LATE CALEDONIAN MAGMAGENESIS IN SOUTHERN SCOTLAND

PAUL SHAND

Doctor of Philosophy

THE UNIVERSITY OF ASTON IN BIRMINGHAM

JUNE 1989

Thesis Summary

The Priestlaw and Cockburn Law intrusions are zoned granitoid plutons intruded into Lower Palaeozoic sediments at the margin of, and prior to closure of, the Iapetus Ocean. They vary from marginal basic rocks to more acid rocks towards their centres. The parental magmas to the plutons were derived from an isotopically depleted mantle modified by melts/fluids during subduction. Zonation in the plutons was caused by combined assimilation and fractional crystallisation (AFC), and rates of assimilation were low relative to rates of fractionation. A series of pyroxene-mica diorites in Priestlaw are however hybrids formed by simple mixing. Porphyrite-acid porphyrite dykes, associated with the plutons, represent chilled portions of the pluton magmas; more evolved quartz porphyry dykes represent crustal melts. Lamprophyre dykes have high LILE and LREE abundances and relative depletions of HFS elements, typical of subduction related ultra-potassic magmas. High Mg numbers, Ni and Cr contents and experimental constraints, imply near primary status for the least evolved lamprophyres. Their enrichments in incompatible elements, high La/Nb, La/Yb, ε Sr and low ε Nd indicate derivation from a previously metasomatised mantle source. Granitoid plutons and lavas in the northern Southern Uplands have high ε Nd and low ε Sr, whereas the younger plutons of the southern Southern Uplands have higher ε Sr, La/Yb and lower ε Nd, consistent with derivation from a more enriched source. No plutons however have remained as closed systems. Three magmatic suites are present in southern Scotland: (1) Midland Valley Suite (2) Northern Southern Uplands Suite and (3) Southern Southern Uplands Suite, consistent with previous models indicating northward underthrusting of English lithosphere below the southern Southern Uplands. Further underthrusting of decoupled lithospheric mantle is indicated by the presence of lamprophyres in the eastern Southern Uplands, and took place between 410 Ma and 400 Ma.

KEY WORDS: assimilation-fractional crystallisation (AFC), Caledonian, granitoid, Iapetus Ocean, lamprophyre.

DEDICATED TO MY FATHER AND MOTHER

Acknowledgements

I would like to thank Dr. J.W. Gaskarth and Dr. N.M.S. Rock for supervising the project. Dr. N.M.S. Rock is also thanked for supplying rock samples 1385-1518. The technical and secretarial staff at Aston University geology department provided the necessary logistical back-up, and their help and friendliness is very much appreciated. Dr. M.F. Thirlwall and Mr. G.A. Ingram provided assistance with rare-earth element and isotopic analysis. Use of the isotope laboratory at Royal Holloway and Bedford New College (RHBNC), where isotopic and REE analysis were determined is greatly appreciated. Dr. N.R.W. Glendinning and Mr. Ian Gill (RHBNC) are thanked for their generous hospitality. Discussions with numerous people over the period of research helped to highlight the many problems involved in igneous geochemistry, and I would like to particularly thank Mr. P.J. Henney, Dr. Martin Menzies, Dr. Matthew Thirlwall and Dr. Chris Ward. Thanks also to Daniel and Araceli, Derek and Carol, Carol, Chris, Pete and Charlie etc. for their friendliness while at Aston.

Dr. N.M.S. Rock, Mr. R.T. Smith and Dr. M.F. Thirlwall kindly criticised Chapter 2. A special thanks to Dr. J.W.Gaskarth for his enormous effort in criticising the various drafts of all the chapters. Thanks to Dr. Jon Naden for help with the Excell spreadsheet on the Mac.

I would like particularly to thank my father for introducing me to all aspects of the natural world at an early age, and both my parents are thanked for their encouragement to do further research, and for their continuing support during my University career.

Last but not least, I would like to especially thank Katherine for her much appreciated help during the collating stages, and for her understanding of the problems involved in both starting to write and trying to finish a PhD !!!

CONTENTS

LIST OF TABLES

LIST OF FIGURES

LIST OF PLATES

1.0 Introduction and general geology

The Caledonian orogeny in Scotland terminated with the collision of two continents and the closure of the intervening Iapetus Ocean. A wide variety of evidence indicates that closure took place along a suture (Iapetus Suture) stretching from south of the Southern Uplands across the Solway Firth and into Central Ireland (Leggett *et al.* 1979; Phillips *et al.* 1976) (Figure 1.1). The oldest rocks in Scotland are 2900Ma. Lewisian gneisses which crop out as refractory granulites in the extreme north-west. This, or younger, basement is overlain further south by a late Pre-cambrian to lower Palaeozoic Moine and Dalradian meta-sedimentary and meta-igneous cover sequence. Older rocks are obscured in the Midland Valley by Lower Palaeozoic and younger sequences of lavas and sediments, but basement is indicated by geophysical studies (Bamford *et al.* 1978), and shown by the presence of granulite xenoliths in Carboniferous vents (Upton *et al.* 1976). The Southern Uplands form part of the non-metamorphic Caledonides (Figure 1.1), and are dominated by Ordovician-Silurian flysch facies sediments.

The ending of the Caledonian orogeny was accompanied by the emplacement of abundant calc-alkaline granitoid plutons (Pankhurst & Sutherland, 1982) and the extrusion of basic-acid lava sequences (Thirlwall, 1979) across the Caledonian Belt. The most voluminous period of granitoid magmatism (late granitoids) occurred from about 430-390 Ma. and are mainly I-type in nature (Chappell & Stephens, 1988; Chappell & White, 1974) and commonly have associated dyke swarms (Rock *et al.* 1988), in contrast to the earlier granitoids (460-430Ma.), many of which have S-type characteristics and lack dyke swarms. The late granitoids represent an areal addition to the crust of Scotland of about 6% (Stephens & Halliday, 1984), and the dyke suites may form as much as 12% of the total volume of igneous rocks (Watson, 1984).

This thesis presents a study of Late Caledonian magmagenesis in the Southern Uplands of Scotland. The geochemical characteristics and relationships between

Aston University

Illustration removed for copyright restrictions

Figure 1.1. Geological map of Scotland. Box 1 shows the main structural units and faults, with the assumed trace of the Iapetus Suture shown as a dashed line. Modified from Harris (1983).

Late Caledonian plutons, minor intrusions (lamprophyres-porphyries) and lavas of an area in the eastern Southern Uplands has been studied in detail. This area stretches from approximately Hawick in the west to St. Abbs Head in the east (Figure1.2), and is covered by published geological 1:50 000 map sheets 17W, 25W, 33W, 33E and 34 of the British Geological Survey. A more broad ranging aspect also covered in this thesis, comprises a rare earth element (REE) and isotopic study of plutons both along and across strike from this area in the Southern Uplands.

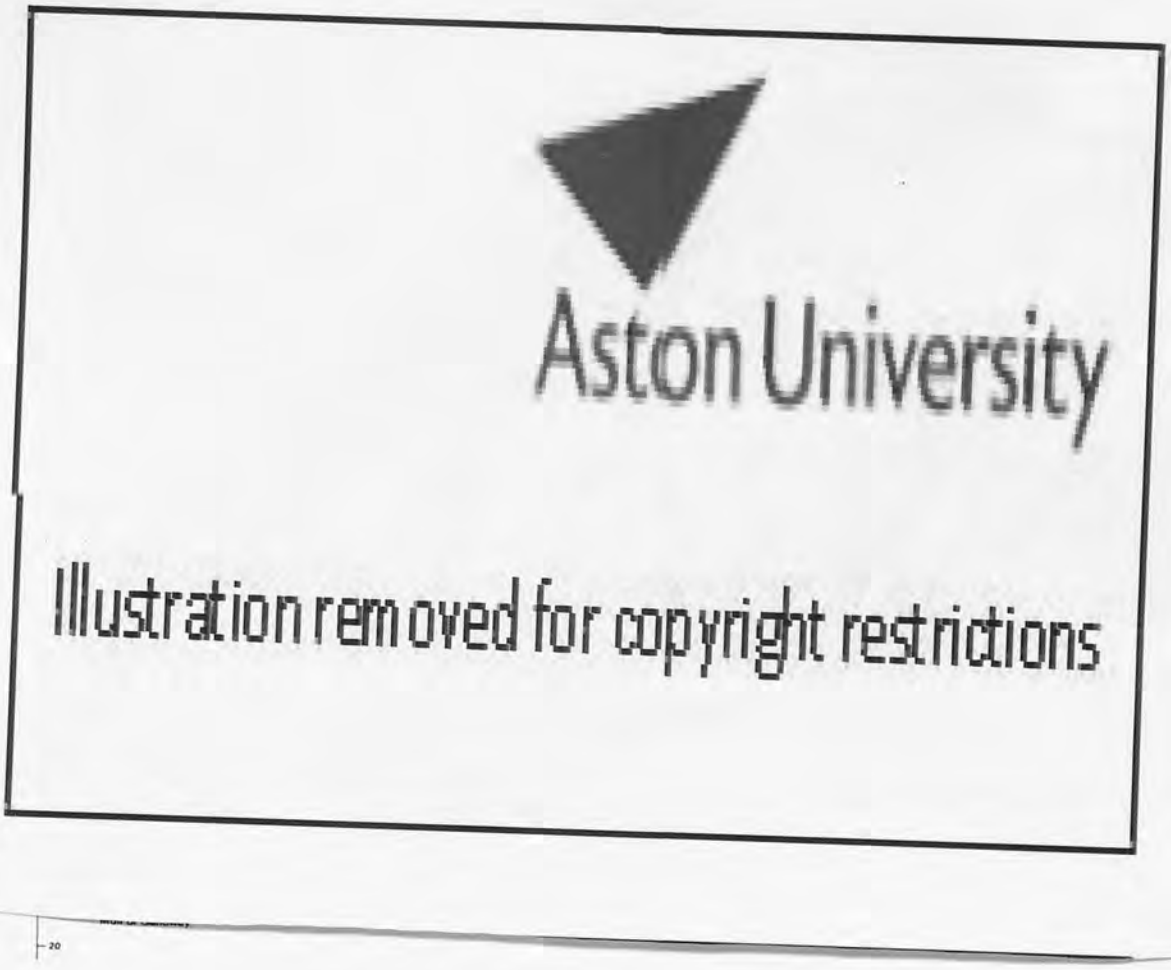

Figure 1.2. Map of the Southern Uplands of Scotland showing localities and detailed area of study, (from Rock *et al.* 1988).

The Southern Uplands is dominated by lower Palaeozoic greywacke sediments. These rocks have been sub-divided into three strike parallel belts: the Northern, Central and Southern Belts (Leggett *et al.* 1979; McKerrow *et al.* 1977). The Northern and Central

belts are separated by the Northern/Central Belts Boundary Fault (Morris, 1987), thought to be a major strike slip fault (Hutton & Murphy, 1987). Stratigraphic sequences in these Belts are in discrete fault bounded tracts within which the rocks predominantly young to the northwest, but the tracts are sequentially younger to the southeast. All three belts are dominated by greywackes, but argillites, cherts and mafic volcanics occur in the Northern Belt.

Tectonic interpretations, to account for the structure of the Southern Uplands, have been the subject of much recent debate (McKerrow, 1988). Early models proposed that the Southern Uplands represented a fore-arc accretionary prism built up during the closure of the Iapetus Ocean (Leggett *et al.* 1979a,b; McKerrow *et al.* 1977). Continental basement is indicated below the northern part of the Southern Uplands from geophysical studies (Hall *et al.* 1983), and Needham & Knipe (1986) thereby proposed a fore-arc model with the sediments representing a "pop-up" structure, partly allochthonous onto Midland Valley type basement, and partly underthrust by basement from the south during ocean closure. Alternatives are a back-arc model, with the the tracts representing a stacked back-arc thrust duplex (Stone *et al.* 1987), or a dual model whereby back-arc rocks of the Northern Belt were subsequently overthrust by rocks of the fore-arc Central and Southern Belts (Hutton & Murphy, 1987; Morris, 1987). Recent geophysical modelling from the North East Coast deep seismic reflection profile suggested the presence of at least four different crustal/terrane types below southern Scotland and northern England: (1) Midland Valley, (2) Sub-continental subduction complex, (3) Lake District and (4) Southern continent, ?Midland Platform (Freeman *et al.* 1988).

The closure of Iapetus has also been the subject of debate, and interpretations as to its timing vary from end-Ordovician (Hutton & Murphy, 1987), through Silurian (Watson, 1984) to Devonian (Soper *et al.* 1987; Thirlwall, 1988). A knowledge of the timing of closure is important in ascertaining the relationship of Late Caledonian magmatism to subduction.

1.2 Previous work

Previous work on the late Caledonian granitoids has concentrated on the larger, more voluminous, plutons of the Highlands and Southern Uplands. The majority of these are compositionally zoned with early mafic rocks marginal to granodiorites and granites (Pankhurst & Sutherland, 1982). The variations in individual plutons suggest that more than one source component, generally both mantle and crust, is necessary to explain this zonation (Halliday, 1984; Halliday *et al.* 1979). The proportions of mantle-derived and crustal components has however been the subject of debate. Recent studies of magmagenesis in the Etive complex in the Highlands for example have argued over either a dominant crustal (Hamilton *et al.* 1980; Clayburn, 1988), or mantle (Thirlwall, 1986) source. The importance of fractional crystallization of basic to intermediate parents has also been emphasised for production of the variation in rock types (Nockolds, 1941; Tindle & Pearce, 1981; Tindle *et al.* 1988), as has combined assimilation and fractional crystallization (Stephens *et al.* 1985). The late Caledonian granitoids have been classified into three petrographical and geochemical suites: (1) the Cairngorm suite comprising plutons of the NE Highlands, (2) the Argyll suite comprising plutons from the SW Highlands, and (3) the S of Scotland suite, including plutons from the Southern Highlands, Midland Valley and the Southern Uplands (Stephens & Halliday, 1984). The Criffell and Fleet plutons in the Southern Uplands were however excluded from these suites because they have features characteristic of S-type granites.

The regional dyke swarms of Scotland have until recently been largely ignored in studies of late Caledonian magmatism. Much recent work has however concentrated on lamprophyres, which occur in both regional swarms unrelated to plutons (Rock *et al.* 1986b), and as abundant dykes marginal to plutons (Rock & Hunter, 1987). These are thought to represent partial melts of metasomatised mantle (MacDonald *et al.* 1985) which may have acted as parents to their spatially associated plutons (MacDonald *et al.* 1986; Rock *et al.* 1988).

Volcanic rocks of similar age occur from the SW Highlands to St. Abbs

head in the Southern Uplands. Isotope and trace element data indicate the presence of old enriched mantle below the SW Highlands, and depleted mantle below the Midland Valley (Thirlwall, 1981, 1986). The variations in these rocks have been modelled as being due to mixing processes in the mantle between the mantle wedge and subducted sediment (Thirlwall, 1983, 1986).

1.3 Sampling and analytical techniques

More than 300 samples (of at least 2kg) from the plutons, dykes, lavas and sediments in the eastern Southern Uplands were collected and, after thin section examination, about 260 samples were selected for geochemical analysis. These were crushed in a tungsten carbide jaw crusher and reduced to a fine powder (-200 mesh). Details of rock processing are given in Appendix 1 and the data are presented in Appendix 3. Ten major (SiO_2, Al_2O_3, Fe_2O_3, MgO, CaO, Na_2O, K_2O, MnO, TiO_2, P_2O_5) and fourteen trace (Zn, Cu, Ni, Rb, Sr, Y, Zr, Nb, Ba, U, Th,Pb, V and Cr) elements were analysed using a PW1400 X-ray spectrometer at Aston University. Major elements were analysed on glass beads using a method similar to that of Norrish & Hutton (1969). Trace elements were analysed on pressed powder pellets (Appendix 1). Precision is estimated from the reproducibility of single samples, one standard deviations being typically SiO_2 0.12%, Al_2O_3 0.06%, Fe_2O_3 0.08%, MgO 0.04%, CaO 0.06%, Na_2O 0.05%, K_2O 0.01%, MnO 0.006%, TiO_2 0.01%, P_2O_5 0.02%, LOI 0.08%, Zn 0.8, Cu 0.9, Ni 1.0, Rb 0.6, Sr 1.9, Y 0.7, Zr 0.9, Nb 0.5, Ba 6.9, U 1.5, Th 1.7,Pb 1.3, V 2.5 and Cr 3.9. Variability in the reproduction of glass beads and pellets give similar standard deviations. Mass absorption effects for the trace elements were compensated for using the Compton scattered Rh tube line. Line overlap corrections for Cr and V (due to interference of the intense Fe Kα line), Zr and Y were used.

Rare earth elements (REE) were determined by isotope dilution using the highly precise method of Thirlwall (1982), and all were determined on aliquots from the solution used for Nd isotope analysis (Appendix 2). REE, Sr and Nd isotopes were

analysed on the VG 354 mass spectrometer, and Rb and Sr concentrations on the X-ray spectrometer at Royal Holloway and Bedford New College (RHBNC). 2 sigma errors on Rb and Sr are + 0.4 and + 1.5 respectively. The Sr standard SRM 987 gave values of $^{87}Sr/^{86}Sr$ = 0.710241+ 22 (2 sd, N=63) over the period of analysis. The Nd standards La Jolla and Aldrich (laboratory standard) gave values of $^{143}Nd/^{144}Nd$ = 0.511857+ 7 (2 sd, N=17) and $^{143}Nd/^{144}Nd$ = 0.511418+ 9 (2 sd, N=47) respectively. Values for the Nd standards varied systematically, and both standards and samples were corrected using: $^{143}Nd/^{144}Nd = (^{143}Nd/^{144}Nd)_m + 0.222(1.14187 - ^{142}Nd/^{144}Nd_m)$, where subscript m is the measured value. This variation is most probably due to the poor peak shape affecting the ^{146}Nd measurement that is used to calculate both $^{143}Nd/^{144}Nd$ and $^{142}Nd/^{144}Nd$ (M.F. Thirlwall, pers. comm.). REE data are presented in Appendix 4 and isotope data in Appendix 5.

1.4 Representation of geochemical data

Major and trace element data for the granitoids, minor intrusions, lamprophyres, sediments and Carboniferous dykes are given in appendices 3a, 3b, 3c and 3d respectively, on a wet basis. REE and isotope data are given in Appendices 4 and 5. All geochemical data plots are done on a volatile free basis. Chondrite normalised plots for spiderdiagrams are normalised to chondrite, except K, P and Ti after Thompson (1982), and REE are normalised to the chondrite values given by Nakasawa (1982). Isotopic data for Sr and Nd are presented as initial ratios and in terms of the parameters ε Nd and ε Sr (DePaolo and Wasserburg, 1976,1977). Initial ratios for the granitoids have been calculated at 410 Ma. for the northern Southern Uplands (Thirlwall, 1988), 397 Ma. for plutons from the southern Southern Uplands (Halliday, 1984) and 400 Ma. for the lamprophyres (Rock and Rundle, 1986). ε Nd values were calculated using $(^{143}Nd/^{144}Nd)_{CHUR}$=0.512638 and $(^{147}Nd/^{144}Nd)_{CHUR}$ = 0.1967, and ε Sr using $(^{87}Sr/^{86}Sr)_{UR}$= 0.7045 and $(^{87}Rb/^{86}Sr)_{UR}$= 0.0839.

1.5 Thesis structure and aims of thesis

The plutons from the eastern Southern Uplands studied here, Priestlaw and Cockburn Law, are small zoned plutons. These are spatially associated with abundant dykes ranging in composition from lamprophyre and porphyrite (andesite porphyry) to quartz-porphyry (rhyolite porphyry). These form the bulk of the present study, and are supplemented with a regional isotopic and REE study of plutons in southern Scotland. The layout of the thesis is as follows:

Chapter 2 presents a detailed major and trace element and Sr and Nd isotopic study of the two zoned plutons, Priestlaw and Cockburn Law, in the eastern part of the Southern Uplands. The aim of this chapter is to ascertain the source component(s) involved in these plutons, and to constrain models for the evolution of zoning. The various models considered are:

(a) Soret-effect diffusion leading to compositional gradients within the melt.

(b) Mass removal in a volatile phase.

(c) Contamination of a single magma by assimilation of wall rocks.

(d) Intrusion of compositionally distinct magmas with possible hybridisation.

(e) Intrusion followed by unmixing of a melt plus restite (restite unmixing model).

(f) Fractional crystallisation of a basic magma, including the formation of marginal cumulates and/or incomplete separation of "cumulus" phase and "liquid".

(g) Mixing of basic and acid magmas.

(h) Fractional crystallisation combined with assimilation(AFC).

Dyke rocks varying in composition from andesite-porphyry to quartz-porphyry are studied using major and trace element data in chapter 3. The aim of this chapter is to study the relationships between the plutons and dykes to ascertain if a genetic relationship exists between the two.

The lamprophyres are treated in chapter 4, where major and trace element and limited REE and Sr and Nd isotopic data are used to constrain the source characteristics of these rocks. Their possible role as parents to the granitoids will also be

discussed.

REE and Sr and Nd isotopes are presented for several plutons in the Southern Uplands and Midland Valley, and compared with the detailed study of Priestlaw and Cockburn Law in chapter 2. The additional plutons considered are Spango and Knipe in the Northern Belt, Carsphairn in the Central Belt, Bengairn, Creetown and Portencorkrie in the Southern Belt and Distinkhorn in the Midland Valley. The aims of this chapter are to constrain the sources of the plutons, in order to constrain models regarding crustal recycling and to relate the geochemical characteristics of these to existing tectonic models.

Chapter 2: The Origin and evolution of the Priestlaw and Cockburn Law zoned plutons in south-east Scotland

2.0 Abstract

The Priestlaw and Cockburn Law intrusions are small, zoned plutons intruded into Lower Palaeozoic sediments at the margin of, and prior to closure of, the Iapetus ocean at ca.410 Ma. The variation in rock types is from marginal olivine norite to dykelets of granite in Priestlaw; and from diorite to patches of granite in Cockburn Law. Combined major and trace elements and Sr and Nd isotopes constrain models for the evolution of this zonation and also constrain end-member compositions of source components. These plutons have more radiogenic initial $^{143}Nd/^{144}Nd$ ratios (εNd = +2.2 to -1.8) than previously published data on Caledonian granitoids, and low initial $^{87}Sr/^{86}Sr$ (0.70416-0.70578). General correlations between isotopes and parameters of fractionation imply that combined assimilation and fractional crystallization (AFC) is an important process in the evolution of zoning. A series of pyroxene-mica diorites in Priestlaw however are hybrids formed by simple mixing. The most basic rocks, except the olivine norites which are cumulates, are similar geochemically and isotopically to the least evolved nearby contemporaneous St. Abbs/Eyemouth lavas (Thirlwall, 1979), implying a parental source from the mantle and not infracrustally derived. These parents are from a time integrated LREE depleted mantle, similar to that below the Midland Valley, that had been previously metasomatized by fluids/melts during subduction. Detailed isotopic modelling implies that rates of assimilation relative to rates of crystallization are low, thus suggesting that mantle addition during the Late Caledonian orogeny has been important. The crustal contaminant is likely to have had a similar Sr and Nd isotopic composition to Southern Uplands Lower Palaeozoic sediments (SULPS). However recent Pb isotopic studies of Southern Uplands plutons and sediments (Thirlwall *et al.* 1989) suggest that SULPS itself is unlikely to have been a contaminant and it appears that ?lower crust which is not exposed but implied by geophysical studies (Hall *et al.* 1983) is the most likely contaminant. The Sr compositions of the parents are well constrained from a consideration of the compositions in marginal basic rocks which represent cumulates, and the variation in the plutons help to constrain the concentration of Sr in the contaminant. A high Sr contaminant would imply implausibly high D_{Sr} during the AFC process. Partial melts of this lower crust must have had very low Nd concentrations (<10 ppm) to satisfy the shapes produced on εNd-εSr diagrams. Such melt compositions could be produced if Nd was retained in some form of restite phase. Accessory minerals which generally contain the REE's provide the most probable source, since experimental studies imply that some of these will behave as restite during low degrees of partial melting.

2.1 Introduction

Concentric zoning in calc-alkaline granitoid plutons is most commonly from more basic to more acid compositions from the margins inward. Models for the evolution of this zoning have largely been unsuccessful in quantifying the various processes that give rise to these compositional changes. This is in part due to the lack of a multi-disciplinary approach to the various types of data, and partly due to the many problems inherent in modelling granitoids. Some of these problems include the following:

(1) Crystallisation in a viscous melt may not produce a clear distinction between "cumulate" and "liquid", therefore the products may be variable mixtures of cumulate and trapped interstitial melt (McCarthy and Hasty, 1976).

(2) The type of crystallisation may lie between the extremes of perfect equilibrium and perfect fractional crystallisation (McCarthy and Hasty, 1976).

(3) Mineral-melt partition coefficients may vary during crystallisation as temperature and composition change (Hanson, 1978; Henderson, 1982).

(4) Minor amounts of accessory minerals e.g. apatite, zircon, allanite and sphene, may control the distribution of some trace elements e.g. REE, Zr, Y (Hurley and Fairbairn, 1957; Sawka *et al.* 1984).

(5) Assimilation or contamination with country rock solids/melts may occur, and may give rise to complex processes such as assimilation/contamination concomitant with crystallisation (De Paolo, 1981).

(6) Isotopic modelling may be complex due to the lack of constraints on the number and compositions of possible end-members, and also the difficulty in ascertaining relative rates of assimilation and crystallisation.

Some of the processes suggested to account for normal zoning in mesozonal plutons were reviewed by Wall *et al.* (1987) and Stephens *et al.* (1985). The use of quantitative mathematical expressions has proved to be very powerful in modelling trace element behaviour in magmatic systems (see Allegre and Minster, 1978, for review). The application of these to simple models of granite petrogenesis was reviewed by Hanson

(1978). The various processes that have been proposed for the generation of zoned plutons include *fractional crystallisation* (Frey *et al.* 1978; Tindle and Pearce, 1981); *restite separation* (White and Chappell, 1977); *assimilation* (Ague and Brimhall, 1987); and *hybridisation* (Cantagrel *et al.* 1984; Kistler *et al.* 1987). More complex models, including *combined fractional crystallisation and assimilation* (De Paolo, 1981), and the effects of *replenishment* with mafic magma (O'Hara, 1977), may approximate more closely to the real physico-chemical conditions. Due to the complexity of these models however, many assumptions are usually required.

2.2 Aims of chapter

In this chapter, major and trace elements, combined with Sr and Nd isotopes, are used to constrain models for the origin of zoning in two plutons, Priestlaw and Cockburn Law (Figure 2.1), in southeastern Scotland. These data will also be used to constrain the source component(s) of the magmas involved in their evolution.

2.3 Priestlaw and Cockburn Law intrusions

The Priestlaw and Cockburn Law intrusions are small plutons intruded into the Central Belt of Lower Palaeozoic flysch facies sediments of the Southern Uplands of Scotland (Figure 2.1). They form part of the suite of "Newer granites" which vary in age from 430Ma to 390Ma (Brown *et al.* 1968), and were emplaced after the main deformation and metamorphism associated with the Caledonian orogeny. They occur from the northwestern Highlands to northern England. The Priestlaw and Cockburn Law intrusions were emplaced on the north-western margin of the Iapetus ocean at c.410 Ma (Thirlwall, 1988). The Southern Uplands is dominated by Lower Palaeozoic greywackes of low metamorphic grade (Oliver and Leggett, 1980), which are subdivided into three parts: (a) the Northern Belt (Ordovician), (b) the Central Belt (Llandovery) and (c) Southern Belt (Wenlock) (Figure 2.1). Tectonic interpretations for the Southern Uplands have varied from a fore-arc accretionary prism (Leggett, 1987 and references therein) to a back-arc basin (Stone

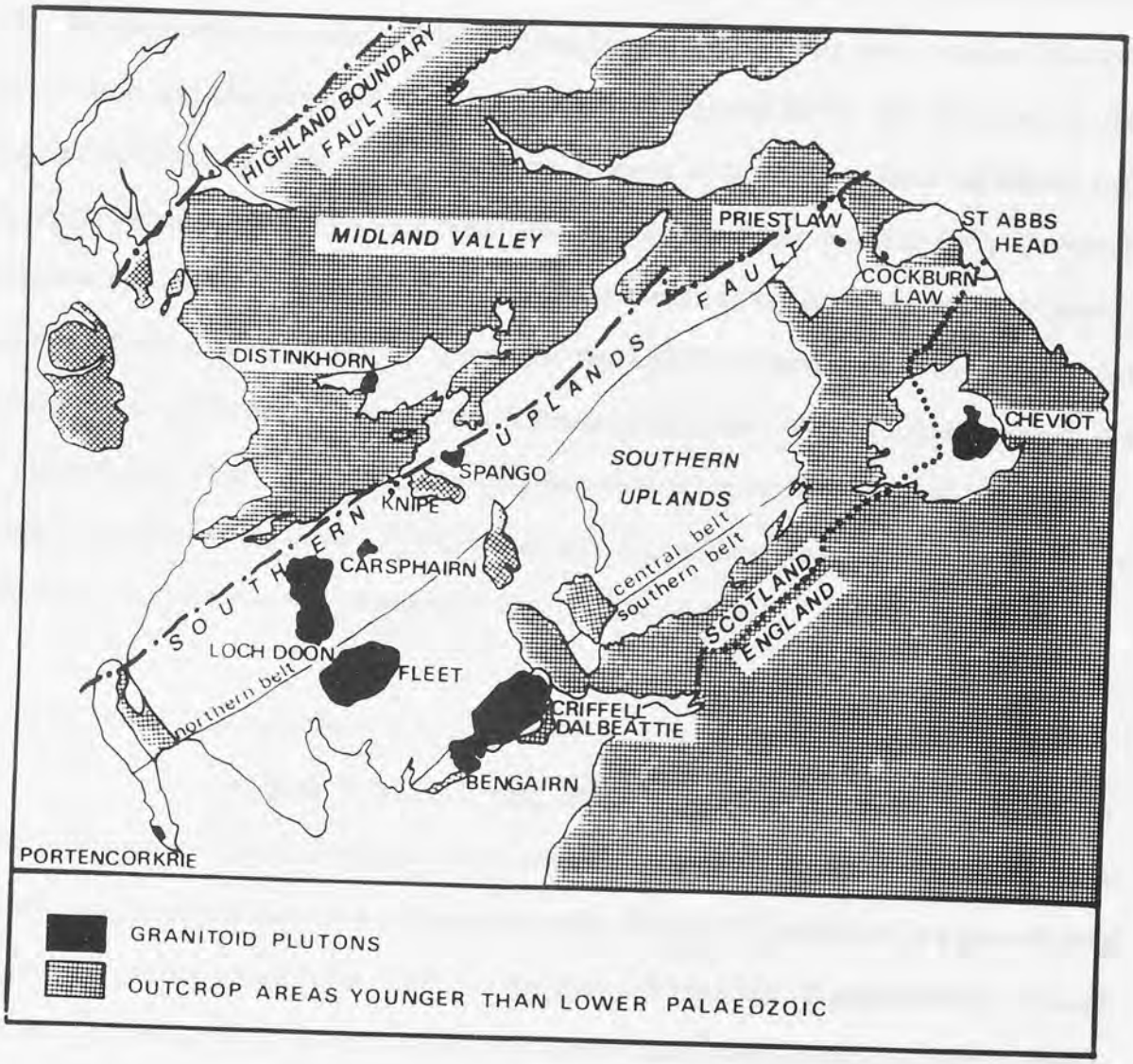

Figure 2.1 Map of southern Scotland showing the distribution of Late Caledonian granitoids.

et al. 1987). Much debate also concerns the timing of collision, and interpretations vary from end-Ordovician (Hutton and Murphy, 1987) to Devonian (Soper *et al.* 1987, Thirlwall, 1988). The importance of strike slip faulting has been emphasised by some workers (Hutton, 1987; Hutton and Murphy, 1987). The Northern and Central Belts are separated by the Kingledores/Orlock Bridge/Slieve Glah fault, thought to be a major fault separating two tectonostratigraphic terranes which were juxtaposed in the late Silurian-early Devonian (Anderson and Oliver, 1986; Morris, 1987). The presence of continental basement beneath southern Scotland is indicated by results of the LISPB seismic refraction experiment (Bamford *et al.* 1978) and the occurrence of lower crustal xenoliths in Carboniferous dykes and plugs (Upton *et al.* 1983). Shallow basement below the northern part of the Southern Uplands, including the area of Priestlaw and Cockburn Law, is indistinguishable seismologically from that of the Midland Valley (Hall *et al.* 1983).

2.4 Zonation of the plutons

Priestlaw is located 5km. north west of Cranshaws (NT 684 618). Exposure is poor and the north-eastern part is buried below the Whiteadder reservoir. Several units are mapped on the basis of a petrographic study (Figure 2.2), and there is a general trend of increasing acidity towards the interior of the pluton from norite to granodiorite, although the outer zone of gabbro is discontinuous. Granite is found only as small (ca.3 cm) dykes in part of the granodiorite (1452d). This general zonation is however interrupted by a pyroxene-mica diorite unit (Figure 2.2). Contacts with country rock are exposed only near the north-eastern margin where granodiorite interfingers with sediment (NT 367 636), but hornfelsing of sedimentary rocks occurs all around the margins of the pluton. The only internal contact exposed is near the northern margin (NT 642 647) which shows altered and decomposed granodiorite intruding sheets of pyroxene-mica diorite. Xenoliths of pyroxene-mica diorite are also present at this locality, and in granodiorite near the centre of the intrusion (NT 644 640). Vugs containing quartz and orthoclase are common in part of the porphyritic unit.

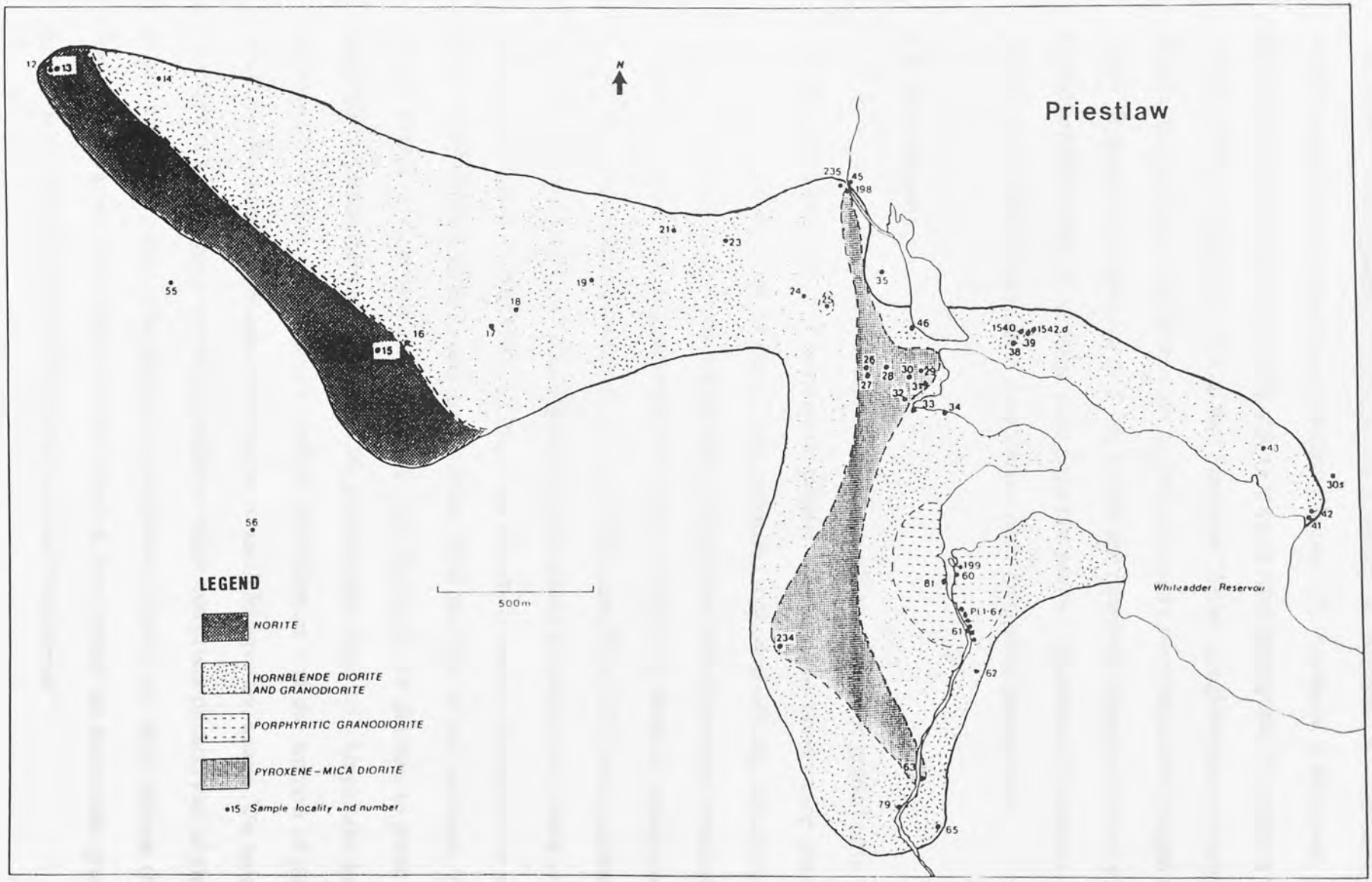

Figure 2.2. The Priestlaw granitoid showing petrographical subdivisions and locations of samples collected.

Cockburn Law is situated 3km. south east of Abbey St. Bathans (NT 758 623), and has a smaller range in rock types than Priestlaw (Figure 2.3). Exposure is also poor, and again there is a general trend of increasing acidity inwards from the margin. No contacts with older country rocks are exposed, but "Old Red Sandstone" facies conglomerates containing blocks of granitoid similar to Cockburn Law lie unconformably over the eastern margin (Midgley, 1946). Rounded autoliths, up to 5 cm across are relatively abundant in one part of the granodiorite (PS 85b), as are felsic segregations or patches. Xenoliths of sedimentary rock are present but uncommon in parts of the pyroxene-mica diorite and granodiorite.

2.5 Petrography

Priestlaw varies from olivine norite to porphyritic granodiorite, and has a few thin (ca.3 cm) dykes of porphyritic granite (1542d). The norites crop out along the north-western margin of the body. They comprise subhedral olivine, orthopyroxene and clinopyroxene in a parallel oriented network of plagioclase laths (bytownite-labradorite) which commonly display bent and deformed twin planes (Plate 2.1). Rods of orthopyroxene also form symplectic textures between olivine and plagioclase (Plate 2.2). Loose boulders (PS 13) from the Kell Burn (NT 615 651, Figure 2.2), previously the only area marked as norite on British Geological Survey 1:50 000 maps, are extremely altered clinopyroxene norites. A series of hornblende diorites and granodiorites form the bulk of the intrusion. The mafic phases change from brown amphibole with little biotite in the diorites, to green euhedral amphibole with more abundant biotite in the granodiorites (Plate 2.3). Amphibole decreases at the expense of biotite in the more evolved granodiorites and the amount of plagioclase (andesine-oligoclase) decreases at the expense of alkali feldspar and quartz. The most evolved rock type is a porphyritic unit of granodiorite which comprises phenocrysts of plagioclase, quartz, biotite and minor orthoclase, in a groundmass of quartz and alkali feldspar (Plate 2.4). Porphyritic granite occurs only as small dykes (ca. 3cm) within the hornblende granodiorite. This basic to acid sequence will be referred to as the "Main Series".

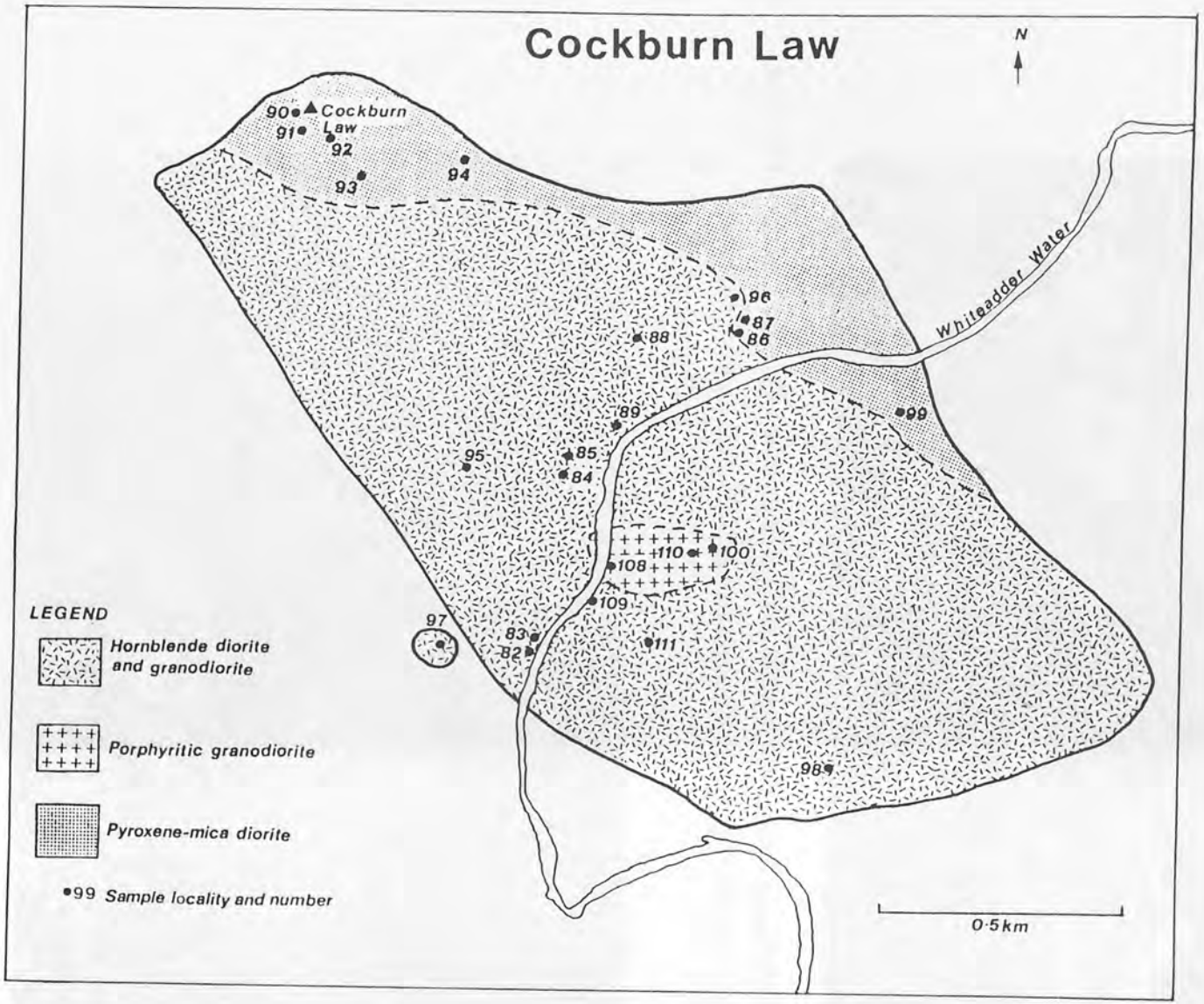

Figure 2.3. The Cockburn Law granitoid showing petrographical subdivisions and locations of samples collected.

Plate 2.1. Olivine norite (PS15) from Priestlaw, showing laminated plagioclase (plag) and subhedral olivine (ol), clinopyroxene (cpx) and orthopyroxene (opx). Field of view (Fov):8.3mm.

Plate 2.2. Olivine norite (PS15) from Priestlaw showing symplectite of orthopyroxene rods formed at the margin of olivine (ol) and plagioclase (plag). Fov: 0.2mm.

Plate 2.3. Hornblende-biotite granodiorite; form Priestlaw (1542), with subhedral hornblende (hbl) and anhedral biotite (bt) poikilitically enclosed in orthoclase (ksp). Fov: 8.3mm.

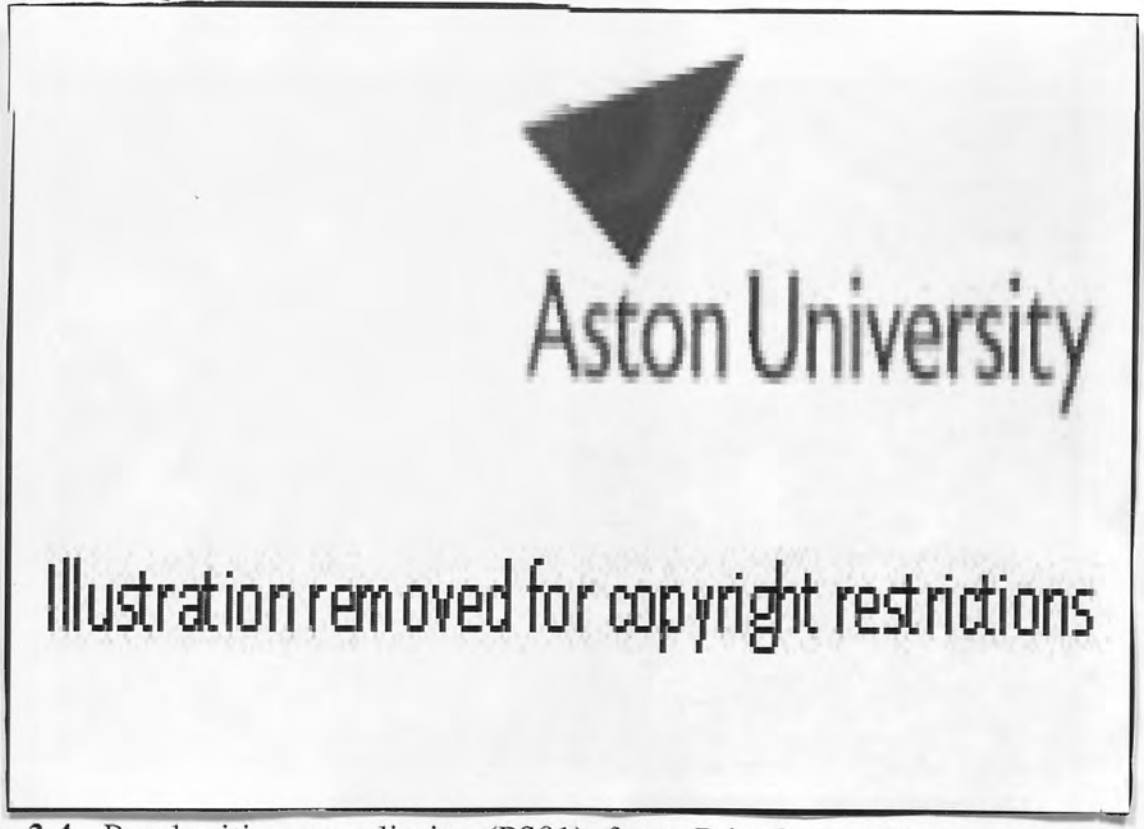

Plate 2.4. Porphyritic granodiorite (PS81) from Priestlaw, with phenocrysts of plagioclase biotite and quartz in a groundmass of plagioclase, quartz and orthoclase. Fov: 8.3mm.

The "Pyroxene-mica Diorite Series" of Priestlaw is a group of dark fine-grained rocks which crop out as an elongated north-south facies through the centre of the intrusion (Figure 2.2). These contain orthopyroxene, clinopyroxene, biotite, plagioclase, alkali feldspar and quartz. They vary from fine-grained rocks with phenocrysts of orthopyroxene (Plate 2.5), to more strongly porphyritic rocks with phenocrysts of plagioclase and more abundant biotite at the expense of pyroxene. In the porphyritic varieties plagioclase commonly contains abundant inclusions of orthopyroxene, biotite and minor clinopyroxene (Plate 2.6). Cumulophyric aggregates of euhedral orthopyroxene are also occasionally seen but are uncommon (PS 25, 26). Xenoliths of the pyroxene-mica diorite Series(PS 198) in granodiorite near to contacts are orthopyroxene-phyric.

Cockburn Law has similar rock types to Priestlaw and is also subdivided petrographically into separate units (Figure 2.3), though no exposures of contacts between individual units are exposed. Coarse-grained (up to 2mm) hornblende diorites crop out at the south western margin and are more altered than similar rock types in Priestlaw, with amphibole being replaced by chlorite, carbonate and minor biotite. Apatite in these rocks is relatively coarse grained (up to 2.6mm). The hornblende diorites grade towards the centre of the pluton into hornblende and hornblende biotite granodiorites (Plate 2.7), some of which contain subhedral clinopyroxene. Enclaves, and felsic patches which grade into the granodiorite, are relatively abundant in one outcrop (PS 85). The enclaves (PS85b) are rich in both clinopyroxene and orthopyroxene, and although the feldspar present is commonly plagioclase, some pyroxene is poikilitically enclosed by large (up to 1mm) orthoclases. Clinopyroxene is common in the host adjacent to these inclusions, but much less common away from the contacts. Porphyritic granodiorites crop out towards, and on, the summit of Stonesheil Hill (NT 774 589). These contain phenocrysts of plagioclase, quartz and lesser amounts of orthoclase and biotite (Plate 2.8).

The pyroxene-mica diorites of Cockburn Law form a discontinuous marginal zone (Figure 2.3). Orthopyroxene phenocrysts are commonly rimmed by chlorite and biotite (Plate 2.9), and all samples contain phenocrysts of plagioclase, commonly with

Plate 2.5. Pyroxene-mica diorire form Priestlaw (PS28), with phenocrysts of subhedral orthopyroxene and biotite in a groundmass of plagioclase and biotite. Fov: 8.3mm.

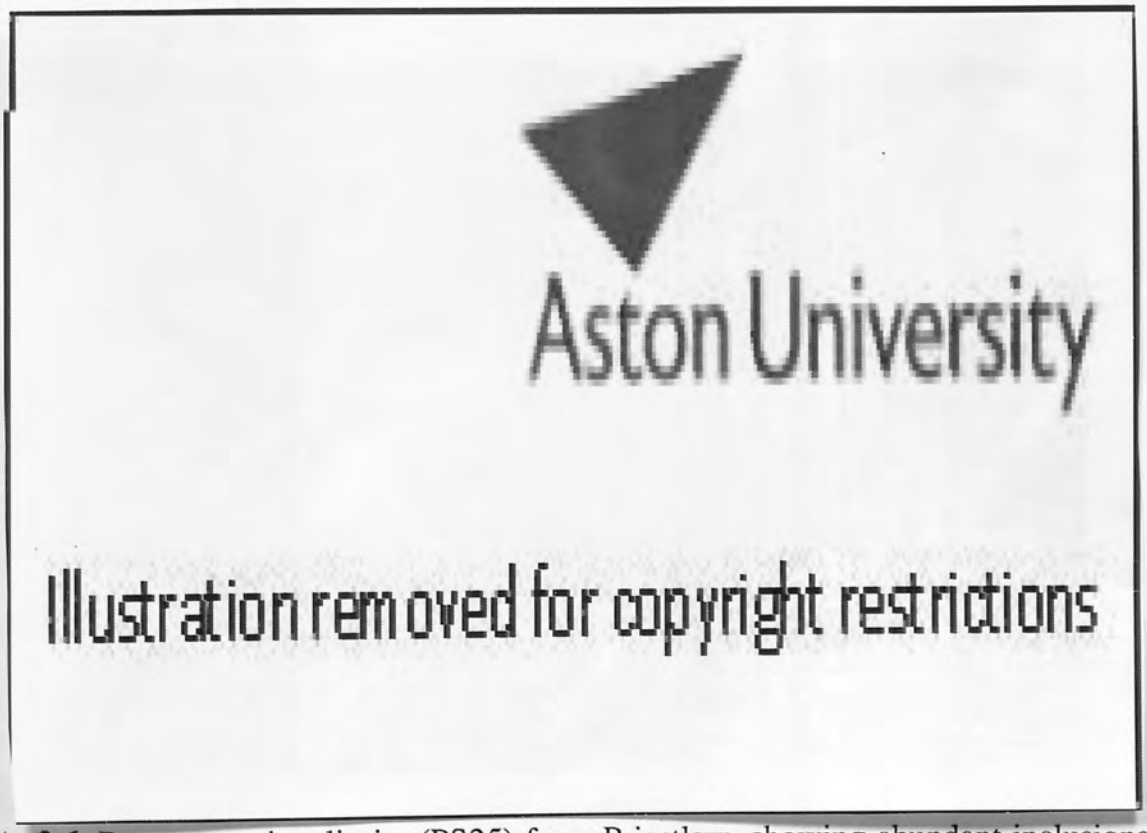

Plate 2.6. Pyroxene-mica diorite (PS25) from Priestlaw, showing abundant inclusions of orthopyroxene, clinopyroxene and biotite in a large phenocryst of plagioclase. Fov: 3.4mm.

Plate 2.7. Hornblende-biotite diorite (PS95) from Cockburn Law, showing patchy alteration in plagioclase. Fov: 8.3mm.

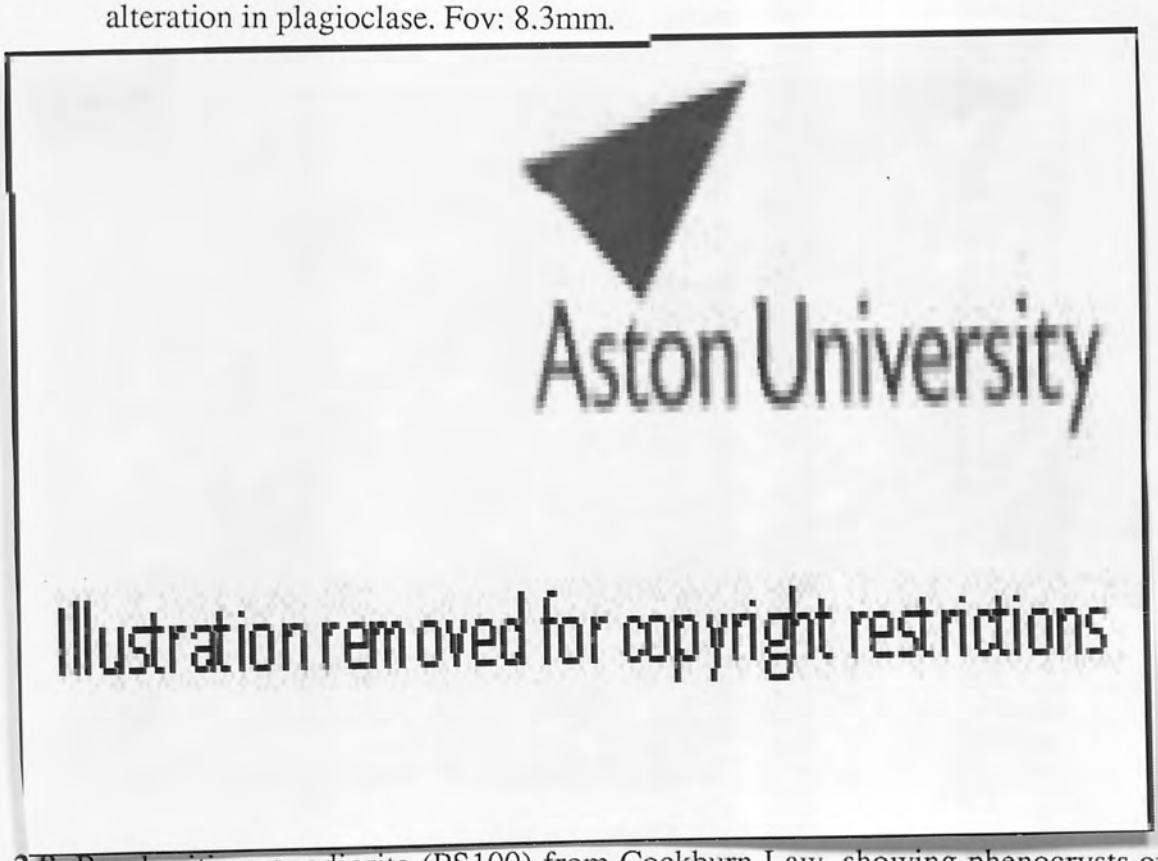

Plate 2.8. Porphyritic granodiorite (PS100) from Cockburn Law, showing phenocrysts of plagioclase, quartz, orthoclase and biotite in a fine-grained groundmass of quartz and orthoclase. Fov: 3.4mm.

Plate 2.9. Pyroxene-mica diorite (PS93) from Cockburn Law, showing euhedral phenocrysts of orthopyroxene with alteration rims of chlorite, in a fine-grained groundmass of plagioclase and biotite. Fov: 8.3mm.

Plate 2.10. Pyroxene-mica diorite from Cockburn Law (PS94), with glomeroporphyritic aggregate of plagioclase, orthopyroxene, clinopyroxene and biotite, in a groundmass dominated by plagioclase with minor biotite. Fov: 3.4mm.

small inclusions of biotite and pyroxene. Coarser grained glomeroporphyritic aggregates comprise euhedral ortho- and clinopyroxene and plagioclase (Plate 2.10). Small biotite-rich xenoliths, similar to hornfelsed country rocks, are relatively common in some samples (PS 99).

Both plutons were probably emplaced at a high level in the crust. Evidence for this is the occurrence of boulders of granitoid similar to Cockburn Law in "Old Red Sandstone" facies conglomerates (probably Upper Devonian) which unconformably overly the south-eastern margin of this intrusion (Midgely, 1946), and abundant vugs which occur near the centre of the porphyritic granodiorite of Priestlaw.

2.6 Constraints on petrogenesis

Major and trace element analyses along with isotope data is used to constrain models for the evolution of compositional variations in these zoned plutons. Representative analyses are given in Table 2.1. In this section a summary of the data will be presented, before assessing the possible contributions of different models.

(a) Major elements

Major element data from Priestlaw and Cockburn Law define a high-K calc-alkaline suite on a K_2O-SiO_2 diagram (Figure 2.4). The Priestlaw Main Series rocks define continuous arrays on Harker diagrams from basic to acid compositions (Figure 2.5), with no apparent compositional gaps. The trends are clear and display both simple linear and curved shapes with increasing SiO_2: Fe_2O_3, TiO_2, Al_2O_3 and MnO decrease linearly; MgO and CaO decrease, which is particularly marked in the basic rocks, and Na_2O and P_2O_5 show an increase followed by a decrease. The olivine norites lie off these trends for some elements e.g. K_2O (Figure 2.4). Although the most evolved pyroxene-mica diorites lie on the trends defined by the Main Series, the least evolved ones for some elements have higher (K_2O and P_2O_5) or lower (Al_2O_3 and Na_2O) values than these trends (Figure 2.5), and have some of the characteristics of shoshonitic rocks (e.g. high K_2O, P_2O_5 and K_2O/Na_2O >1). The

No.	PS15	PS17	PS28	PS60	PS65	PS82	PS92	PS95	PS99
Pluton[a]	Plw	Plw	Plw	Plw	Plw	Clw	Clw	Clw	Clw
Type[b]	N	D	Pmd	pGd	Gd	D	Pmd	Gd	Pmd
SiO_2	50.50	51.42	58.86	69.56	60.30	48.48	64.16	61.66	63.58
Al_2O_3	18.57	17.74	15.89	14.71	16.82	18.91	16.27	16.23	16.77
Fe_2O_3	7.28	8.16	5.86	2.99	6.06	6.98	4.39	5.51	4.35
MgO	8.89	6.62	4.61	1.74	3.17	2.62	2.51	3.32	2.37
CaO	9.53	7.40	5.18	2.03	4.12	10.14	3.94	4.35	4.59
K_2O	0.19	1.51	4.04	4.14	2.76	1.10	2.62	3.08	2.31
Na_2O	2.63	3.00	3.03	3.41	3.82	3.52	4.03	3.74	3.80
MnO	0.12	0.12	0.10	0.06	0.10	0.09	0.08	0.10	0.06
TiO_2	0.42	1.19	0.92	0.42	0.85	1.42	0.61	0.74	0.66
P_2O_5	0.03	0.18	0.35	0.13	0.21	0.35	0.15	0.22	0.15
LOI	1.35	2.21	1.13	0.98	1.80	5.61	0.74	1.06	1.04
Total	**99.60**	**99.55**	**99.96**	**100.15**	**100.00**	**99.24**	**99.50**	**100.01**	**99.68**
Zn	69	81	89	31	59	61	66	64	62
Cu	10	8	18	5	14	25	61	28	15
Ni	129	75	49	64	48	41	56	59	42
Rb	11	34	67	103	76	29	74	77	70
Sr	680	557	1773	359	503	588	411	604	363
Y	8	29	25	21	28	23	24	24	24
Zr	17	108	266	168	178	80	160	183	151
Nb	2	6	11	12	9	8	10	10	10
Ba	214	443	1518	600	725	326	564	625	499
U	0	2	3	4	2	2	5	3	3
Th	1	4	12	26	12	3	12	11	11
Pb	5	14	22	15	12	14	23	20	18
V	98	212	140	51	126	174	95	102	124
Cr	274	153	115	47	47	30	60	83	69
La	2.49	13.07	46.25	39.81	28.01	13.37	23.34	30.89	23.23
Ce	5.31	30.52	101.66	68.58	57.20	29.22	46.09	65.54	47.53
Nd	3.174	18.377	50.279	24.450	26.278	16.551	20.118	30.604	21.477
Sm	0.8471	4.509	8.621	4.009	5.091	3.769	4.029	5.709	4.447
Eu	0.671	1.267	2.292	0.901	1.293	1.444	1.036	1.390	1.078
Gd	n.d.[c]	4.74	6.20	3.25	4.45	3.85	3.67	n.d.	n.d.
Dy	1.04	4.96	4.31	2.66	4.32	3.68	3.37	3.91	3.81
Er	0.69	2.87	2.20	1.60	2.51	1.97	1.98	2.14	2.19
Yb	0.65	2.46	1.97	1.75	2.41	1.70	1.91	2.07	2.07
Lu	0.097	0.35	0.29	n.d.	n.d.	0.27	0.31	n.d.	n.d.
$(^{87}Sr/^{86}Sr)_o$	0.70416	0.70448	0.70420	0.70469	0.70506	0.70492	0.70513	0.70460	0.70576
εSr	+2.1	+6.7	+3.1	+9.7	+14.9	+12.9	+16.2	+8.5	+25.1
$(^{143}Nd/^{144}Nd)_o$	0.512209	0.512201	0.512225	0.512203	0.512161	0.512202	0.512147	0.512191	0.512023
εNd	+1.9	+1.8	+2.2	+1.8	+1.0	+1.8	+0.8	+1.6	-1.8

Table 2.1. Representative geochemical analysis of the Priestlaw And Cockburn Law plutons.

a Plw: Priestlaw
Clw: Cockburn Law

b N: norite
D: diorite
Gd: granodiorite
pGd: porphyritic granodiorite
Pmd: pyroxene-micadiorite

c n.d.: not determined

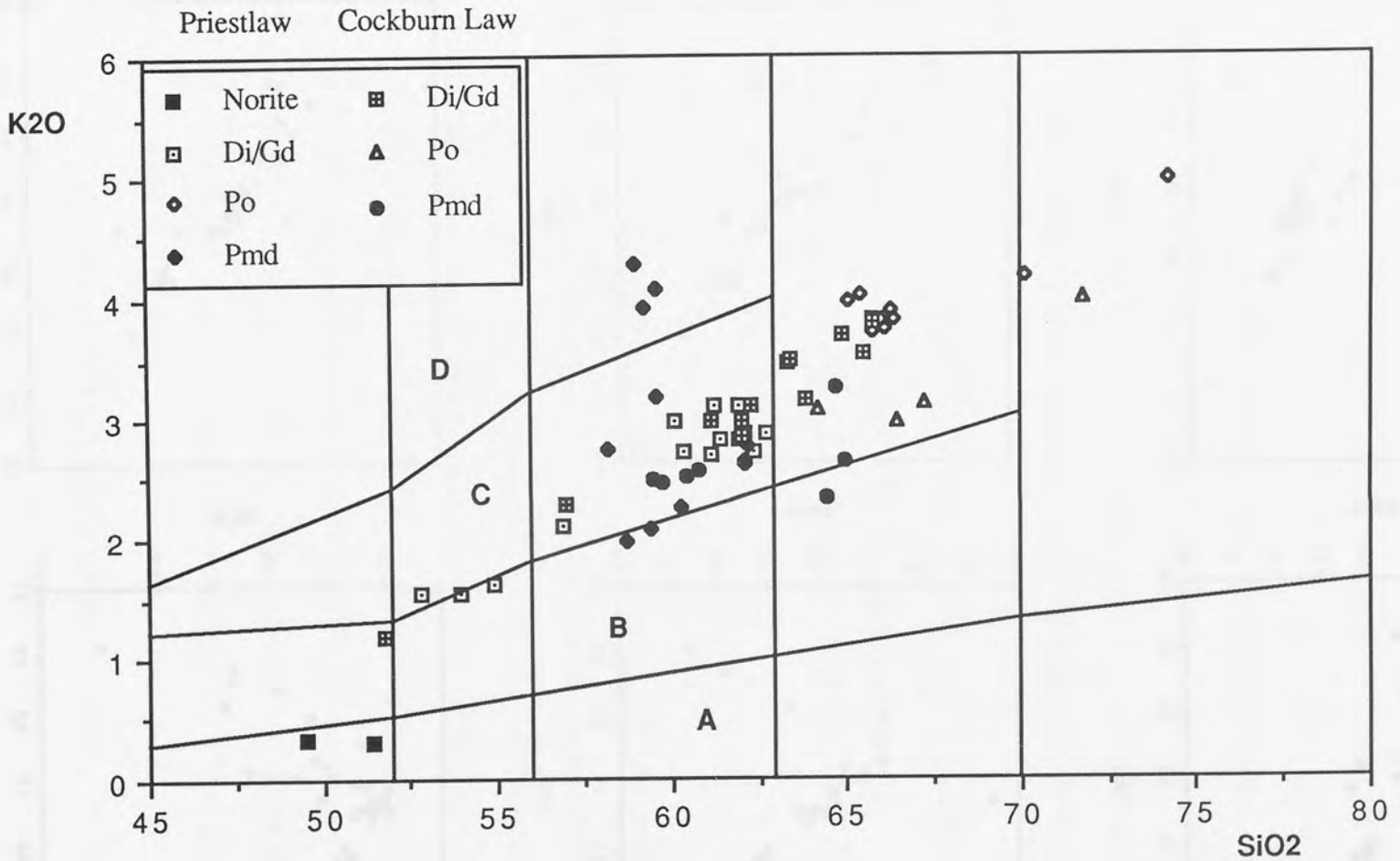

Figure 2.4 K_20-SiO_2 diagram for Priestlaw and Cockburn Law. Legend symbols: Norite: olivine norite; Di/Gd: hornblende diorite and granodiorite; Po: porphyritic granodiorite and granite; Pmd: pyroxene-mica diorite. Fields for calc-alkaline rocks after Peccerillo & Taylor (1976): A: arc-tholeiite series; B: calc-alkaline series; C: high-K calc-alkaline series; D: shoshonite series.

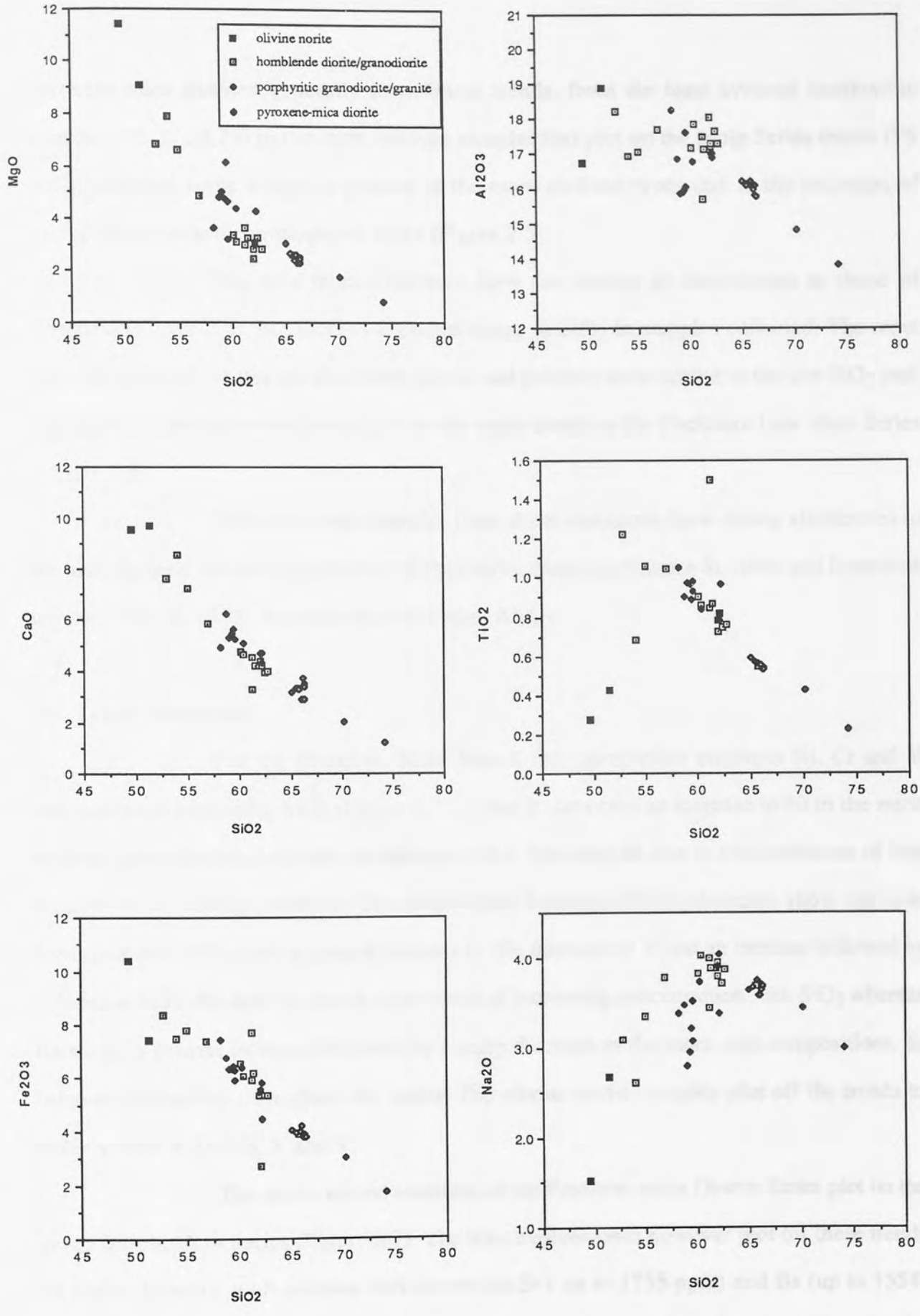

Figure 2.5 Selected major element Harker diagrams for Priestlaw.

pyroxene-mica diorites generally form linear trends, from the least evolved shoshonitic varieties (PS 27,28,29) to the more evolved samples that plot on the Main Series trends (PS 30G), although some scatter is present in the more evolved types due to the inclusion of altered xenoliths and cumulophyric rocks (Figure 2.5).

The data from Cockburn Law are similar in abundances to those of Priestlaw (Figure 2.6), but there is a smaller range in SiO_2 in samples collected. The most basic hornblende diorites are also more altered and produce some scatter at the low SiO_2 end. The pyroxene-mica diorites here all lie on the same trends as the Cockburn Law Main Series (Figure 2.6).

The most basic samples from these intrusions have strong similarities to the least evolved members (andesites) of the nearby contemporaneous St. Abbs and Eyemouth lavas (Thirlwall, 1979), but have slightly higher Al_2O_3.

(b) Trace elements

For the Priestlaw Main Series, the compatible elements Ni, Cr and V decrease with increasing SiO_2 (Figure 2.7). There is however an increase in Ni in the most evolved granodiorites, but with no increase in Cr. This may be due to contamination of low Ni acid rocks during crushing. The High Field Strength (HFS) elements show variable behaviour with SiO_2; with a general increase in Nb, decrease in Y and an increase followed by a decrease in Zr. Rb and Th plot as clear trends of increasing concentration with SiO_2 whereas Ba shows a general increase followed by a sharp decrease in the more acid compositions. Sr behaves compatibly throughout the series. The olivine norites notably plot off the trends to lower values of Zr, Nb, Y and V.

The most evolved members of the Pyroxene-mica Diorite Series plot on the trends for the Main Series (Figure 2.7). The least evolved ones however plot off these trends for some elements: with extreme enrichments in Sr (up to 1755 ppm) and Ba (up to 1554) and to a lesser degree Zr at similar SiO_2. Ni and Cr are also slightly higher in the pyroxene-mica diorites, with the highest values in the xenoliths of these. The two samples

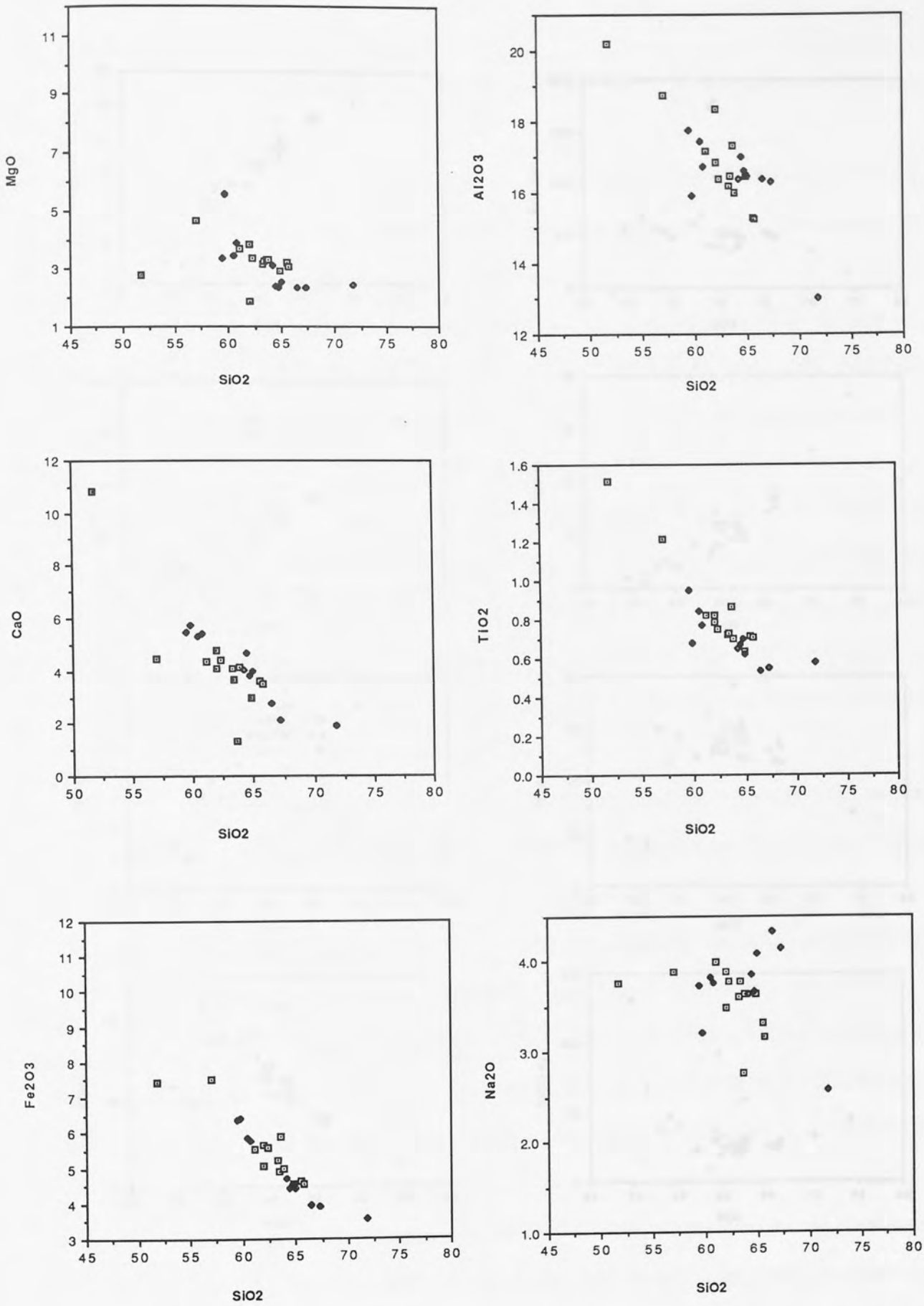

Figure 2.6 Selected major element Harker diagrams for Cockburn Law. Symbols as in Figure 2.5

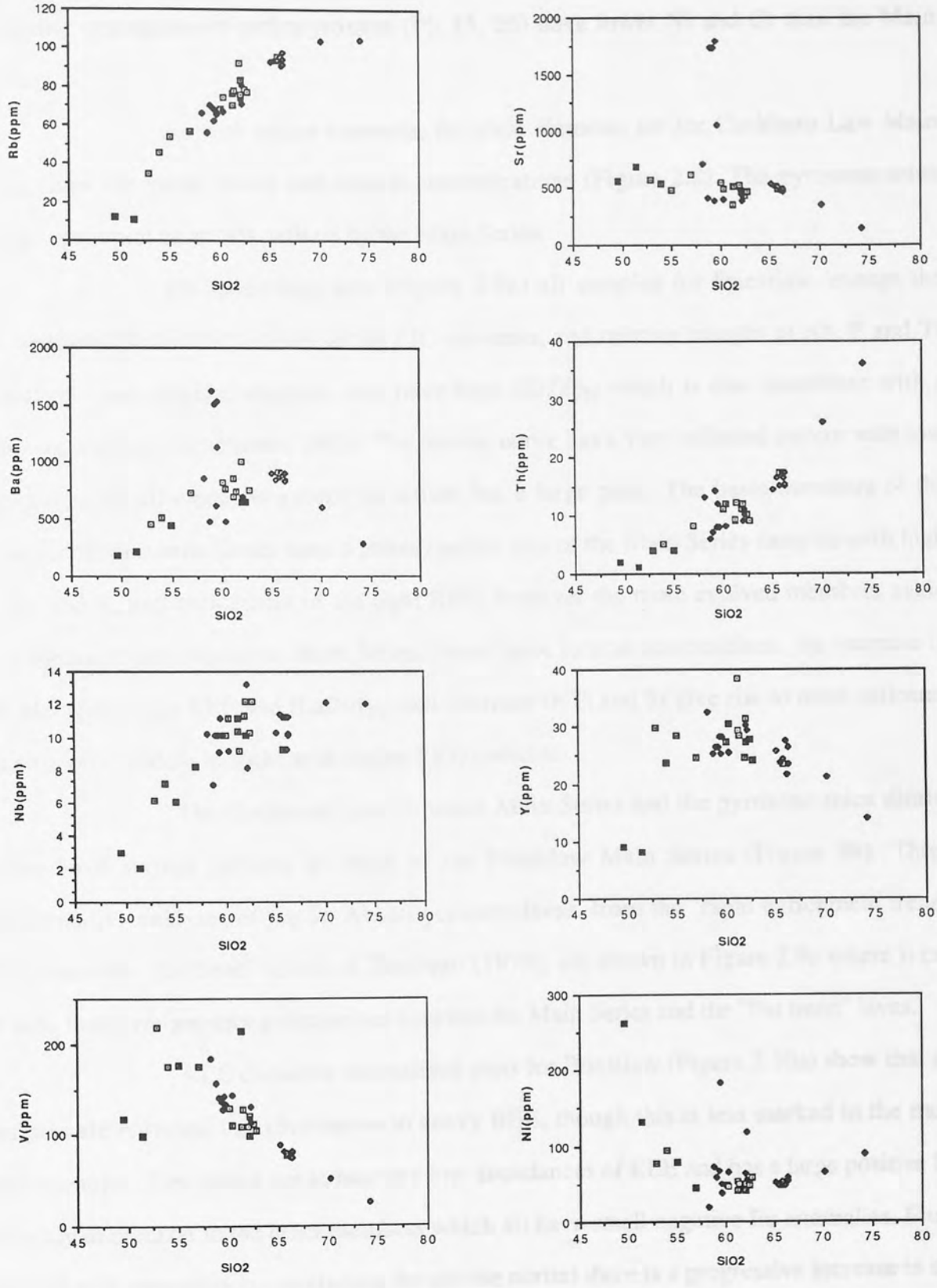

Figure 2.7 Selected trace element Harker diagrams for Priestlaw. Symbols as in Figure 2.5.

containing aggregates of orthopyroxene (PS 25, 26) have lower Ni and Cr than the Main Series.

As with major elements, the trace elements for the Cockburn Law Main Series show the same trends and similar concentrations (Figure 2.8). The pyroxene-mica diorites again plot on trends defined by the Main Series.

On spiderdiagrams (Figure 2.9a) all samples for Priestlaw, except the olivine norite, have enrichments in the LIL elements, and relative troughs at Nb, P and Ti typical of calc-alkaline magmas, and have high $(Zr/Y)_N$ which is also consistent with a continental arc setting (Pearce, 1983). The olivine norite has a very inflected pattern with low abundances of all elements except Sr, which has a large peak. The basic members of the pyroxene-mica diorite Series have a pattern unlike any of the Main Series samples with high Sr, Ba and K, and enrichment of the light REE; however the more evolved members again have identical patterns to the Main Series. From basic to acid compositions, the increase in LIL elements, light REE and $(La/Nd)_N$, and decrease in Ti and Sr give rise to more inflected patterns very evident in rocks with higher SiO_2 contents.

The Cockburn Law intrusion Main Series and the pyroxene-mica diorite Series have similar patterns to those of the Priestlaw Main Series (Figure 9b). Three representative analyses of the St. Abbs/Eyemouth lavas, from the "rapid enrichment trend" (SA1) and the "flat trend" (SA5) of Thirlwall (1979), are shown in Figure 2.9c where it can be seen that there are strong similarities between the Main Series and the "flat trend" lavas.

REE chondrite normalised plots for Priestlaw (Figure 2.10a) show that all samples are enriched in light relative to heavy REE, though this is less marked in the most basic samples. The olivine norite has very low abundances of REE and has a large positive Eu anomaly in contrast to the other members which all have small negative Eu anomalies. From basic to acid compositions (excluding the olivine norite) there is a progressive increase in the light REE, La and Ce; a decrease in the heavy REE, Gd-Lu; and an increase followed by a decrease in the middle REE, Nd-Eu. The basic pyroxene-mica diorites have the greatest enrichment in light REE and have no Eu anomaly, whereas the evolved pyroxene-mica

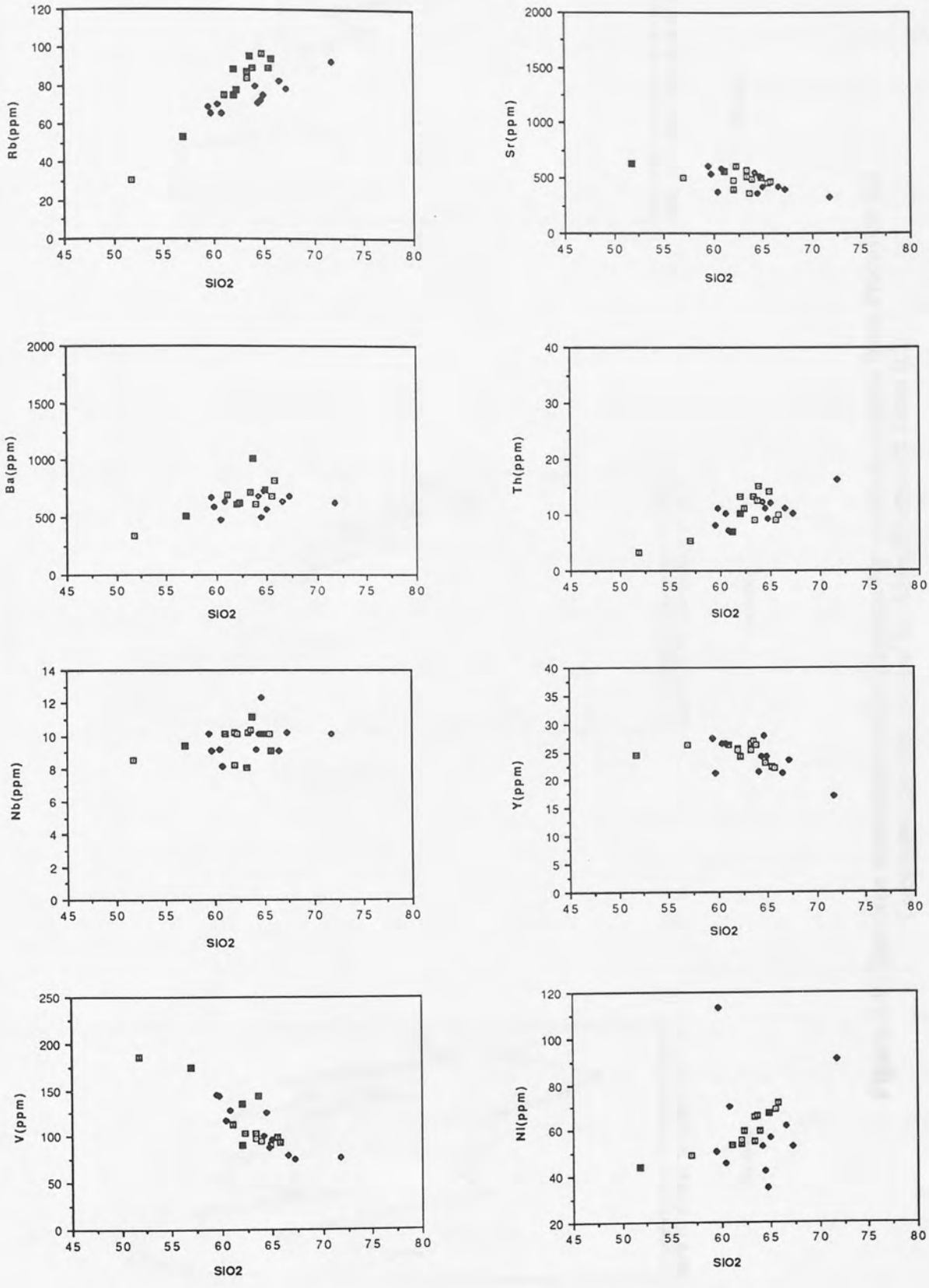

Figure 2.8 Selected trace element Harker diagrams for Cockburn Law. Symbols as in Figure 2.5.

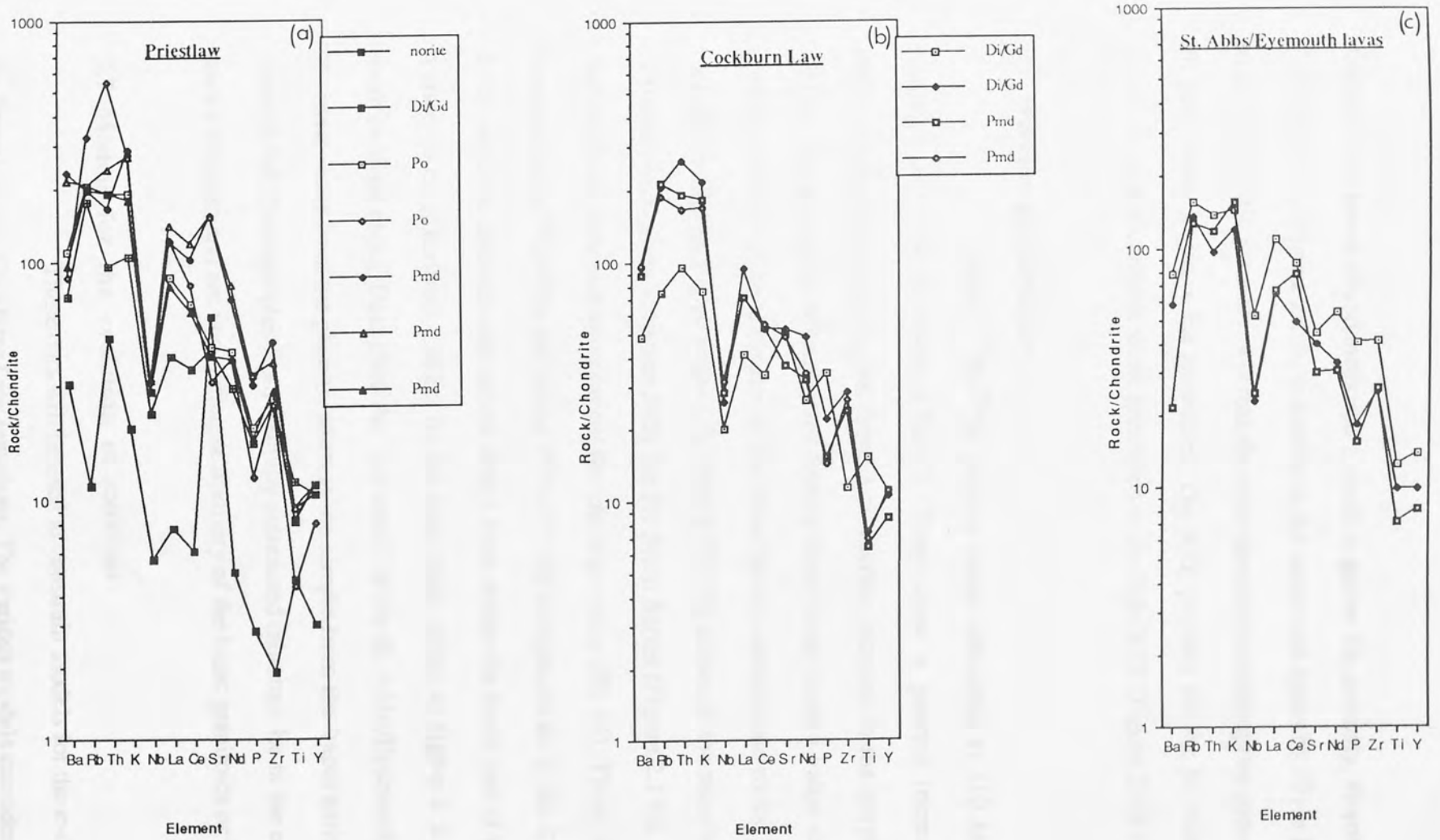

Figure 2.9 Chondrite normalised spiderdiagrams for selected samples from Priestlaw (a), Cockburn Law (b) and the St. Abbs/Eyemouth lavas (c).

diorites have lower abundances and a small negative Eu anomaly. Hornblende diorite from Cockburn Law (Figure 2.10b) is similar to the same rock type (PS 17) at Priestlaw, but has a small positive Eu anomaly, whereas the other samples (including two pyroxene-mica diorites) all have small negative Eu anomalies. The REE profiles for the St. Abbs/Eyemouth lavas show similar enrichments to the granitoids in the light REE (Figure 2.10c).

(c) Isotope geochemistry

Initial $^{87}Sr/^{86}Sr$ isotope ratios calculated at 410 Ma for the Priestlaw intrusion are low (0.70416-0.70517). They show a general increase from basic to intermediate compositions, but there is no further increase in the porphyritic unit (Figure 2.11a). The pyroxene-mica diorites form a linear array from a value similar to that of the olivine norite up to ones similar to the Main Series intermediate rocks. The Cockburn Law rocks have slightly higher values (0.70460-0.70578), although the most basic sample (PS 82) is altered, increasing at higher SiO_2 for the Main Series (Figure 2.11b). The pyroxene-mica diorites show little variation except for one high value (PS 99). There is a good correlation between initial $^{87}Sr/^{86}Sr$ and initial $^{143}Nd/^{144}$ Nd isotopes on an ε Nd- ε Sr diagram (Figure 2.12), with the data defining narrow arrays from within the lower part of the field for Midland Valley lavas (Thirlwall, 1982a) for the more basic rocks, to higher ε Sr and lower ε Nd in more evolved rocks. Data from the "flat trend" of the St. Abbs/Eyemouth lavas are similar to the basic rocks from the plutons, whereas the sample from the "rapid enrichment trend" plot to lower ε Nd. Two samples from spatially associated minettes lie in the enriched quadrant on such a diagram and are very different from any of the basic granitoids or lavas (Figure 2.12).

2.7 Models for the evolution of zonation

These data will be used to constrain models for the evolution of zonation in the Priestlaw and Cockburn Law intrusions. The various models considered are:

(1) Soret effect diffusion leading to compositional gradients within the melt.

(2) Mass removal in a volatile phase.

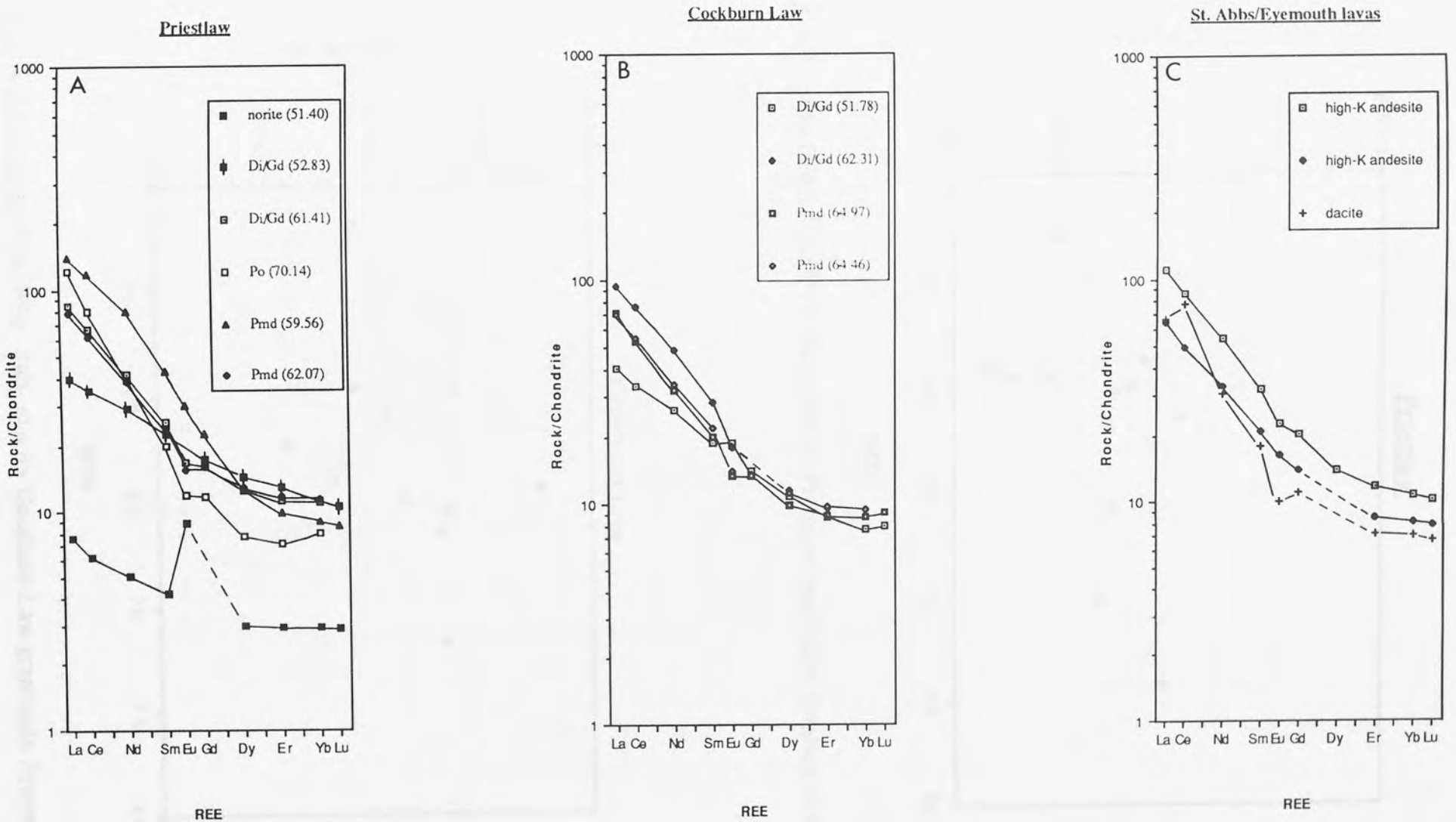

Figure 2.10 Chondrite normalised REE diagrams for Priestlaw (A), Cockburn Law (B) and the St. Abbs/Eyemouth lavas (C). SiO_2 contents of the granitoids are given in brackets in the legends.

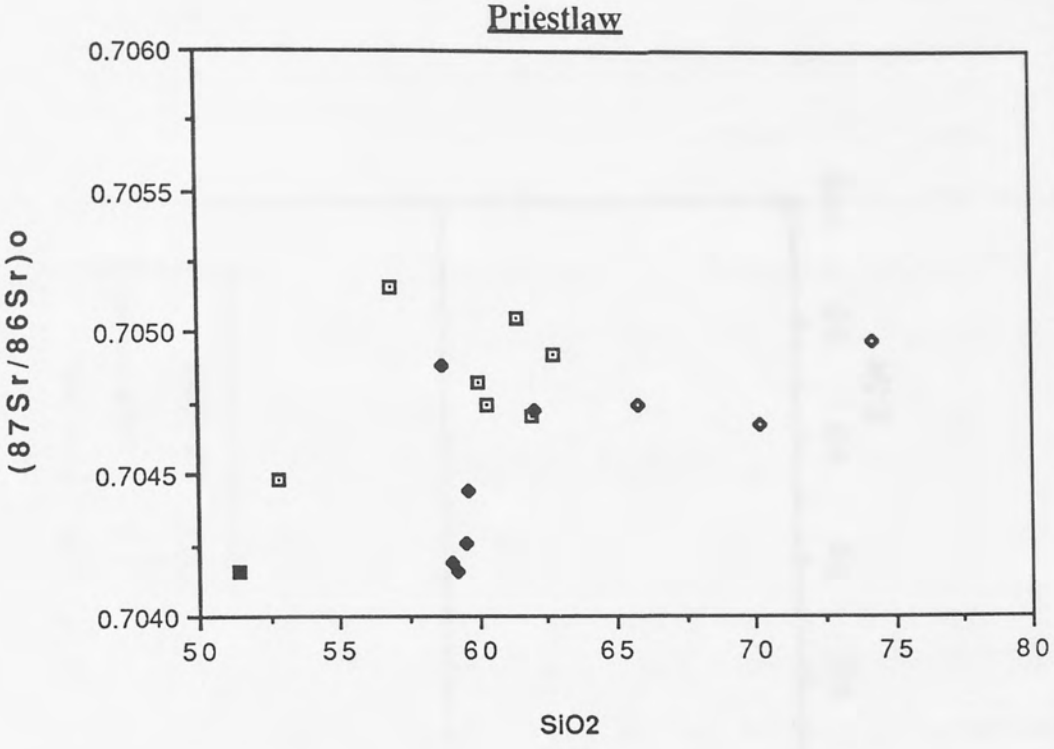

Figure 2.11a Initial $^{87}Sr/^{86}Sr$ - SiO_2 plot for Priestlaw granitoids. Symbols as in Figure 2.5.

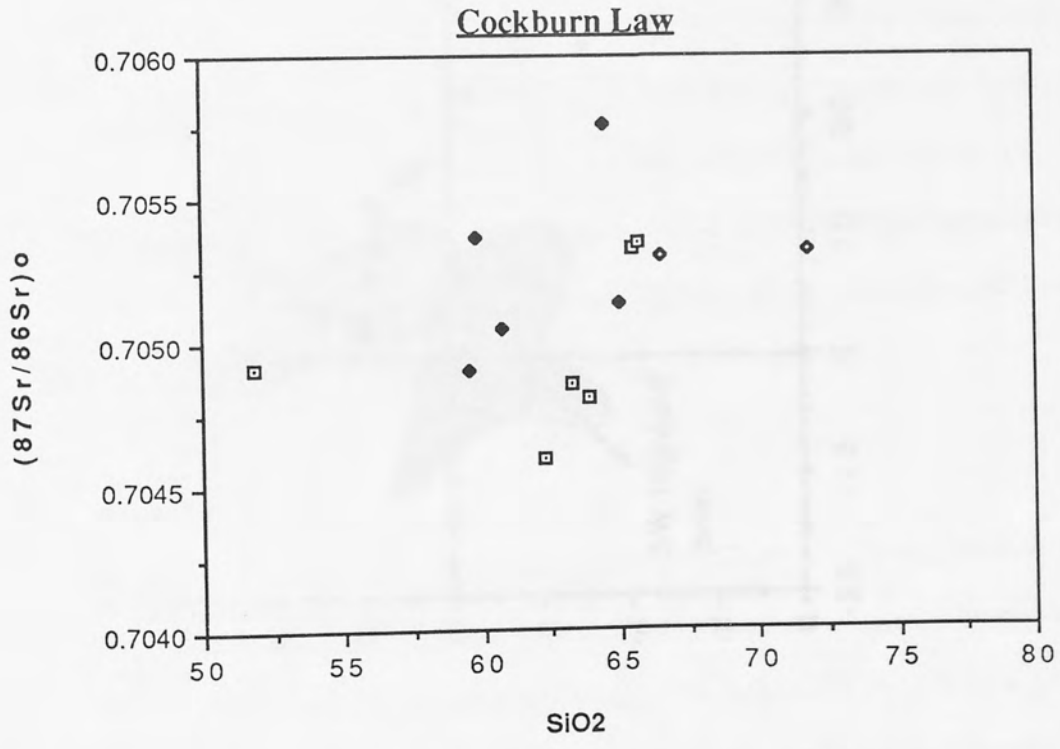

Figure 2.11b Initial $^{87}Sr/^{86}Sr$ - SiO_2 plot for Cockburn Law granitoids. Symbols as in Figure 2.5.

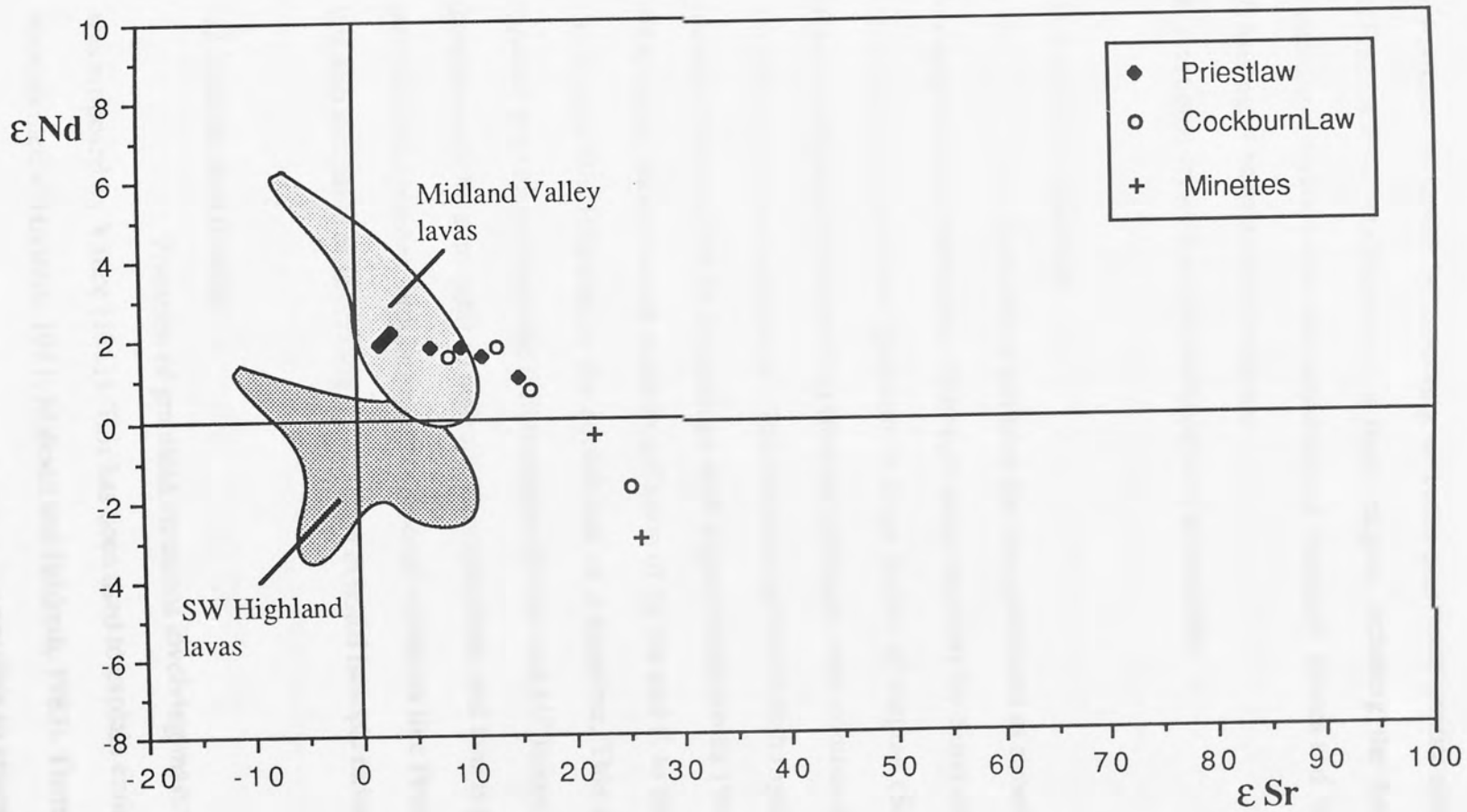

Figure 2.12 ε Nd - ε Sr diagram showing the Priestlaw and Cockburn Law granitoids and minettes of the eastern Southern Uplands. The fields for the Midland Valley and SW Highland lavas (Thirlwall, 1982a) are shown for comparison.

(3) Contamination of a single magma by assimilation of wall rocks.

(4) Intrusion of compositionally distinct magmas with possible hybridisation.

(5) Intrusion followed by unmixing of a melt plus restite (restite unmixing model).

(6) Fractional crystallisation of a basic magma, including the formation of marginal cumulates and/or incomplete separation of "cumulus" phases and "liquid".

(7) Mixing of basic and acid magmas.

(8) Fractional crystallisation combined with assimilation.

(1) Soret-effect diffusion

Soret-effect diffusion has been postulated as a mechanism that can give rise to compositional variations. Although mass transport by Soret diffusion cannot develop significant compositional gradients in large bodies of magma (Schott, 1983), significant effects could occur if Soret-effect (thermal diffusion) were combined with convection to give "thermogravitational separation". This has been applied to both rhyolites (Hildreth, 1981) and granites (Whalen, 1983). By analogy with experimental results (Walker and DeLong, 1982, 1984) such a model would result in diffusion of Si, Na and K to the hotter side and Fe, Mg, Ca, Ti and Mn diffusion to the cooler side of a chamber. This is the reverse of what is required to explain magmatic differentiation (Baker and McBirney, 1985). The process may therefore only be applicable to high silica compositions, and thus is probably unimportant as a mechanism in plutons with large compositional variations like Priestlaw and Cockburn Law. It is also incapable of generating the variation in initial isotopic ratios.

(2) Volatile mass transfer

Zonation of granitoid intrusions involving mass transfer in a volatile phase was proposed by Vance (1961). This has been used to explain enrichments in highly charged trace elements (Hildreth, 1981; Mahood and Hildreth, 1983). There is little experimental data available in support of this process, thus it is not possible to assess its applicability properly, and it has been rejected in favour of ordinary fractionation by Baker and McBirney (1985),

because ordinary fractionation can also explain the variation in data.

Loss of alkalis in a volatile phase may drive the magma to peraluminous compositions (Clarke, 1981; Goad and Cerny, 1981), however although there is a change from metaluminous to peraluminous compositions in rocks in both Priestlaw and Cockburn Law, K_2O increases linearly throughout the silica range. The decrease in Na_2O and the change from metaluminous to peraluminous compositions can be explained by processes such as plagioclase and hornblende fractionation. Evidence for vapour saturation is minor and only occur as some miarolitic cavities (no pegmatites are found) in the centre of the porphyritic unit of Priestlaw (PS60). Volatile loss cannot explain the good correlations between some elements and the general correlations of isotopic parameters with indices of fractionation. Its influence is thus considered to be minimal even for the most evolved compositions.

(3) Contamination by assimilation of wall rocks

Models for the zonation of some Californian batholiths by assimilation of pelitic wall rocks have been proposed by White *et al.* (1986) and Ague and Brimhall (1987). Evidence for wall rock assimilation of metasedimentary rocks is also presented by Meucke and Clarke (1981) and Clarke and Meucke (1985) for the South Mountain batholith.

Textures of xenoliths from plutons in the Southern Uplands show that partial melting has occurred, leaving plagioclase and biotite as refractory phases (Tindle and Pearce, 1983). Due to the refractory nature of several phases it is unlikely that complete assimilation would take place, and xenoliths in various stages of digestion should therefore be present. The rarity of xenoliths in the margins of the Priestlaw and Cockburn Law intrusions implies that assimilation is a minor process. Although sediments are hornfelsed at the margins of both intrusions (PS 30S, 35), there is no evidence for partial melting. Two sedimentary rocks taken from near the margin of Priestlaw have initial strontium ratios greater than 0.712, whereas the marginal igneous rocks of the intrusion commonly have the lowest ratios, and there is an increase towards more acid compositions towards the centres of plutons. A pyroxene-mica diorite (PS 99) from Cockburn Law however has a relatively high Sr initial

ratio of 0.70578. This sample, from close to the margin, has small, biotite-rich inclusions which may represent partially digested sedimentary xenoliths. Contamination through the roof of a chamber into the core of the pluton, cannot account for the rarity of xenoliths or the gradational nature of the two intrusions. *In situ* assimilation of local country rocks therefore appears not to be a dominant process in the evolution of the plutons, and as argued by Stephens *et al.* (1985) it would require considerable energy for a large amount of melting of low grade, prehnite-pumpellyite facies metasediments (Oliver and Leggett, 1980).

(4) Intrusion of compositionally distinct magmas

Some features of the Priestlaw and Cockburn Law intrusions are suggestive of separate pulses of magma implying that the zonation was not produced *in situ*.. These features include the discontinuous nature of the outer zones, the large chemical variation over such small (1km) areas, and the observed sharp contacts between the Main Series and the pyroxene-mica diorites. These imply that separate pulses of magma have been involved, however it does not necessarily follow that the pulses are unrelated. The fact that the Main Series rocks from both plutons show continuous variation and good trends from basic to acid compositions for both major and trace elements, does suggest these are closely related. The most basic pyroxene-mica diorites however have large differences in the concentrations of Ba, Sr, K_2O, P_2O_5 and Zr compared with the Main Series, and it would appear likely that these represent a distinct magma. It is unlikely that these diorites can be related through any kind of crystallisation history to the Main Series but two hypothetical possibilities exist:

(a) The basic pyroxene-mica diorites are parental to the Main Series rocks giving rise to SiO_2-poor marginal rocks (i.e. which represent cumulates) and SiO_2-rich compositions (liquids) in the interior of the pluton. If this were the case then it would be expected that the parental magma would have concentrations of elements intermediate between the basic and acid rock types, which is clearly not seen. Since the basic Main Series rocks are dominated by plagioclase, the Sr concentrations in the proposed cumulate rocks should be higher than or similar to the parental liquid since D_{Sr} is usually >2 for plagioclase. The pyroxene-mica

diorites are however much more enriched in Sr than the basic marginal rocks. Since the basic marginal rocks are depleted in incompatible elements (including LREE) relative to the pyroxene-mica diorites, the more evolved rocks should show correspondingly higher values, and again this is not seen: the basic pyroxene-mica diorites are more enriched in incompatible elements than all of the Main Series rocks. It is untenable therefore that the basic pyroxene-mica diorites are parental to the Main Series rocks in the intrusion.

(b) Fractional crystallisation of a basic magma similar to that which produced the Main Series basic rocks, to produce the pyroxene-mica diorites. This is possibly an important process for the intermediate rocks of the Main Series (discussed later; model 6) but is unlikely for the basic pyroxene-mica diorites. The bulk distribution coefficients for Sr and Ba would have to be very low to produce the large enrichments in these elements. This could be achieved if all of the fractionating phases had low partition coefficients such as olivine, pyroxenes or spinel, and the magma had undergone extensive fractionation of these minerals. Such fractionation would however produce large depletions in the structural components and trace elements of these minerals (such as MgO, CaO, TiO_2, Ni, V etc.) in the pyroxene-mica diorites. The pyroxene-mica diorites have similar to slightly greater contents for these elements and elements of basic association than the Main Series, thus the pyroxene-mica diorites cannot be produced from the same magma as that which gave rise to the Main Series rocks.

The most basic (shoshonitic) pyroxene-mica diorites thus appear to represent a compositionally distinct magma unrelated to that of the Main Series by any process of fractional crystallisation. The more evolved members of the Pyroxene-mica Diorite Series do however plot on the Main Series trends and may be more closely related. The fact that the most basic pyroxene-mica diorites and the marginal olivine norite have identical initial $^{87}Sr/^{86}Sr$ and very similar $^{143}Nd/^{144}Nd$ ratios is suggestive of these having a similar source perhaps being formed by different degrees of partial melting. The enrichment in incompatible elements (including the LREE and higher La/Yb) of the basic pyroxene-mica diorites relative to the Main Series, fits a derivation from a magma produced by smaller degrees of partial

melting than the Main Series magma. The Priestlaw and Cockburn Law intrusions are composite, and for each, the Main Series rocks probably formed by a single similar process. However, the basic pyroxene-mica diorites of Priestlaw constitute a compositionally distinct magma. The relationship between the more evolved pyroxene-mica diorites to the Main Series will be discussed in model (7).

(5) Restite unmixing

A restite unmixing model has been proposed to account for compositional variations in granitoid suites of eastern Australia (White and Chappell, 1977) and in the Scottish Caledonides (Chappell & Stephens, 1988). In this model geochemical and petrological variation is produced by the progressive unmixing of restite (unmelted solid residue) from felsic minimum melt as both rise from the source area. This model apparently explains the common occurrence of linear trends for major and trace elements on Harker diagrams. The restite component is represented by mafic inclusions (enclaves), mafic "clots" and individual crystals e.g. complexly zoned plagioclase and pyroxene cores to amphibole. There is considerable debate on the role of restite unmixing in granitoid plutons as both the linear trends on Harker diagrams and mafic enclaves are also considered compatible with fractional crystallisation and mixing of magmas (Vernon, 1983; Wall *et al.* 1987).

The non-linear trends for several major and trace elements on Harker diagrams for Priestlaw and Cockburn Law (Figures 2.5-2.8), are not compatible with restite unmixing as a major process in these plutons. Although linear trends may be slightly modified by other processes, it is difficult to see how non-linear trends, such as those shown by Na_2O, Zr and Ba, where there is an increase in concentration followed by a decrease, could be achieved by restite unmixing. The dominance of the euhedral to subhedral shapes of phases found in both intrusions is also difficult to reconcile with the anticipated anhedral shapes of restite phases more typical of the relatively high temperature and pressure regime in which the magma first formed. Mafic clots, consisting of orthopyroxene and calcic-plagioclase, occur in one sample of the pyroxene-mica diorite from Priestlaw. They are identical petrographically to

individual phenocrysts and both display euhedral shapes thus they are interpreted as cognate inclusions. Fine-grained and dark-coloured round to ovoid enclaves occur at one locality in the Cockburn Law intrusion. They are composed of clino- and orthopyroxene, plagioclase and K-feldspar, are much finer grained than the enclosing hornblende granodiorite, have almost identical major and trace element compositions to their host, and may represent a quenched portion of the host granodiorite. Initial Sr isotopic ratios of the enclaves (PS 85b) are the same as the host granodiorite (PS 85) and associated felsic patches (PS 85f), though this could be explained by the re-equilibration of the Sr isotopes as has been shown for enclaves in the Criffell pluton of south west Scotland (Holden *et al.* 1987). The coherence and variation in isotopic signatures with fractionation would also be difficult to explain by the restite model. From the above the evidence in favour of restite separation in Priestlaw and Cockburn Law would therefore appear to be minimal on both petrological and geochemical grounds.

(6) Fractional crystallisation of a basic magma.

Fractional crystallisation of a basic magma is the basis of models for the zonation of the contemporaneous Loch Doon (Tindle and Pearce, 1981) and Cairnsmore of Carsphairn (Tindle *et al.* 1988) plutons which lie along strike to the south west of the Priestlaw and Cockburn Law intrusions (Figure 2.1). Major and trace element data have been used to suggest *in situ* fractional crystallisation of a dioritic parent for Loch Doon and successive intrusion of a fractionating dioritic magma for Cairnsmore of Carsphairn. Fractional crystallisation is also applied for the normally zoned Tuolumne Intrusive Series of the Sierra Nevada batholith (Bateman and Chappell, 1979). Frey *et al.* (1978) from REE data for the same series, also suggested a fractional crystallisation history, particularly of amphibole. The possibility of granites being mixtures of "cumulus" phases and interstitial melt was discussed by McCarthy and Hasty (1976). Although their work refers to granites (*sensu stricto*), where the magmas involved would be more viscous, cumulate formation may be an important process in any plutonic environment.

The pyroxene-mica diorites of Priestlaw show such large changes in the abundances of some trace elements (Sr, Ba) over such a low silica interval (Table 2.1), that a simple fractional crystallisation history is untenable. These will be discussed in more detail in the following section.

In each of the units of the Main Series rocks the variation of major and trace elements (Figures 2.5-2.8) is consistent with fractionation of the phases observed. Two of the complicating factors in modelling fractionation however are that; (1) the proportions of fractionating phases are continually changing and (2) the partition coefficients for trace elements vary in relation to liquid composition, in general being greater in more acid magmas (Hanson, 1978). The decline, particularly in the basic rocks, in MgO, Ni and Cr can be explained by the fractionation of olivine and the pyroxenes in the least evolved rocks followed by pyroxenes with amphibole and then dominated by amphibole. Evidence of the importance of amphibole is the general decrease in Y and middle-heavy REE from marginal hornblende diorites (e.g.PS17) to evolved granodiorites (e.g.PS60). Plagioclase is a dominant mineral in all rock types and the decrease in CaO, Al_2O_3 and Sr throughout the Series, and Na_2O and Ba in the later stages, is probably controlled dominantly by plagioclase fractionation. The similar linear decreases in TiO_2, Fe_2O_3 and V throughout the sequence are probably a response to fractionation of titano-magnetite as well as the mafic phases. Apatite and zircon control the later decreases in P_2O_5 and Zr respectively.

Trace elements have been particularly successful in semi-quantitative modelling of variation in magmas (Allegre and Minster, 1978, Hanson, 1978). It is necessary however to have a knowledge of the proportions of phases crystallising and the partition coefficients for trace elements in these phases. Because partition coefficients for trace elements vary due to changes in liquid composition, the partition coefficients used here refer to those of intermediate compositions as far as possible. The trace elements Ba, Rb and Sr occur mainly in the major silicate minerals, and not in the accessory phases, consequently they are particularly useful for modelling granitoids (McCarthy and Hasty, 1976).

Models for Ba-Rb and Sr-Rb in the Priestlaw Main Series are shown

(Figs.2.13a,b), assuming perfect Rayleigh fractionation of the phases which occur in the rocks in the following proportions: 60% plagioclase, 20% amphibole, 8% orthopyroxene, 4% clinopyroxene, 6% biotite and 2% titano-magnetite. The proportions are based on average estimates of the proportions in the least evolved samples. The assumption is made that the phases are crystallising out in constant proportions and that partition coefficients do not change, both of which are extremely unlikely. Modelling therefore is used to define general trends. Priestlaw has a general trend, from hornblende diorite to hornblende granodiorite with increasing Rb and Ba and decreasing Sr. This is consistent with the dominant control of plagioclase and hornblende during fractionation both of which are present in thin section. The porphyritic granodiorites and granite however have decreasing Ba and Sr at relatively constant Rb concentrations. Although the Rb concentrations show little variation, the most evolved samples depart from the Main Series trend to produce a flatter trend (Figure 2.7). This is unlikely to be related to volatile loss because it affects Rb only to a very minor extent and K not at all (Figure 2.5). It is therefore more likely that the changes result from the fractionation of minor amounts of biotite which is the only mineral with $K_{DRb} > 1$, and this also explains the decrease in Ba in these rocks. It is difficult to establish whether any parts of the intrusions represent pure liquids or mixtures of "cumulus" and interstitial liquid, since fine-grained, non-porphyritic chilled margins are not seen.

The coarse grain-size and texture of the olivine norite from Priestlaw, along with the fact that it lies off the trends for the rest of the Main Series on Harker diagrams and has extreme depletions of some trace elements (e.g. Zr 8ppm; Rb 10ppm), suggests that this may represent a cumulate. The very inflected spidergram pattern, low abundances of REE, large positive Eu anomaly and mineralogy are also consistent with the cumulate nature for this rock. The texture and geochemistry of the olivine norites thus support the idea that these represent cumulates. The fact that these do not plot on the model cumulate trend is to be expected because this sample contains a different mineral assemblage (i.e. olivine + pyroxenes + plagioclase) from that of the general model. Its cumulate character is still obvious from the graph however. The data from Cockburn Law define similar trends resembling those of

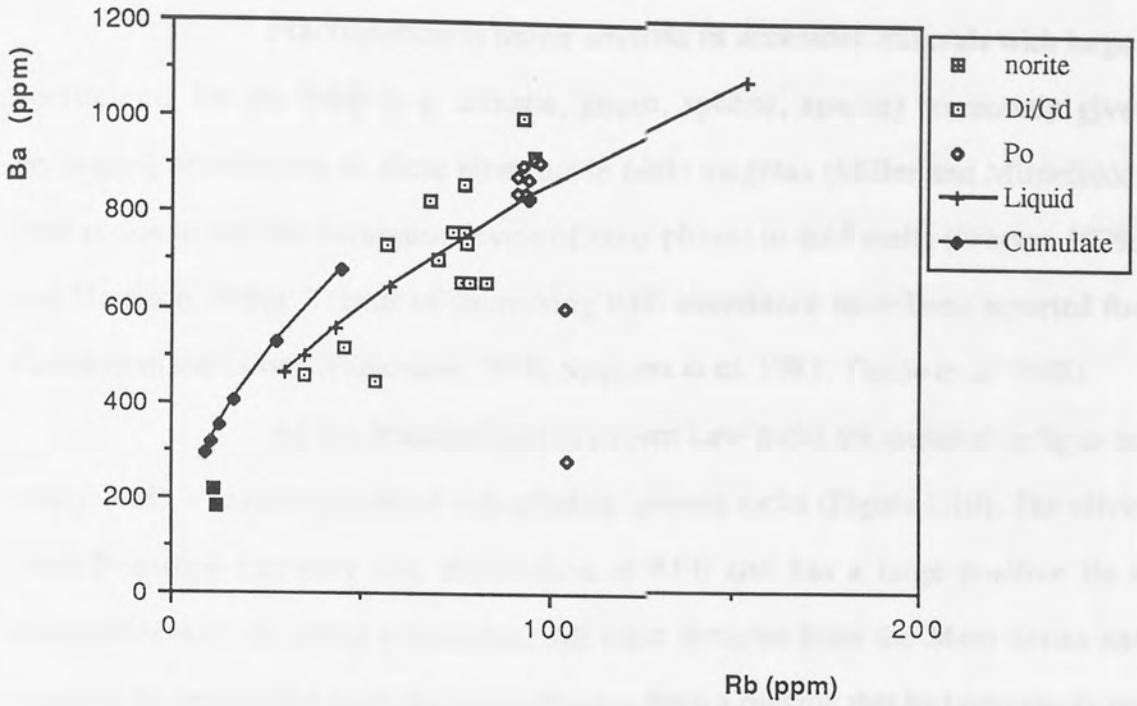

Figure 2.13a Ba-Rb diagram showing the trends of the Priestlaw Main Series and modelled trends. See text for discussion.

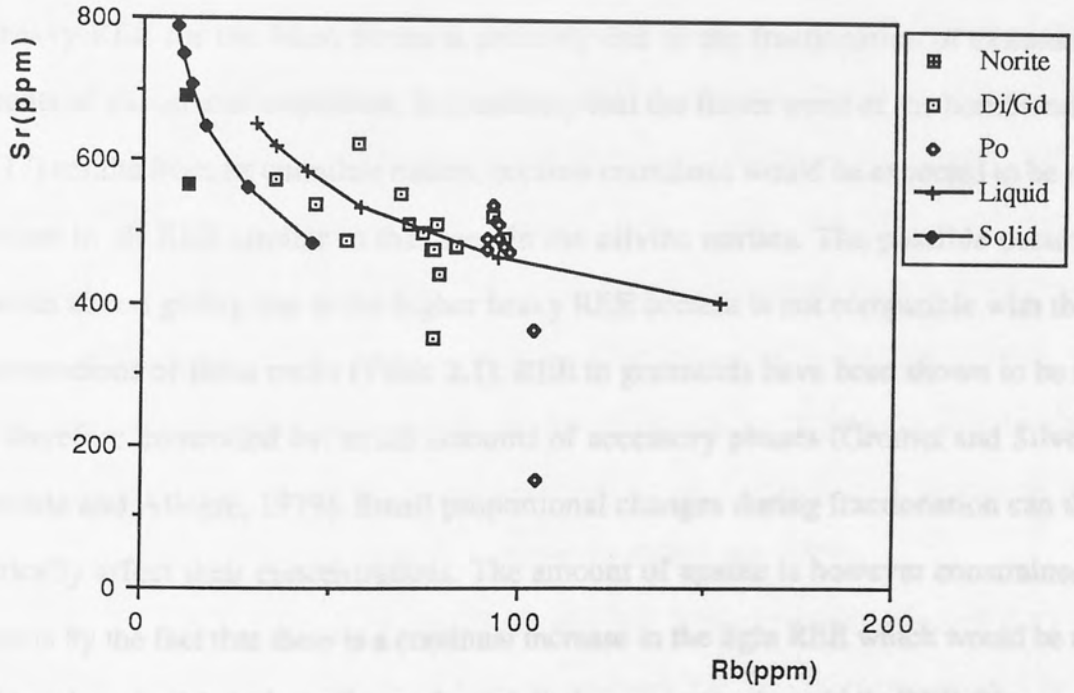

Figure 2.13b Sr-Rb diagram showing the trends of the Priestlaw Main Series and modelled trends. See text for discussion.

Priestlaw, and can be interpreted in a similar manner.

Fractionation of minor amounts of accessory minerals with large partition coefficients for the REE (e.g. allanite, zircon, sphene, apatite) commonly gives rise to decreasing abundances of these elements in felsic magmas (Miller and Mittlefehldt, 1982). This is due to the low saturation levels of these phases in acid melts (Watson 1979; Watson and Harrison 1984). Trends of decreasing REE abundance have been reported for several Caledonian intrusions (Pankhurst, 1979; Stephens *et al.* 1983; Tindle *et al.* 1988).

All the Priestlaw and Cockburn Law rocks are enriched in light- relative to heavy-REE, a feature typical of calc-alkaline igneous rocks (Figure 2.10). The olivine norite from Priestlaw has very low abundances of REE and has a large positive Eu anomaly compatible with its being a cumulate. All other samples from the Main Series have small negative Eu anomalies implying crystallisation from a magma that had previously undergone some plagioclase fractionation. The lack of a large negative Eu anomaly and the general decrease in the middle REE is expected because fractionation of amphibole preferentially incorporates the middle-heavy REE but less particularly Eu relative to the others. The pyroxenes also contribute to a positive Eu anomaly (Hanson, 1978). The slight decrease in the heavy REE for the Main Series is probably due to the fractionation of extremely small amounts of zircon and amphibole. It is unlikely that the flatter trend of the hornblende diorite (PS 17) results from its cumulate nature, because cumulates would be expected to be relatively depleted in all REE similar to that seen in the olivine norites. The possible occurrence of cumulus zircon giving rise to the higher heavy REE content is not compatible with the low Zr concentrations of these rocks (Table 2.1). REE in granitoids have been shown to be fixed in, and therefore controlled by, small amounts of accessory phases (Gromet and Silver, 1979; Fourcade and Allegre, 1979). Small proportional changes during fractionation can therefore drastically affect their concentrations. The amount of apatite is however constrained to low amounts by the fact that there is a continual increase in the light REE which would be removed by this mineral; although apatite preferentially incorporates the middle REE (Hanson, 1978), the partition coefficients are high for all REE. The general shapes of the REE patterns are

therefore also consistent with fractionation dominated by plagioclase and amphibole but necessitating small amounts of zircon and possibly apatite in the later stages of evolution.

Fractional crystallisation of a basic/intermediate magma appears therefore to be a viable model for the Main Series of both Priestlaw and Cockburn Law. Based on major and trace element data, the good trends and general abundances are compatible with a fractional crystallisation model involving the phases observed in the rocks. Although it would appear that fractional crystallisation has been an important process in the zonation of these plutons, closed system fractionation cannot explain the range and correlation of Sr and Nd isotopes. These isotopic signatures imply that some form of open system behaviour must have occurred during the evolution of the plutons.

(7) Mixing of basic and acid magmas

Magma mixing has been shown to be of widespread occurrence in calc-alkaline associations (Eichelberger and Gooley, 1977; Kay and Kay, 1983). Mixing of basic and acid magmas has been suggested to account for the continuous variation in Hercynian granitoids and enclaves (Cantagrel *et al.* 1984) and is considered to be an important mechanism in parts of the Sierra Nevada batholith (Reid *et al.* 1983; Kistler *et al.* 1986). Petrological evidence for magma mixing or mingling, such as xenocrysts or basic inclusions showing crenulated, chilled margins and vesiculated cores is commonly preserved in volcanic rocks (Cantagrel *et al.* 1984). In the plutonic environment, however, such petrological evidence may be obscured because of slow cooling and crystallisation rates. Geochemical data should however preserve evidence of mixing. Simple mixing is the classic cause of linear trends of major and trace elements on Harker diagrams. Isotopic data should also reveal pseudo-isochrons and mixing lines; and straight lines are the product of mixing on ratio-ratio plots, where each axis has the same denominator (MacCaskie, 1984).

The range of initial Sr and Nd isotopic ratios (Figure 2.12) in both Priestlaw and Cockburn Law show that the magmas cannot simply be related to a closed system. Because isotopic ratios are not affected by crystallisation processes, some form of

mixing or assimilation must have occurred. The non-linear trends for the Main Series rocks on Harker diagrams however support the fractional crystallisation process as discussed in the previous section. A scatter rather than a straight line is evident on Ba/Sr vs. Rb/Sr (Figure 2.14a) and $(^{87}Sr/^{86}Sr)_I$ vs. 1000/Sr (Figure 2.14b) plots for the Main Series, showing that simple mixing is not a tenable model for these. It would appear therefore that the evidence for fractional crystallisation and/or mixing must be combined in a more complex model for the Main Series, and will be discussed later.

The linear trends on Harker diagrams for the Priestlaw pyroxene-mica diorites are however indicative of mixing (Figures 2.5, 2.7), and some petrographic features e.g. the zones of pyroxene and biotite inclusions in plagioclase, are similar to those described for mixed magmas (Eichelberger and Gooley,1977; Vernon,1983). Ratio-ratio plots involving trace elements (Fig. 2.14a) and isotopic ratios (2.14b) with both axes having the same denominator, also have good linear correlations which supports mixing. Because the most evolved pyroxene-mica diorites all lie on the Main Series trends for both major and trace elements and for isotopes, it appears likely that one end member is an intermediate magma of the Main Series. The least evolved pyroxene-mica diorites represent a compositionally distinct magma having undergone a different degree of partial melting (of the same mantle) as the Main Series parent, as shown in model (4). It is more difficult to say whether any of the pyroxene mica diorites represent an end member, but the fact that they have similar isotopic compositions to the olivine norite and no Eu anomaly may suggest that they are isotopically close to the end member rather than representing a mixture. The pyroxene-mica diorites are probably a series of hybrids between a compositionally distinct magma (shoshonitic) and an intermediate magma of the Main Series.

(8) Assimilation-fractional crystallisation (AFC)

Description of the process of combined fractional crystallisation and assimilation extends as far back as the classic studies of Bowen (1928). More recently Taylor (1980) pointed out that heat balance considerations support the coupling of these two

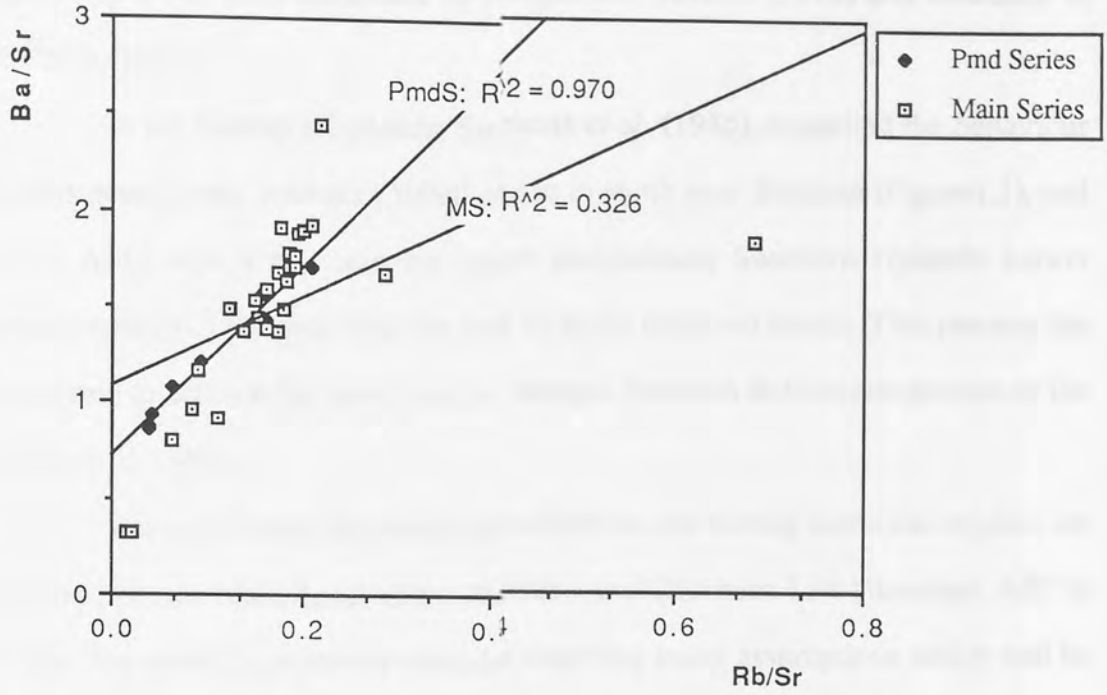

Figure 2.14a Ba/Sr-Rb/Sr diagram for the Priestlaw Main Series (MS) and Pyroxene-mica diorite Series (Pmd), showing the good linear trend in the Pyroxene-mica diorite Series.

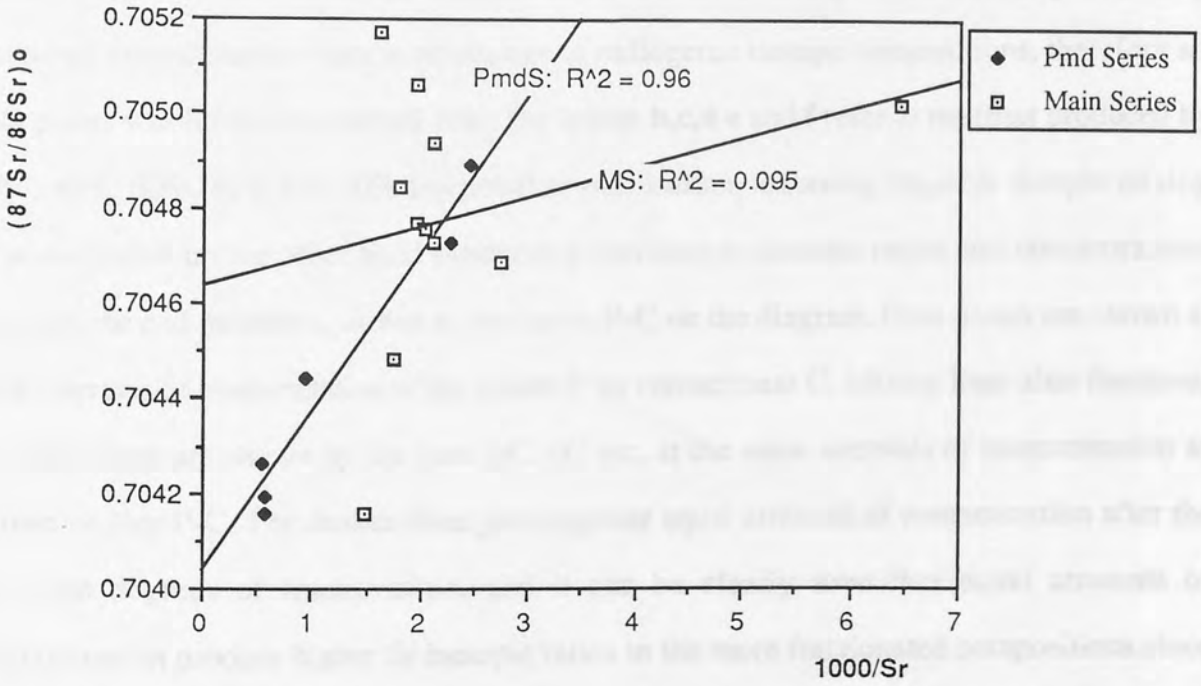

Figure 2.14b $^{87}Sr/^{86}Sr$-1000/Sr diagram for the Priestlaw Main Series (MS) and Pyroxene-mica diorite Series (Pmd), showing the good linear trend in the Pyroxene-mica diorite Series and scatter in the Main Series.

processes; with the latent heat of crystallisation providing the heat required for assimilation. Equations for this process were described by Allegre and Minster (1978) and modelled in detail by De Paolo (1981).

In the Southern Uplands, Stephens *et al.* (1985) modelled the behaviour of REE and Sr isotopes in the younger Criffell pluton in south west Scotland (Figure1.1), and concluded that AFC with a granodiorite parent assimilating Southern Uplands Lower Palaeozoic sediments (SULPS) provided the best fit to the observed trends. This process has also been suggested to account for the O and Sr isotopic variation in Miocene plutons of the Aegean (Altherr *et al.* 1988).

Because neither fractional crystallisation nor mixing alone can explain the geochemical data from the Main Series of the Priestlaw and Cockburn Law intrusions, AFC is considered here. The model is relatively complex requiring many assumptions which will be discussed after comparing AFC with fractional crystallisation and mixing.

Some of the differences between the fractional crystallisation and mixing models can be highlighted by $^{87}Sr/^{86}Sr$ vs. Sr diagram (Figure 2.15a). A parent magma (e.g. basalt) is represented by **P** on the diagram and a contaminant (e.g. upper crust) by **C**. During fractional crystallisation there is no change in radiogenic isotope compositions, therefore all data points will lie on a horizontal line. The letters **b,c,d e** and **f** refer to magmas produced by 20%, 40%, 60%, 80% and 90% fractional crystallisation, assuming D_{Sr}=1.6. Simple mixing or assimilation on the other hand produces a variation in isotopic ratios and concentrations between the end members, shown as the curve **P-C** on the diagram. Data points are shown at 20% intervals of contamination of the parent **P** by contaminant **C**. Mixing lines after fractional crystallisation are shown by the lines b**C**, c**C** etc. at the same intervals of contamination as shown on line **P-C**. The dashed lines join together equal amounts of contamination after the different degrees of fractionation, and it can be clearly seen that equal amounts of contamination produce higher Sr isotopic ratios in the more fractionated compositions since the Sr concentrations are much less relative to the contaminant. It is obvious therefore that if fractional crystallisation has occurred, the concentrations as well as the isotopic ratios have to

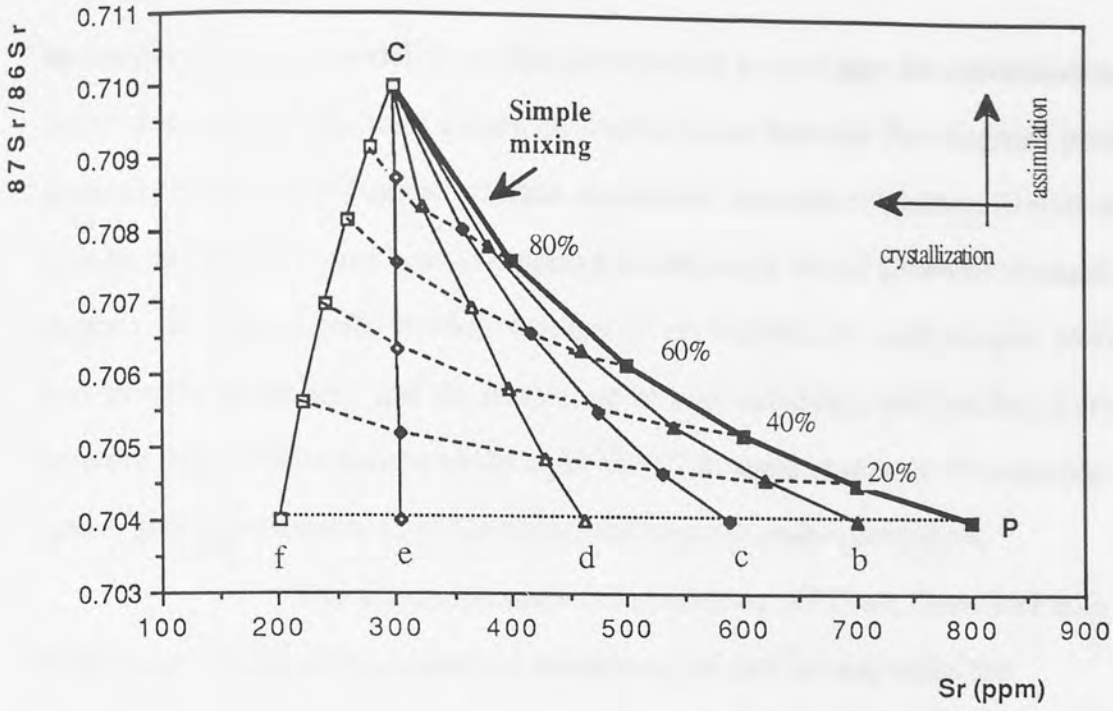

Figure 2.15a Initial $^{87}Sr/^{86}Sr$-Sr diagram showing simple mixing and fractional crystallisation trends. See text for discussion.

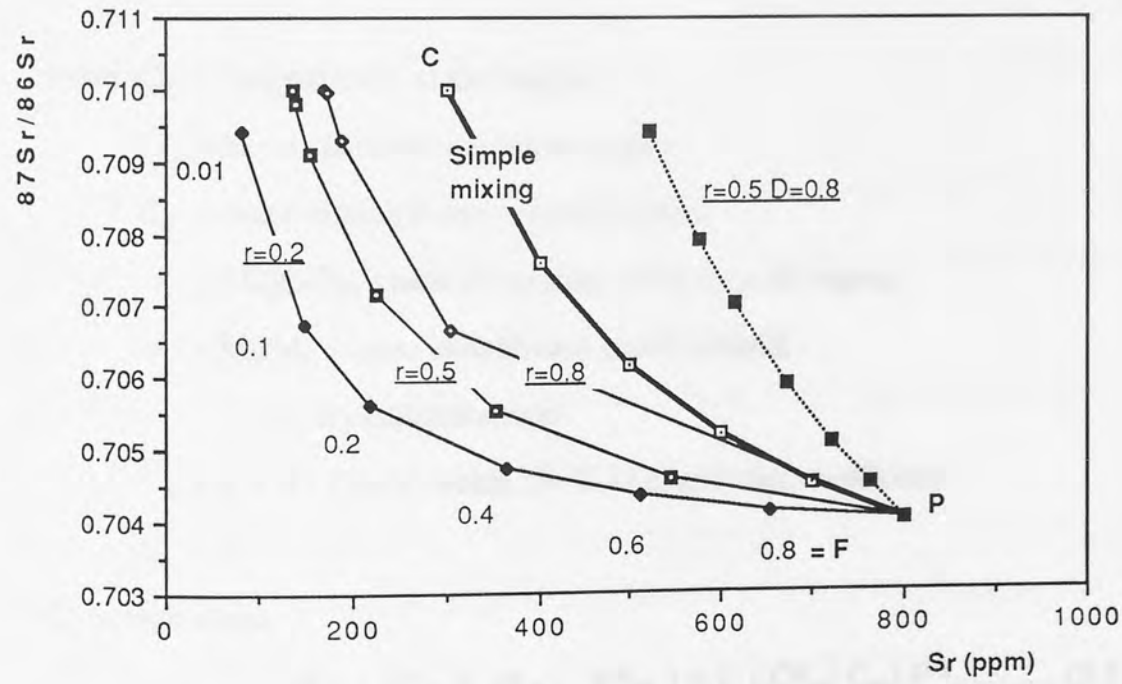

Figure 2.15b Initial $^{87}Sr/^{86}Sr$-Sr diagram showing simple mixing and assimilation-fractional crystallisation trends. See text for discussion.

be considered in any model. It is difficult however to envisage the contamination process as being important in the later stages of fractionation because the magmas produced would generally not be hot enough to promote substantial amounts of melting. Simple mixing would also be unlikely because heat lost during assimilation would promote crystallisation of the magma. In this simple model, fractional crystallisation and simple mixing are two end-member processes, and the likelihood of both occurring will produce curves or scatter between them. Points may lie to the right of **P-C** in some instances; for example in a situation where Sr is incompatible (D<1) or where the rocks represent cumulates.

The equations used for modelling AFC are from DePaolo (1981), and those used for calculating elemental concentrations and isotopic ratios are:

(1) concentrations:

$$C_m/C^o_m = F^{-z} + (r/r-1)\,[C_a/(z\,C^o_m)]\,(1- F^{-z}) \quad \text{.....(3.1)}$$

where C_m = concentration in the magma

C^o_m = initial concentration in the magma

C_a = concentration in assimilated wallrock

F = M_m/M^o_m = mass of magma/ initial mass of magma

r = M_a/M_c = mass assimilation rate/fractional crystallisation rate

z = $(r + D - 1)/(r-1)$ where D= Bulk distribution coefficient

(2) isotopic ratios

$$(\varepsilon_m - \varepsilon^o_m)/(\varepsilon_a - \varepsilon^o_m) = 1-(C^o_m/C_m)\,F^{-z} \quad \text{.....(3.2)}$$

where ε_m and ε_a refer to epsilon units (or isotopic ratios) of the magma and assimilate

respectively.

The curves for AFC are represented for a constant value of r, which is the rate of assimilation relative to the rate of crystallisation, and examples are shown on Figure 2.15b for various r and D values. The points and numbers on the curve are representative values of F. As noted by DePaolo (1981), this model differs from fractional crystallisation in that for elements with D>1 a steady state value is always reached, and is represented by:

$$C_m = r\, C_a / (r + D - 1) \quad \text{.....(3.3)}$$

AFC also differs from simple mixing in that on isotope-isotope diagrams it may result in correlations that do not point to or reach the end member. This only occurs, however, when the bulk distribution coefficients for the two elements are significantly different and where substantial crystallisation has occurred. The trends become more similar to fractional crystallisation as r tends to zero, and to simple mixing as r tends to infinity. In this case even moderately low r (r= 0.8) values are similar to simple mixing at higher values for F . AFC also produces much larger shifts in initial isotopic ratios (Figure 2.15b) for a similar amount of contamination than simple mixing and simple mixing followed by fractional crystallisation (Figure 2.15a).

Data from the Priestlaw Main Series on a $(^{87}Sr/^{86}Sr)_0$ vs. Sr diagram (Figure 2.16), fall on lines with relatively shallow slopes. In modelling these data with AFC, however, two important assumptions have to be made on:

(1) the isotopic ratios and concentrations of the parent and contaminant.

(2) the bulk distribution coefficients of the elements modelled.

The only exposed rocks older than the granitoids are SULPS thus these will first be considered as a possible contaminant. Two samples of Silurian turbidites analysed from near to the margin of Priestlaw (PS30s, PS35; Figure 2.2) have high initial $^{87}Sr/^{86}Sr$ ratios >0.712 (Table 2.1, Appendix 5). This is higher than the average SULPS value of 0.7075 (Halliday *et al.* 1980); however it is probably more representative because the average was

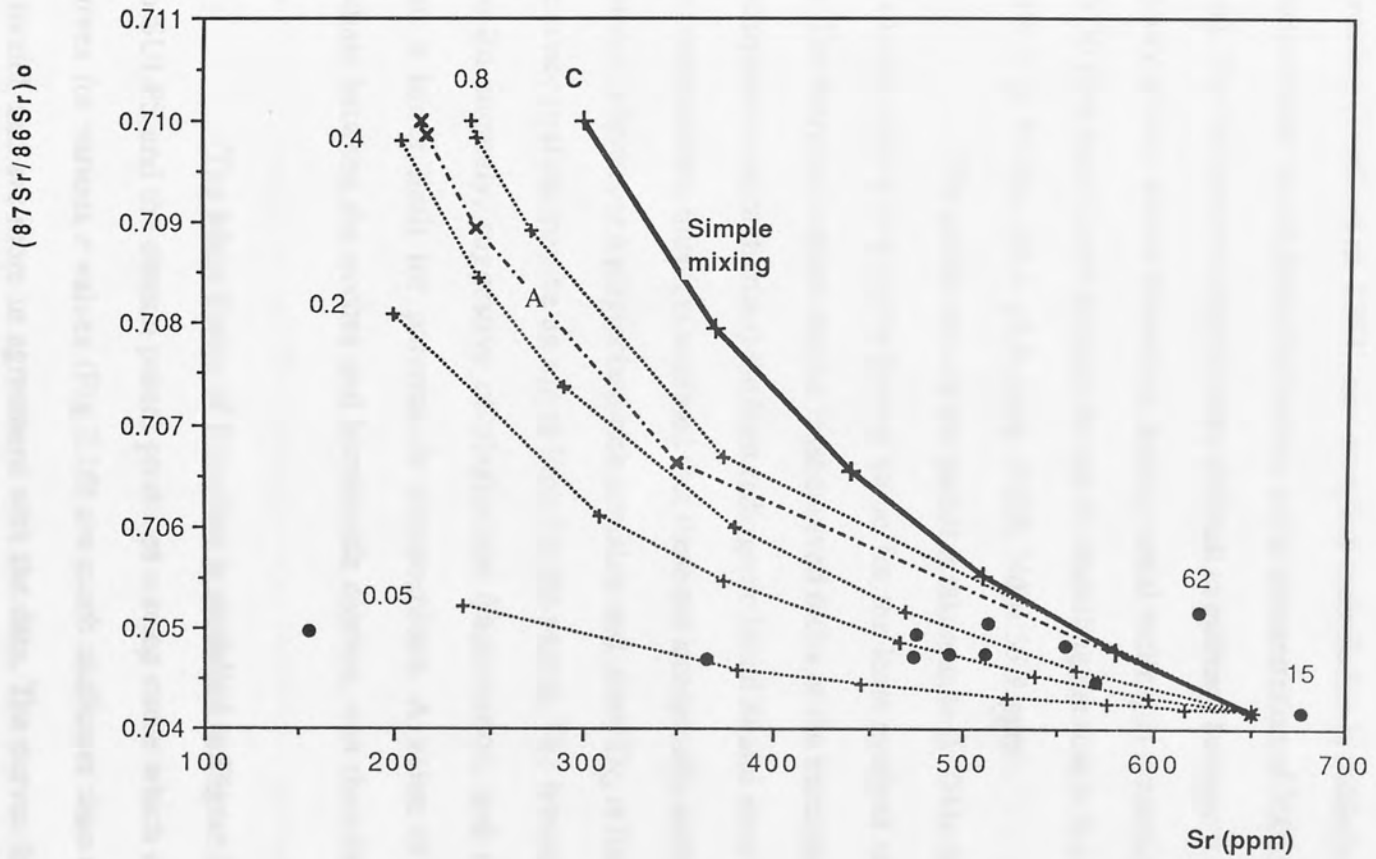

Figure 2.16 Initial $^{87}Sr/^{86}Sr$ - Sr diagram showing data from the Priestlaw Main Series. Modelled trends are for simple mixing (solid line) and AFC (dotted lines) assuming D=1.2 and the assumptions for the end-members made in the text. r values are shown adjacent to each curve. The dashed curve (A) is for a high Sr (750 ppm) contaminant with D = 2.5.

based partly on basic greywackes not present in the area of Priestlaw and Cockburn Law. The extensive Nd isotope study of Scottish sedimentary and metasedimentary rocks (O'Nions *et al.* 1984), showed an average ε Nd value of -6 in greywackes and shales of the Southern Uplands consistent with a higher initial Sr ratio. An initial $^{87}Sr/^{86}Sr$ ratio of 0.710 was chosen for modelling purposes. Because plagioclase would tend to stay in restite during partial melting (Tindle *et al.* 1983), and complete assimilation is unlikely, the Sr concentration of the contaminant would probably be low, and a concentration of 300ppm Sr was chosen for modelling. The Nd concentration is more difficult to estimate because it is likely to be present in accessory phases whose behaviour during partial melting is presently poorly understood; however 30 ppm was chosen initially for use in modelling because it is a typical concentration in SULPS (e.g. PS30s, Nd = 27.9 ppm; PS35, Nd = 35.9 ppm).

The initial ratio of the parent is taken to be 0.70416 because it is the value for the olivine norite and is the lowest value for the least evolved of the pyroxene-mica diorites. The marginal norites are the least evolved rocks of the intrusion having (along with the basic pyroxene-mica diorites) the least radiogenic initial Sr and most radiogenic initial Nd isotopic compositions, thus it is assumed that these are isotopically similar to the parent. The olivine norite is however a plagioclase-rich cumulate and since D_{Sr} is likely to be greater than 1, its Sr concentration may be an upper limit for the parent. The hornblende diorites have a negative Eu anomaly, suggestive of plagioclase fractionation, and these are thought to represent a lower limit for parental Sr compositions. A value of 650ppm, which is intermediate between the norites and hornblende diorites, was therefore chosen for use in models.

The Main Series of Priestlaw is modelled in Figure 2.16. Simple mixing between SULPS and the chosen parent produces a steep curve which does not fit the data. AFC curves for various *r* values (Fig 2.16) are much shallower than those for the simple mixing model, and are more in agreement with the data. The curves for higher values of *r* (e.g.*r* =0.8) are more similar to simple mixing, particularly during the initial stages of AFC. It would clearly be more difficult to choose between the two models on such a diagram. Because

most of the data depart drastically from the simple mixing trend, and since cumulate formation and fractional crystallisation have previously been shown to be important in the least evolved rocks of the Main Series (model 6), the AFC models are favoured. As M_a/M_c approaches zero, the AFC curves become more comparable with fractional crystallisation trends, which can be used to explain the trend from hornblende granodiorite to the porphyritic granodiorite and granite where there is little variation in initial isotopic ratios.

Two samples sit to the right of the simple mixing curve and are more similar to the case of $D_{Sr}<1$ (Figure 2.16) or possibly involving a higher Sr contaminant; however the evolution of the plutons, even the least evolved rocks is dominated by plagioclase fractionation, hence it is very unlikely that D_{Sr} would be less than 1. A very high Sr contaminant is also unlikely because this would require very large D_{Sr}. Since one of these samples (PS 15) has been shown to be a cumulate, consequently it would seem likely that the other, PS62, (Figure 2.16) has a similar origin. This latter sample is from the the margin of the pluton and is much more coarsely grained than the majority of samples collected, thus further favouring a cumulate rich origin.

Similar arguments can be presented for Nd although the behaviour of this element is difficult to model in more evolved rocks because of the extremely high bulk distribution coefficients for accessory minerals. Nd data from Priestlaw and Cockburn Law are plotted on Figure 2.17a along with the modelled trends for simple mixing and AFC with variable D and r values. Apart from one sample (PS 99) which contains small biotite-rich clots interpreted as xenoliths and with a low ε Nd, the data plot more closely to the modelled trends with low D and r values. The inferred r values are however extremely low (0.01-0.1) compared to those suggested by the Sr isotopes. Large enrichments in Nd are also implied as F becomes small: up to 55 ppm at F =0.1 and 129 ppm at F =0.01.

Further modelling in which the concentration of Nd in the contaminant was varied to 6 ppm also produces arrays that initially describe the granitoid data (Figure 2.17b). Again trends with low D and r values best fit most of the data. The values of r (0.3-0.6) are more compatible with those for the Sr isotope data. The lack of variation in Nd

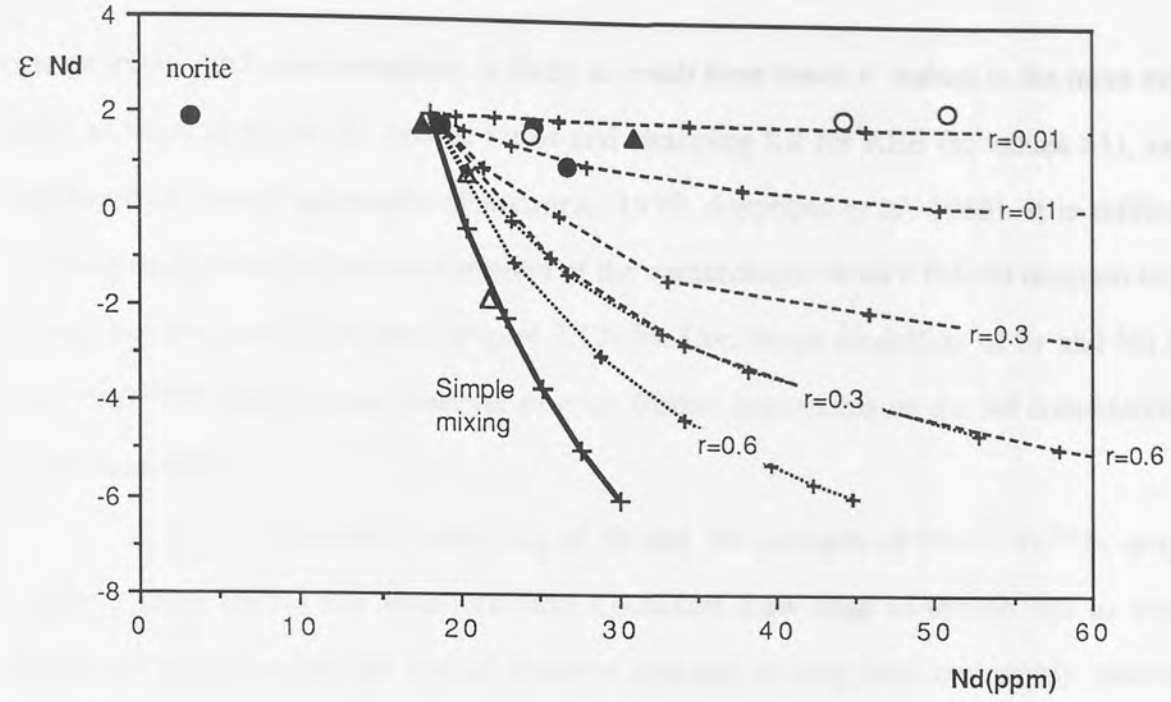

Figure 2.17a ε Nd-Nd diagram showing granitoid data and modelled trends for simple mixing (solid line) and AFC (dotted: $D = 0.8$; dashed: $D = 0.6$), assuming Nd=30ppm in the contaminat. r values shown adjacent to curves. Data symbols: Priestlaw: circles; Cockburn Law: triangles; Main Series: solid symbols; Pyroxene-mica diorite Series: open symbols.

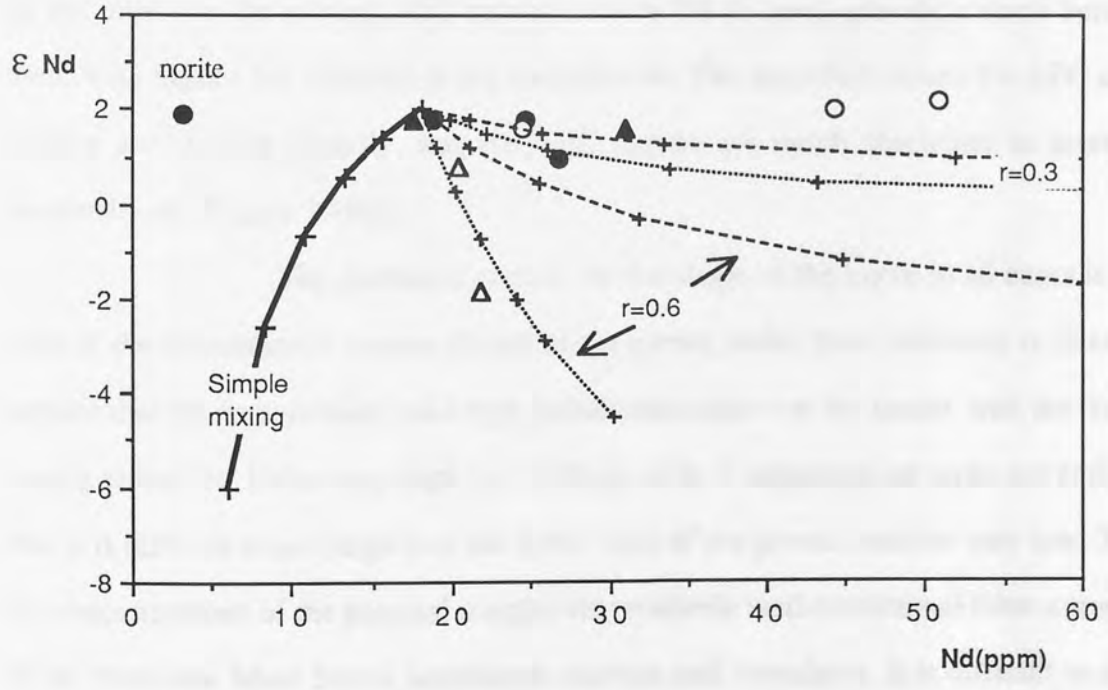

Figure 2.17b ε Nd-($^{87}Sr/^{86}Sr$)o diagram showing data and modelled trends for simple mixing (solid line) and AFC (dotted: $D = 0.5$; dashed: $D = 0.3$) assuming Nd=6ppm in the contaminant. r values shown adjacent to curves. Data symbols as in Figure 2.17a.

isotope ratios and concentrations is likely to result from lower r values in the more evolved rocks as implied by the Sr isotope ratios and changing Kd for REE (to values >1), as seen elsewhere in zoned granitoids (Pankhurst, 1979; Stephens *et al.* 1985). It is difficult to precisely determine the Nd concentration of the contaminant on an ε Nd-Nd diagram because various models can fit the data (Figure 2.17a,b). Combined modelling of Sr and Nd on an εNd- $^{87}Sr/^{86}Sr$ diagram can however provide further constraints on the Nd concentration in the contaminant.

Combined modelling of Sr and Nd isotopes (ε Nd- $^{87}Sr/^{86}Sr$ diagram, Figure 2.18a). shows the Priestlaw and Cockburn Law data to define flat to concave downward slopes unlike the typical concave upwards mixing lines commonly involved in mantle-crust interaction. Curves for simple mixing for the two modelled Nd concentrations in a contaminant (Figure 2.18a) show that low Nd (6ppm) in the contaminant provides a better fit, with a higher Sr/Nd ratio in the contaminant relative to the parent controlling the shape of the curves. The AFC curve for Nd=30ppm (Figure 2.18b) is shallower than that for simple mixing but nevertheless, the trends are similar, and the data for Priestlaw and Cockburn Law do not plot near the curves. AFC curves for low Nd (6 ppm) provide a much better fit than those with higher Nd (30ppm) in the contaminant. The modelled curves for AFC and simple mixing are similar initially, but the AFC curves are much shallower in more evolved compositions (Figure 2.18b).

The dominant control for the shape of the curve in all cases is the Sr/Nd ratio of the contaminant relative to that of the parent, rather than variations in D and r. This implies that the contaminant had a high Sr/Nd ratio relative to the parent, with the contaminant having either low Nd or very high (ca. 1500 ppm) Sr. Continental arc rocks are enriched in Sr thus it is difficult to envisage how the Sr/Nd ratio of the parent could be very low. The Sr and Nd concentrations of the parental magma are relatively well constrained from a consideration of the Priestlaw Main Series hornblende diorites and cumulates. It is difficult to envisage a high Sr contaminant, because Sr would tend to be held in plagioclase in restite during partial melting of the crust. A high Sr contaminant (ca. 750ppm assuming Nd = 30ppm in the

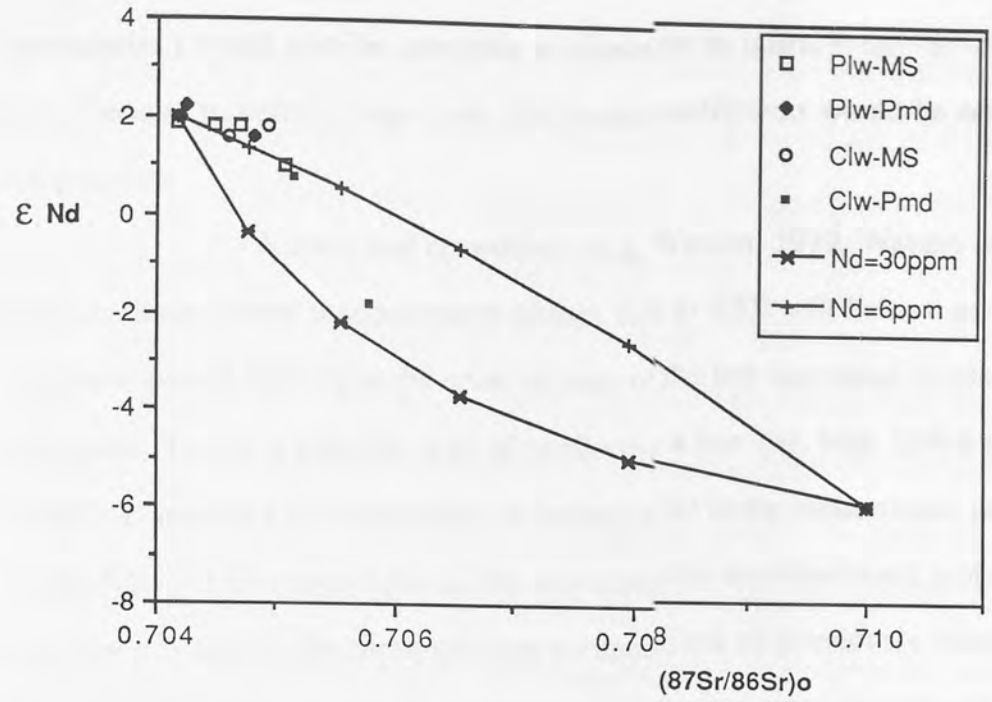

Figure 2.18a ε Nd-($^{87}Sr/^{86}Sr$)o diagram showing granitoid data and modelled trends for simple mixing assuming Nd=30ppm (crosses) and 6ppm (plus signs) in the contaminat.

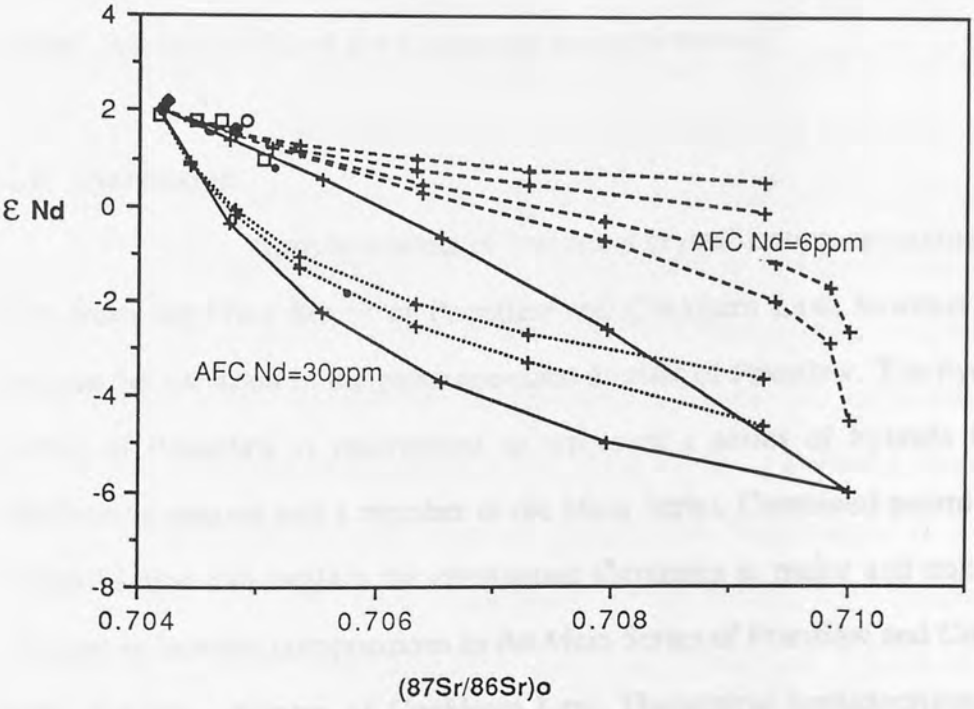

Figure 2.18b ε Nd-($^{87}Sr/^{86}Sr$)o diagram showing data and modelled trends for simple mixing and AFC assuming Nd=30ppm (dotted curves) and 6ppm (dashed curves) in the contaminat. AFC curves are for variable D and r values which describe the actual data on isotope - trace element diagrams (Figures 2.16 and 2.17).

contaminant) would also be untenable as shown on an initial $^{87}Sr/^{86}Sr$ -Sr diagram (Figure 2.16), because extremely large bulk distribution coefficients would be necessary in all rock compositions.

Watson and co-workers (e.g. Watson, 1979, Watson & Harrison, 1984) however, have shown that accessory phases rich in REE will behave as restite during low degrees of partial melting in the crust because of the low saturation levels of these phases in acid melts. This is a possible way of producing a low Nd, high Sr/Nd contaminant. AFC modelling, assuming a concentration of 6ppm for Nd in the contaminant, produces the best fit for the data. The data do not plot all the way along this modelled trend probably because of the very low r value in the more evolved compositions as previously shown for Sr isotopes (Figure 2.16), where fractional crystallisation becomes more important in the cooler, more evolved magmas.

AFC modelling thus explains the major and trace element and isotopic changes in Priestlaw and Cockburn Law much better than any previous models, and the low r values, indicated from modelling, show that fractional crystallization is dominant in the genesis of zoning of the plutons. Assuming r values of 0.4-0.6, it is estimated from the model, that ca.10-15% of the plutons are crustally derived.

2.8 Discussion

Simple models of fractional crystallisation or mixing cannot explain the data from the Main Series of Priestlaw and Cockburn Law, however simple mixing can explain the variation in the pyroxene-mica diorites of Priestlaw. The Pyroxene-mica Diorite Series of Priestlaw is interpreted to represent a series of hybrids between a separate shoshonitic magma and a member of the Main Series. Combined assimilation and fractional crystallisation can explain the continuous variations in major and trace elements, and the changes in isotopic compositions in the Main Series of Priestlaw and Cockburn Law and the pyroxene-mica diorites of Cockburn Law. Theoretical considerations imply that it is a probable mechanism when basic magmas with high liquidus temperatures traverse continental

crust with much lower solidus temperatures. Because trace element concentrations are not independent of fractionation processes, much use has been made of combining two isotope systems (e.g. Sr and Nd). The trends on ε Nd-ε Sr diagrams however may not be unique, and various combinations of the parameters used in AFC can give rise to similar trends. In the case of Priestlaw and Cockburn Law, the trends are dominantly controlled by the Sr/Nd ratio of the contaminant relative to the parent and give little information on the concentrations involved. An additional but often ignored constraint can be placed on these theoretical curves by choosing the curves that agree not only with isotopic parameters, but also with the daughter isotope elemental concentrations e.g. on εSr-Sr and εNd-Nd diagrams. One of the main assumptions in AFC modelling is the choice of r ; low values are preferred in the case of Priestlaw and Cockburn Law, and are also favoured on thermal grounds (Marsh, 1989). The other major assumption concerns the choice of end-member compositions, and this will be discussed prior to comparison with models proposed for other intrusions.

The crustal end-member has been assumed to be SULPS because these are the only rocks cropping out which are older than the plutons. AFC modelling for the Criffell pluton, which occurs along strike from Priestlaw and Cockburn Law (Figure 2.1), has also been done using SULPS using Sr and O isotopes and REE (Stephens *et al.* 1985). The presence of shallow basement (Hall *et al.* 1983) and of lower crustal xenoliths in Carboniferous dykes (Upton *et al.* 1983) in the area of study suggests that contamination might possibly be from below SULPS. As there are no isotopic data available for the lower crustal samples, contamination in the lower or middle crust cannot be ruled out. The occurrence of a few xenoliths in Priestlaw and Cockburn Law, and in Criffell (Stephens *et al.* 1985), and of some partially melted xenoliths (Tindle and Pearce, 1983) in the Loch Doon pluton, suggests that contamination by country rock has occurred in at least some of these plutons. Thirlwall *et al.* (1989) suggested on the basis of a Pb isotope study of southern Scotland granitoids (including Priestlaw) and lavas, that SULPS is unlikely to be the contaminant, because the more evolved and contaminated granitoids have higher Pb isotopic compositions than SULPS. The various models produced in the present study, which were

derived assuming constraints provided by SULPS, give a relatively good fit to the data and may imply that the actual contaminant, if not SULPS, is isotopically similar in terms of Sr and Nd isotopes.

The least evolved rock types in both intrusions including the Priestlaw olivine norite, the basic pyroxene-mica diorites of Priestlaw and the hornblende diorite of Cockburn Law, all have similar Nd isotopic compositions, thus it is assumed that these values are representative of the parent magmas to the intrusions. The initial $^{87}Sr/^{86}Sr$ ratio of the Cockburn Law hornblende diorite is higher than that of the two Priestlaw samples measured, but this rock is extremely altered and it is likely that its ratio has been changed by the alteration. The radiogenic initial $^{143}Nd/^{144}Nd$ and unradiogenic $^{87}Sr/^{86}Sr$ ratios data indicate that the parent to the granitoids is dominantly from a long term light REE depleted mantle. The granitoids (and St. Abbs/Eyemouth lavas) are geochemically and isotopically similar to the Midland Valley lavas (Figure.2.12), which Thirlwall (1982a, 1986) interprets as depleted mantle modified by subducted lithosphere, and thus, a similar source may be involved for the parental magmas to the granitoids. The geochemical similarity of the less evolved parts of the plutons to the St. Abbs and Eyemouth lavas with high Ni and Cr imply a mantle as opposed to infracrustal source (Chappell and Stephens, 1988). In such a case, the production of granitoid plutons strongly suggests ponding of basic magma within the crust with the likelihood that initial fractional crystallization was dominated by mafic minerals plus or minus plagioclase. The effect of this process would be to reduce the compatible elements Ni and Cr; thus low values of these elements do not necessarily imply infracrustal derivation. The occurrence of a few, relatively high Ni and Cr, diorite xenoliths in Priestlaw (Figure 2.7) and the presence of olivine cumulates, supports this suggestion.

Although the isotopic compositions of the norites and the least evolved pyroxene-mica diorites are likely to be similar to the parents of the intrusion, it is less clear to what extent these are similar to the mantle below this part of the Southern Uplands. It is possible that the trends produced by the granitoids on isotope-isotope diagrams (Figures 2.12, 2.18) represent parts of mixing lines from a more depleted source eg. similar to the most

depleted Midland Valley lavas which are similar to island arc tholeiites (IAT). The shapes of the granitoid data (straight to concave down) on an ε Nd - ε Sr diagram (Figure 2.12) cannot be produced from these however, since island arc tholeites have similar Sr/Nd ratios to the granitoids, and thus would produce typical concave upward shapes. If the data from the Priestlaw and Cockburn Law intrusions are part of a typical mantle-crust curve, then inspection of Fig 2.12 would imply that the contaminant plotted in the upper right hand quadrant whereas one data point from Cockburn Law plots in the lower right hand quadrant. Although lithospheric mantle xenoliths from Streap Comlaidh have suitable isotopic characteristics that sit in the upper right hand quadrant, these occur only in the northern Highlands in dykes intruding old crust (Menzies *et al.* 1988), and these appear not to be present beneath the Midland Valley to the south (Halliday *et al.* 1985). One further difficulty with the least evolved granitoids being derived from a much more isotopically depleted mantle is that the data would lie on the lower parts of a mixing curve, closer to the contaminant which generally implies extensive contamination. The products should therefore have more evolved characteristics than found in the granitoids and lavas, such as higher SiO_2 and low Ni and Cr.

Contamination of a slightly more depleted source by lower crust to give values similar to those of basic rocks, followed by AFC processes in the upper crust, cannot be ruled out. This hypothesis is thought to be unlikely however, because it would require that the most basic rocks from both Priestlaw and Cockburn Law, the pyroxene-mica diorites of Priestlaw, and the one sample from the 'flat trend' of the St. Abbs lavas (with very different Sr and Nd concentrations), all have undergone different amounts of contamination, and yet all ended up with similar values. It is proposed that the isotopic compositions for the least evolved parts of Priestlaw and Cockburn Law and the pyroxene-mica diorites of Priestlaw are similar to those for the mantle below this part of the Southern Uplands at ca. 410 Ma. This will be discussed in more detail in chapter 5 in relation to additional data from other Southern Upland plutons.

2.9 Comparison with other models

The process of AFC has largely been ignored in geochemical studies of granitoids, probably partly due to the lack of combined isotopic and major and trace element studies. Because AFC models require much less contamination to produce enriched isotopic characteristics, they cannot be ignored in models of crustal evolution through geological time. A study of S- and I-type granitoids from eastern Australia (McCulloch and Chappell, 1982) showed by isotopic modelling that the genesis of I-type granitoids is compatible with their being mixtures of mantle and crust. The large amounts of contamination necessary are however inconsistent with major and trace element abundances, possibly because a MORB like mantle end member was chosen or that fractional crystallisation was ignored. Identification of contamination of MORB with crustal material may be relatively simple, but numerous studies (Menzies and Murthy, 1980; Hawkesworth *et al.* 1983) have shown that old lithospheric mantle may have geochemical characteristics similar to that found in the crust; hence making the detection of contamination much more difficult. Added to this MORB is unlikely to represent the parental magma for granitoids in continental arcs for the following reasons:

(1) it is never erupted through continental crust.

(2) the mantle wedge above subduction zones is likely to be metasomatised by fluids/melts released from the downgoing slab.

(3) studies of continental magmas and geophysical studies (Jordan, 1988) implying a deep tectosphere below continents suggest that a more enriched mantle and not MORB will probably be tapped beneath continents.

The most isotopically depleted parent likely to be found in areas of active or recently terminated subduction, would be similar to island arc tholeiites (IAT), and general mixing of this source with continental crust has been effectively modelled for the Sierra Nevada and Peninsular ranges granitoids of California (DePaolo, 1980, 1981). The lithospheric mantle below Scotland is however extremely heterogeneous (Halliday *et al.* 1985; Menzies *et al.* 1988), a factor which must be considered in models of granitoid genesis. The

most depleted and probably youngest mantle is that found below the Midland Valley during the Late Caledonian (Thirlwall, 1982a) and Carboniferous times (Smedley, 1986,1988). This mantle is however distinct from MORB and has been suggested to be more similar to OIB (Smedley, 1986). It is clear that distinct mantle domains exist below different crustal blocks in Scotland (Menzies and Halliday, 1988; Rock *et al.* 1988) and their importance must be emphasised when forming general models of crustal evolution. The mantle source below the northern Southern Uplands is unlikely to be MORB or IAT since this would most likely require considerable contamination for the St. Abbs lavas and granitoids. Models for the evolution of granitoids using MORB or IAT as an end-member, are likely to overemphasise the proportion of crustally derived material in their genesis

Simple mixing models can also overemphasise the proportion of crustally derived material in cases where fractional crystallisation is also important; particularly if the element concerned is compatible and has a lower concentration than that in the parental magma. The relationship between isotopic ratios and element concentrations (Figures 2.16-17) in conjunction with those on isotope-isotope diagrams (Figure 2.18) can help to constrain the role of fractional crystallisation.

Fractional crystallisation models have commonly relied only on major and trace element studies for modelling (Tindle and Pearce, 1981; Tindle *et al.* 1988). The good trends and progressive evolution of the Priestlaw and Cockburn Law intrusions can also, in the absence of isotopic data, be modelled well with a fractional crystallisation history (Figures 2.5-8, 2.13). Although contamination of a mantle derived magma by crustal materials may give rise to considerable scatter, particularly if the crust is heterogeneous, it is evident from this study that the extent of such scatter very much depends on the actual process. It is also evident that contamination in the Priestlaw and Cockburn Law intrusions would be difficult to detect without an isotopic study, and this may also be the case for many other plutons. This conclusion has important consequences for models that do not have a multi-disciplinary geochemical approach, since least squares and trace element modelling do not generally constrain the number of components as effectively as isotopes. One of the main problems with

a simple major and trace element study of calc-alkaline rocks, is that fractional crystallisation produces magmas that tend to granitoid (i.e. minimum melt) compositions. Progressive contamination with low degree partial melts of the crust (also minimum melt) may only appear to enhance this tendency for major and trace elements, and thus, is extremely difficult to detect. The correct identification of crustal contamination by geochemical fingerprinting therefore requires a combined major and trace element and isotope approach. Tindle and Pearce (1981) showed for example, that fractional crystallisation is important in the Loch Doon intrusion, but the variation in initial $^{87}Sr/^{86}Sr$ and O isotopes (Halliday *et al.* 1980) is clear evidence for more than one component. The importance of both processes occurring in this pluton make it probable that AFC type processes have been important.

The restite-unmixing hypothesis would appear to be untenable on both petrological and geochemical grounds in Priestlaw and Cockburn Law. AFC best explains the variation in isotopic signatures, and the non-linear trends for some elements. If only the more evolved compositions of these plutons are considered however, then linear to only slightly curved trends are apparent which are interpreted as AFC trends in the present study. Wall *et al.* (1988) have shown that linear trends can also be produced during fractional crystallisation depending on the compositions and proportions of the fractionating assemblage. Linear plots with a limited range in compositions are not evidence therefore for restite unmixing (or any form of mixing). Many of the eastern Australian granitoids that have been modelled on the restite unmixing hypothesis also show variations in isotope geochemistry (McCulloch & Chappell, 1982), and it may be possible to model these more successfully by AFC processes. The fact that simple mixing models for Sr and Nd isotopes imply different proportions of contamination from that indicated by major and trace elements (McCulloch and Chappell, 1982) suggests that a reappraisal of the restite unmixing model for these may be necessary.

2.10 Summary

1. Fractional crystallisation of a basic/intermediate magma appears to be an important process in the evolution of the zoned Priestlaw and Cockburn Law intrusions.

2. Sr and Nd isotope data show that simple fractional crystallisation must however be accompanied by assimilation, the assimilant probably having isotopic characteristics similar to the local country rocks.

3. The model that best satisfies the major and trace element data of Cockburn Law and the Main Series of Priestlaw is that of assimilation-fractional crystallisation (AFC).

4. Magma mixing is used to explain the series of pyroxene-mica diorites in the Priestlaw intrusion. Mixing occurred between a distinct shoshonitic magma and a magma of the Main Series.

5. AFC modelling using probable end members suggests that the Sr/Nd ratio of the contaminant was high, and it is concluded that during partial melting Nd probably remains in a REE enriched restite phase during partial melting.

6. Variation in mixing lines on isotope-isotope diagrams can be explained by:

   (a) Difference in isotopic ratios between contaminant and parent.

   (b) Changing Sr/Nd in crystallising magma.

   (c) r and D values selected for AFC modelling.

   (d) REE enriched phases behaving as restite in the crust during partial melting due to their low saturation levels.

For Priestlaw and Cockburn Law (a) and (c) are likely to have been the most important constraints on the shapes of the curves. r is however important in the more evolved compositions because as it tends to 0, the curves become more like fractional crystallization.

7. Mantle addition to the crust has been important during the Late Caledonian orogeny. The parent magmas of the Priestlaw and Cockburn Law intrusions are likely to have been mantle derived melts (and not underplated basaltic melts). Crustal recycling is important and models indicate that ca. 10-15% of the granitoids are crustally derived.

Chapter 3: Late Caledonian Dyke swarms of South eastern Scotland

1: The Porphyrite-Porphyry Series.

3.0 Abstract

Several hundred dykes are spatially and temporally associated with the small plutons of the eastern Southern Uplands of Scotland. They are fine-grained, commonly porphyritic rocks which vary in composition from porphyrite (andesite porphyry) to quartz porphyry (rhyolite porphyry), and the mineral phases present are similar to those found in the plutons. Alteration is present in all rock types, but generally more intense in the more evolved dykes. Major and trace element concentrations and trends in the porphyrites and acid porphyrites (dacite porphyries) are identical to those of the plutons which suggests that they are fine-grained representatives of the pluton magmas. The similarities in concentrations of compatible and incompatible elements in both groups implies that the plutonic rocks are not cumulates. The quartz porphyries form a distinct, separate group on some trace element diagrams (e.g. Zr-Nb) compared to the other rock types. Petrological and geochemical considerations imply that these may represent crustal melts, with the heat necessary for their formation coming from the magmas parental to the plutons and the less evolved dykes. This explains the close spatial and temporal association of the quartz porphyries to the plutons and less evolved dykes.

3.1 Introduction

One of the most neglected aspects of Late Caledonian magmatism in Scotland is the origin of the regional dyke swarms. Diverse suites of minor intrusions, varying in composition from basic lamprophyres to quartz porphyries, are associated with many of the Late Caledonian granitoids of Scotland (Richey, 1932). The dyke swarms are best developed in association with the compositionally zoned I-type (Halliday *et al.* 1980) plutons such as Ben-Nevis, Lochnagar, Strontian and Criffell. Granites with S-type or A-type characteristics (Fleet, Cairngorm) lack dyke swarms. These minor intrusions are represented mainly by dykes, but bosses, sills, vents and breccia pipes are also known (Bowes & Wright, 1967; Rock *et al.* 1986).

In most areas porphyrites (andesite-porphyries), acid porphyrites (dacite-porphyries) and quartz porphyries (rhyolite-porphyries) predominate, accompanied

by aphyric felsites. Lamprophyres are however the most common type around some intrusions e.g. those around the Glen Tilt complex in the Highlands and the Newry pluton of Northern Ireland. The dyke rocks of the Southern Uplands have a similar diversity in composition to those of the Caledonian belt as a whole, varying from appinite and lamprophyre to quartz-porphyry (Barnes *et al.* 1986).

The dyke swarms provide evidence for the existence of a tensional tectonic environment following the main Caledonian orogeny. Regional trends of the dykes across Scotland vary from generally EW in the northern Highlands, NE and NNE in the Grampian Highlands, NNE and NNW in the Midland Valley to ENE in the Southern Uplands (Richey, 1932). In the west and north-west of Ireland no obvious regional pattern is apparent, and the dyke swarms around particular intrusions have no distinct trends. The orientations of the minor intrusions, as with the plutons, appear to be structurally controlled using pre-existing fault structures to aid their emplacement (Smith, 1979; Watson, 1984).

The relationship of the dykes to the plutons is clearly seen in some of the better exposed granitoids of the metamorphic Caledonides. In the Etive and Ben Nevis complexes for example, a swarm of porphyrite dykes (similar in composition to the lavas) cut the lavas, the Glencoe ring dyke and the outer granitoids of both intrusions, and are in turn cut by the central granites (Bailey and Maufe, 1960). Similar relationships are seen in the Rosses centre in Donegal and in the Criffell intrusion of the Southern Uplands. The relationship of basic to acid dykes is generally more complex. In the Northern Highlands, the more acid dykes consistently cross-cut more basic types (Smith, 1979). Basic appinite and lamprophyre intrusions are generally earlier than both granitoid plutons and porphyrite-porphyry series dykes (Bowes and Wright, 1961,1967). However, the presence of lamprophyre dykes intruding the evolved members of plutons (Phillips, 1955) and syn-plutonic mafic dykes in several plutons (Holden *et al.* 1987), show basic magmas to have been available also during later stages of magmatic evolution.

In the western part of the Southern Uplands, dykes are very abundant and are spatially associated with the zoned plutons of Loch Doon, Criffell, Portencorkrie

and Cairnsmore of Carsphairn (Figure 3.1). The Black Stockarton Moor area, north-west of Criffell, is a zone of extremely abundant dyke intrusions (mainly porphyrites) forming part of a sub-volcanic complex (Leake and Cooper, 1983) and south of this area, lamprophyre and porphyrite dykes are closely associated with basaltic intrusions and agglomerate/breccia pipes (Rock *et al.* 1986a). Several lamprophyres have been dated from the Kirkcudbright area and give K-Ar ages from 418±9 Ma. to 409±9 Ma (Rock *et al.* 1986b). Most of the minor intrusions show some degree of alteration, and in many cases replacement by secondary minerals is extensive. King (1937) proposed that this alteration (albitisation and chloritisation) is the result of "autolysis" from residual solutions rich in water, carbon dioxide, soda and silica. Barnes *et al.* (1986) noted limited chemical compositions in the dykes of the Wigtown Peninsula with porphyrites forming a group with ca. 57 per cent SiO_2, and acid porphyrites and porphyries ca. 63-71 per cent SiO_2. An apparent silica gap is also found in the dykes around the Criffell pluton (as well as in the pluton itself) with the porphyrites forming a group between 57-59 per cent SiO_2 and the acid porphyrites and quartz porphyries 64-71 SiO_2. The dyke rocks from the Wigtown Peninsula (Barnes *et al.* 1986) have been modelled to show that the porphyrite and porphyry intrusions are not simply lamprophyric fractionates, but may be derived from at least two parent magmas, represented by crustally-contaminated lamprophyre or entirely crustal melts.

Apart from brief petrological observations of some rocks in the BGS memoirs (e.g. M^{c}Adam & Tulloch, 1985), no work has been completed on the minor intrusions of the eastern Southern Uplands (the area of this study). In the eastern part of the Southern Uplands several small granitoid intrusions are exposed (Figure 3.1). The largest of these is Priestlaw (ca.4km^2) and Cockburn Law (ca.2km^2) which vary from gabbro to granite and diorite to granodiorite respectively (chapter 2). Other smaller intrusions are Lamberton beach (NT 968 590), Stobshiel (NT 496 632) and Kidlaw (NT 513 643). These smaller intrusions are however much more altered (M^{c}Adam & Tulloch, 1985). A gravity and magnetic anomaly near Lammer Law (NT 524 618) led Bennet

Aston University

Illustration removed for copyright restrictions

Figure 3.1 Generalised distribution of intermediate and acid dykes in southern Scotland. From Rock *et al* (1988).

(1969) to suggest the presence of a roughly circular stock-like intrusion, the Lammer Law 'granite', at a depth of 150-300m. Other evidence for the presence of a buried pluton comes from thermally altered dykes and sedimentary rocks forming a metamorphic aureole (McAdam & Tulloch, 1985). Lagios & Hipkin (1979) postulated that a buried granite batholith (the 'Tweedale granite') underlies much of the eastern part of the Southern Uplands and possibly extends across much of the strike (Figure 1.2). Rock *et al.* (1988) noted that whereas mafic and intermediate dykes are the commonest type in the western Southern Uplands, felsic dykes are uncommon and appear to be restricted to the northern and eastern parts, associated with the geophysically inferred subcrop of the "Tweedale granite" (Figure 3.1). A sequence of extrusive rocks, varying from andesite to rhyolite, with some associated agglomeratic vents is exposed between St. Abbs Head and Eyemouth on the east coast of the Southern Uplands (Thirlwall, 1979).The dyke rocks here in the east are diverse varying from lamprophyre to quartz porphyry. All the lamprophyres spatially associated with the plutons are mica-lamprophyres with hornblende varieties being present only near Hawick (sheet 17W) where no intermediate to acid rocks are exposed. The lamprophyres will be treated separately from the porphyrite-porphyry series for the following reasons:

(1) Mica-lamprophyres form part of a regional zone of high-K magmatism ca. 10km wide and >300km long stretching from Northern Ireland to St. Abbs Head (Rock *et al.* 1985). No hornblende lamprophyres are associated with the granitoid intrusions.

(2) Field and geochemical evidence (chapter 4) suggest that the mica lamprophyres are younger than the granitoids and lavas, and may therefore have no genetic relationship with the latter.

3.2 Aims of chapter

The main aim of this chapter is to study the evolution of the dyke rocks, and to ascertain whether the porphyrite-porphyry series are more fine-grained equivalents

of the plutonic bodies, or are a distinct series of magmas.

Models for the evolution of the minor intrusions is important in Caledonian magma-genesis for the following reasons:

(1) the minor intrusions have an aggregate volume which may represent as much as 10-20% of the combined volume of plutonic and volcanic rocks.

(2) there are close spatial, temporal and (?)genetic associations of the minor intrusions with the larger plutonic bodies. The minor intrusions generally cover a wider range of compositions and may record the earliest and latest phases of magmatism.

(3) although many of the dyke rocks are porphyritic, they may approximate more closely to liquid compositions than the more coarsely grained plutonic equivalents.

Over 200 samples were collected from dyke rocks in the eastern Southern Uplands and thin sectioned for petrographic description. The freshest of these were selected for geochemical analysis along with a representative sample of altered and/or weathered rocks in order to study the effect of alteration on geochemistry. These were analysed using X-ray fluorescence for both major and trace elements.

3.3 Nomenclature

The porphyritic character and naturally high volatile content (particularly the lamprophyres) of many of the dyke rocks make modern chemically based classifications inapplicable. Barnes *et al.* (1986) used the long established B.G.S. petrographical classification whereby the dykes were divided into lamprophyres (mesocratic to mafic, mafic phenocrysts only, little or no quartz), porphyrites (mesotype, intermediate plagioclase, hornblende and biotite phenocrysts, little alkali feldspar, some quartz), acid porphyrites (acid plagioclase, sparse ferromagnesian phenocrysts, more quartz and alkali feldspar than porphyrites), quartz porphyries (leucocratic, essential alkali feldspar and/or quartz as phenocrysts in quartzo-feldspathic groundmass) and felsites (aphyric or fine-grained felsic rocks). The porphyrites, acid porphyrites and quartz porphyries *broadly* correspond to andesites, dacites and rhyolites respectively.

This petrographic classification is however very general and arbitrary, and since most of the dykes in the study area are altered, a classification based on mineral compositions is best avoided. Pseudomorphs in the dyke rocks are however generally easy to recognise from their shapes and type of mineral replacement. The following general classification, based on B.G.S. 1:50,000 maps, is therefore used for the porphyrite-porphyry series:

Porphyrites (P): Mesotype rock with phenocrysts of plagioclase (intermediate in fresh rocks) + hornblende ± biotite in a matrix of the same minerals with minor alkali feldspar, quartz, apatite and opaque oxides.

Acid porphyrites (Fpt): Similar to porphyrites but with phenocrysts of plagioclase (acid in fresh rocks) ± biotite ± minor alkali feldspar ± quartz, and more quartz and alkali feldspar in the groundmass, minor opaque oxides and apatite.

Quartz porphyries (qFp): Leucocratic pale coloured porphyry, with phenocrysts of quartz ± alkali feldspar ± minor plagioclase ± rare biotite in a quartzo-feldspathic groundmass with opaque oxides and rare apatite.

Felsites (F): Aphyric to fine-grained non-porphyritic quartzo-feldspathic rocks with sparse opaque oxides.

Microgranodiorites (Fmd): Pale medium grained rock containing quartz, orthoclase, plagioclase, hornblende and/or biotite. May have phenocrysts of feldspar.

All of the dykes collected, which were mapped as felsites on B.G.S. maps, were altered members of the porphyrite-porphyry group of rocks, and these have been reclassified.

3.4 Field relationships

The minor intrusions cut Ordovician and Silurian sediments of the eastern Southern Uplands (Figure 3.1), and several acid porphyrites and quartz porphyries (PS 19,21,23,24) also intrude the intermediate members of the Priestlaw granitoid (Figure 2.2). Exposure is generally poor however and contacts with country rock commonly are not seen. The only intrusions mapped as cutting rocks of 'Old Red Sandstone' facies are of

monchiquite (PS 214), dolerite (1466b-c, PS 177) and felsite (1400a-b, 1401a-b) all of probable Carboniferous age (Appendix 3e), and a minette dyke near St. Abbs Head (1421-3, PS 181-2).

One of the most conspicuous features of the dyke swarms is their clustering around granitoid plutons. The minor intrusions form four obvious clusters and their associated plutons are:

(1) Lamberton Beach granite: St. Abbs Head (NT 910 690) to SW of Lamberton Beach (NT 950 580) associated with a faulted sliver of granite (Lamberton Beach granite), lavas and agglomeratic vents.

(2) Cockburn Law: Exposed on the northern side of Cockburn Law where the Silurian meta-sediments are not covered by Carboniferous rocks.

(3) Priestlaw: Surrounding the Priestlaw granitoid and continuing west along strike to (4).

(4) Lammer Law: Associated with a metamorphic aureole (NT 540 610) and the Stobshiel and Kidlaw granitoids.

Most samples were collected from better exposed stream sections, and the majority of the intrusions are near vertical dykes and sheets with thicknesses of the order of 1-2m. Some of the more evolved intrusions however attain thicknesses of 5-10m (1416, PS 8) and have relatively shallow dips. Some quartz porphyries, SE of St. Abbs Head have been mapped as larger intrusions with dimensions up to 1.5 by 0.5 km (1429). Several minor intrusions have been classified as microgranodiorites (1385, 1398, 1416, 1418) and one as granite (1482), and for the most part the dykes appear to be petrologically homogeneous. In one of the microgranodiorites however there is a variation from more mafic to more felsic compositions from the margins inward (1416a-f). Flow banding is a common feature at the margins of many of the acid dykes (PS 9,10).

Most dykes have a general NE trend similar to the strike of the country rocks, though some have trends varying from NNE (PS 120,165) to NNW (1395, PS125). Both groups appear petrographically and geochemically identical.

3.5 Petrography

(a) Porphyrites (P)

Textural variation in the porphyrites is quite diverse. They are characterised by phenocrysts and microphenocrysts of plagioclase and/or hornblende, and commonly biotite. Pyroxenes, or pseudomorphs after pyroxene, are present in some specimens.

Plagioclase (labradorite-andesine) with normal zoning is the most common phenocryst phase and commonly forms cumulophyric aggregates. Some phenocrysts of plagioclase also have overgrowth rims of albite. Euhedral shapes are the norm but many feldspar have embayed margins (1397) indicative of resorption. Other features include tapered ends of crystals with hollow centres and ragged margins of broken crystals. Several porphyrites have very fresh plagioclase (1411,PS12), but the majority show some degree of alteration. Patchy replacement by sericite is common (1397,1510), and this varies from extensive (1391) to patchy (PS 56) kaolinisation. The feldspar in altered rocks is albite-oligoclase which probably represents albitisation of the plagioclase.

Green or brown hornblende is the most common mafic phase and, although cumulophyric aggregates are found, in most instances forms discrete euhedral crystals (Plate 3.1). Four rocks (1396, 1410-11 and PS 150), marked as lamprophyres on B.G.S. maps, contain abundant feldspar phenocrysts, thus they are porphyrites according to the accepted definition (Rock, 1984). Amphibole occasionally poikilitically encloses plagioclase (1396) as in the hornblende diorite of Priestlaw, but is commonly enclosed in plagioclase (1397). Some of the fresher porphyrites (1396, 1510) contain, in addition to fresh plagioclase, both brown and green amphibole. Replacement of amphibole by chlorite, carbonate and micaceous aggregates is however the norm in these rocks.

Pyroxene is not common and where present is generally pseudomorphed by carbonate and chlorite (1426,1477-9), though some relics of fresh clinopyroxene are present (1426,1467,1468). Pseudomorphs of quartz after ?olivine occur in one dyke (1394). Biotite is present as a phenocryst in some porphyrites, and although

Plate 3.1. Hornblende- plagioclase-phyric porphyrite (1510) showing, euhedral phenocrysts of hornblende and sericitised plagioclase, in a fine-grained altered groundmass of plagioclase, hornblende, quartz and alkali feldspar. Fov: 8.3mm.

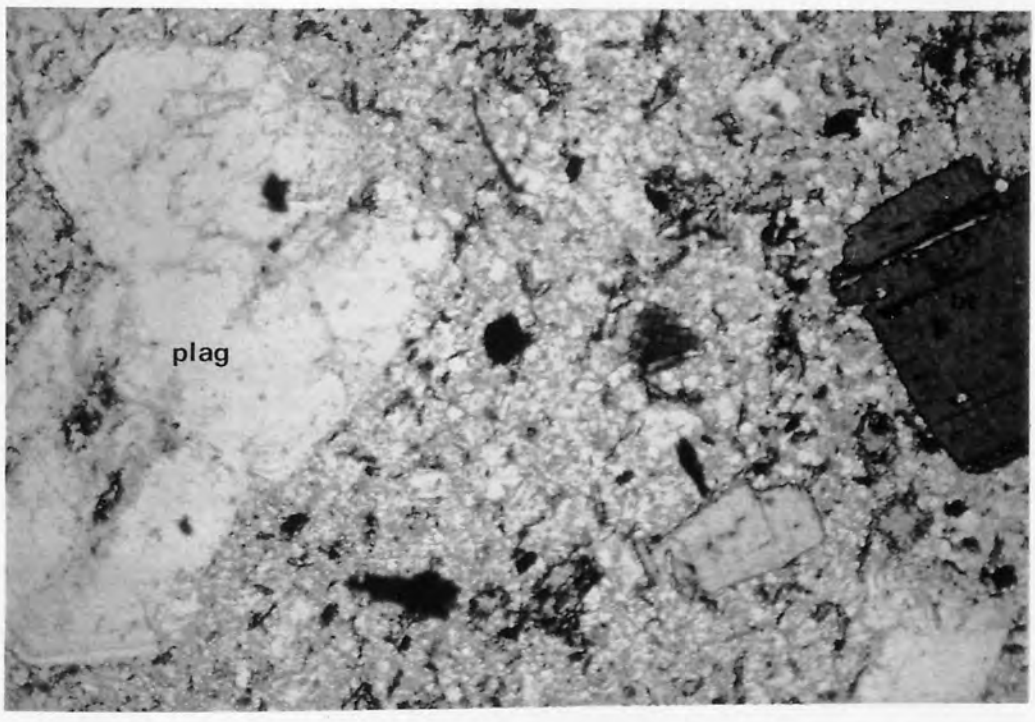

Plate 3.2. Plagioclase-biotite-phyric acid porphyrite (1413) with fresh plagioclase and biotite, in a fine grained groundmass of plagioclase, biotite, quartz and alkali feldspar. Fov: 3.4mm.

fresh euhedral phenocrysts are common, replacement by chlorite is sometimes extensive (1475).

The groundmass mainly comprises plagioclase, minor alkali feldspar, mafic minerals and minor zircon, apatite and opaque oxides. The textures vary from a plexus of laths of feldspar (some being trachytic) to extremely fine-grained and granular. Apatite, less commonly zircon and opaque oxides are commonly enclosed in mafic minerals particularly biotite.

(b) Acid porphyrites (Fpt)

The acid porphyrites are characterised by phenocrysts of plagioclase of more sodic (albite-oligoclase) composition than those of the porphyrites, commonly biotite, and some hornblende or quartz. Alteration in these rocks is generally much more intense than in the porphyrites but textures are similar.

Cumulophyric aggregates of feldspar are also present, as well as individual phenocrysts, and plagioclase is generally highly sericitised and/or kaolinised. Fresh plagioclase is present in only a few dykes (Plate 3.2), but fresh patches within some dykes contain fresh phenocrysts. The more sodic composition of the plagioclase in altered dykes is probably primary since these are also found in the freshest dykes, but the reported presence of a few remnants of more calcic plagioclase (M^{c}Adam & Tulloch, 1985) indicates that some of the dykes may be albitised.

Phenocrysts of biotite are more numerous (Plate 3.2) and green amphibole less common than in the porphyrites. Where present amphibole is largely pseudomorphed by chlorite and carbonate. Biotite is commonly fresh enclosing apatite, zircon and opaque oxides. Replacement by chlorite, carbonate and colourless mica is however extensive in the more altered dykes.

Subhedral quartz occurs in some dykes as large crystals commonly with corroded margins and reaction rims of chlorite. These are possibly xenocrysts derived from deeper crustal materials.

The groundmass of the acid porphyrites is variable, with fine grained plagioclase present as turbid, sericitised, laths and with more abundant granular quartz than in the porphyrites. Alkali feldspar is also more abundant in the groundmass, along with biotite and, in some specimens muscovite. Alteration of the groundmass is generally intense, being similar to that in the phenocryst phases, and in addition hematitisation is common along grain boundaries and as veinlets in very altered samples.

(c) Quartz porphyries (qFp)

The quartz porphyries are leucocratic rocks characterised by abundant phenocrysts of quartz and less abundant ones of feldspar (Plate 3.3). Alteration is typically extensive with complete kaolinisation and sericitisation of the feldspar and replacement of biotite with chlorite, carbonate and hematite. Biotite is not very common in most dykes, however it is prominent in a few fresh dykes (1469) where it is sometimes enclosed in quartz. Pale green to colourless micaceous aggregates with associated hematite are present and may be pseudomorphs after biotite.

The feldspar in these rocks is usually too altered (kaolinised) for optical determination but both altered plagioclase and alkali feldspar occur in the fresher samples.The feldspars vary from only slightly sericitised albitic plagioclase, commonly rimmed by orthoclase (1493,1509), to albite plus orthoclase or microperthite (1512,1514).

Quartz generally forms subhedral to euhedral crystals (Plate 3.3), commonly with embayed margins enclosing biotite similar to that forming phenocrysts, thus suggesting that these are phenocrysts rather than xenocrysts. Several specimens have phenocrysts and glomeroporphyritic aggregates of phenocrysts consisting of quartz and alkali feldspar micrographic intergrowths (Plate 3.4).

The groundmass is composed of a mosaic of quartz and altered (kaolinised and sericitised) alkali feldspar varying from very fine (1493) to quite coarsely grained (1509). Spherulitic texture is developed in some samples (PS6). Colourless to pale green mica replaces a few phenocrysts of (?)biotite and colourless mica is common in the

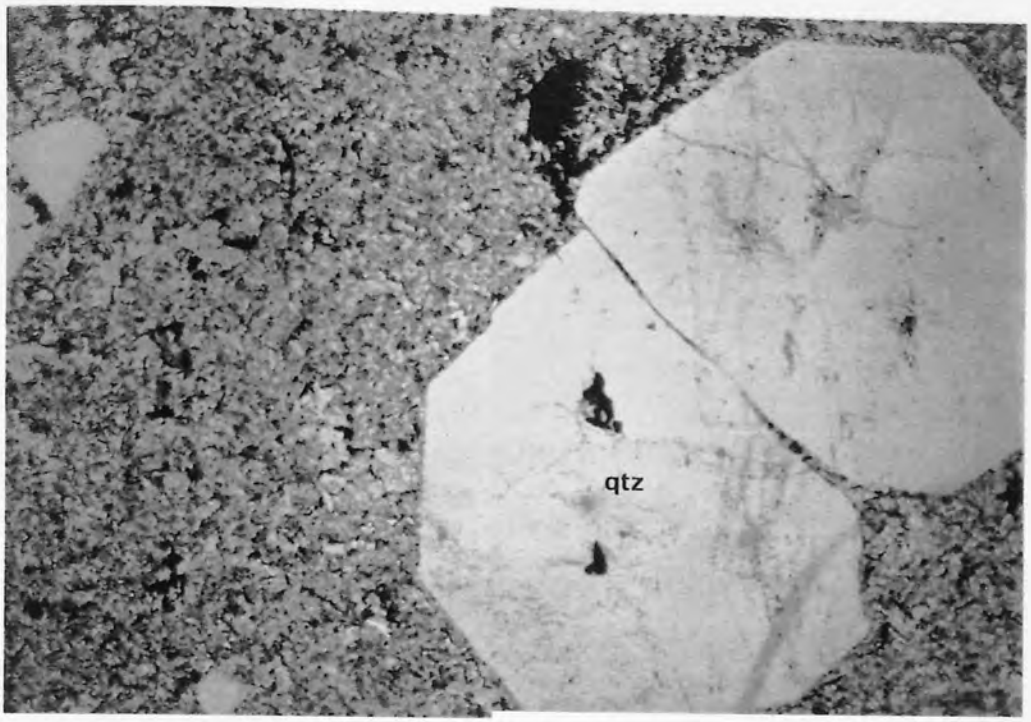

Plate 3.3. Quartz porphyry (1493) showing euhedral quartz phenocrysts in fine-grained groundmass of quartz and kaolinised alkali feldspar. Fov: 3.4mm.

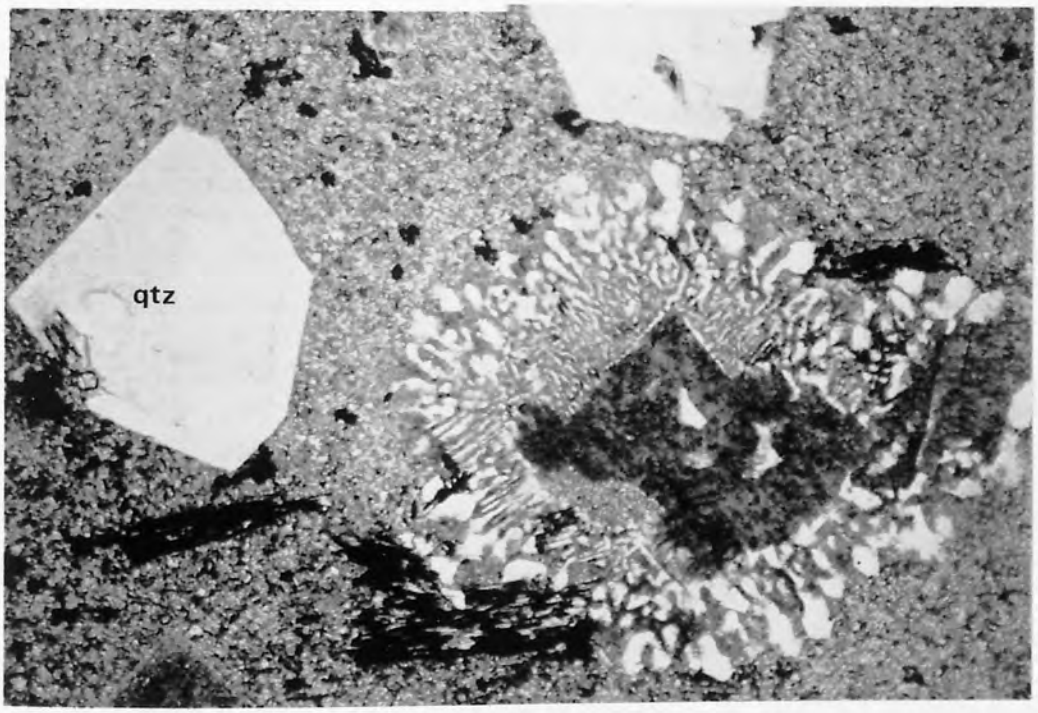

Plate 3.4. Quartz porphyry (1513) with phenocrysts of quartz and hematitised mica, and graphic intergrowth of quartz and alkali feldspar around an extremely altered plagioclase crystal. Fov: 8.3mm.

groundmass. The groundmass mica is colourless and occurs as small sheaves interstitial to quartz and feldspar.

Quartz and quartz-hematite veins are relatively abundant in some altered dykes.

(d) Microgranodiorite (Fmd)

The microgranodiorites are fine- to medium-grained rocks and appear similar to the more finely grained facies of the plutonic bodies. Plagioclase, some of which occurs as phenocrysts, is andesine-oligoclase and is generally normally zoned. Biotite, orthoclase and lesser amounts of amphibole and quartz and accessory apatite and zircon are also present in these rocks.

One large (6m) microgranodiorite dyke (1416a-f) adjacent to the Cockburn Law intrusion varies from a mafic-rich marginal phase, with felsic segregations, to a more felsic interior. This rock is comprised of plagioclase and biotite set in a slightly finer groundmass of plagioclase, biotite, alkali feldspar and quartz. The felsic segregations composed of alkali feldspar, quartz and minor plagioclase are present near to the margin of the dyke.

3.6 Geochemistry

The porphyrite-porphyry series, are similar to the granitoids in defining a high-K calc-alkaline series on a K_2O-SiO_2 diagram (Figure 3.2). Harker diagrams for major elements have continuous arrays from basic to acid compositions, covering the field of the plutons and extending beyond (Figure 3.3). Rocks with the geochemical characteristics of the "cumulate" olivine norites of Priestlaw are however missing from the dyke suite, and the least evolved porphyrites have slightly lower MgO, CaO and Al_2O_3 and higher TiO_2 than the olivine norites of Priestlaw.

Although many of the acid porphyrites and quartz porphyries are extensively altered, MgO, Fe_2O_3, CaO and TiO_2 show good trends and strong similarities

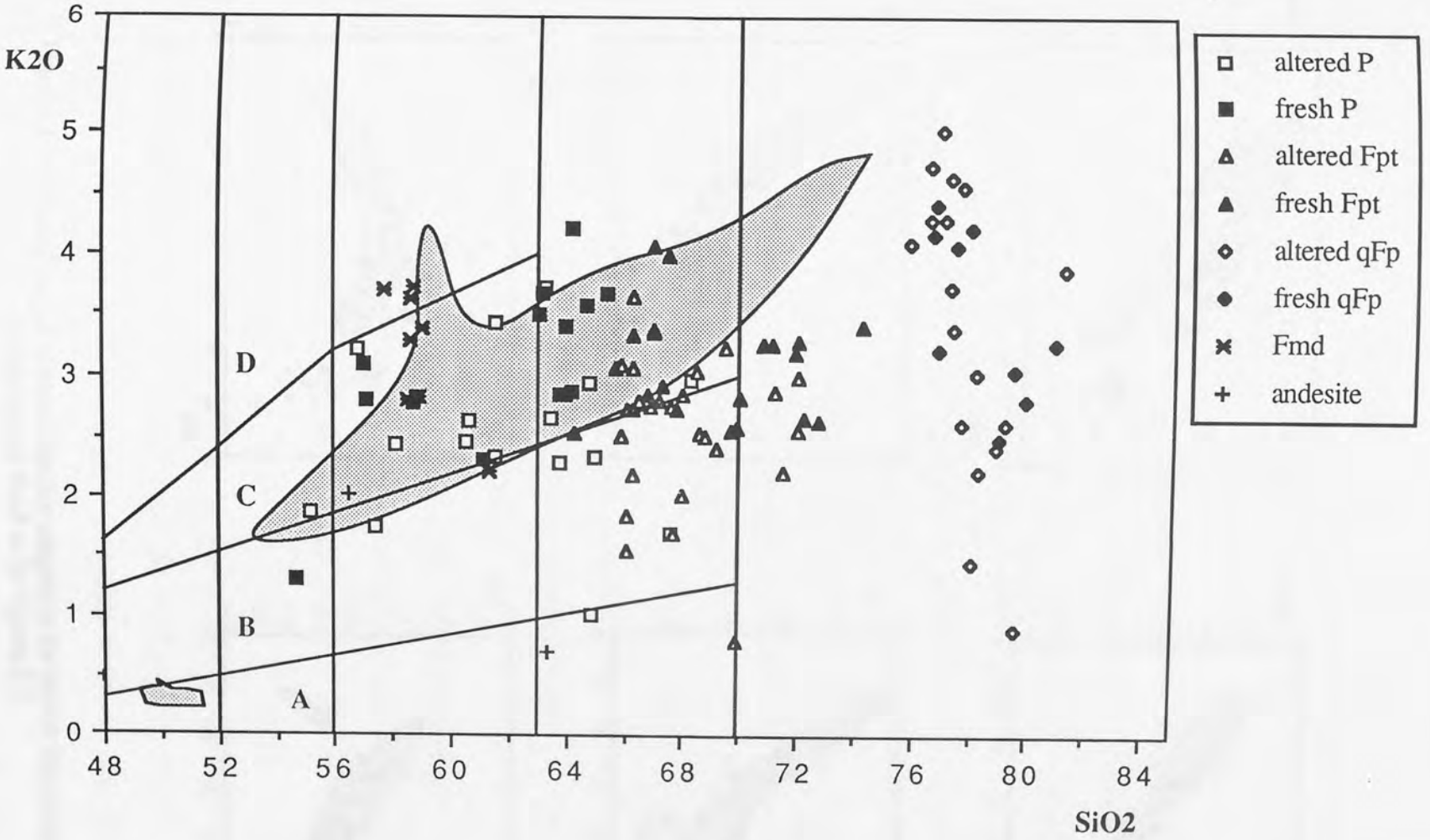

Figure 3.2 K_2O-SiO_2 diagram for minor intrusions and lavas (andesites). Legend symbols are ; P: porphyrites; Fpt: acid porphyrites; qFp: quartz porphyries; Fmd: microgranodiorites. The Priestlaw and Cockburn Law granitoids (Chapter 2) are shown as the shaded field for comparison. Fields for the arc rocks after Peccerillo & Taylor (1976); A: arc tholeiite series; B: calc-alkaline series; C: high-K calc-alkaline series; D: shoshonite series.

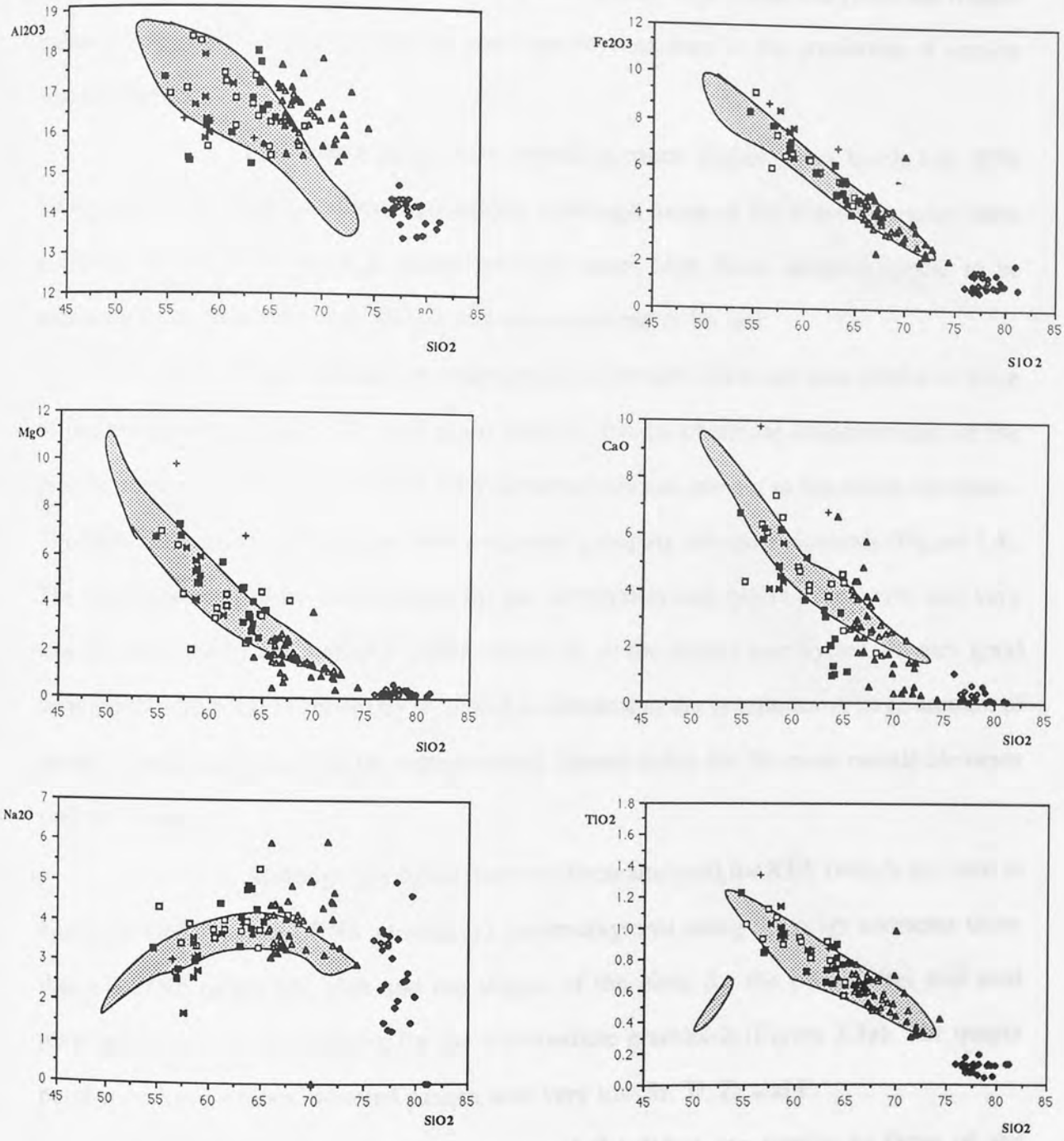

Figure 3.3 Selected major element Harker diagrams for minor intrusions and lavas. Symbols and field as in Figure 3.2.

with the granitoids. There is some scatter however in the more evolved dykes for the more mobile elements K_2O, Na_2O and MnO down to lower abundances in the altered rocks. Some altered intermediate to acid rocks also have higher Al_2O_3 and TiO_2 than the fresher rocks. P_2O_5 is also slightly higher in some porphyrites than in the granitoids of similar silica content.

The quartz porphyries extend to much higher silica levels (ca. 80% SiO_2) than any of the Caledonian granitoids. Although many of the altered samples show evidence of silicification (e.g. quartz veinlets) some high silica samples appear to be relatively fresh, and their high SiO_2 levels are considered to be real.

Trace element abundances in the freshest dykes are also similar to those of the granitoids (Figure 3.4), and again some of the geochemical characteristics of the olivine norites (high Ni, Cr and low HFS elements) are not present in the minor intrusions. The high silica quartz porphyries form a separate grouping for some elements (Figure 3.4). The HFS elements show some scatter for the porphyrites and quartz porphyries, and very low abundances of Zr, and to a lesser degree Y, in the quartz porphyries. A very good correlation with SiO_2 is shown by V, which is identical to the granitoids. A large amount of scatter is seen particularly in the more evolved altered dykes for the more mobile elements such as Rb and Sr.

Although the dykes have not been analysed for REE (which are used to highlight the presence of Nb anomalies), spiderdiagrams using the other elements show that LILE/Nb ratios are high and the shapes of the plots for the porphyrites and acid porphyrites are similar to those for the intermediate granitoids (Figure 3.5a). The quartz porphyries have a more inflected pattern with very low Sr, Ti, Zr and P.

Although trends for most of the dykes are similar to those of the granitoids on Harker diagrams, much scatter is apparent. The freshest samples (those with LOI < 3 wt.%) are plotted as *solid* symbols on Figures 3.3, 3.4 and 3.5(b) and altered rocks with *hollow* symbols in order to ascertain the geochemical effects of alteration. The quartz porphyries generally have low LOI (< 2 wt. %), but since these rocks contain

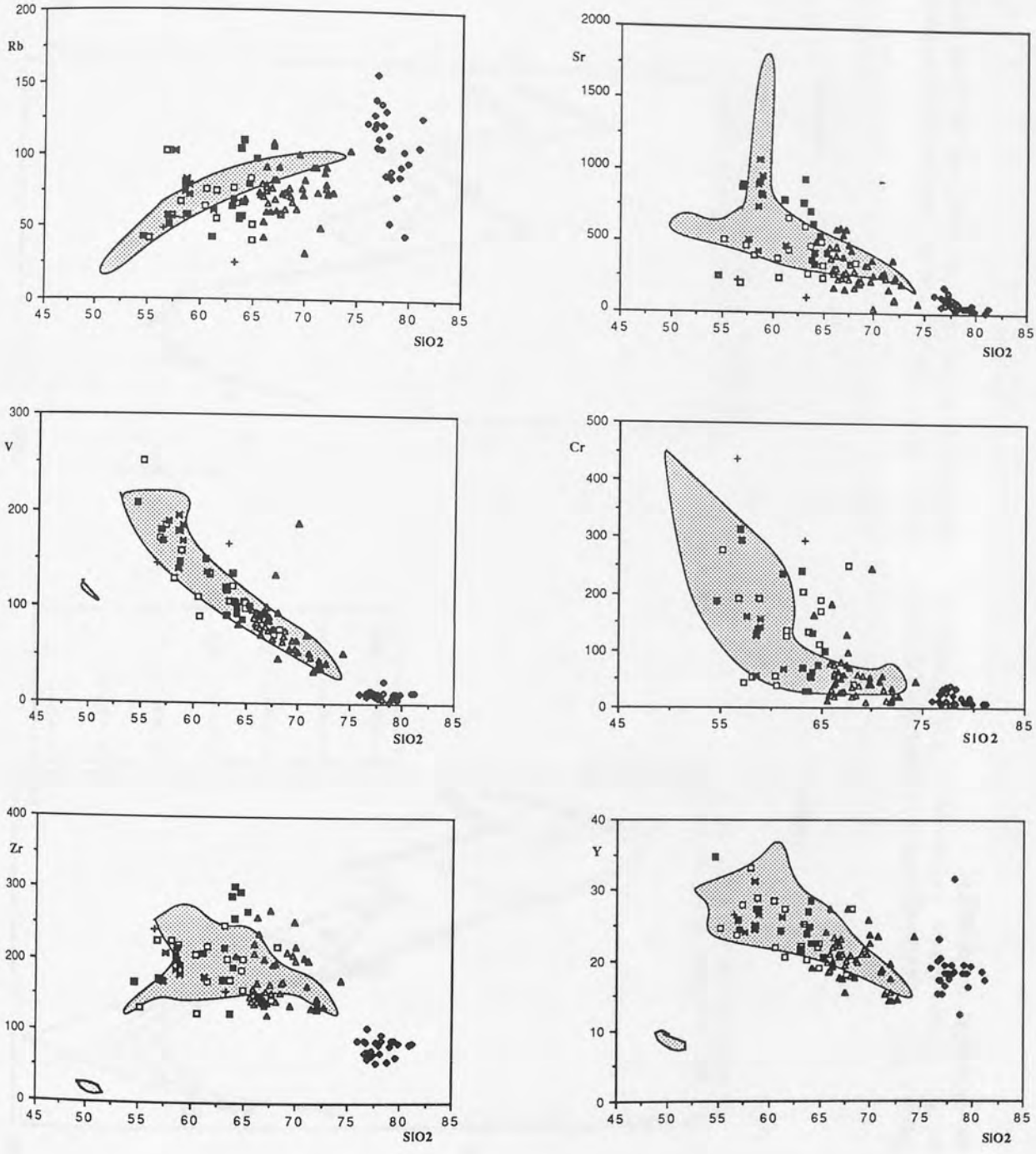

Figure 3.4 Selected trace element Harker diagrams for minor intrusions and lavas. Symbols and field as in Figure 3.2.

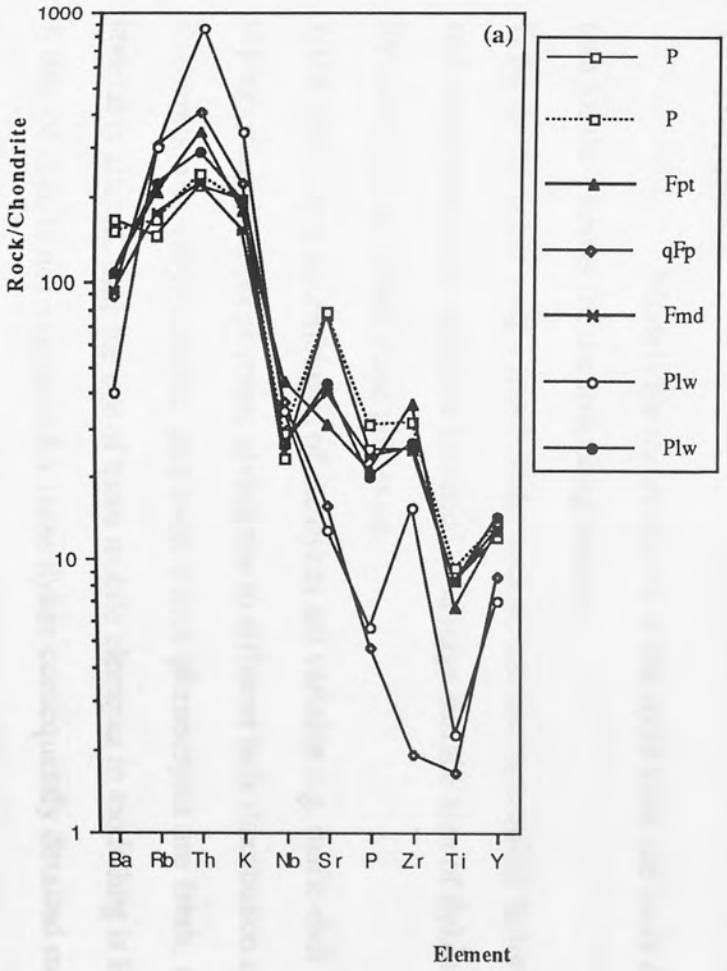

Figure 3.5a Spiderdiagram with selected elements for the freshest dykes. Two samples from Priestlaw are shown for comparison.

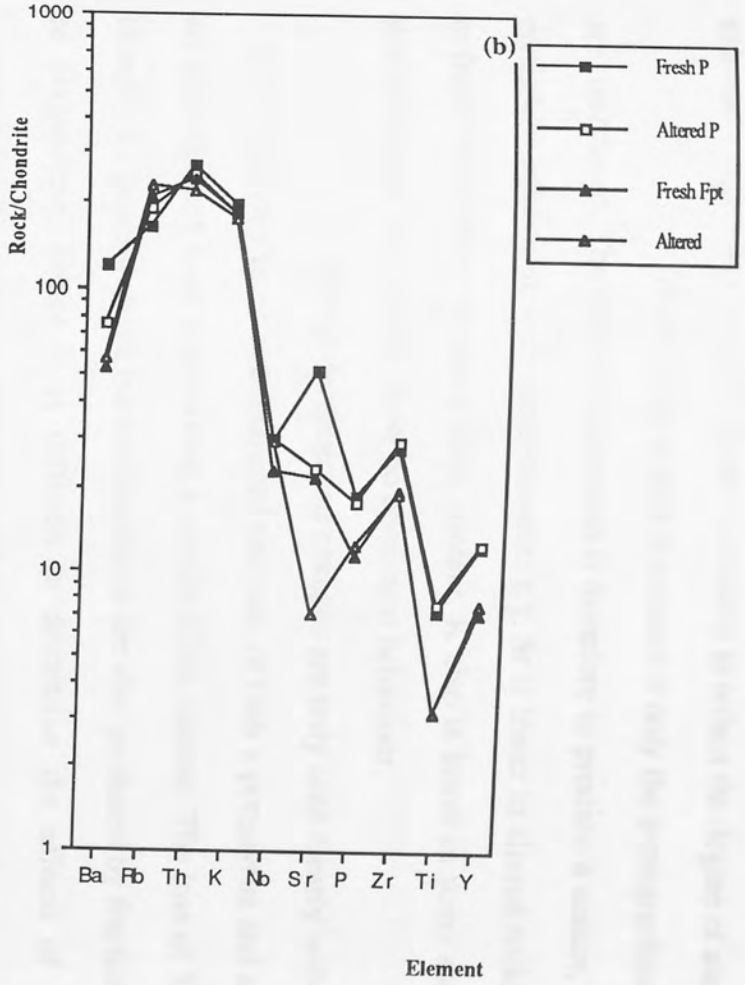

Figure 3.5b Spiderdiagram with selected elements showing fresh and altered porphyrite and acid porphyrite.

extremely high silica, the LOI figure is unlikely to reflect the degree of alteration.

Much of the scatter is reduced if only the petrographically freshest rocks are considered. The effect of alteration is therefore to produce a scatter, but there is some consistent behaviour with some elements e.g. Sr is lower in altered rocks when compared to fresh rocks with the same SiO_2 content. K also is lower in some rocks but there is a general scatter. Rb and Ba show no consistent behaviour.

On spiderdiagrams changes are only seen clearly with Sr e.g. in Figure 3.5(b) where an altered and unaltered analyses of both a porphyrite and an acid porphyrite are plotted, each rock type having a similar silica content. The loss of Sr in altered rocks changes the general shape but similar effects are also produced by fractional crystallisation of plagioclase, hence it is difficult to determine the effects of alteration using log-normalised diagrams to discriminate between alteration and fractionation processes.

3.7 Discussion

Models for the evolution of the dyke suite are more difficult to produce than for the plutons for the following reasons:

1. the dykes occur over a much wider area where the controlling factors of crystallisation and assimilation may be more localised. The large surface area of dykes or intrusive sheets for example may affect these processes.
2. the phenocryst assemblages of the dykes are variable e.g. mafic-rich - plagioclase-poor to plagioclase-rich porphyrites, giving rise to different bulk distribution coefficients.
3. alteration is very variable, and even where phenocrysts are fresh, the groundmass is invariably altered, thus the use of more mobile elements in modelling is limited.
4. isotope data is not available for these dykes consequently detailed modelling of source components is not possible.

Major element abundances in the granitoids and in the freshest dyke rocks are very similar, the only exceptions being the "cumulate" olivine norites of Priestlaw and the very high silica quartz porphyries of the dyke suite. The geochemical and

petrological similarity between the plutonic bodies and the porphyrites and acid porphyrites is compatible with a genetic relationship.

The elements Ba, Rb and Sr, which are useful for modelling of rocks with wide compositional variations, are prone to the effects of alteration particularly of feldspar and biotite. Sr-Rb and Ba-Rb diagrams (Figure 3.6a,b) reveal scatter with much overlap between the groups. There is however a general decrease in Sr and increase in Rb from porphyrites to quartz porphyries (Figure 3.6a). Hornblende porphyrites, with minor phenocryst plagioclase, have the highest Sr contents and thus are unlikely to reflect cumulus plagioclase. The large scatter of Rb in the acid porphyrites and quartz porphyries probably reflects the general increase of alteration in more evolved rock types. Although the scatter is greater than in the granitoids abundances at similar silica levels are similar (Figure 3.4). A poor correlation is shown on a Ba-Rb diagram (Figure 3.6b) but a general decrease in Ba from porphyrites to acid porphyrites is evident. These trends are consistent with the modelled fractionation sequence of the granitoids (Chapter 2), dominated by plagioclase. The only mineral phases with published partition coefficients >1 for Ba are K-feldspar and biotite; however these phases as phenocrysts are not present in many basic and intermediate rocks. This plus the close correspondence of Ba with Sr, not only in the dyke rocks but also in the granitoids (where only minor biotite fractionation is likely to have occurred), may imply that Ba is a trace component in plagioclase.

The "immobile" HFS elements have been extensively used in geochemical modelling and discrimination diagrams (Pearce & Cann, 1970; Pearce & Norry, 1979) for altered rocks. The use of these elements in quantitative modelling of evolved rocks is limited in more evolved calc-alkaline rocks since they are commonly controlled by fractionating minor accessory phases, particularly in calc-alkaline rocks (Pearce & Norry, 1979). The best trend on Harker diagrams is that of TiO_2, where there is a good negative correlation with SiO_2, but the quartz porphyries form a distinct separate group (Figure 3.3). Zr-, Y- and Nb-SiO_2 diagrams show much more scatter, even in the freshest rocks, with the quartz porphyries forming a tight group slightly distinct from the

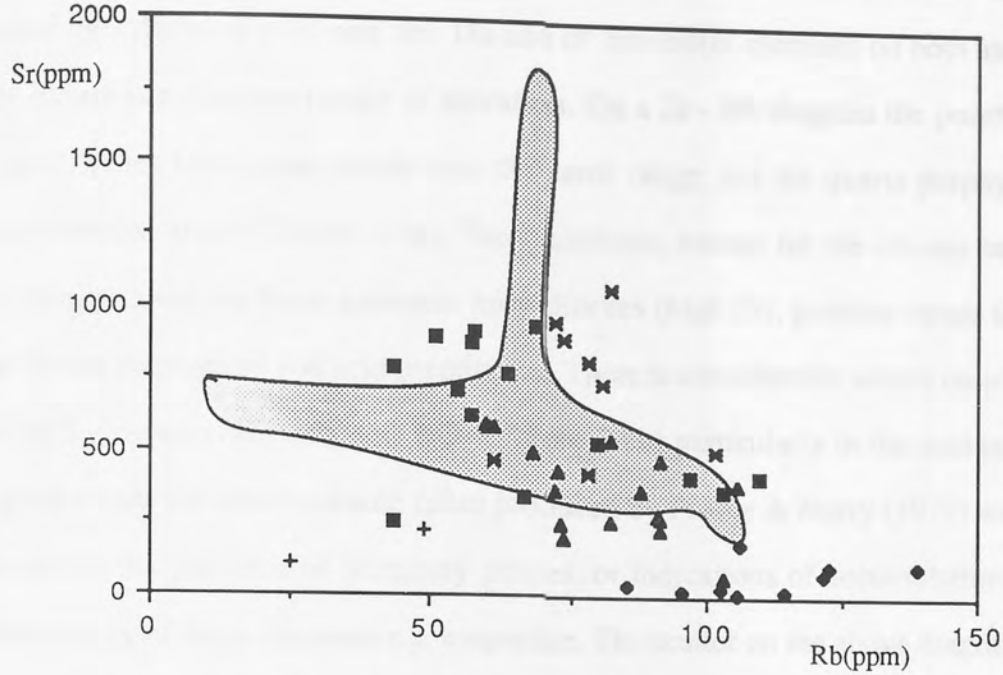

Figure 3.6(a). Relationship between Sr and Rb for the freshest dykes and granitoids. Symbols and field as in fig. 3.2.

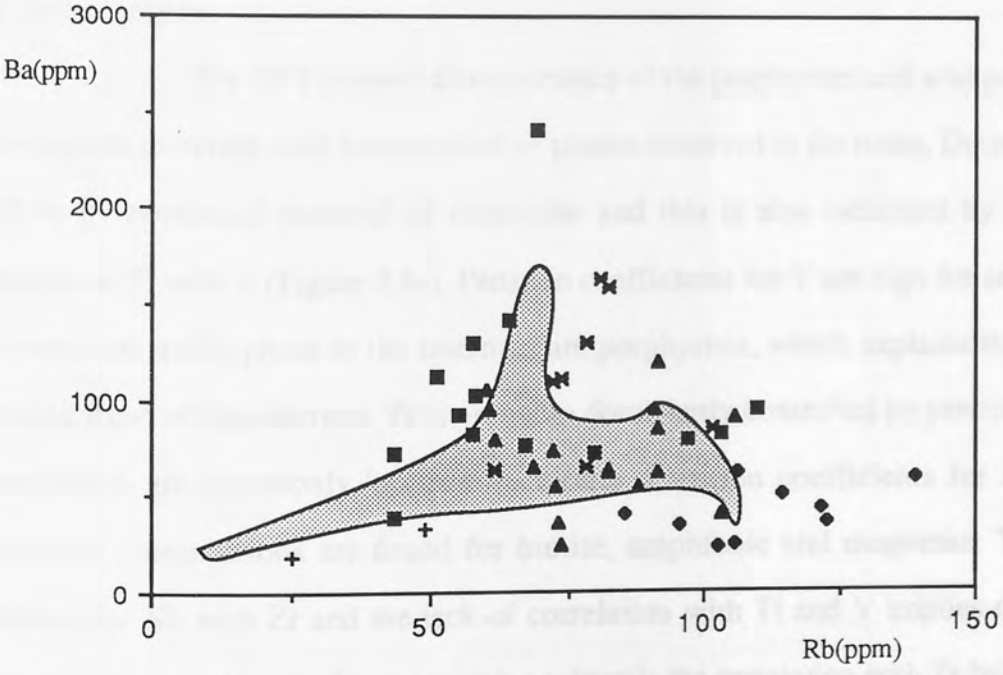

Figure 3.6(b). Relationship between Ba and Rb for the freshest dykes and granitoids. Symbols and field as in fig. 3.2.

more basic dykes (Figure 3.4). There is an overall general decrease in Y and an increase followed by a decrease in Zr and Nb. The use of 'immobile' elements on both axes can test if this scatter is a function purely of alteration. On a Zr - Nb diagram the porphyrites and acid porphyrites form good trends over the same range, but the quartz porphyries again form a separate group (Figure 3.7a). The granitoids, except for the olivine norites (low HFS elements) and the basic pyroxene mica diorites (high Zr), produce trends identical to those for the porphyrites and acid porphyrites. There is considerable scatter on plots for the other HFS elements elements e.g. TiO_2 (Figure 3.7b) particularly in the acid porphyrites. The good trends for some volcanic suites produced by Pearce & Norry (1979) were on data screened for the presence of accessory phases, or indications of accumulation of phases containing any of these elements e.g. magnetite. The scatter on the above diagrams is most likely caused by the crystallisation of such minor accessory phases. Ti and Zr for example form essential structural components in titano-magnetite and zircon respectively, and as such do not obey Henry's Law for the partitioning of trace elements.These minor phases are commonly found enclosed in biotite and amphibole and fractionation of the latter may cause further scatter.

The HFS element characteristics of the porphyrites and acid porphyrites are compatible therefore with fractionation of phases observed in the rocks. Decrease in Ti would be by continued removal of magnetite and this is also indicated by the good correlation of Ti with V (Figure 3.8a). Partition coefficients for Y are high for amphibole, the commonest mafic phase in the intermediate porphyrites, which explains the general decreasing trend of this element. Zr is probably dominantly controlled by precipitation of zircons which are commonly 'trapped' in biotite. Partition coefficients for Nb >1 in intermediate compositions are found for biotite, amphibole and magnetite. The good correlation for Nb with Zr and the lack of correlation with Ti and V implies that Nb is dominantly controlled by the ferromagnesian minerals the correlation with Zr being due to these phases enclosing zircon.

Cr and, to a lesser degree, Ni correlate well with MgO (Figure 3.8b),

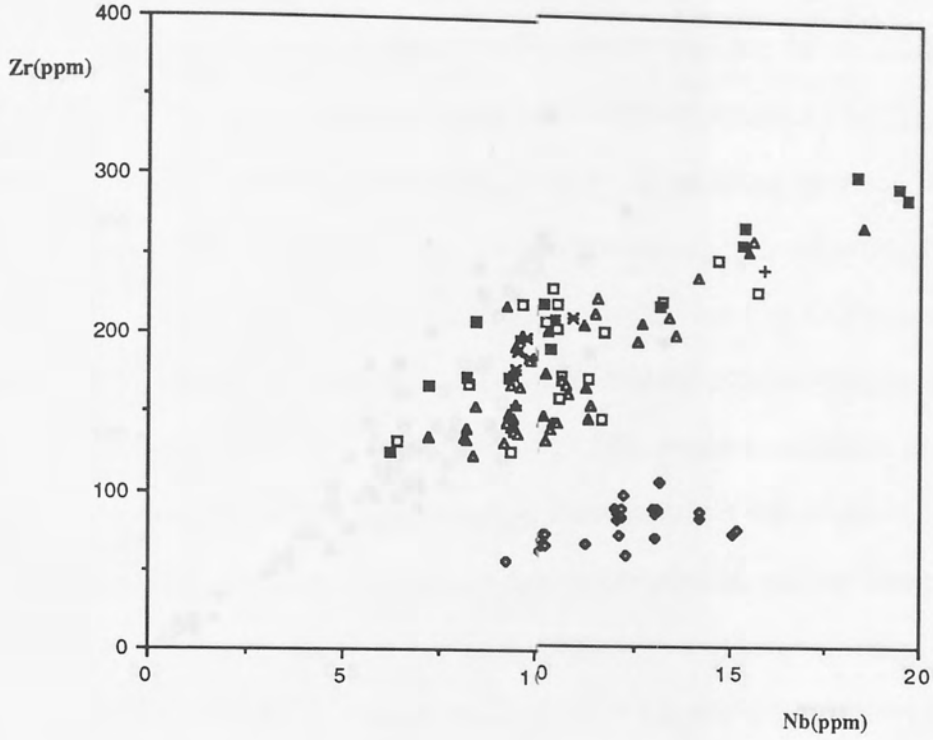

Figure 3.7a Zr-Nb plot for minor intrusions and lavas. Symbols as in Figure 3.2.

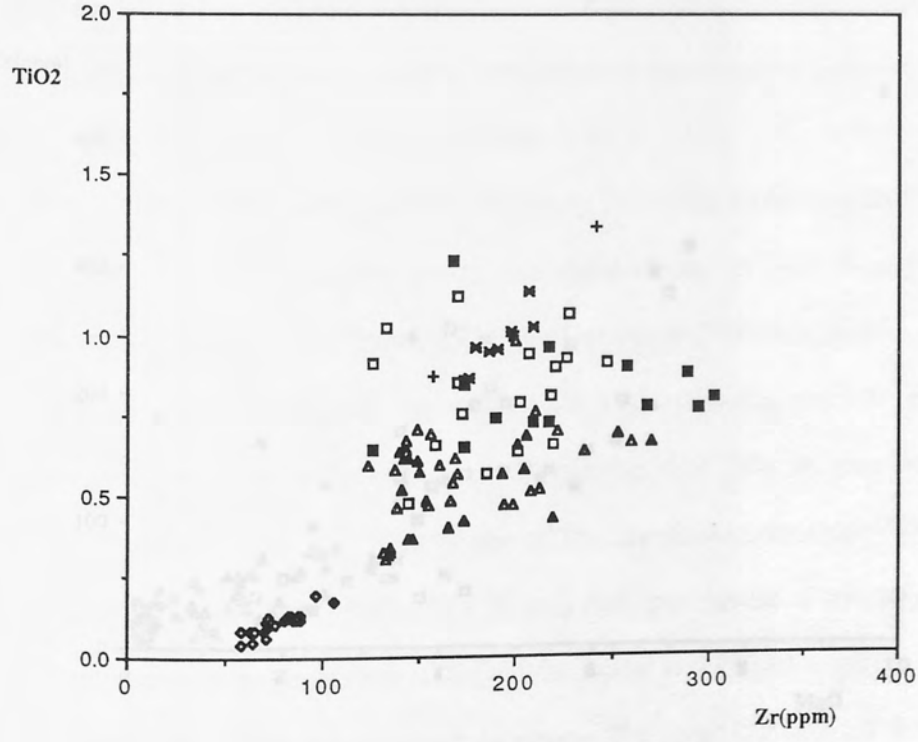

Figure 3.7b TiO_2-Zr plot for minor intrusions and lavas. Symbols as in Figure 3.2.

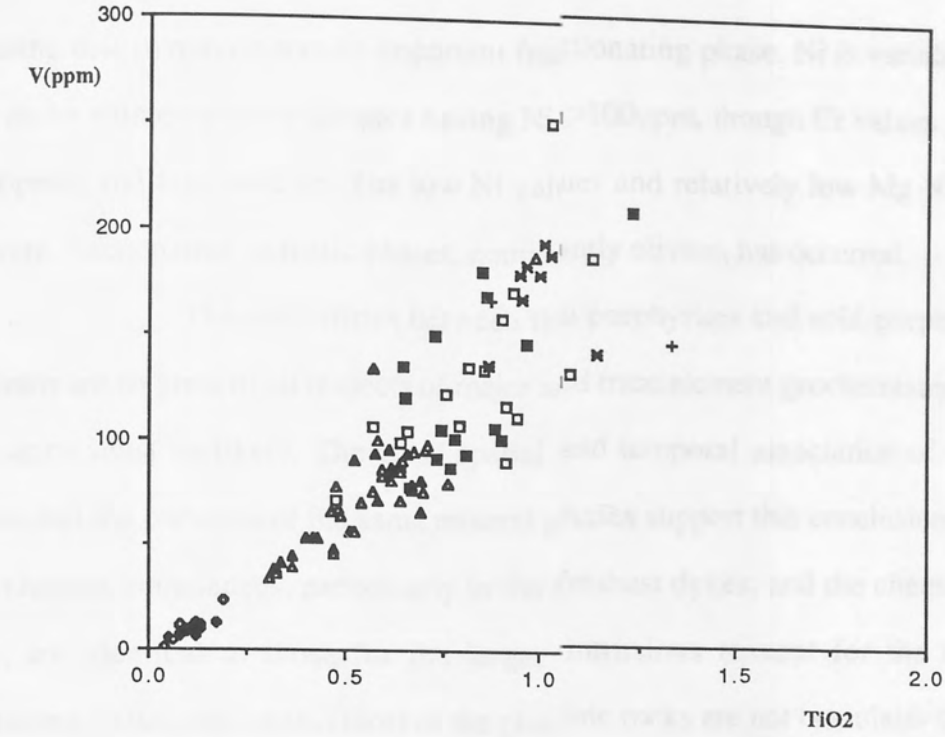

Figure 3.8a V-TiO_2 plot for minor intrusions and lavas. Symbols as in Figure 3.2.

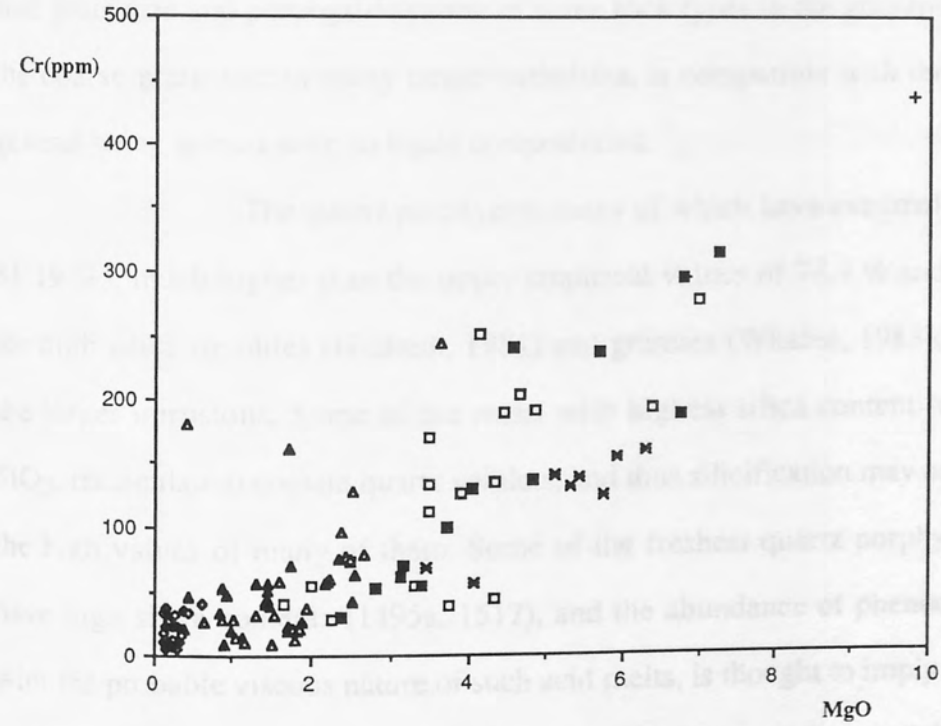

Figure 3.8b Cr-MgO plot for minor intrusions and lavas. Symbols as in Figure 3.2.

indicating that pyroxene was an important fractionating phase. Ni is variable in the most basic rocks with only three samples having Ni >100ppm, though Cr values are higher (up to 300ppm) and less variable. The low Ni values and relatively low Mg Numbers imply that some fractionation of mafic phases, dominantly olivine, has occurred.

The similarities between the porphyrites and acid porphyrites and the granitoids are so great in all respects of major and trace element geochemistry that a genetic association must be likely. The close spatial and temporal association of the dykes and plutons and the presence of the same mineral phases support this conclusion. The fact that trace element abundances, particularly in the freshest dykes, and the chemical trends for these, are identical to those for the larger intrusions (except for the olivine norite "cumulates") also implies that most of the plutonic rocks are not cumulates (*sensu stricto).* Cumulates would have enrichments in trace elements compatible with the fractionating phases e.g. Ni, Cr, Sr and depletions in elements incompatible with these phases e.g. Rb. If the granitoids were cumulates, they should show enrichments in Sr, Ni and Cr, and depletions in Rb and K relative to the dykes (liquids) which are not present. The relatively fine grain size and porphyritic nature of some rock types in the granitoids, compared with the coarse grain size in many larger batholiths, is compatible with the plutonic rocks in general being at least *near* to liquid compositions.

The quartz porphyries, many of which have extremely high silica (up to 81.19 %), much higher than the upper empirical values of 74.4 % and 78.50 % reported for high silica rhyolites (Hildreth, 1981) and granites (Whalen, 1983), are not present in the larger intrusions. Some of the rocks with highest silica content (e.g. 1498: 81.19% SiO_2, recalculated) contain quartz veinlets, and thus silicification may account for many of the high values of many of them. Some of the freshest quartz porphyries however also have high silica contents (1495a, 1517), and the abundance of phenocryst quartz, along with the probable viscous nature of such acid melts, is thought to imply that some samples are SiO_2-rich because of accumulated quartzes. The large quartz crystals are interpreted as phenocrysts, as opposed to their being of xenocrystic origin, because many have euhedral

to subhedral shapes and do not have reaction rims (Plate 3.3). Although some resorption features are present, as in rhyolites in general, they merely indicate a change in the physico-chemical conditions in the magma.

The quartz porphyries are the only dykes with colourless to pale-green mica in fresh rocks showing similarities to the S-type Fleet pluton and the interior of the Criffell pluton. The presence in some dykes of large glomeroporphyritic aggregates of quartz and alkali feldspar with graphic intergrowths is unusual (Plate 3.4). The coarse nature and anhedral shapes of these aggregates and the phases in them may imply that they are xenoliths, although no reaction relationships are obvious.

The distinctive geochemical grouping of the quartz porphyries, away from the porphyrite-acid porphyrite and granitoid trends, implies that a direct genetic relationship between them is unlikely. A model for their evolution by greater amounts of contamination than for the less evolved dykes does not account for the overlap of some elements (SiO_2, CaO and MgO) and the distinct and separate grouping for others (Ti, Zr), or the distinct grouping on a Zr-Nb plot. The values for Ni and Nb are higher than those found in many of the acid porphyrites and may be accounted for by a separate derivation. If indeed these are from a different source to that for the less silicic dykes, then they are a restricted compositional group, nevertheless spatially associated with the other rocks.

It is possible the quartz porphyries represent small degree partial melts of the crust. The aggregates of quartz-feldspar with graphic intergrowths could thus be interpreted as remnants of partially-melted country rock. Calculated melts from a study of graywacke xenoliths in the Loch Doon pluton (Tindle & Pearce, 1983) have similarities to the quartz porphyries e.g. low Al_2O_3 and CaO; however the femic constituents are quite high in these calculated melts. The melt fractions calculated by these authors were however large (69-88%) since these xenoliths were probably sitting "*stewing* " in a magma chamber for a long period of time. Smaller degrees of partial melting e.g. around the margins of plutons would probably yield melts with higher SiO_2 and lower MgO contents. An isotopic study would be necessary in order test this crustal melt hypothesis for the quartz

porphyries. Because the isotopic ratios in the plutons are well constrained for Priestlaw and Cockburn Law, and are very different from the greywackes (chapter 2), a Rb-Sr and Sm-Nd isotopic study would provide a good test. The association of the quartz porphyries with the plutons would not be unexpected because the magmas for the plutons could provide the necessary heat for crustal melting.

3.8 Summary

(1) A series of dykes varying from porphyrite (54% SiO_2) to quartz porphyry (81% SiO_2) occur closely associated with numerous small granitoid bosses in the eastern Southern Uplands.

(2) The phenocryst assemblages and some of the textural features of the porphyrites and the more evolved acid porphyrites are similar to those in the spatially and temporally associated plutons.

(3) Major and trace element characteristics of the porphyrites and acid porphyrites are identical to those of the associated exposed plutonic rocks implying that the dyke rocks are merely more finely grained, porphyritic varieties of the plutons. The plutons therefore are probably quite close to liquid compositions and are not "cumulates"(*sensu stricto*)

(4) The quartz porphyries are geochemically a distinct and separate group (Figures 3.3, 3.4, 3.7a) and they are thought not to be genetically linked to the more basic dykes. It is postulated that they represent small degree partial melts of country rock, either Lower Palaeozoic greywackes or possibly deeper crustal melts. The heat source for melting is likely to have been the basic/intermediate magmas of the plutons, thus the close spatial and temporal association with the plutons and other less evolved dykes is explained.

Chapter 4: Late Caledonian dyke swarms of south-eastern Scotland 2: Lamprophyres.

4.0 Abstract

Calc-alkaline lamprophyre (minette) dykes in the eastern Southern Uplands form part of a swarm nearly parallel to the inferred Iapetus Suture, stretching from the Ards Peninsula of Northern Ireland to St. Abbs Head in the east of Scotland. The dykes are clustered close to several small granitoid bosses (chapter 2), but appear to be younger than the plutons and their associated porphyrite-porphyry dykes. Mica- (minette and kersantitic-minette) and hornblende-lamprophyres are present further west near Hawick where no intermediate-acid plutons or dykes occur. The lamprophyres have enrichments in LILE and LREE and relative depletions of HFS elements typical of subduction related ultra-potassic magmas. These incompatible element enrichments are present in rocks with high Mg number and Ni and Cr contents, which combined with experimental constraints, their fine grained nature and presence of chilled margins, imply a near primary status for the least evolved varieties. High values of LREE, LILE, La/Nb, La/Yb, ε Sr and low ε Nd imply derivation from a previously metasomatised source. The minettes were probably derived from a source containing garnet and phlogopite, and the hornblende varieties from a shallower source in the stability field of amphibole. The minettes of the eastern Southern Uplands have not provided a parental component to the 410 Ma. granitoids which were derived from more depleted source. Emplacement of lamprophyre dyke swarms is likely to be structurally controlled, and the presence of these swarms in the Southern Uplands may indicate the presence of large faults of Caledonian trend below the Lower Palaeozoic sediments.

4.1 Introduction

Calc-alkaline lamprophyres are a widespread and, until recently, much neglected group of rocks (Rock, 1984). They are porphyritic dyke rocks rich in amphibole and/or phlogopite and in both ultramafic related (Mg, Ni, Cr), and incompatible (e.g. K, Na, Ba, Sr), elements. Nomenclature for these rocks is defined on the proportions of amphibole to biotite and plagioclase to K-feldspar (Table 4.1). Close compositional equivalents to the lamprophyres are found amongst members of the the absarokite-shoshonite-banakite rock series of rocks (Joplin, 1968). Although they are similar in some respects to other high-K rocks such as lamproites and leucitites, their enrichments are less extreme.

	Dominant mafic mineral	
	Biotite-phlogopite	amphibole
Dominant feldspar		
K-feldspar	Minette	Vogesite
Plagioclase	Kersantite	Spessartite

Table 4.1. Lamprophyre rock types based on Streckeisen (1979).

Worldwide calc-alkaline lamprophyres have three apparent petrological associations (Rock, 1984). These are with:

(A) calc-alkaline granitoid plutons

(B) shoshonitic volcanic and sub-volcanic suites

(C) appinite-breccia-pipe complexes.

The actual chemical and mineralogical definition of calc-alkaline lamprophyre in the past has been ambiguous. A series of chemical and mineralogical screens are used to separate them from related rocks (Rock, 1984), and the reader is referred to this paper for further details. The close association of granitoids with appinites and the heteromorphic nature of the latter with spessartites (Barnes *et al.* 1986) indicates that associations A and C are genetically related. Calc-alkaline lamprophyres (hereafter referred to simply as lamprophyres) are considered to be petrogenetically linked with subduction because of their close association with shoshonitic rocks in island arcs and on continental margins, and their emplacement both during and immediately following subduction.

It has been suggested that lamprophyres represent parental magmas to calc-alkaline granitoid (Leat *et al.* 1987; Rock & Hunter, 1987; Suzuki & Shiraki, 1980) and syenitoid plutons (Thompson & Fowler, 1986). Although in some instances emplacement of lamprophyres is later than that of the associated plutons (Turpin *et al.*

1988), in many instances field and isotopic data show *contemporaneity* of lamprophyres with associated plutons (Macdonald *et al.* 1986) and acid magmas (Rock & Hunter, 1987).

4.2 Origin of lamprophyres

A plethora of models for the origin of lamprophyres have been published, and are summarised in Rock (1984). There is agreement amongst modern workers that the high Mg numbers, Ni and Cr contents are indicative of a mantle source since they are high enough to be in equilibrium with a peridotitic source region. Some of the clearest evidence in support of this comes from the Navajo (e.g. Thumb, Buell Park) area of south western U.S.A. (Ehrenberg, 1982; Roden, 1981). Garnet peridotite xenoliths entrained in minette from the Thumb equilibrated within a restricted depth range (100-120 km) and at temperatures of 950-1250 °C (based on the geothermobarometric calculations of Ehrenberg, 1982), thus confirming the deep mantle origin of the minettes. Some of these peridotites also contain phlogopite in apparent textural equilibrium with surrounding anhydrous phases. The parental magmas are thought to have formed from very small degrees of partial melting of a garnet peridotite containing accessory phlogopite and apatite (Roden, 1981), and the compositional range of the minettes from mafic to felsic, was probably produced by fractional crystallisation (Roden, 1981). The abundance of lherzolite inclusions (xenoliths) in the felsic rocks (Ehrenberg, 1977; Roden & Smith, 1979) indicates that the differentiation process occurred in the uppermost mantle (Ehrenberg, 1977). The variation in isotopic ratios from mafic (lower εSr & higher εNd) to felsic compositions along with the occurrence of crustal xenoliths was taken to indicate that most, if not all, of the minettes have been contaminated with continental crust or lithospheric mantle or recycled material (Alibert *et al.* 1986). Isotope characteristics of megacrystalline xenoliths from the Thumb are similar to those of ocean island basalts (OIB) and are unlike any minette. If the xenoliths had previously crystallised from the minette magma it would imply that the minettes had undergone contamination.

Several authors have proposed an origin in a previously metasomatised mantle enriched in LILE and light REE (Bachinski & Scott, 1979; Jones & Smith, 1983; Venturelli *et al.* 1984), and it has been suggested that ancient subcontinental mantle, involved in the collision zone of the Sunda arc, is the source of the high-K lamprophyres found in that area (Varne, 1985). Additional evidence for a source in old lithospheric mantle comes from Pb isotope ratios found in lamprophyres across the Hercynian belt of Europe identical to those measured on Hercynian continental crust. These ratios combined with a Sr and Nd isotopic and geochemical study, were used to discount upper level assimilation and to propose an origin by melting lithospheric mantle enriched by recycled crustal material (Turpin *et al.* 1988). Minettes associated with syenites in north west Scotland have a proposed deep *asthenosphere* source, modified by *infusion* from previously subducted lithosphere (Thompson & Fowler, 1986).

Metasomatism of depleted mantle by fluids derived from two different sources has been suggested for lamprophyres in northern England (MacDonald *et al.* 1986): (1) incompatible element enrichment from aqueous subduction-related fluids and (2) HFS element enrichment from CO_2-rich fluids related to degassing sub-lithospheric sources.

Ultrapotassic rocks (e.g. lamproites, leucitites) from Leucite Hills and West Kimberly appear to be of the same magmatic lineage as minettes, but with more extreme enrichments in incompatible elements (Menzies & Hawkesworth, 1987). These enrichments in both groups of ultrapotassic rocks led Rock (1984) to propose that lamprophyres are produced by crustal modification of K-rich lamproitic or leucititic magmas.

Experimental studies have been confined to minettes and Ruddock & Hamilton (1978a,b) showed that in the Di-Lc-Qtz system minette magmas would yield phlogopite+diopside+sanidine+quartz. This is not an equilibrium assemblage, however it can be accounted for if minettes represent chilled liquids and are thus not necessarily crystal

mushes (Rock, 1984). A comparison between experimental results and natural minettes of the Thumb implies that mafic minettes preserve a near-liquidus assemblage crystallised in the upper mantle ($fO_2 \geq QFM$) in the presence of a H_2O-bearing phase (Esperanca & Holloway, 1987). These authors also showed that in primitive minettes, the preservation of olivine in equilibrium with phlogopite phenocrysts can be explained by lamprophyre magmas brought to near surface conditions at temperatures of 1,000-1,200 ^{o}C and chilled rapidly. This thus precludes a process dominated by AFC in a shallow magma chamber.

4.3 Late Caledonian lamprophyres of Britain

Late Caledonian lamprophyres are spatially and temporally associated with many of the *Newer Granites* throughout Scotland and with syenites in the Northern Highlands (Figure 4.1). They occur across the entire Caledonian Belt from the Lewisian foreland (Rock *et al.* 1987) to the English Lake District (MacDonald *et al.* 1985). Many are spatially associated with Permo-Carboniferous and Tertiary dyke swarms, intruded parallel to Caledonian trends, but are distinguished on petrological and geochemical grounds (Morrison *et al.* 1987).

The association of lamprophyres with syenites (association B of Rock, 1984), although locally developed within some dykes (MacDonald *et al.* 1986), is restricted to the Northern Highlands (Figure 4.1). A major and trace element study of these syenites (Thompson & Fowler, 1986), showed that minettes are close analogues to parental magmas, which have subsequently undergone fractional crystallisation. These authors proposed an asthenospheric source for the parents as opposed to the multi-source origin suggested for the Lake District lamprophyres (MacDonald *et al.* 1985).

A preliminary study of lamprophyres across a traverse of the Caledonides (Rock *et al.* 1988) showed that Sr, Ba, P, Rb, Y, Zr, Nb and possibly K increase outward from a minimum in central Scotland both northward and southward and that K/Th increases monotonically from the Lake District to north-west Scotland.

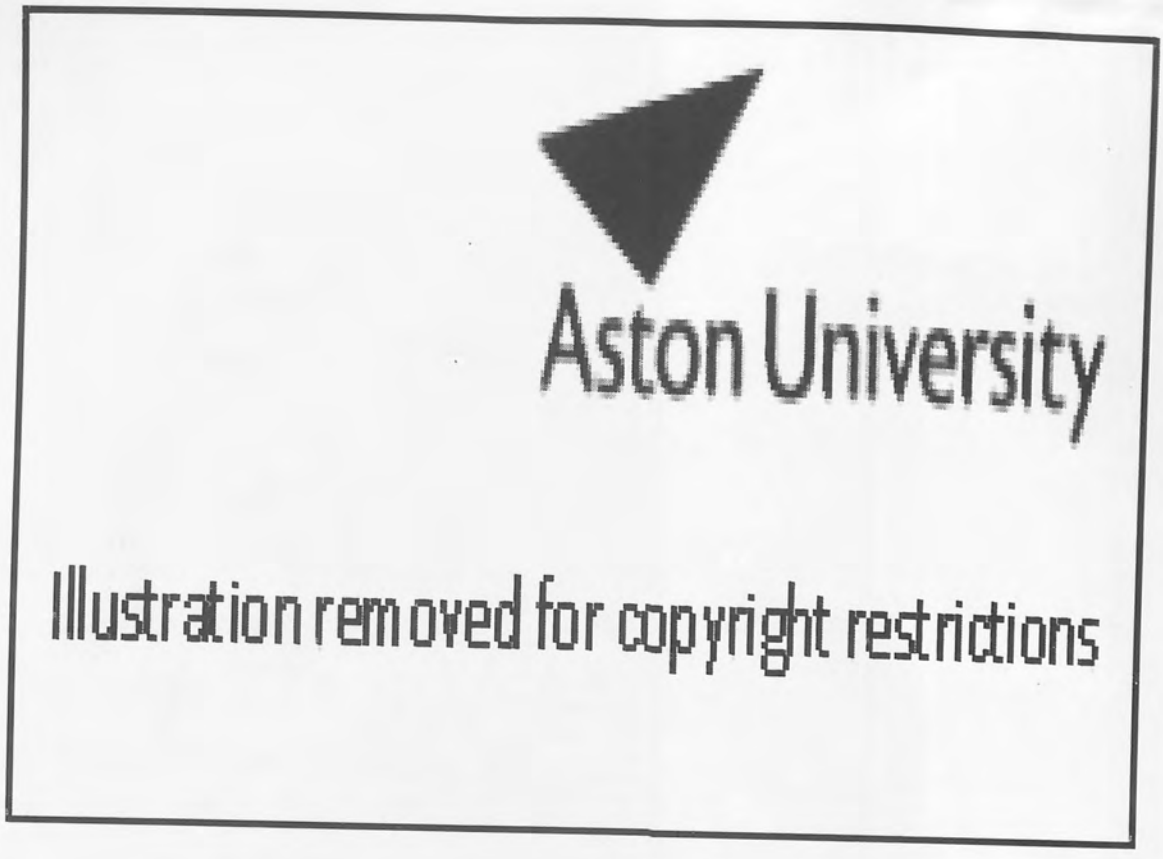

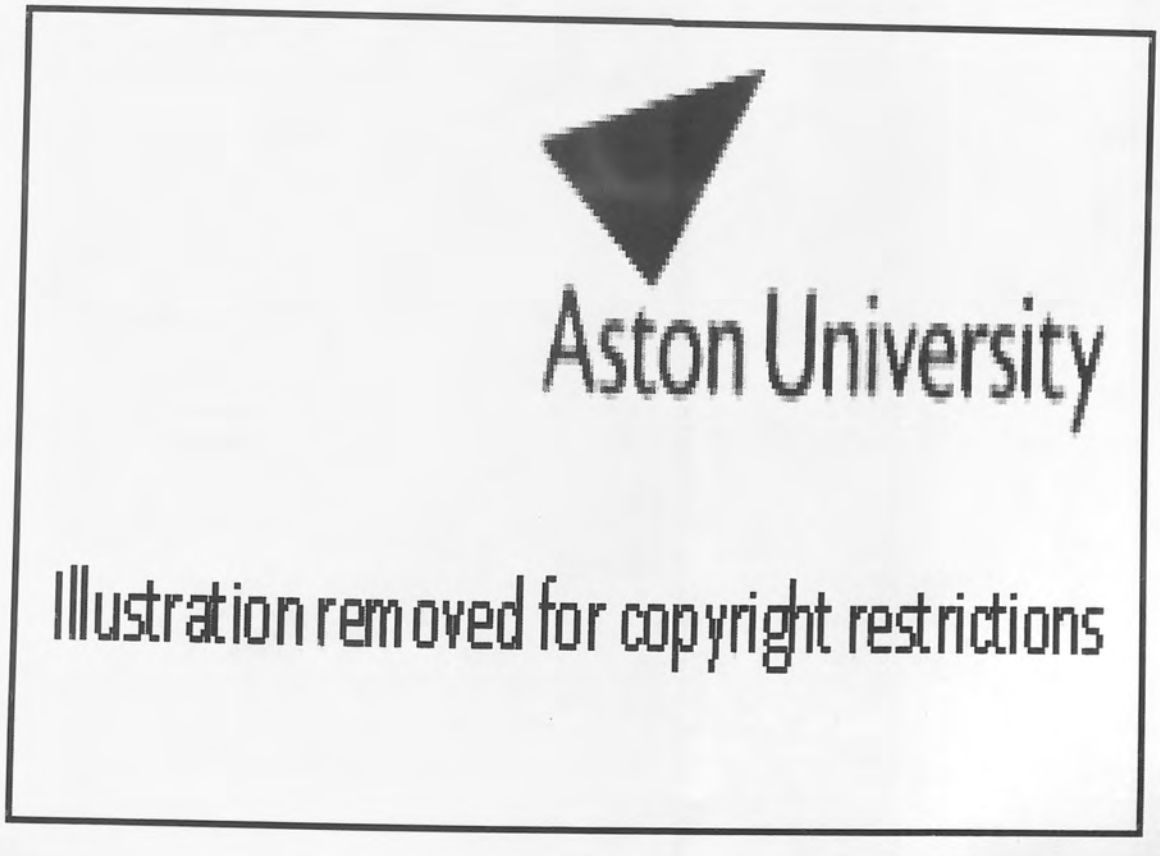

Figure 4.1 Map of Scotland showing Late Caledonian lamprophyres and associated granitoid plutons (from Rock *et al.* 1988).

The close spatial and temporal association of many lamprophyres with the zoned I-type plutons has led to the suggestion that these lamprophyric magmas represent a postulated high Sr, Ba, K parent for many of these plutons (Harmon *et al.* 1984). The *Newmains* dyke (spessartite) in southwest Scotland has variation from hornblende- and pyroxene-rich cumulates to patches of quartz syenite and granite. The syenites are explained by fractionation of the lamprophyric magma and the granites by contamination of that magma by the graywacke country rocks (MacDonald *et al.* 1986). These authors further suggested that lamprophyres may have been parental to the nearby Criffell pluton and possibly all Caledonian granitoids. The intimate relationships of lamprophyre dykes with composite and multiple sheets, varying from "malchite" [lamprophyric, plagioclase-phyric (quartz)-micro (monzo) diorites] to microgranites around the Ross of Mull pluton, was also taken to be evidence of the parental role of lamprophyres in the genesis of granitoids (Rock & Hunter, 1987).

The intrusion of lamprophyres, as well as other Late Caledonian rocks, is likely to have been structurally controlled by deep Caledonian lineaments (Smith, 1979; Watson, 1984; Wright & Bowes, 1979). It is worth noting in this context the distribution of lamprophyres in the Southern Uplands where basement is covered by Lower Palaeozoic sediments. A regional zone of lamprophyres ca. 10km wide and >300km long stretches from the Ards Peninsula in Northern Ireland to St. Abbs Head (Figure 4.2) (Rock *et al.* 1985). This zone is dominated by mica-bearing lamprophyres away from plutons and hornblende-bearing varieties around plutons, however both mica- and hornblende-bearing varieties occur close to the Criffell pluton. Lamprophyres (mainly hornblendic) are also clustered around the Loch Doon pluton further north.

4.4 Sampling and aims of chapter

26 samples, from 13 dykes, were collected from the area of exposed plutons and intermediate to acid dykes in the eastern part of the Southern Uplands. These were analysed

Aston University

Illustration removed for copyright restrictions

Figure 4.2 Distribution of lamprophyre dykes in southern Scotland (from Rock *et al*, 1988)

by XRF for both major and trace elements. The two freshest dykes (1388 & 1424) were analysed for Sr and Nd isotopic ratios and REE. The data set was augmented by 20 samples from 14 dykes in the vicinity of Hawick to the southeast, where abundant lamprophyres occur and are not associated with any Late Caledonian intrusions.

The aims of this chapter are several fold:

(1) to present new XRF, REE and Sr and Nd data from lamprophyres in southeastern Scotland to complement studies elsewhere in the Caledonides.

(2) to use this data to constrain the source(s) of lamprophyres

(3) to test whether the lamprophyre-granitoid association is genetic in the study area.

4.5 Field geology

The lamprophyres occur as thin (<3m), near vertical, dykes with chilled margins, and some exhibit flow layering (1443). Exposure is generally poor but some dykes can be traced for >100m along strike (PS192). The mica lamprophyres are generally fine-grained, dark grey to black in colour and have conspicuous microphenocrysts of biotite/phlogopite. Lamprophyres with large (up to 3mm) phenocrysts of mica typical of lamprophyres elsewhere in the Caledonides, are not present in the study area. Ovoid patches of calcite up to 18cm across are common near the margins of some dykes (PS1M) and throughout others (PS191). Hornblende-lamprophyres only occur around Hawick and generally have large, euhedral (PS220) to acicular (PS227M,MC) amphiboles in a grey-green groundmass, though in altered specimens (PS222) the groundmass is commonly pink.

Feldspathic globular structures (from 10mm to < 1mm) are common in both types of lamprophyre. These are usually most abundant closer to the chilled margin than the centre of the dykes (PS1, 221, 227M-C). The interiors of the dykes are more coarsely grained and where present globular structures are larger though less abundant.

Composite dykes with more evolved compositions are common in other parts of the Caledonides (Rock & Hunter, 1987), but are not present here. One poorly exposed dyke however (PS227M-227C) has variation from altered fine-grained hornblende-lamprophyre at the margin to a fresh hornblende-mica-lamprophyre at the centre, and will be referred to as a kersantitic spessartite. Quartz xenocrysts are common in most dykes and abundant xenoliths of quartzite up to 30cm (PS220) are present in two (1414 ,PS220). Similar inclusions are reported from other dykes as far west as Dumfries (Rock *et al.* 1985). The country rock graywackes are extensively brecciated and veined with calcite (PS184Br) adjacent to one dyke (PS184). Carbonate veinlets are relatively common within several others, and generally confined to within the intrusions (1473, PS173).

Most dykes are intruded into Silurian graywackes but two altered dykes (along strike from each other thus probably represent the same intrusion) intrude "Old Red Sandstone" lavas and also cut Lower Devonian conglomerates near St. Abbs Head. This dyke yielded a K-Ar biotite age of 400±9 Ma (Rock & Rundle, 1986). This age is younger than the Priestlaw and Cockburn Law intrusions dated ca.410Ma (Thirlwall, 1988), however both these dates are within error of each other. Field relationships also indicate a younger age for the lamprophyres i.e.

(1) several lamprophyre dykes (173-4,1473) are also seen to intrude the Lamberton Beach granite further east.

(2) one dyke (192,1415) is intruded into the metamorphic aureole of the Cockburn Law granitoid, but itself shows no sign of thermal metamorphism.

(3) Lower Devonian conglomerates, containing granitoid clasts similar to Cockburn Law, unconformably overlie the intrusion and as mentioned above these sediments are intruded by a lamprophyre dyke. No cross cutting relationships with the porphyrite-porphyry series dykes are present.

4.6 Petrography

(a) Mica lamprophyres: Where feldspar is fresh and can be identified, the mica-lamprophyres are all minettes (Plate 4.1). Kaolinisation is the main feldspar alteration product, however in most dykes patches of K-feldspar are generally preserved, thus it is likely that most if not all these mica-lamprophyres are minettes.

The dominant phenocrysts are (20-60%) castellated, pseudo-hexagonal biotite/phlogopite and they are pale brown in colour and have dark-brown rims (one probe analysis from the centre of a phenocryst shows it to be a Ti-rich phlogopite; Table 4.2). The phenocrysts are small (≤1mm) and generally fresh even in rocks which appear extremely altered. Flow alignment of phlogopite is conspicuous in one dyke (1443). Pseudomorphs after euhedral olivine (≤4mm) are present in most dykes. The olivine is replaced by 'pilite' (Velde, 1968) or chlorite + opaque oxides and in one dyke (1421-3) by quartz + opaque oxides (Plate 4.2). Small remnants of fresh olivine were seen in only one dyke (PS227M). Fresh phenocrysts, and microphenocrysts, of clinopyroxene occur in one dyke (1388, PS191), however in the majority they are commonly replaced either by carbonate or in a few instances by quartz and chlorite. The dominant groundmass phase is K-feldspar which occurs most commonly as sub-radiating sheaves (Plate 4.1), which, although extremely fresh in several dykes (1424, 1452), is variably replaced by patchy (1388) to extensive (225) kaolinisation.

1388 Phlogopite core

SiO_2	TiO_2	Al_2O_3	FeO	MnO	MgO	CaO	Na_2O	K_2O	Cr_2O_3	NiO	Total
39.23	4.33	15.81	5.97	0.00	20.96	0.02	0.00	6.72	0.63	0.12	93.78

Table 4.2. Probe analysis of phlogopite core from minette (1388).

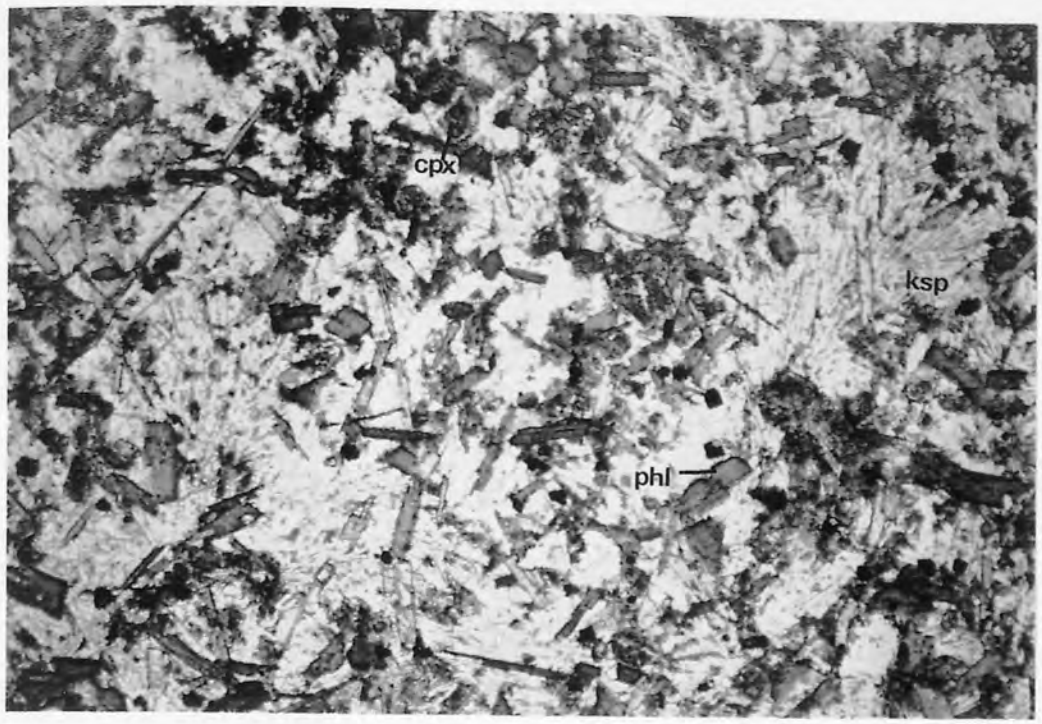

Plate 4.1. Minette (1424) showing micro-phenocrysts of phlogopite (phl) with dark rims and altered clinopyroxene (cpx), in a groundmass of fresh sub-radiating sheaves of K-feldspar (ksp) and opaque oxides. Fov: 3.4mm.

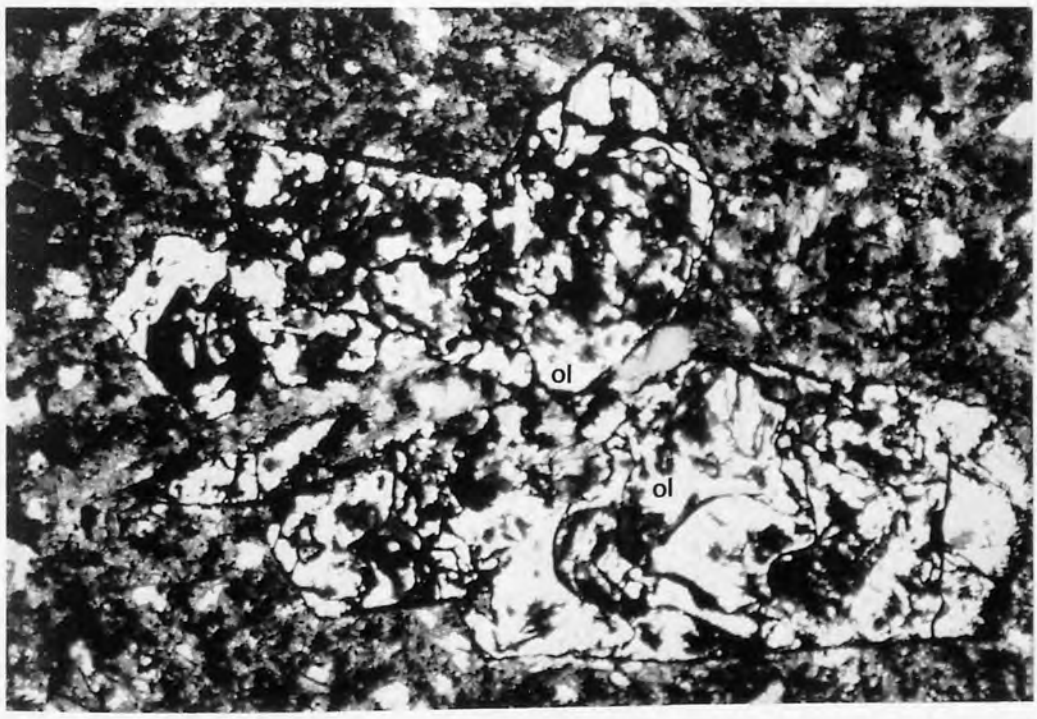

Plate 4.2. Quartz-hematite-opaque oxide pseudomorphs after phenocryst olivine (ol), in the altered St. Abbs dyke (1422). Fov: 3.4mm.

Accessory phases include interstitial quartz and relatively abundant acicular apatite occurring both in the feldspathic groundmass and as numerous inclusions in phlogopite (Plate 4.5). Subhedral opaque oxides (magnetite or titano-magnetite) and interstitial carbonate are scattered throughout the groundmass and thin irregular veinlets of carbonate cut some specimens (173,1473).

"Globular structures" (Rock, 1984), up to 4cm in diameter, are a ubiquitous feature of the mica lamprophyres and generally increase in size towards the centre of dykes. These structures are generally sharply defined from the rest of the rock by their much lower colour index and have rims of tangential phlogopite (Plate 4.3), though some however partly merge with the host rock. Shapes vary from spherical, which is the most common (PLate 4.4) to 'flattened'. Sometimes one globule occurs enclosing another, and larger structures appear to comprise several *coalesced* smaller bodies. Stellate sheaves of K-feldspar are dominant (60-90%) in the structures with quartz, chlorite and carbonate being more common in the larger structures towards their centres. Graphic intergrowths of quartz and K-feldspar are present in larger structures, phlogopite occurs in coalesced ones, and a small (<<1mm) euhedral amphibole occur in one large structure (1388).

Partly chloritised, larger, subhedral, dark-brown, biotite crystals containing abundant anhedral inclusions of opaque oxides are present in several bodies. These are similar to biotites of the country rocks and are thought to be xenocrysts. Other xenocrysts are partially resorbed quartzes (Plate 4.5) a few which have reaction rims of chlorite (probably after clinopyroxene or biotite), and a few resorbed, and extremely altered, plagioclases. One very altered dyke (1414) contains abundant rounded quartzite xenoliths (Plate 4.6).

(b) Hornblende lamprophyres: As mentioned in the previous section these are only found amongst the Hawick suite and are much less numerous than mica-lamprophyres. Spessartites are the dominant type, however one dyke (PS227;

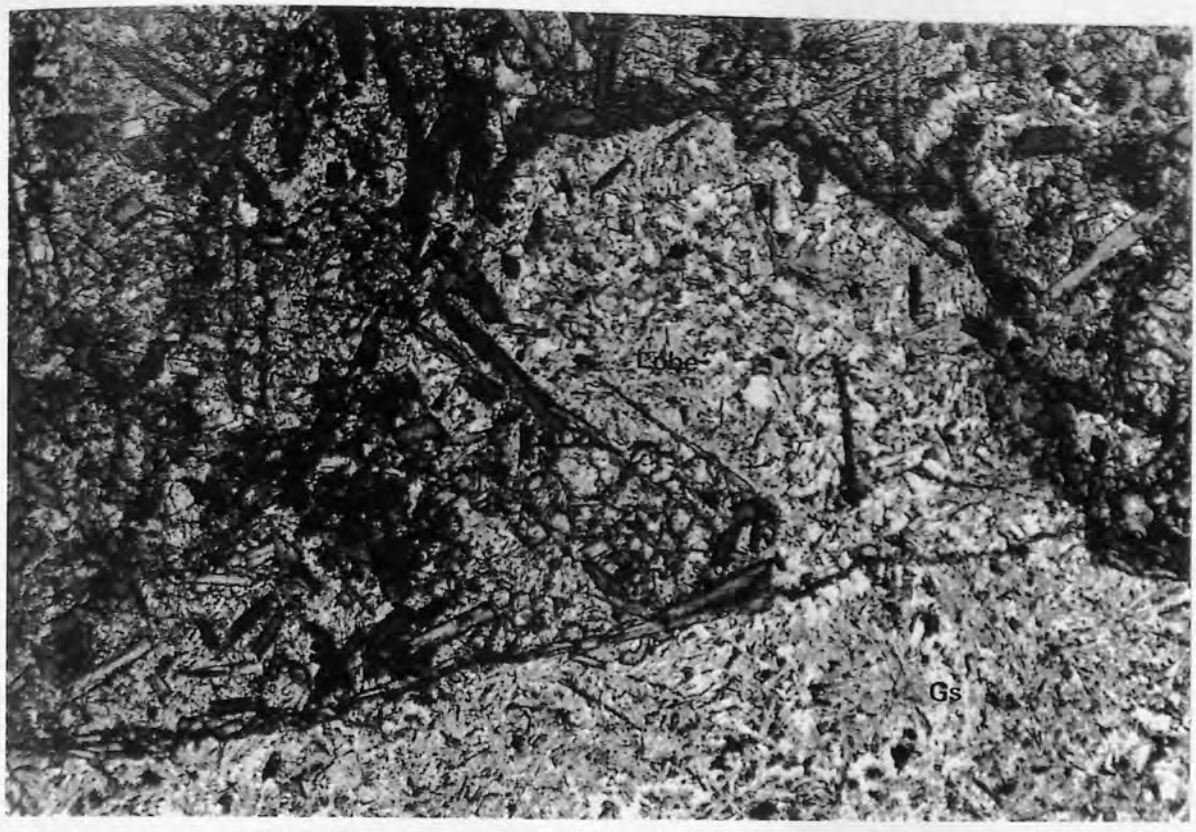

Plate 4.3. Globular structure (Gs) in minette (1388) with smaller coalesced globular lobe (Lobe). Note distinct tangential rim of phlogopite around structure. Fov: 3.4mm.

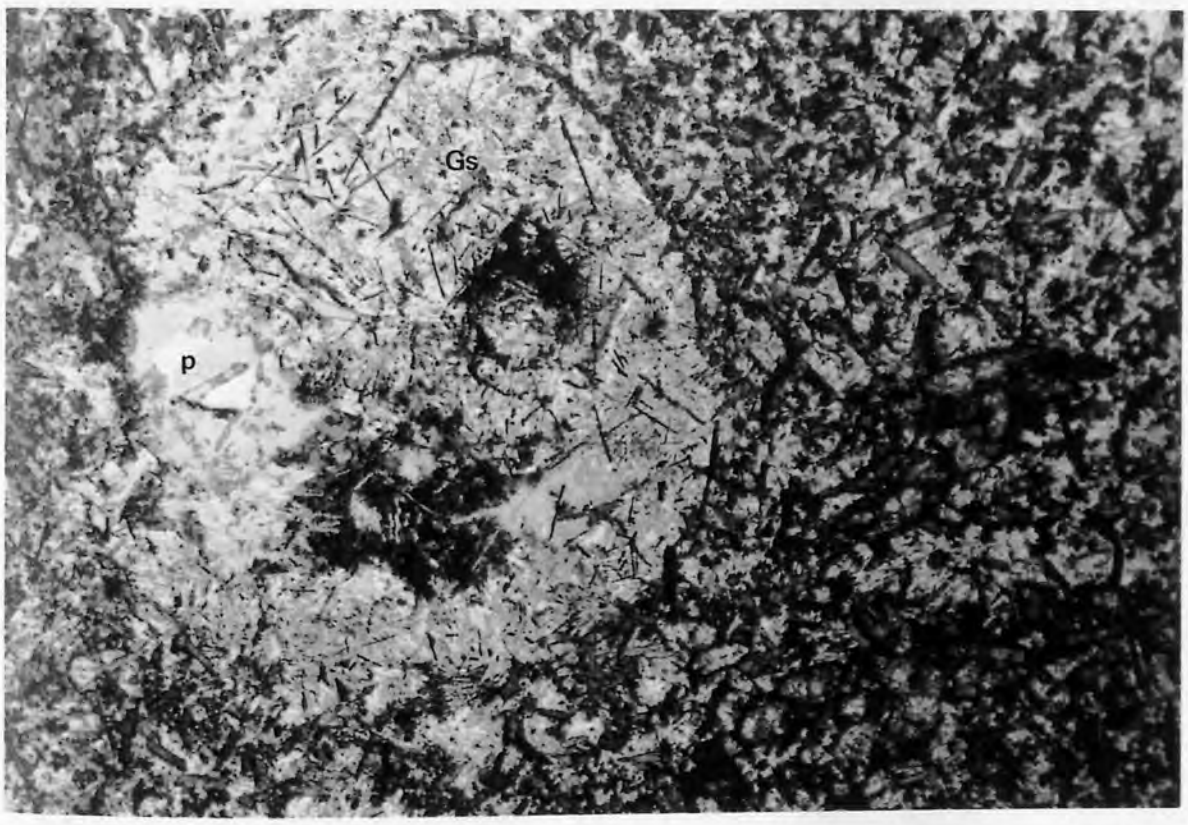

Plate 4.4. Large rounded globular structure (Gs) in minette (1424), composed dominantly of K-feldspar sheaves with minor biotite and patches of quartz-chlorite-carbonate (p) Fov: 8.3mm.

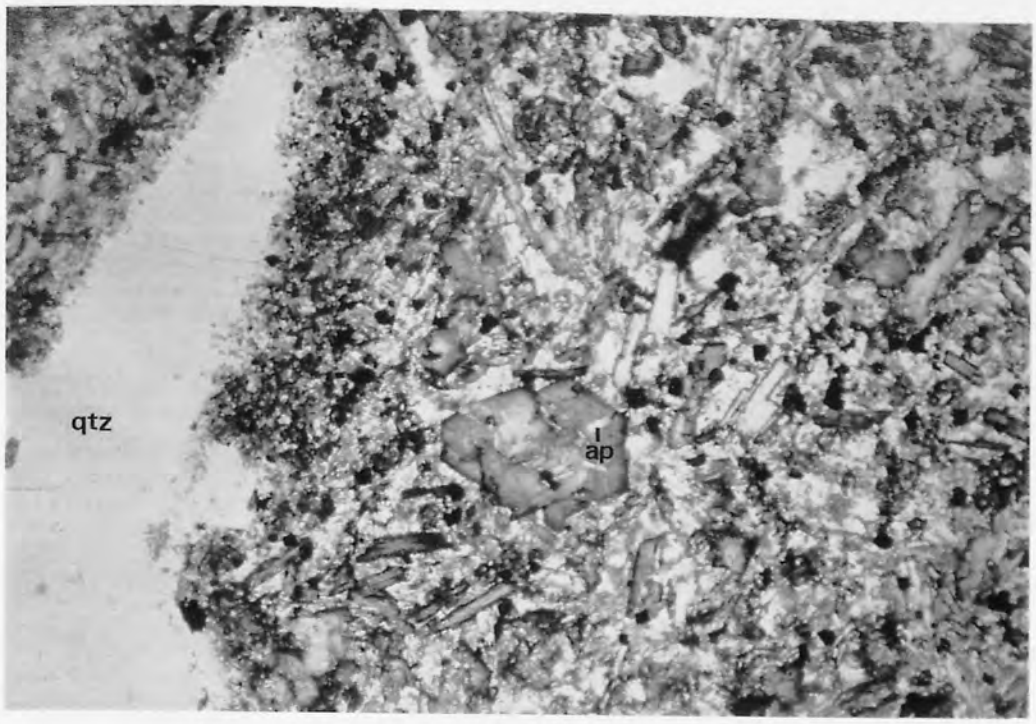

Plate 4.5. Partially resorbed quartz (qtz) xenocryst in minette (1415). Note abundant inclusions of apatite (ap) in phlogopite phenocryst near centre. Fov: 3.4mm.

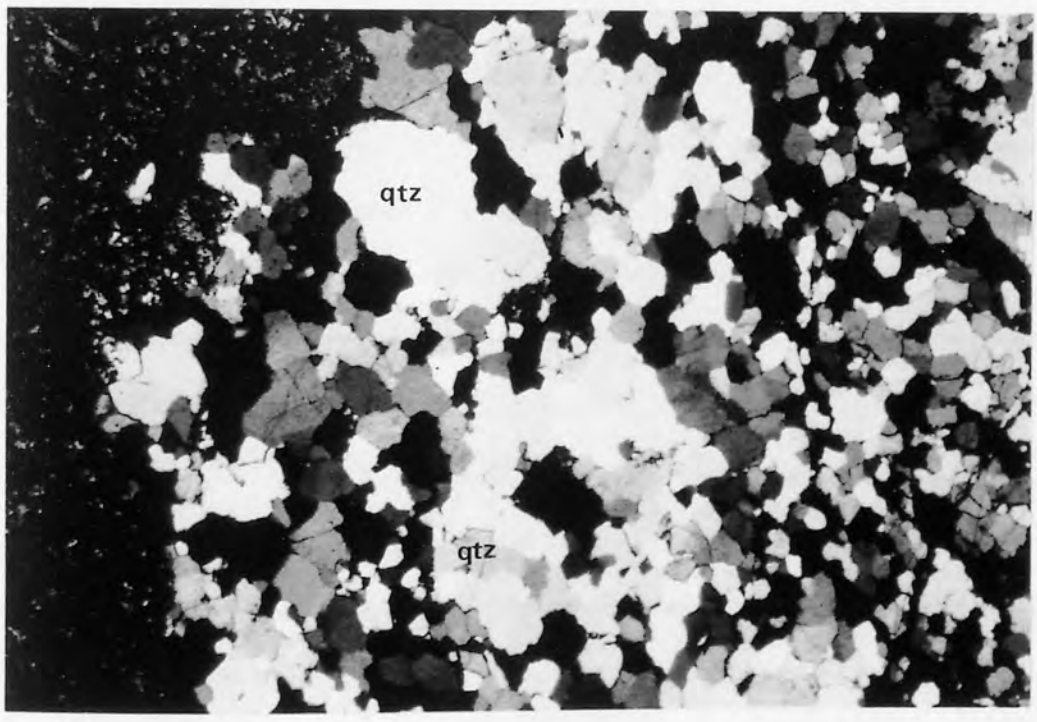

Plate 4.6. Rounded quartzite xenolith (qtz) in altered mica lamprophyre (1414). Note recrystallised texture and purity of the xenolith. Fov: 8.3mm.

kersantitic spessartite) varies from fine-grained spessartite, with some K-feldspar and phlogopite, to a hornblende-lamprophyre with abundant phlogopite (227C). The hornblende-lamprophyres typically have panidiomorphic, brown, amphibole phenocrysts (≤1cm) in more coarsely grained varieties (PS220), and the more finely grained rocks have acicular amphibole (PS227M,MC). The groundmass feldspar is plagioclase in euhedral to subhedral laths. In one dyke (PS220), the laths are enclosed in a pinkish fine grained groundmass (Plate 4.7). The feldspars, where altered are dominantly sericitised, though some kaolinite is common. Apatite is present as small squat prisms in the groundmass or as microphenocrysts. Opaque oxides are present but are not as abundant in these rocks as in the mica-lamprophyres. Quartz is a minor, interstitial phase.

Globular structures are confined to the more finely grained varieties and comprise up to 25% of parts of the dyke (227MC). They consist dominantly of sodic plagioclase with minor amphibole in a fine-grained mesostasis.

Xenocrysts of quartz, with reaction rims of chlorite, are commonly present and one fresh dyke (220) has abundant (ca. 60%), rounded, pure quartzite xenoliths (≤ 30cm diameter), showing partial, to almost complete, recrystallisation. Extremely small fluid inclusions are abundant particularly along grain boundaries and fractures in the quartzites. Spectacular reaction rims around the xenoliths of clinopyroxene are common, though pyroxene is not a constituent of the lamprophyre away from the margins of xenoliths. Inside the pyroxene rim is a zone where quartzite is replaced by a pinkish, feldspathic mesostasis containing abundant fine-grained and microcrystalline clinopyroxene (Plate 4.7). Adjacent to xenoliths some clinopyroxene is partially enclosed by brown amphibole identical to that found away from the xenoliths (Plate 4.8), implying that at least some crystallisation of amphibole occurred after entrainment of the xenoliths.

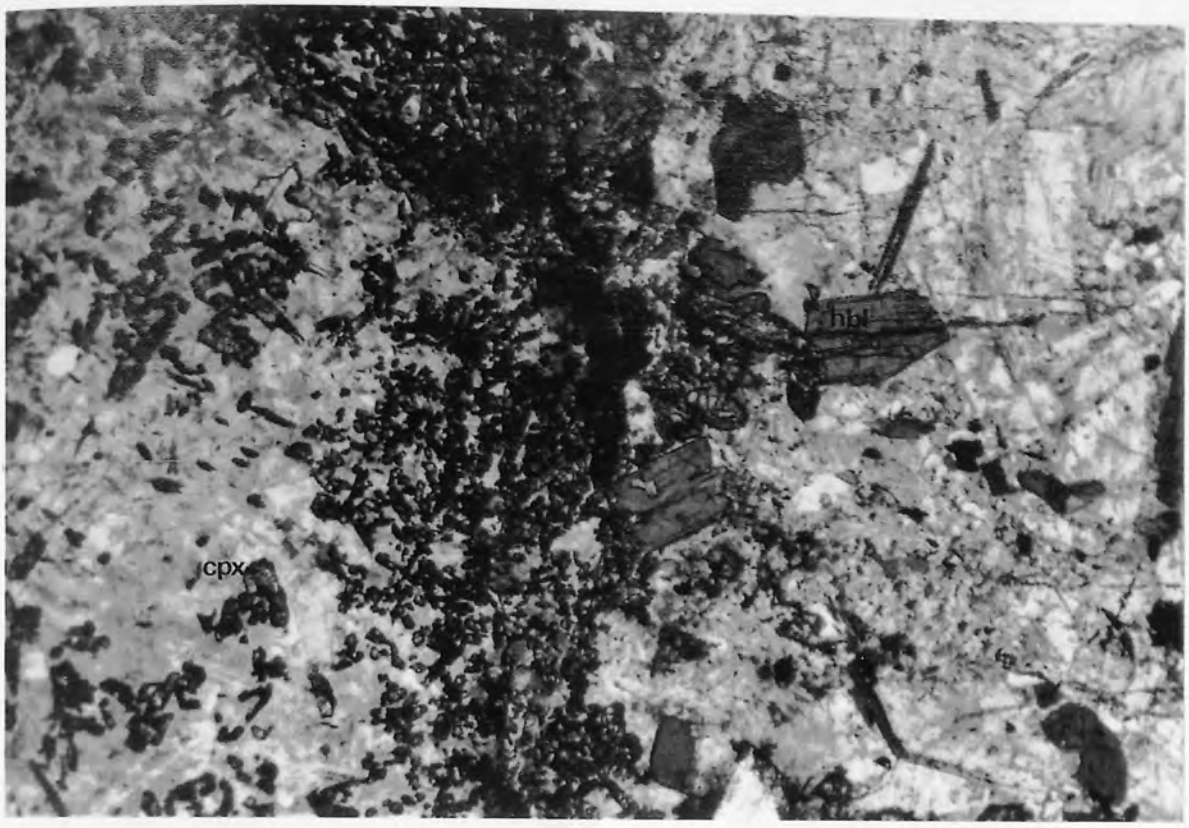

Plate 4.7. Rim of clinopyroxene developed around a quartzite xenolith, the latter of which is now replaced by feldspar and fine-grained clinopyroxene (left half), in spessartite, PS 220 (right half). Fov: 8.3mm.

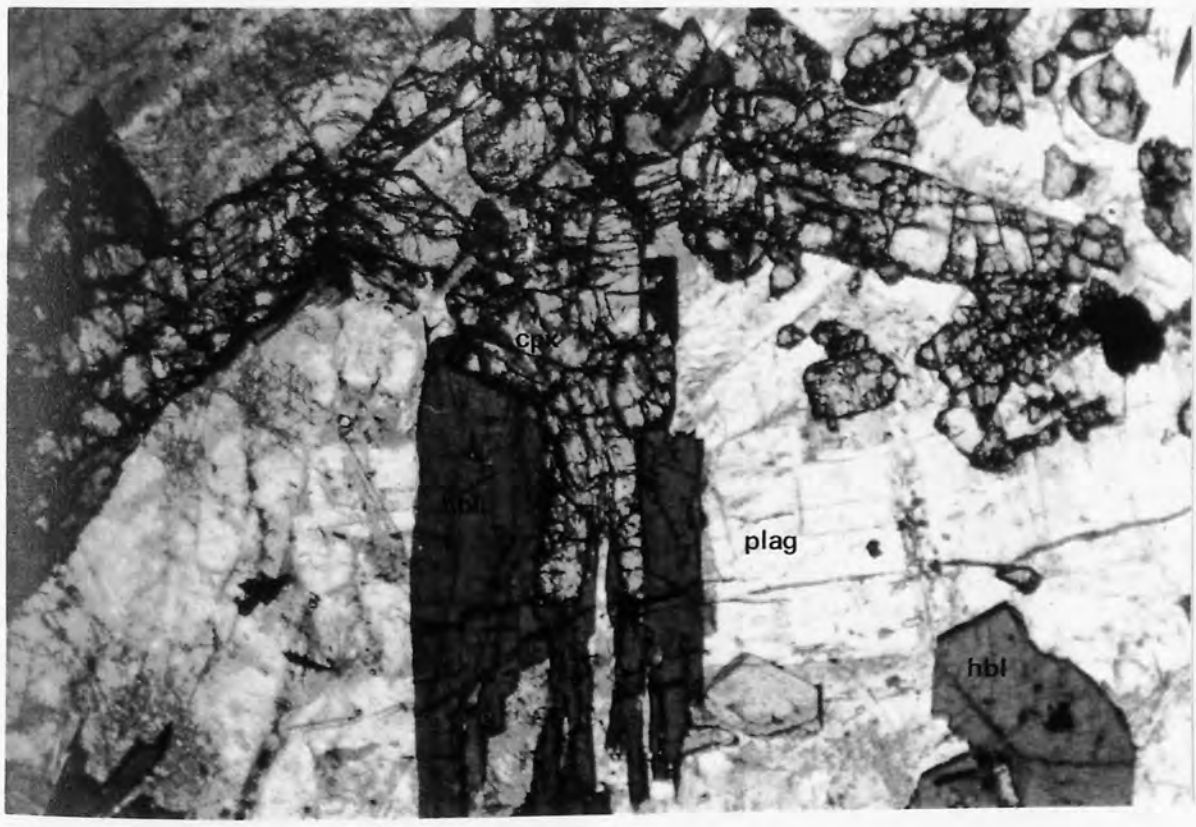

Plate 4.8. Clinopyroxene from rim of quartzite xenolith (see Plate 4.7), partially enclosed by brown amphibole in spessartite (PS220). Fov: 8.3mm.

4.7 Geochemistry

The lamprophyres vary from low (45%) to intermediate (64%) silica levels and plot in the fields of absarokites, shoshonites and banakites on a K_2O-SiO_2 diagram (Figure4.3). The major and trace element data are listed in Appendix 3c, however some typical analyses are given in Table 4.3.

High LOI (H_2O+CO_2) contents of the lamprophyres are believed to be primary (Rock, 1984) but may in part be due to alteration (carbonatisation, chloritisation) because very high CaO is associated with very high LOI (Appendix 3c), however the freshest rocks all have relatively high CaO (5-8%). A comparison of petrographically fresh rocks to altered ones indicates mobility of some elements implying that alteration leads to generally lower K_2O, P_2O_5, Al_2O_3 and Sr and a scatter for Na_2O and Ba (Figure 4.4 and 4.5) in altered relative to fresh samples. All the lamprophyres have high MgO contents, even those with the higher SiO_2 contents, and Mg numbers vary between 52 and 80, though the majority are in the range 70-80. Both mica- and hornblende-bearing varieties have similar values which are close to those expected for primary magmas in equilibrium with mantle peridotite. Ni and Cr contents are likewise very high being up to 317 ppm and 679 ppm respectively.

In fresh rocks Al_2O_3 is generally low but is variable. This is typical of magmas having formed from a deep source, with values of 13-15% for the mica-lamprophyres and 13-17% for hornblende varieties. Minettes from Hawick have higher Al_2O_3 contents at similar MgO than those further east (Figure 4.4a). There is an increase of Al_2O_3 with decreasing MgO (r=0.66) in the hornblende varieties implying that plagioclase fractionation has not been important. Al_2O_3/TiO_2 ratios are low and similar to MORB as is the case for the Lake District lamprophyres (MacDonald *et al.* 1985). There is little correlation with MgO for most elements in the mica-lamprophyres except perhaps Fe_2O_3 (Figure 4.4b), whereas correlations are relatively good for some elements of the hornblende-lamprophyres (K_2O, r=0.79; Na_2O, r=0.71; Figure 4.5). K_2O, Na_2O and

No.	1388	1422	1424	1452	PS1	PS220c	PS222	PS227c
Type*	M	M	M	M	M	S	S	K-S
Area$^{\tau}$	E	E	E	H	H	H	H	H
SiO_2	53.40	52.54	45.18	52.22	47.76	54.63	55.84	40.79
Al_2O_3	13.92	12.10	13.01	14.66	13.77	12.97	14.30	13.69
Fe_2O_3	6.37	6.62	7.27	6.31	6.58	7.41	5.83	9.08
MgO	7.08	5.62	7.73	6.94	7.41	8.20	6.33	8.46
CaO	5.88	5.33	9.12	5.47	7.31	7.86	4.17	9.45
K_2O	4.97	5.67	4.01	3.68	5.47	1.81	2.78	2.34
Na_2O	2.58	0.04	1.86	2.98	1.22	2.17	3.19	2.62
MnO	0.12	0.12	0.11	0.11	0.09	0.11	0.07	0.13
TiO_2	1.08	1.48	1.14	0.97	0.93	1.18	0.84	1.50
P_2O_5	0.83	0.67	1.06	0.53	0.68	0.40	0.26	1.37
LOI	4.23	9.66	8.90	4.76	7.72	2.93	5.85	8.21
Total	100.47	99.85	99.39	98.62	98.92	99.67	99.40	97.62
Zn	84	50	93	74	92	77	78	105
Cu	55	44	134	41	52	27	26	46
Ni	264	195	297	222	303	257	158	215
Rb	111	108	84	81	120	45	49	57
Sr	1248	261	1532	1090	443	744	335	1016
Y	25	25	36	20	25	22	22	32
Zr	337	804	525	355	341	167	156	393
Nb	22	15	32	15	18	10	9	30
Ba	2048	1451	1878	1774	1529	784	682	3688
U	5	4	3	3	6	1	3	4
Th	24	16	20	20	29	2	8	25
Pb	26	11	21	23	30	13	15	28
V	125	145	150	145	172	162	151	227
Cr	301	470	335	343	416	535	347	241
K_2O/Na_2O	1.9	141.8	2.2	1.2	4.5	0.8	0.9	0.9
Mg No.*	76.2	70.9	75.3	76.0	76.4	76.1	75.7	72.8
Zr/Nb	15.3	53.6	16.4	23.7	18.9	16.7	17.3	13.1
Zr/Y	13.5	32.2	14.6	17.8	13.6	7.6	7.1	12.3
$(La/Yb)_N$	48.7		53.9					
εSr	17.0		25.8					
εNd	-0.45		-2.99					

Table 4.3. Representative analysis of lamprophyres from the eastern Southern Uplands.

* M=minette, S=spessartite, K-S=kersantitic spessartite.
τ E=eastern area, H=Hawick area.
* Fe normalised to Fe^3/Fe_t cation ratio of 0.3 in calculation.

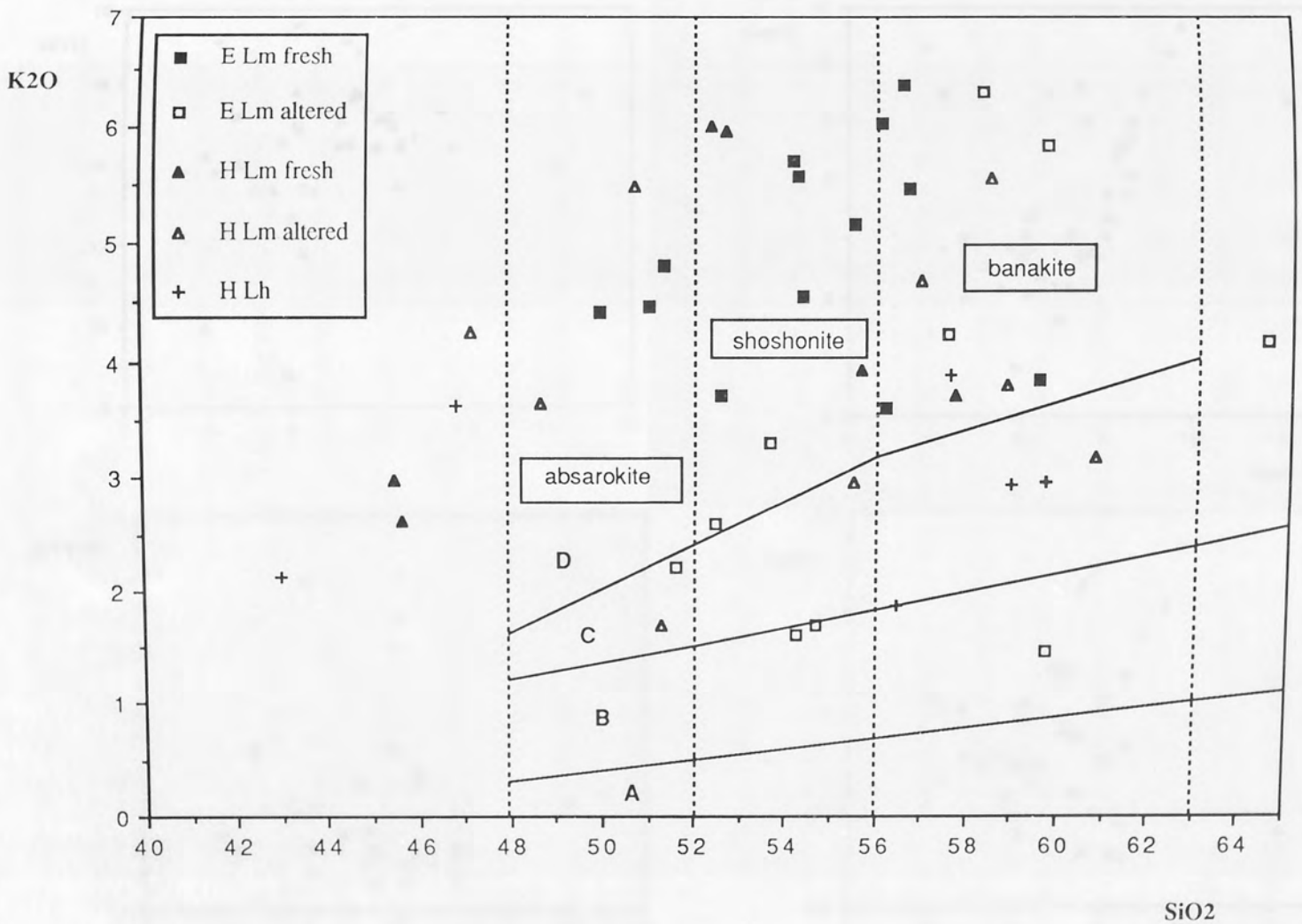

Figure 4.3 K_2O-SiO_2 diagram for lamprophyres Legend symbols are ; E: eastern part of Southern Uplands; H: Hawick; Lm: minette; Lh: hornblende lamprophyre. Fields for the arc rocks after Peccerillo & Taylor (1976) are: A: arc tholeiite series; B: calc-alkaline series; C: high-K calc-alkaline series; D: shoshonite series. Individual fields for the shoshonite series are named.

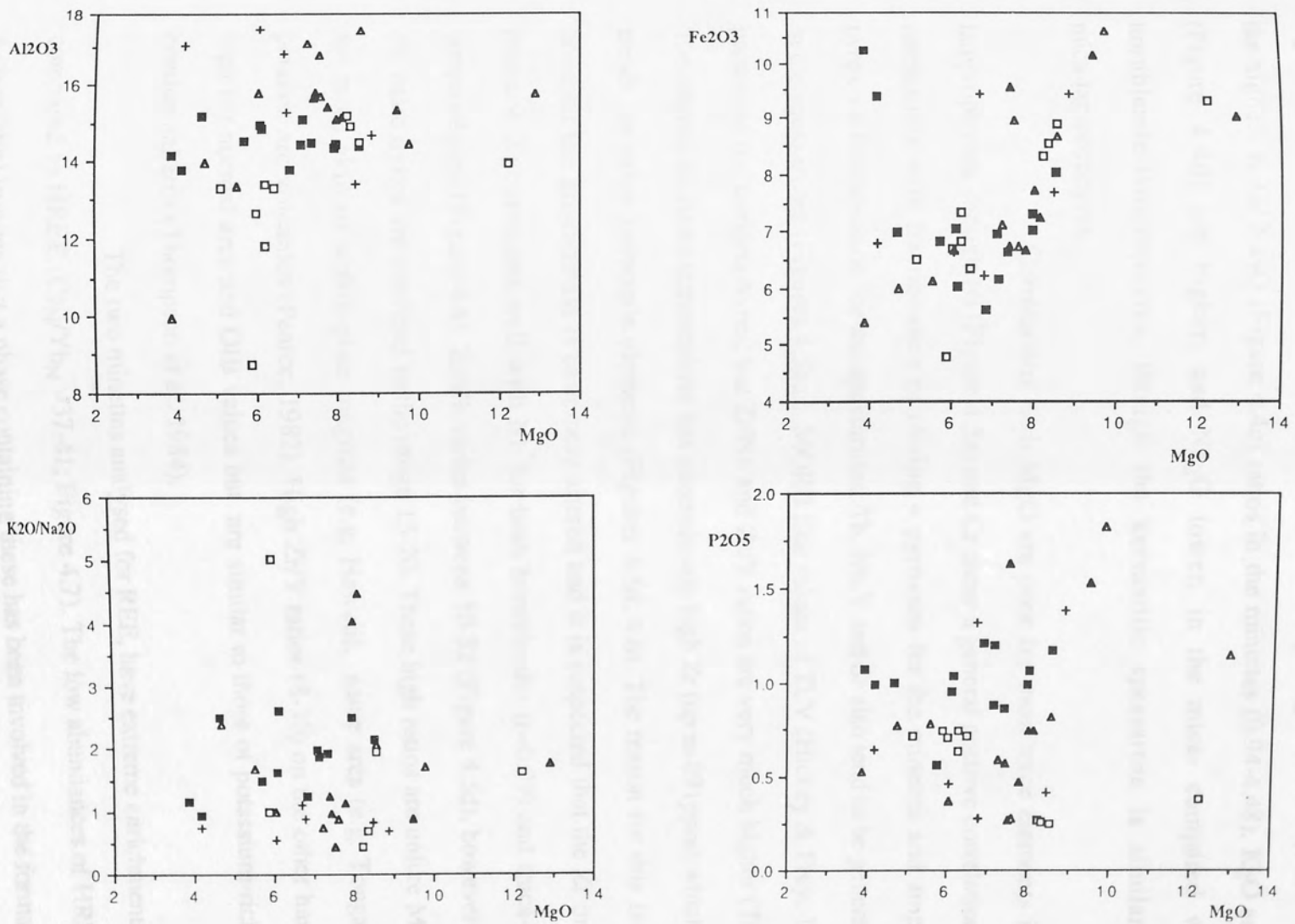

Figure 4.4 Selected MgO-SiO_2 plots for major elements in lamprophyres. Symbols as in Figure 4.3.

K_2O/Na_2O are high even in the freshest rocks and at high MgO contents (Table 4.3) with the highest K_2O/ Na_2O (Figure 4.4c) ratios in the minettes (0.94-4.48). K_2O and P_2O_5 (Figure 4.4d) are higher, and Na_2O lower, in the mica- compared with the hornblende-lamprophyres, though the kersantitic spessartite is similar to the mica-lamprophyres.

Correlations with MgO are poor for most trace elements in all the lamprophyres, though Ni (Figure 4.5a) and Cr show a general positive correlation. This is compatible with fractionation of olivine + pyroxene for the minettes and amphibole ± pyroxene fractionation for the spessartites. Th, Nb,Y and Sr also tend to be generally lower in the spessartites (Figures 4.5b,c). MORB like values of Ti/V (Hickey & Frey, 1982), are present in the lamprophyres, but Zr/Nb and Zr/Y ratios are very much higher (Table 4.3). The altered St. Abbs lamprophyre has anomalously high Zr (up to 891ppm) which plots off trends for other immobile elements (Figures 4.5d, 4.6). The reason for this is not clear however the groundmass is extremely altered and it is suspected that the Zr may not be primary. Zr correlates well with Nb for both hornblende- (r=0.99) and mica- (r=0.71) lamprophyres (Figure 4.6). Zr/Nb varies between 10-32 (Figure 4.5d), however values in the basic dykes are confined to the range 15-20. These high ratios are unlike MORB and are more akin to within-plate magmas (e.g. Hawaii), some arcs (e.g. Tonga arc) and potassic arc volcanics (Pearce, 1982). High Zr/Y ratios (8-30) on the other hand are too high for normal arcs and OIB values but are similar to those of potassium-rich suites of continental arcs (Thompson *et al.* 1984).

The two minettes analysed for REE, have extreme enrichments in LREE compared to HREE (Ce_N/Yb_N =37-41; Figure 4.7). The low abundances of HREE (ca. 10 x chondrite) implies that a phase containing these has been involved in the formation of the magma. The presence of garnet during partial melting for example would produce magmas with similar HREE contents but varying degrees of LREE enrichment. The very high LREE contents in these minettes (Ce_N= 247-343) also indicate that even with low degrees

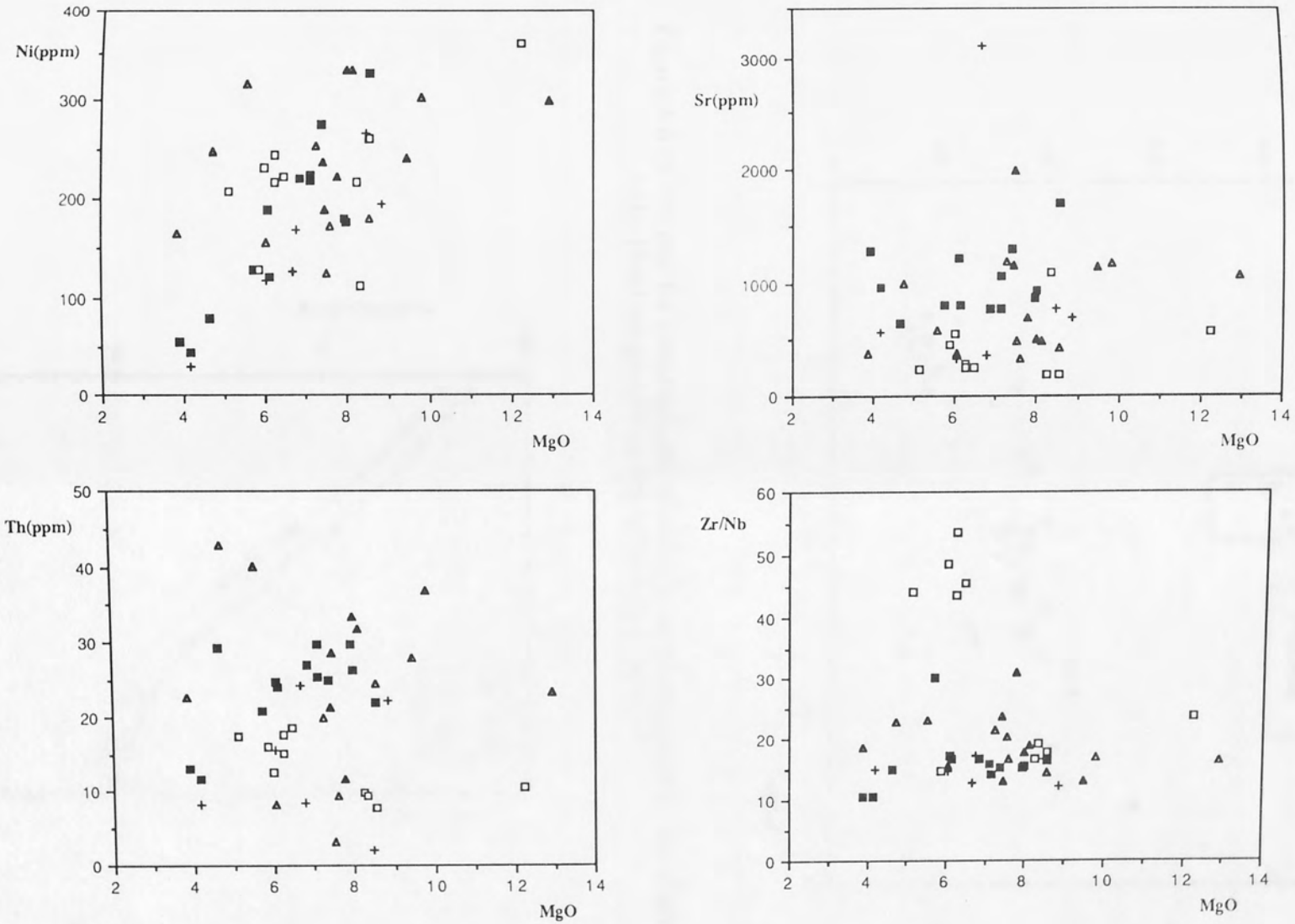

Figure 4.5 Selected MgO-SiO_2 plots for trace elements in lamprophyres. Symbols as in Figure 4.3.

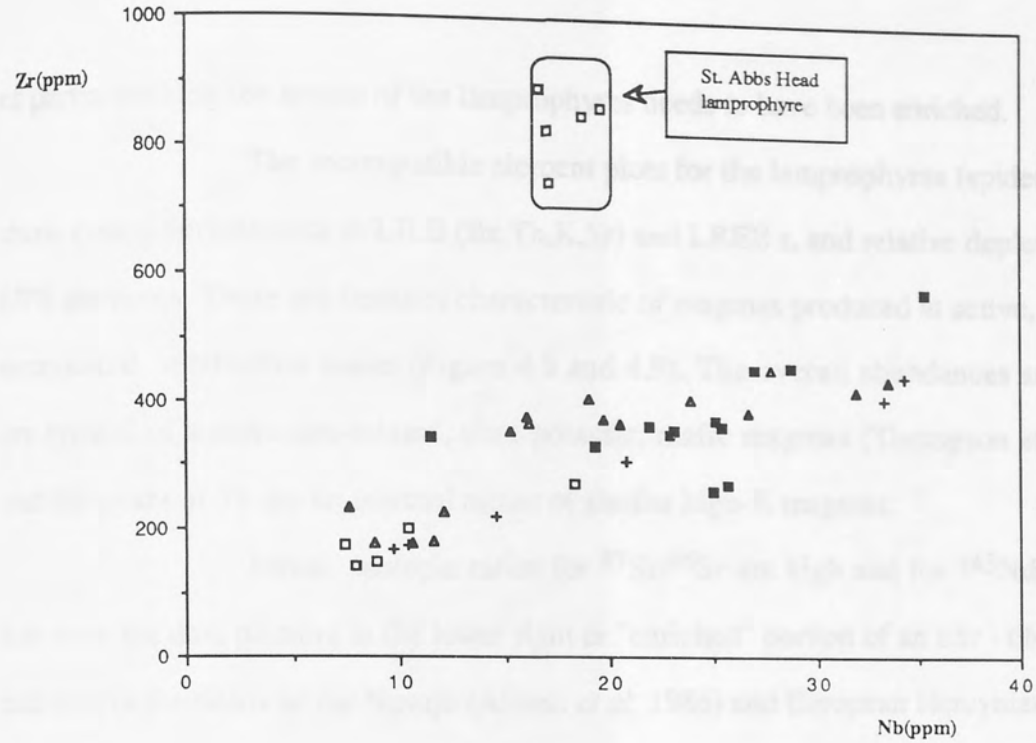

Figure 4.6 Zr-Nb plot for lamprophyres showing good trend except for the altered St. Abbs Head lamprophyre. Symbols as in Figure 4.3.

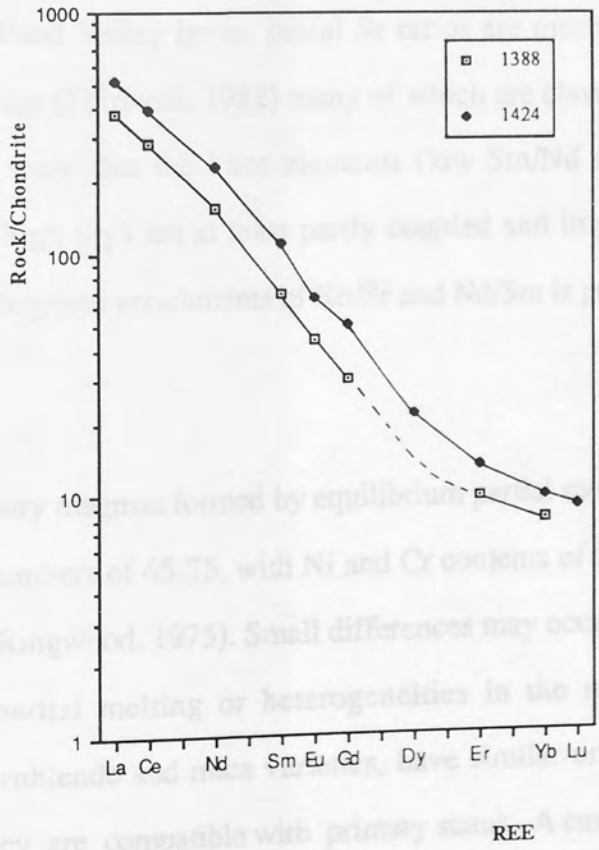

Figure 4.7 Chondrite normalised REE diagram for minettes 1388 and 1424.

of partial melting the source of the lamprophyres needs to have been enriched.

The incompatible element plots for the lamprophyres (spiderdiagrams), show strong enrichments in LILE (Ba,Th,K,Sr) and LREE s, and relative depletions of the HFS elements. These are features characteristic of magmas produced at active, or recently terminated, subduction zones (Figure 4.8 and 4.9). The overall abundances and patterns are typical of subduction-related, ultra-potassic, mafic magmas (Thompson *et al.* 1984), and the peaks at Th are an unusual aspect of similar high-K magmas.

Initial isotopic ratios for $^{87}Sr/^{86}Sr$ are high and for $^{143}Nd/^{144}Nd$ are low with the data plotting in the lower right or "enriched" portion of an εSr - εNd diagram, and plot in the fields of the Navajo (Alibert *et al.* 1986) and European Hercynian (Turpin *et al.* 1988) mica-lamprophyres (Figure 4.10). These two values are also within the range reported for lamprophyres from south-west Scotland and the Lake District (Henney *et al.* 1989). The lamprophyres do not overlap with either of the least evolved granitoids of Priestlaw and Cockburn Law, which have strong characteristics of a depleted mantle (chapter 2), or the Midland Valley lavas. Initial Sr ratios are much higher than for the south-west Highland lavas (Thirlwall, 1982) many of which are classified as shoshonites. The lamprophyre data show that the trace elements (low Sm/Nd and high Rb/Sr) and isotopes (low Nd_I and high Sr_I) are at least partly coupled and imply that at least one component with time integrated enrichments of Rb/Sr and Nd/Sm is present in their source.

4.8 Petrogenesis

Primary magmas formed by equilibrium partial melting of peridotite are expected to have Mg-numbers of 65-75, with Ni and Cr contents of 2-300 ppm and about 500 ppm respectively (Ringwood, 1975). Small differences may occur as a result of either different degrees of partial melting or heterogeneities in the mantle. Many of the lamprophyres, both hornblende and mica varieties, have similar or higher values to the above consequently they are compatible with primary status. A cumulate-origin for the

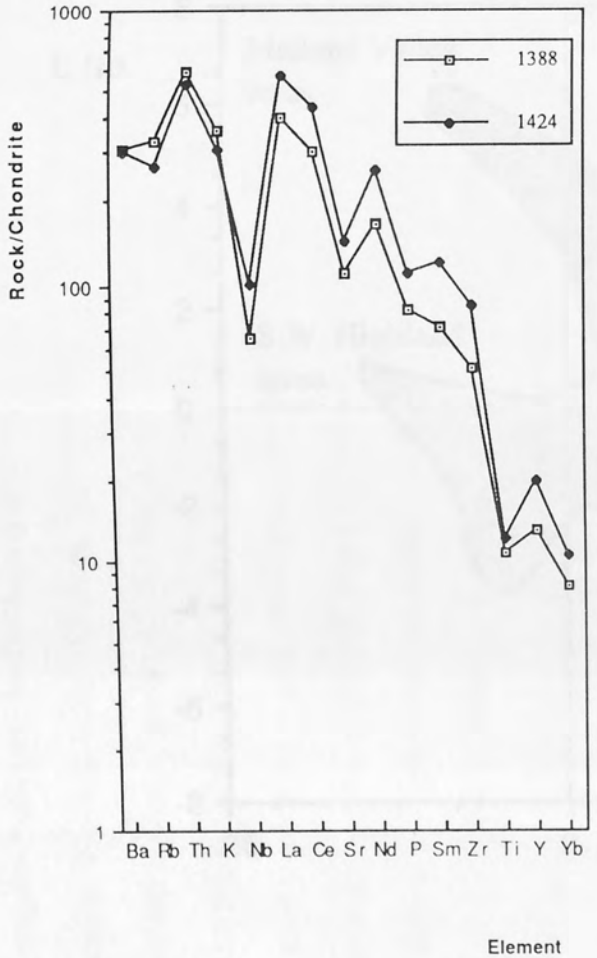

Figure 4.8 Spiderdiagram for minettes 1388 and 1424.

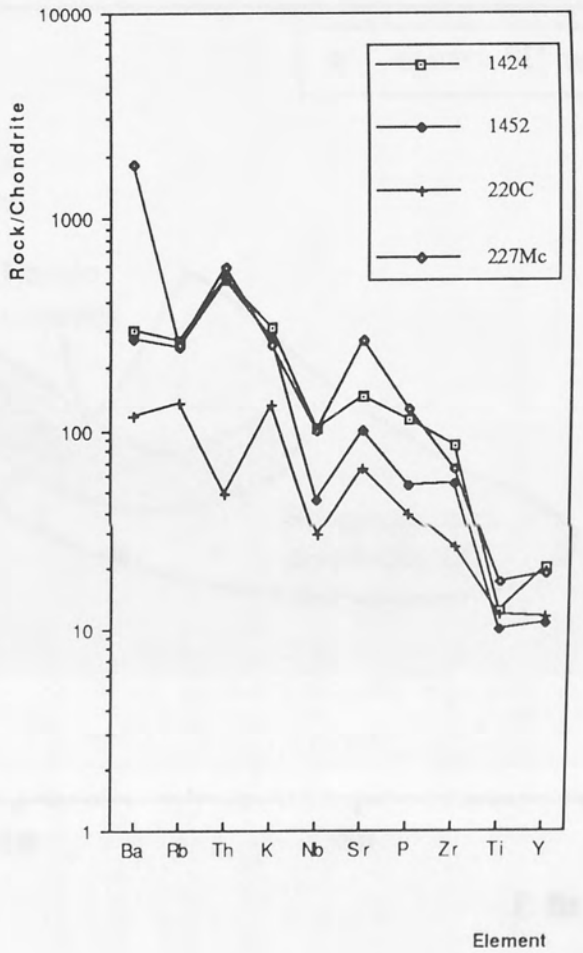

Figure 4.9 Spiderdiagram using selected elements for mica- and hornblende-lamprophyres from the eastern area and Hawick.

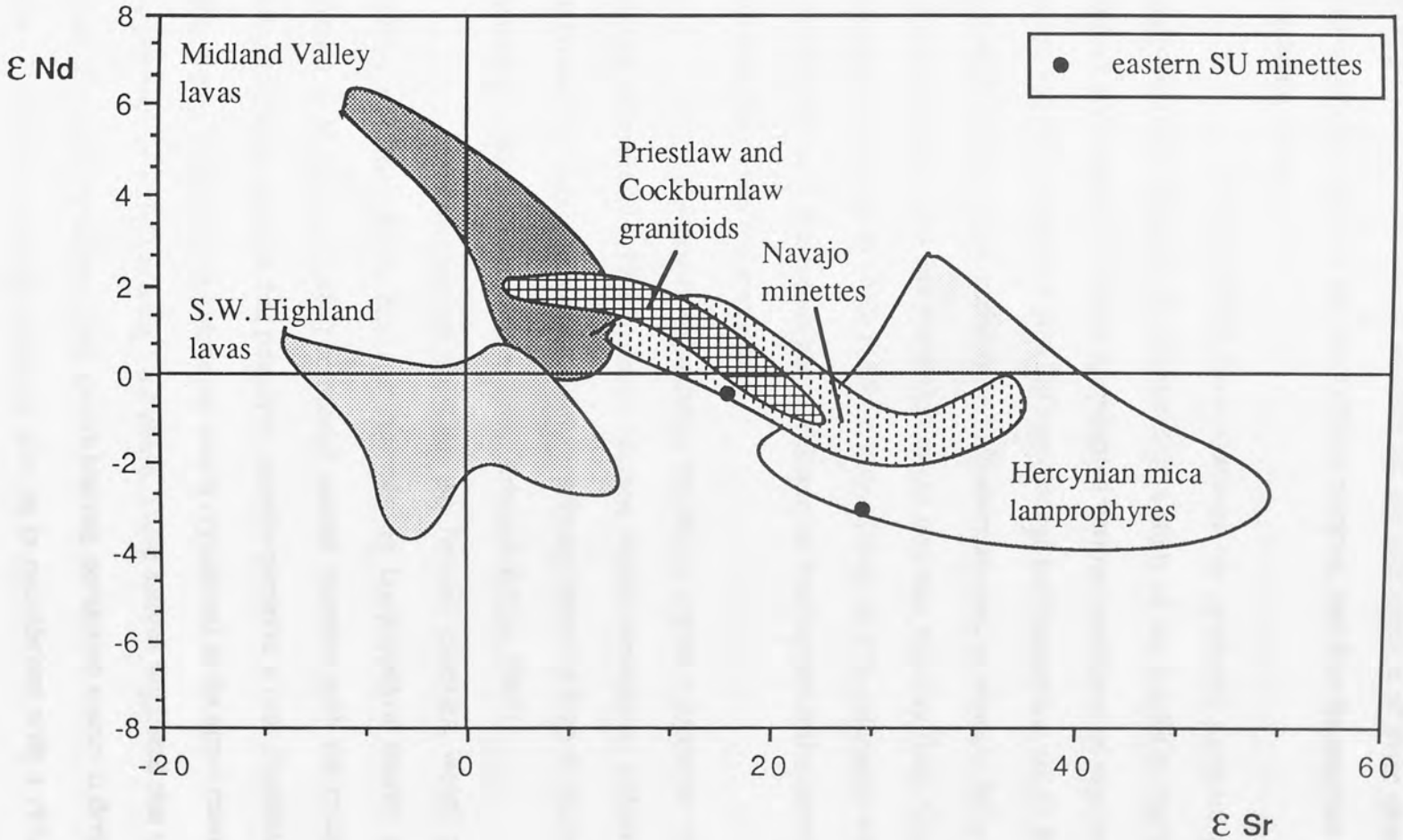

Figure 4.10 ε Nd- ε Sr diagram for samples 1388 and 1424. Fields for the Midland Valley and SW Highland lavas (Thirlwall, 1982a), Navajo minettes (Alibert *et al*) and Hercynian mica-lamprophyres (Turpin *et al* 1988) are shown for comparison.

lamprophyres cannot be used to account for the high content of these elements, because most rocks are fine-grained and have chilled margins, and thus the magmas were probably close to being liquids.

Experimental investigations on synthetic systems provide some constraints on the source of K-rich rocks. In a study of the $KAlSiO_4$-MgO-SiO_2 system, Wendlandt and Eggler (1980a,b) investigated various conditions of vapour absence, CO_2 saturation and CO_2 saturation plus H_2O present but buffered at low aH_2O. Potassic liquids formed in all three systems varied from SiO_2-oversaturated to strongly SiO_2-undersaturated with increasing pressure and expansion of the enstatite stability field. Quartz-normative liquids were formed up to 14Kb (~50km) in conditions of CO_2 saturation with H_2O present with phlogopite as a subsolidus phase. Phlogopite bearing peridotite melts incongruently and is characterised by the reaction:

phlogopite + enstatite + sanidine + vapour = forsterite + liquid.

At higher pressure (14-17 Kb) melts became leucite-normative. Subsequent work on natural rocks are also in agreement with the primary nature of high-K liquids derived from the mantle (e.g.Barton & Hamilton, 1982; Arima & Edgar, 1983).

Experimental work on the Navajo minettes, which contain mantle xenoliths, provides more realistic controls on lamprophyre source characteristics. Esperanca & Holloway (1987) compared natural minettes with the results produced in experiments; they showed that primitive minettes preserve a near-liquidus assemblage of olivine, diopside and Ti-rich phlogopite which crystallised in the upper mantle ($fO_2 \geq$QFM) in the presence of a H_2O-bearing fluid phase. These authors suggested that minette magmas *originated* from a metasomatised, garnet-bearing, peridotitic source at deeper levels in the mantle (P≥20 Kb), although they can also be in equilibrium with a phlogopite-bearing wehrlite (± opx) source at 17-20 Kb under reducing or oxidising conditions. At lower pressures the olivine field expands and in the presence of water the reaction:

3 olivine + 3 leucite + H_2O = 2 phlogopite + 2 K-feldspar,

takes place at shallower depths. Potassic magmas, retaining volatiles during cooling at low pressure, may include phenocrysts of K-feldspar in addition to phlogopite. They concluded that any minette containing olivine + clinopyroxene + phlogopite ± opaque oxide could not have been significantly re-equilibrated at low pressure and temperature. The preservation of this assemblage precludes processes dominated by AFC in a shallow magma chamber and supports a model whereby minettes are brought to near surface conditions at temperatures in the range of 1,000-1,200 ^{o}C and chilled rapidly (Esperanca & Holloway, 1987). The presence of leucite-bearing rocks (± K-feldspar phenocrysts) with similar geochemistry to minettes, but associated with volcanic centres, provides evidence of similar origins but different evolutionary P-T histories through the crust, and may explain the distinct lack of lamprophyre lava flows (Rock, 1984).

The experimental data thus provides strong constraints for the origins of minettes in southeastern Scotland, where the preservation of olivine + clinopyroxene + phlogopite as phenocrysts, the presence of chilled margins and fine-grained textures is consistent with rapid ascent and chilling of a hot magma, and precludes their emplacement as a crystal mush (Rock, 1984). Lamprophyres with lower Mg numbers and relatively low Ni and Cr contents are compatible with olivine- and clinopyroxene-controlled fractionation at deep levels in the crust or upper mantle. Although quartz xenocrysts occur in the minettes it is thought unlikely that major contamination (e.g. AFC) has been important in the upper crust because this would destroy the primary assemblage and would substantially lower Mg numbers and Ni and Cr contents.

The relationship of the hornblende-lamprophyres to the minettes is less clear because there is little direct experimental data. With the exception of the kersantitic spessartite, the spessartites, at similar MgO contents, have generally lower K_2O, K_2O/Na_2O, P_2O_5, Rb, Th, Nb and Y than the minettes. Although the spessartite data set is small, differences between the two groups have been noted elsewhere in the Southern Uplands with mica-lamprophyres generally having higher CaO, K_2O, K_2O/Na_2O, P_2O_5,

Rb, Ba, Zr, Nb and LREE but lower SiO_2 (Rock *et al.* 1987). These differences may be due to the balance of H_2O- vs. CO_2-dominated melting regimes (Rock *et al.* 1987), and the stability limit of amphibole. Mica lamprophyres may be produced at levels below the stability field of amphibole (26-30 Kb) where CO_2 is the dominant control on melting behaviour (Wyllie, 1978, 1979, Morse, 1980). The higher CaO content of minettes and the more abundant carbonate (primary , primary remobilised , secondary ?) is compatible with these being produced from a mantle source with primary carbonate (Ruddock & Hamilton, 1978a,b). The solubility of carbonate at high pressures (>16 Kb) and its effectiveness as a buffer for CO_2 however, ensures that any free fluid/vapour, after the hydration of mica, will be H_2O-rich at high pressures, and that fluids at low pressures may be CO_2-rich. Hydrous fluids are capable of leaching and transporting greater concentrations of ions than either pure CO_2 or $CO_2 + H_2O$, and melts are much better agents of causing metasomatism and transporting elements than fluids (Eggler, 1987). Carbonic metasomatism may for example be caused by nephelinite-carbonatite *melts* (Green & Wallace, 1988, Menzies *et al.*, 1987). The mechanics of enrichment processes and compositions of metasomatic agents is however still contentious and much more work is necessary to identify the origin and extent of metasomatic domains in the mantle. The higher K_2O/Na_2O contents of minettes, nevertheless implies that these are derived from a deeper, phlogopite-bearing source than the hornblende-lamprophyres. Mica amphibole lamprophyres such as the kersantitic spessartite having characteristics of both types of lamprophyre may have formed in intermediate domains between the two source areas. The higher abundances of LILE, HFS elements and LREE in the minettes may be a function of smaller degrees of partial melting, or derivation from a more extensively metasomatised mantle, or a function of different fluid compositions.

The range in incompatible trace element ratios (e.g. Zr/Nb) of the most basic lamprophyres is small and may imply that the variation is due to different degrees of partial melting of a similar source. There is however a variation in the Nd isotopic values

which is not consistent with derivation of all the lamprophyres from a single homogeneous source. The variation in isotopic compositions of the mica- and hornblende-lamprophyres in southern Scotland implies that the source of the lamprophyres is heterogeneous and/or that more than one component is involved.

Extreme enrichments in incompatible elements in minettes imply that the source was enriched and that extremely small degree partial melts are involved (Alibert *et al.* 1986). The extraction of small degree melts is a feasible process by compaction under stress (McKenzie, 1985) and it is likely that high primary volatile contents of lamprophyres would facilitate this process.

The globular structures are dominantly of feldspar similar petrographically to that of the host rock. In addition some contain carbonate ± quartz ± chlorite in the centres and larger ones may also have phlogopite or amphibole. They may also be seen to be 'squashed' in dykes showing flow textures. The most likely origin for these globular structures is through expansion of more volatile-rich areas of the magma (not liquid immiscibility). These areas expanded on ascent through the crust thus displacing phlogopite or amphibole which now appear as continuous or semi-continuous tangential rims. Larger structures, nearer the centres of dykes, appear to have formed by coalescence of smaller structures and, as indicated from textural relationships may thus include phlogopite or amphibole. The overall features of the structures suggest crystallisation from a melt, as opposed to a vapour phase, and they are texturally distinct from amygdales proposed by Nemec (1971) and Read (1926).

The presence of abundant quartzite xenoliths in some lamprophyre dykes shows that at least some have interacted with continental crust. In the freshest example, a spessartite (PS 220), the quartzite is rimmed with clinopyroxene similar to reaction rims around quartzite reported elsewhere (Reynolds, 1936, 1938). Fresh clinopyroxene and amphibole, apparently in textural equilibrium (as in PS 220), also occurs in some dykes in south west Scotland (P.J. Henney, pers. comm.), and may result

from sudden loss of volatiles through interaction with the middle to lower crust. Large parts of the xenoliths are replaced with a pinkish fine-grained mesostasis enclosing fine-grained to microcrystalline clinopyroxene. This type of reaction, between lamprophyres and crustal rocks, forming felsic products which may also be rheomorphic (Reynolds, 1936), may represent processes taking place at depth, and thus is relevant to considerations of apparent genetic relationships between lamprophyres and granitoids (MacDonald *et al.* 1986, Rock *et al.* 1987) . It is thought likely that with loss of volatiles at high levels in the crust, lamprophyre magmas would tend to freeze, because their solidus and liquidus would be increased with a loss of volatiles. The quartzite xenoliths originate from rocks below the Lower Palaeozoic sediments but these are not exposed at the surface. Quartzite xenoliths occur in other lamprophyre dykes across the Southern Uplands (Rock *et al.* 1986) and as clasts in Silurian conglomerates of the Midland Valley (Longmann *et al.* 1979). They may be either metasedimentary quartzites or alternatively, quartz veins from high grade metamorphic terranes. The purity of the xenoliths, the abundance of fluid inclusions in them, and their similarity in hand specimen to vein quartz is thought to make the latter source most probable.

4.9 Discussion

The high LREE content and La/Yb, and the enriched isotopic characteristics of the lamprophyres, as well as high Zr/Y and Zr/Nb, ratios are interpreted to imply derivation from an enriched and metasomatised mantle. The calc-alkaline shoshonitic nature of the magmatism provides evidence for the interaction of fluids/melts derived from a subducting plate with the mantle above. The source characteristics of this mantle are however debatable. A subduction component is present in the lamprophyric magmas, but to what degree this is overprinting a previously metasomatised mantle is not clear. The presence of a crustal component, probably related to subduction of sediment, is indicated by e.g. low Sr/Nd (10-12) in the minettes compared with most peridotites and

oceanic magmas (15-20), because both clays and siliceous melts have low Sr/Nd ratios (Alibert *et al.* 1986). An asthenospheric melt modified by infusion from previously subducted lithosphere has been suggested (Thompson & Fowler, 1986) for the minettes from northwest Scotland which are located at a large distance from the Iapetus suture. A multi-component origin comprising (a) depleted lithospheric mantle, (b) enrichment in LILE related to subduction and (c) CO_2-rich phase from degassing of the mantle after ocean closure, has been suggested for lamprophyres of northern England close to the Iapetus Suture (MacDonald *et al.* 1985). The enrichment in LILE and relative depletions in HFS elements is thought to be a primary feature of lamprophyres because these occur in rocks with primary characteristics and is ubiquitous in calc-alkaline rocks. It is thought that a deep asthenosphere source for the minettes in southern Scotland is unlikely because they are too close to the suture zone. In the multi-component model of MacDonald *et al.* (1985), the evidence for a depleted mantle component was implied by the similarity of Al_2O_3/Ti, Ti/V and Ti/Sc ratios to those in MORB. However Ti, as one of the HFS elements, is characteristically depleted in calc-alkaline suites, thus ratios involving this element are best avoided until a viable model for this depletion is understood and accepted. The above authors displayed their model on a MORB normalised diagram using the empirical procedure adopted by Pearce (1983). A similar diagram for a minette from south eastern Scotland is shown in Figure 4.11a . Zone A represents the depleted mantle component, zone B the enrichment due to a CO_2-rich phase and zone C the enrichment due to subduction. A similar model may be applied to any of the lamprophyres. Although zone B (the *within plate component* ; Pearce, 1983) is rather large for the lamprophyres it is present in all continental calc-alkaline suites and also in OIB's. It may thus represent an OIB-*like* parent or a component of continental lithospheric mantle, subsequently overprinted by a subduction component. Island arc magmas display an enrichment in LILE elements only relative to that expected to be produced from a depleted source, and can be modelled with zones A+C (Pearce, 1983). An OIB from Hawaii (geological standard

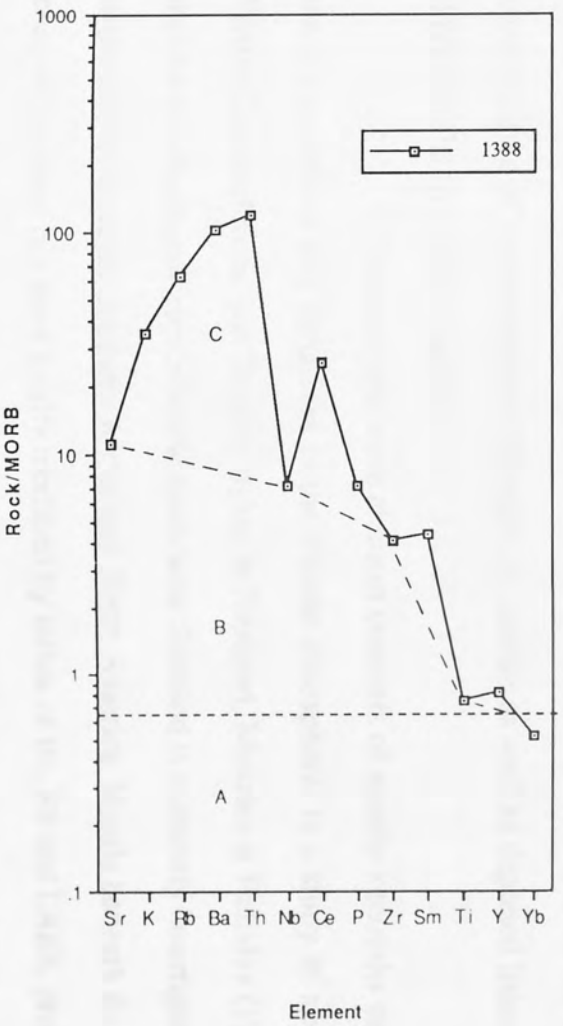

Figure 4.11a MORB-normalised element plot for minette 1388 showing multi-component model of MacDonald *et al* (1985). See text for discussion.

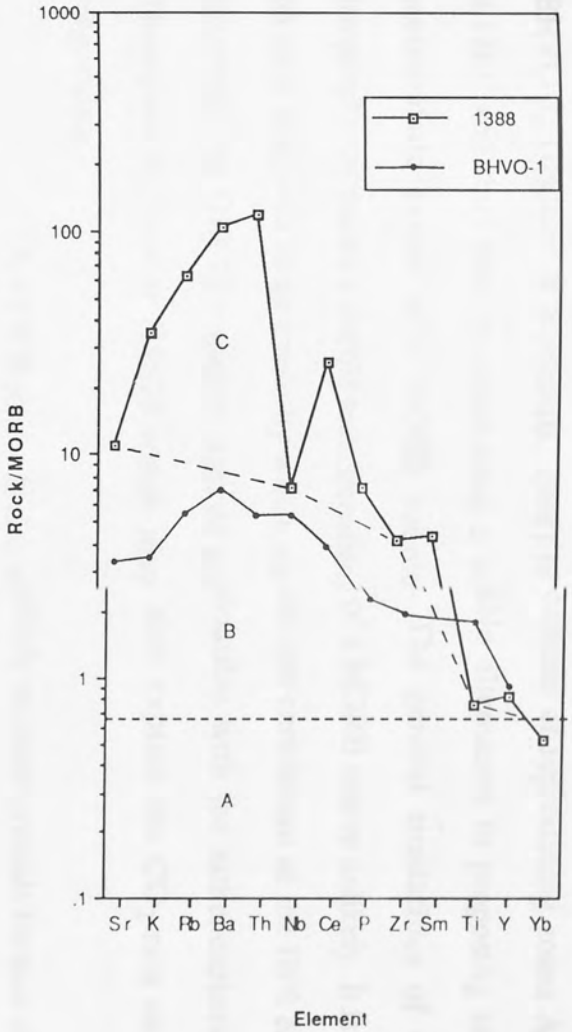

Figure 4.11b MORB-normalised element plot as in Figure 11a with OIB BHVO-1 also plotted for comparison. See text for discussion.

BHVO-1; Gladney & Roelandts, 1988) is capable of reproducing zones A+B (Figure 4.12b), and thus may be considered a viable alternative to proposing two separate metasomatic events of a MORB source. The general similarities of Caledonian lamprophyres makes a double metasomatism of a MORB source unlikely. It is impossible on such diagrams to ascertain by which means the enrichment of the HFS elements has occurred. An OIB-like source is more compatible with the asthenospheric model of Thompson & Fowler (1987) which may also explain the CO_2-rich nature of the magmatism.

A MORB source is also unlikely on other grounds because of the lack of any MORB magmatism from below continental crust (chapter 2). Previous metasomatism of sub-crustal mantle below the continents is likely to produce enrichments and heterogeneities. It is now fairly well established that modal metasomatism of the lithosphere occurs in response to the passage of Fe- and Ti-rich silicate melts and K-rich hydrous fluids (Hawkesworth *et al.* 1984, Menzies *et al.* 1987). This allows for the possible contributions of metasomatised lithospheric mantle as well as depleted lithosphere or an ultimate OIB like asthenosphere.

Isotopic and trace element contents of mantle xenoliths may constrain the compositions and variations in the mantle lithosphere. In a study of xenoliths from Permo-Carboniferous and Tertiary dykes in Scotland, Menzies & Halliday (1988) showed that the sub-Archaean mantle below north-west Scotland is extremely heterogeneous similar to the mantle beneath Southern Africa and North America. Mantle beneath the Proterozoic crust of Scotland has been locally modified by influx of Ba, Rb and LREE, probably due to subduction and the mantle beneath the Midland Valley is similar to OIB. It was suggested that the presence of these lithospheric domains could be explained by previous subduction and extensional regimes. The dykes sampled the lithospheric mantle in Permo-Carboniferous and Tertiary times however, and it is difficult to ascertain the character of the lithospheric mantle in Late Silurian-Early Devonian times, because

subduction of Iapetus and subsequent extension in the Lower Carboniferous (with OIB magmatism; Smedley, 1986) have modified this mantle. Thinning and modification (e.g. by OIB) of the sub-Midland Valley lithospheric mantle for example may explain its OIB-like character, and sinking of unstable lithospheric mantle followed by underplating may be an important process following orogeny. The evidence of Menzies & Halliday (1988) make it clear that the lithospheric mantle below Scotland north of the Southern Uplands fault has had a long and complex history.

There is to date no published isotopic data on mantle xenoliths from below the Southern Uplands. The magmatic products of the northern Southern Uplands have come from at least two mantle sources (Figure 4.10):

(1) a depleted mantle source that provided the parental magmas for the Priestlaw and Cockburn Law granitoids.

(2) an enriched mantle that produced the minettes.

The two minettes have low ε Nd and high ε Sr indicating that their source had time integrated high Rb/Sr and Nd/Sm ratios. The variation in initial Nd isotopes in southwest Scotland (Henney *et al.* 1989) from +2 to -2 implies that both a depleted and enriched components are present. Because a stable lithosphere allows such isotopic characteristics to develop it seems likely that they were produced at least in part from such a source. Whether the source of the lamprophyres is from a heterogeneous mantle previously metasomatised by fluids/melts, or whether the metasomatism was directly related to subduction cannot be solved because of the present lack of data. Some sub-lithospheric oceanic magmas (OIB), from e.g. Kerguelan have also developed such characteristics and it is not possible to model the various components that gave rise to the minettes with the presently available data. Old, extremely enriched, sub-lithospheric mantle is preserved under the Lewisian of northwestern Scotland, and a study of the lamprophyres in that area would provide constraints into asthenospheric/lithospheric components.

The lamprophyres of southern Scotland are spatially close to the Iapetus

Suture whereas rocks of the shoshonite association are found at large distances behind the trench (Chen & Moore, 1979, Whitford & Nicholls, 1979). The young age of the St. Abbs dyke at 400± 9 Ma (Rock & Rundle, 1986) means that it was intruded post-closure (see chapter 5) and therefore is similar tectonically to post-collisional lamprophyres (Rock, 1984).

In areas of low heat flow (e.g. at trenches) it is likely that extensive amphibole and/or mica crystallisation may occur (Foley, 1988). The lamprophyres therefore probably represent very small degree partial melts of a mantle previously metasomatised due to subduction (possibly overprinting older ?enriched lithosphere) in a post-collisional setting and that melting was initiated during the readjustment of isotherms following the cessation of subduction. The low Nd and high Sr isotopic ratios and the extreme enrichments of several elements make it more likely that lithospheric mantle has played a major role in their genesis.

The differences in isotopic compositions between the minettes and the granitoids precludes a genetic link between them. Hornblende lamprophyres would appear to have a closer spatial and ?genetic link with the granitoids and it interesting to note that the commonest lamprophyres associated with the Criffell pluton are hornblende-bearing varieties (Phillips, 1956).

The geochemistry of the eastern Southern Uplands lamprophyres show strong similarities with those of the Lake District (MacDonald *et al.* 1985) and have higher abundances for many elements (e.g. Ba, Th, K) than seen on the regional trends across Scotland of Rock *et al.* (1987). This does not affect the trends drastically but merely shows that the increase in certain elements occurs further to the north in the eastern Southern Uplands than in the west. The lower values further west in the Southern Uplands reflects the dominance of hornblende-lamprophyres there. Lamprophyres are concentrated along a main narrow zone close to the Iapetus suture in the west, but which extends further north in the east (Figure 4.2). This probably is a structurally controlled trend similar to that reported

elsewhere for Caledonian dykes (Smith, 1979, Watson, 1982), as it is nearly parallel to the accepted trace of the Iapetus Suture. The more northerly extension of lamprophyres in the eastern Southern Uplands may result from a bend in the trace of the suture or, more likely (as will be discussed in chapter 5), to more extensive underthrusting of the southern continent below this part of Scotland. The lamprophyres were intruded later (ca.400 Ma) than the granitoids and hence probably post-date closure of the Iapetus ocean. Their tectonic setting is therefore similar to the younger (ca. 397 Ma.) granitoids (Criffell, Fleet) of the Southern Uplands, with which they are intimately associated.

4.10 Summary

(1) Calc-alkaline lamprophyres in the eastern Southern Uplands are minettes forming part of a dyke swarm extending from the Ards Peninsula in Northern Ireland east to St. Abbs Head in Berwickshire. They occur close to several small Late Caledonian granitoid plutons and associated intermediate to acid dykes (chapter 2). Further west, near Hawick both hornblende- and mica-lamprophyres occur and no more acid plutons or dykes are exposed.

(2) The lamprophyres have enrichments in LILE and LREE, and relative depletions in Nb and Ti and abundances of incompatible elements typical of subduction-related ultra-potassic magmas.

(3) The high Mg numbers and high Ni and Cr contents are consistent with primary status of mantle derived melts.

(4) The phenocryst assemblage olivine + clinopyroxene + phlogopite implies that the minettes represent mantle melts brought to near surface conditions at temperatures of ca. 1,000-1,200 ^{o}C and chilled rapidly.

(5) The geochemical characteristics of the lamprophyres i.e. high values for LREE, LILE, La/Nb, ε Sr and low ε Nd, imply derivation from a previously metasomatised source. The minettes are derived from a source with garnet and phlogopite present,

and hornblende lamprophyres may be derived from a shallower source in the stability field of amphibole.

(6) Metasomatism was probably caused by H_2O-rich melts/fluids derived from the subducting plate, and by possibly CO_2-rich melts/fluids coming from deeper sources during or previous to subduction. An isotopic study of lamprophyres across the Caledonian Belt would give clearer insights into asthenospheric/lithospheric source components.

(7) The variation in ε Nd in lamprophyres from the Southern Uplands indicates that more than one mantle component is necessary to explain their source.

(8) Globular structures are interpreted as volatile-rich parts of the magma that expanded at lower pressures as they ascended.

(9) The Priestlaw and Cockburn Law granitoids have characteristics of a more depleted mantle, and therefore their parents are not of lamprophyric origin

(10) Quartzite xenoliths (up to 30cm) in lamprophyre dykes provide direct evidence (Upton *et al.* 1983) for continental crust below the Southern Uplands and may represent vein quartz typical of high-grade metamorphic terranes.

(11) The emplacement of Southern Uplands lamprophyres is likely to have been structurally controlled by the Iapetus Suture, and the more northerly extension of this zone may be related to underthrusting of southerly basement during the later stages of ocean closure.

Chapter 5 : Regional geochemical characteristics of the Late Caledonian plutons of southern Scotland.

5.0 Abstract

REE and Sr and Nd isotope data are presented for small granitoid plutons and lavas in the Southern Uplands and Midland Valley of Scotland. Granitoid plutons and lavas in the northern Southern Uplands (410 Ma.) have high ε Nd and low ε Sr and were derived from a long term depleted mantle modified by subduction in a manner similar to that proposed for lavas in the Midland Valley (Thirlwall, 1986). Plutons from the southern Southern Uplands (397 Ma.) have generally higher ε Sr, La/Yb and lower ε Nd and are consistent with derivation from a more enriched mantle as opposed to an infracrustal source. None of the plutons studied have remained as closed systems, and general correlations with indices of fractionation imply that a process akin to assimilation-fractional crystallisation (AFC) has been important. A consideration of ages and isotopic data show three different magmatic suites to be present in southern Scotland: (1) Midland Valley suite (2) northern Southern Uplands suite and (3) southern Southern Uplands suite. These are consistent with geophysical (Freeman *et al.* 1988) and structural (Needham & Knipe, 1986) models in implying northward underthrusting of English lithosphere below the southern Southern Uplands. The spatial association of ca.400Ma. minettes, similar geochemically to lamprophyres further south, with plutons in the northern Southern Uplands are interpreted as evidence for more northerly underthrusting of decoupled English lithospheric mantle. Final closure of the Iapetus ocean, represented by this underthrusting occurred between 410Ma. and ca.400Ma. The 410Ma. and previous magmatism occurred therefore whilst subduction was active, hence the two are probably linked.

5.1 Introduction

The Late Caledonian granitoid plutons of Scotland (Figure1.1) were emplaced during the period 440-390 Ma., during and after closure of the Iapetus Ocean. These plutons define a series of high-K calc-alkaline rocks which are commonly zoned (see summary in Pankhurst & Sutherland, 1985), in general becoming progressively more acid inwards. There is a considerable variation in rock types within the plutons, varying overall from peridotites and associated lamprophyric rocks to granites. The latter are generally I-type granitoids, however S-type granitoids occur in the Southern Uplands as the

Cairnsmore of Fleet pluton and also in the interior of the Criffell-Dalbeattie pluton. They are divided into three suites on the basis of geochemistry (Stephens & Halliday, 1984) :

(1) the Cairngorm Suite comprising plutons from the NE Highlands.

(2) the Argyll Suite comprising plutons from the SW highlands.

(3) the S of Scotland Suite comprising plutons from the southern Highlands, the Midland Valley and the Southern Uplands.

The Criffell and Cairnsmore of Fleet plutons (Figure 5.1) are excluded from this classification because in part they have distinctive chemical features similar to S-type granitoids. The more alkaline nature and dominantly high-SiO_2 content of the Cairngorm suite (Plant *et al.* 1980) make these plutons more similar to A-type granitoids. Hornblende diorites are commonly associated with plutons in the Argyll suite, whereas pyroxene bearing diorites are associated with those from the S of Scotland suite. The boundary between the Argyll and S of Scotland suites is the mid-Grampian line of Halliday (1984) This line, which has no obvious surface manifestation as a major structural discontinuity, was postulated to be a terrane boundary by Halliday (1984) on the basis of a change in isotopic characteristics of granitoids (southerly limit to ε Nd > -6).

Recent isotopic dating of the Late Caledonian lavas and plutons has shown variations in the ages of magmatism across the Caledonian belt (Thirlwall, 1988). Old Red Sandstone lavas in the Highlands are dated around 420Ma, with plutonism continuing from 423Ma to around 408Ma. In the Midland Valley both volcanism and plutonism occurred between 415 and 410Ma. In the Southern Uplands there is a contrast in the ages of plutons and lavas between the northern and southern parts. In the northern part (e.g. Priestlaw, Carsphairn, Loch Doon) magmatism is dated at around 408Ma whereas near to the Iapetus Suture (e.g. Criffell, Cheviot, Fleet) it occurred around 394Ma (Thirlwall, 1988).

The source of the granitoids has been the subject of much debate. Pidgeon & Aftalion (1978) showed that most of those from the area north of the Highland Boundary Fault contained zircons with a marked isotopic memory of old radiogenic lead,

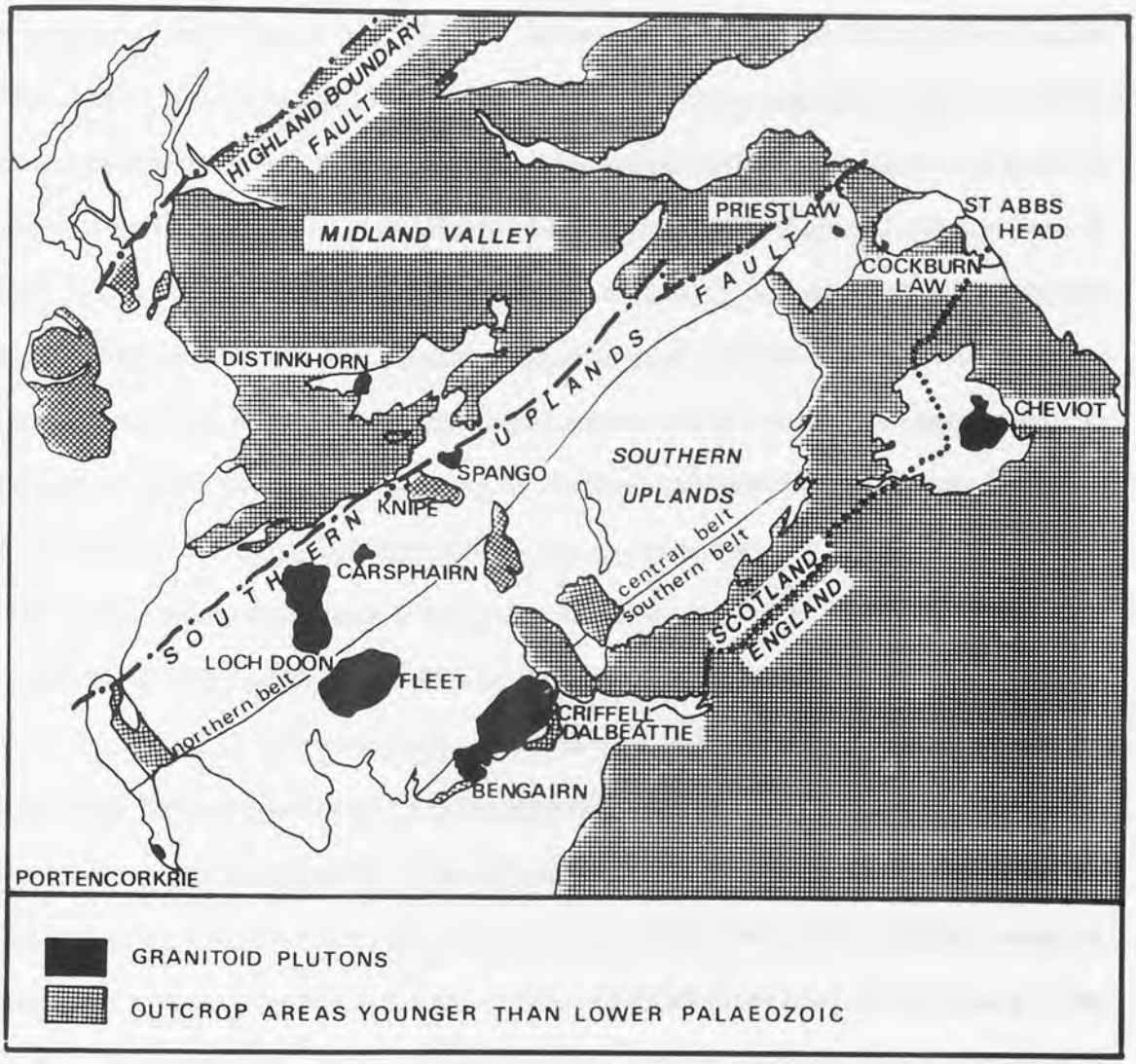

Figure 5.1 Map of southern Scotland showing the distribution of Late Caledonian granitoid plutons and Northern, Central and Southern Belts.

whereas those further south contain little or no isotopic memory of older zircon. These authors suggested that the granitoids contain a substantial crustal component and that the lower crust was older north of this fault. Although recent Nd-Sr-Pb isotopic studies (Halliday *et al.* 1980, Halliday, 1984, Harmon *et al.* 1984) have suggested that the Scottish granitoids are mixtures of mantle and crustal components, debate continues as to which is dominant. An example of this is the Etive complex in the SW Highlands where Frost & O'Nions (1985) proposed a model dominantly involving crustal recycling, whereas Thirlwall (1986) preferred a more dominant mantle source. Much of this debate concerns the choice of the chemistry of the mantle end-member and is particularly concerned as to whether the mantle is enriched below parts of the Scottish Highlands. Although changes in ε Nd occur across Scotland (Halliday, 1984), there is no increase in $^{87}Sr/^{86}Sr$ or $^{18}O/^{16}O$ isotopic compositions, as is found in the granitoids of the cordillera of the Western United States (Kistler & Peterman, 1978 ; DePaolo, 1981).

It is now generally accepted that continental crust is underlain by heterogeneous lithospheric mantle, produced by the interaction of varied silicate melts and fluids with the preexisting mantle. Although enriched mantle is known to exist under old cratonic areas e.g. South Africa (Richardson *et al.* 1985), other old cratonic areas are underlain by depleted mantle e.g. South-western USA (Menzies *et al.* 1985). Many of the differences between the Scottish granitoid suites are paralleled by similar changes in inclusions from younger volcanics and hypabyssal intrusions which are thought to represent fragments of mantle lithosphere (Halliday *et al.* 1985). A study of lithospheric xenoliths and their host magmas along a traverse from the Midland Valley to the Archaean Lewisian foreland shows the variability of the Scottish sub-continental mantle (Menzies *et al.* 1988), and indicates that distinct lithospheric domains exist under Scotland, however geochemical data on xenoliths from the Southern Uplands have not been published. Lamprophyre intrusions, across Scotland, including the Southern Uplands, show a zonation (enrichment) in some trace elements both north and south from minima around the present Midland Valley (Rock *et al.* 1987).

Detailed isotopic studies for most individual plutons in the Caledonides are lacking, with the published data tending to concentrate on a few analyses from the larger plutons. The choice of end-member components is important for modelling source compositions, but a knowledge of the mechanisms of zoning in plutons, as shown in Chapter 3, is also of fundamental importance in allowing constraints to be placed on modelling crustal evolution e.g. AFC generally requires less contamination than simple mixing to produce similar changes in isotopic ratios. It is thus very important to combine major and trace element and isotopic studies in order to deduce the form of mixing. Most of the work to date has been on the intermediate to evolved components of the plutons and this has been difficult because of the differing amounts of fractionation and contamination.

5.2 Regional geology and tectonics

The Southern Uplands of Scotland are dominated by a series of lower Palaeozoic flysch facies sediments which are sub-divided into three strike parallel belts: the Northern, Central and Southern Belts (Leggett *et al.* 1979; Morris 1983). The Northern Belt rocks although dominated by greywackes, also contain Llanvirin-Landelo argillites and chert and mafic volcanic rocks mainly Arenig in age,and are entirely Ordovician in age. This is separated from the Central belt by the Northern/Central Belts Boundary fault (Morris 1987). The Central and Southern belts are also dominated by greywackes, although argillites, cherts and mafic volcanic rocks are rare. Stratigraphic sequences in all three belts occur in discrete fault bounded tracts, which predominantly young to the NW but become sequentially younger to the SE (Leggett *et al.* 1979, McKerrow *et al.* 1979).

Tectonic interpretations to account for this structure have been the subject of much recent debate (McKerrow, 1988). Early models proposed that the lower Palaeozoic sediments represented a fore-arc accretionary prism built up during the closure of Iapetus (McKerrow *et al.* 1977; Leggett *et al.* 1979 a,b). The presence of basement below the Midland Valley and Southern Uplands was indicated by results of the LISPB seismic refraction experiment (Bamford *et al.* 1978), and later by the occurrence of lower

crustal xenoliths in Carboniferous dykes and vents (Upton *et al.* 1983). This was accommodated in the fore-arc model by postulating that the accretionary prism was at least in part allochthonous (Leggett *et al.* 1982). Other geophysical studies (Hall *et al.* 1983) indicate that crystalline rocks of continental affinity occur at shallow depth (1-5km) below parts of the Southern Uplands. This basement continues 15-20km southwards below the Southern Uplands and is indistinguishable from that below the Midland Valley (Hall *et al.* 1983). Seismic reflectors also extend from the Midland Valley across the Southern Uplands Fault into the Southern Uplands. A further fore-arc model has the Southern Uplands as a "pop-up" structure, partly allochthonous onto Midland Valley type basement, and partly underthrust by basement from the south during the final stages of closure of the Iapetus ocean (Needham & Knipe, 1986). Subsequent structural and petrographical studies of Southern Uplands Lower Palaeozoic Sediments (SULPS) have led to a divergence of views from the traditional one of a fore-arc complex (Leggett, 1987) to that of a back-arc thrust duplex (Stone *et al.* 1987). Further modifications produced a dual model, with the Northern belt rocks having formed in a back-arc basin, and the Central and Southern belts formed in a fore-arc situation (Hutton & Murphy, 1987 and Morris, 1987). Recent geophysical data from the North East Coast deep seismic reflection profile (NEC) which runs from the Midland Valley to south of the Lake District, has suggested the presence of at least four types of crust based on their reflectivity (Freeman *et al.* 1988). These authors have suggested that these represent four different crustal/terrane types: (1) Midland Valley, (2) Sub-continental subduction complex, (3) Lake District and (4) Southern continent (Midland Platform?).

The importance of strike-slip faulting has been emphasised by some workers (Hutton, 1987; Hutton & Murphy, 1987), and the fault separating the Northern and Central Belts has been postulated to separate two tectonostratigraphic terranes which were juxtaposed in the late Silurian/early Devonian. An isotopic study of granitoid boulders from Northern Belt conglomerates showed many to be similar to intrusions now exposed in Newfoundland, and this was interpreted as evidence that these areas were juxtaposed early

in the history of closure (Elders, 1987).

Much debate also concerns the timing of collision, and interpretations vary from end-Ordovician (Hutton & Murphy, 1987) to end-Silurian/early Devonian (McKerrow, 1987; Soper *et al.* 1987, Thirlwall, 1988).

5.3 Plutons studied and aims of chapter

REE and Sr and Nd isotope data are presented from several small plutons from southern Scotland (Figure 5.1). These include the Priestlaw and Cockburn Law intrusions in the northern Southern Uplands (see Chapter 3). The other plutons analysed here for REE and Sr and Nd isotopes are Spango (5 samples) and Knipe (4 samples) from the Northern belt both of which sit very close to the Southern Uplands Fault, Cairnsmore of Carsphairn (3 samples) from the Central Belt and Bengairn (4 samples) and Portencorkrie (2 samples) from the Southern Belt. One specimen from Creetown in the Southern belt and another from Distinkhorn in the Midland Valley were also analysed. Spango and Knipe have not been dated but as all other plutons from the northern Southern Uplands give ages around 410Ma and as these have strong geochemical similarities to these plutons, a similar age is extremely likely. The close spatial and temporal association of Bengairn with Criffell and the similar age of Portencorkrie (J.W. Gaskarth, pers. comm.) also display the distinct grouping of ages between the northern and southern Southern Uplands. A summary of the major and trace element characteristics (M.F. Thirlwall, unpublished data) of these plutons will first of all be described (section 5.4) in order to compare and contrast along and across strike in the Southern Uplands.

The main aims of this chapter are as follows:

(a) to present new REE and Sr and Nd isotopic data for several plutons in southern Scotland in order to constrain models for the recycling and addition of continental crust in the later stages of the Caledonian orogeny.

(b) to study the geochemical characteristics of these plutons and to fit these into the framework of granitoid suites proposed by Stephens & Halliday (1984).

(c) to compare the geochemical characteristics of plutons from along and across strike in the Southern Uplands, and to relate them to existing tectonic models.

5.4 Major and trace element geochemistry.

Major element trends and concentrations for all the Southern Uplands plutons are remarkably similar (e.g. Figure 5.2a,b,c), the only real difference being slightly higher Na_2O in plutons in the south (Figure 5.2d), except the S-type Cairnsmore of Fleet. Previously published data for the larger plutons of Loch Doon, Criffell and Cairnsmore of Fleet (Tindle & Pearce, 1981; Stephens & Halliday, 1986; Tindle *et al.* 1988) are also plotted. The range in silica of the southern plutons is relatively limited (58-74%) reflecting the lack of basic diorites marginal to these. Although several smaller plutons are associated with basic rocks (e.g. Portencorkrie, Glencluce), there is as yet no published data on these.

The plutons generally have similar trace element characteristics but some differences are apparent:

(a) There is a gradual increase in Rb when plotted against SiO_2 for the basic-intermediate compositions (Figure 5.3a), but this is more dramatic increase at higher SiO_2 for some plutons (Loch Doon, Criffell, Carsphairn) similar to the high values found in Fleet. This increase is most marked in rocks of granitic composition including aplites and cordierite microgranites.

(b) Plutons from the southern Southern Uplands have higher abundances of Sr at similar SiO_2 than the majority of northern ones (Figure 5.3b), but are lower than the pyroxene-mica diorites of Priestlaw.

(c) At similar SiO_2, Y and Yb are lower in plutons from the southern part (Figure 5.3c) but have overlapping fields for La giving rise to higher La/Y and La/Yb (Figure 5.3d) in these plutons than for those in the northern part.

(d) K/Rb ratios in the plutons decrease with increasing SiO_2 and there is a good trend for K/Rb vs. Rb. The exceptions to this are Priestlaw and Cockburn Law

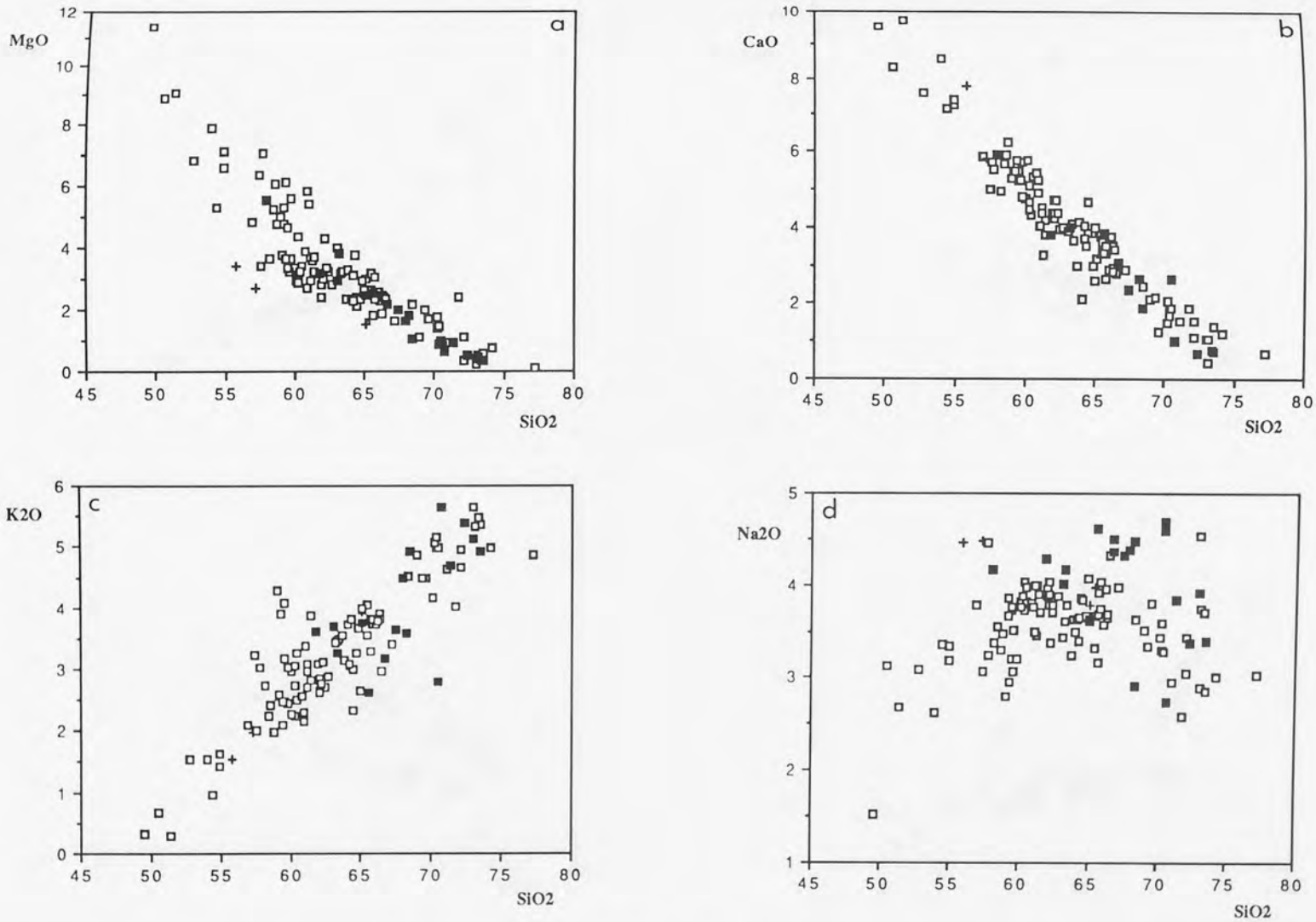

Figure 5.2 Selected major element Harker diagrams for southern Scotland granitoid plutons. Symbols are: open squares: northern Southern Uplands; closed squares: southern Southern Uplands plutons; crosses: Midland Valley. Data sources: this study, Stephens & Halliday (1984) and Tindle & Pearce (1981).

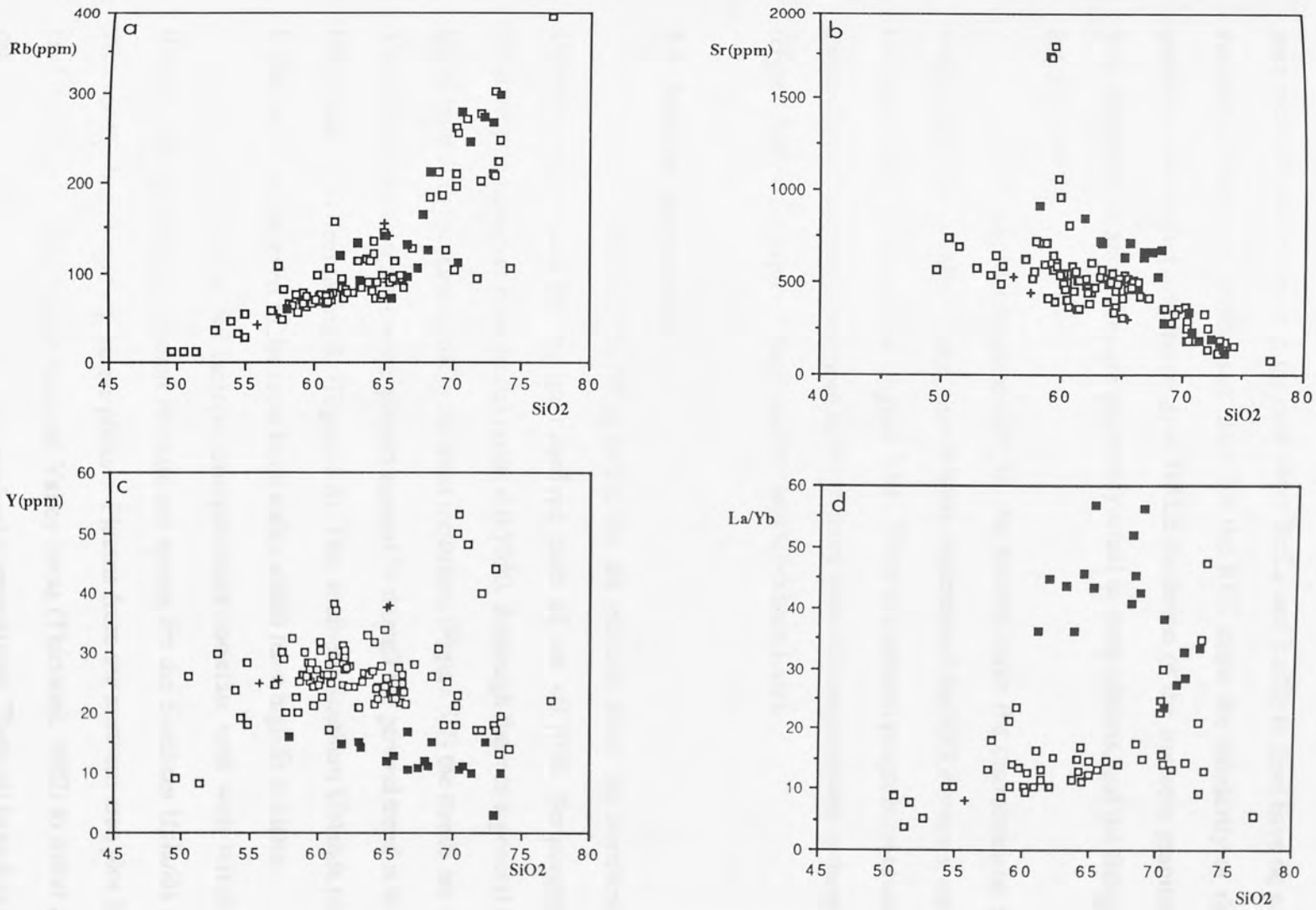

Figure 5.3 Selected trace element Harker diagrams for southern Scotland granitoid plutons. Symbols as in Figure 5.2.

which show a general increase and some scatter of points on the diagram (Figure 5.4).

Apart from these differences the plutons have similar abundances of other trace elements and ratios e.g. the data show Ba/La and La/Nb to have have no geographical variation. Chondrite normalised plots for the REE show the similarity of the northern plutons to each other and the relative HREE depletion of the southern granitoids (Figure 5.5). Negative Eu anomalies are extremely small in most plutons, and the Bengairn diorite has no anomaly.

Spiderdiagrams for all the plutons have the characteristic patterns of within-plate calc-alkaline rocks, with relative depletion of the HFS elements, enrichment of LILE and high $(Zr/Y)_N$ ratios (Figure 5.6a). There is a general progression towards a much more inflected pattern from more basic to more evolved compositions in these intrusions (Figure 5.6b, c.f. chapter 3 for Priestlaw and Cockburn Law).

5.5 Isotope geochemistry

Initial $^{87}Sr/^{86}Sr$ ratios for all plutons from the northern Southern Uplands are low and for the least evolved parts all are <0.7050. No plutons from the southern part however have initial ratios < 0.7050. Although there is a general increase in initial ratio with increase in SiO_2 for most intrusions (Figure 5.7) the trends are not simple. There is also some scatter when plotted against Sr though the general trend is to increasing initial ratio with decreasing Sr (Figure 5.8). The southern Southern Uplands plutons have higher initial ratios even in the most basic rocks which have high Sr contents.

Initial Nd isotopic compositions correlate well with initial $^{87}Sr/^{86}Sr$ (Figure 5.9) however published Nd data are sparse for the Southern Uplands intrusions, even for the better studied, larger plutons. Plutons from the northern area plot from within the lower part of the field of Midland Valley lavas (Thirlwall, 1982) to lower and higher εNd and εSr respectively in the more evolved compositions. These all have less radiogenic initial $^{143}Nd/^{144}Nd$ than the Distinkhorn diorite (ε Nd=+2.9) which is the highest value yet recorded for a Caledonian granitoid. The Carsphairn intrusion plots in the lower

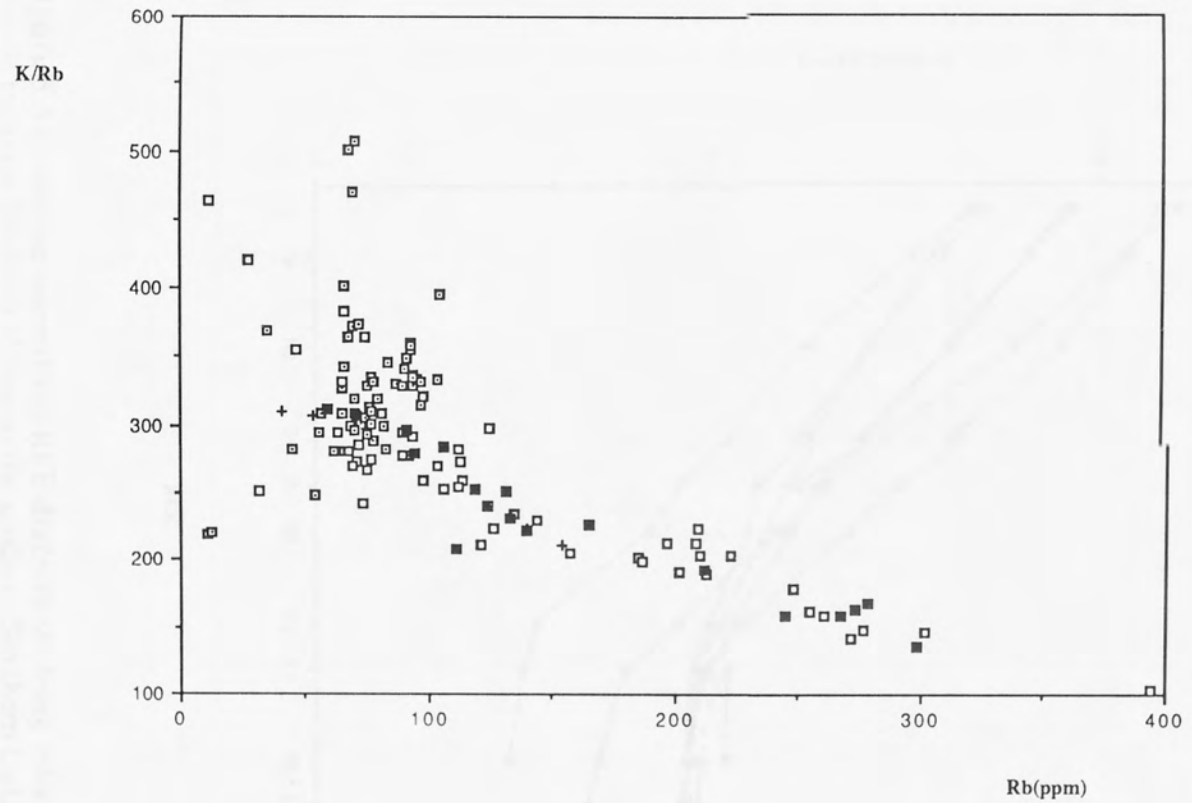

Figure 5.4 K/Rb-Rb plot for southern Scotland granitoid plutons. Symbols as in Figure 5.2 except for Priestlaw and Cockburn Law which are shown as squares with central dot.

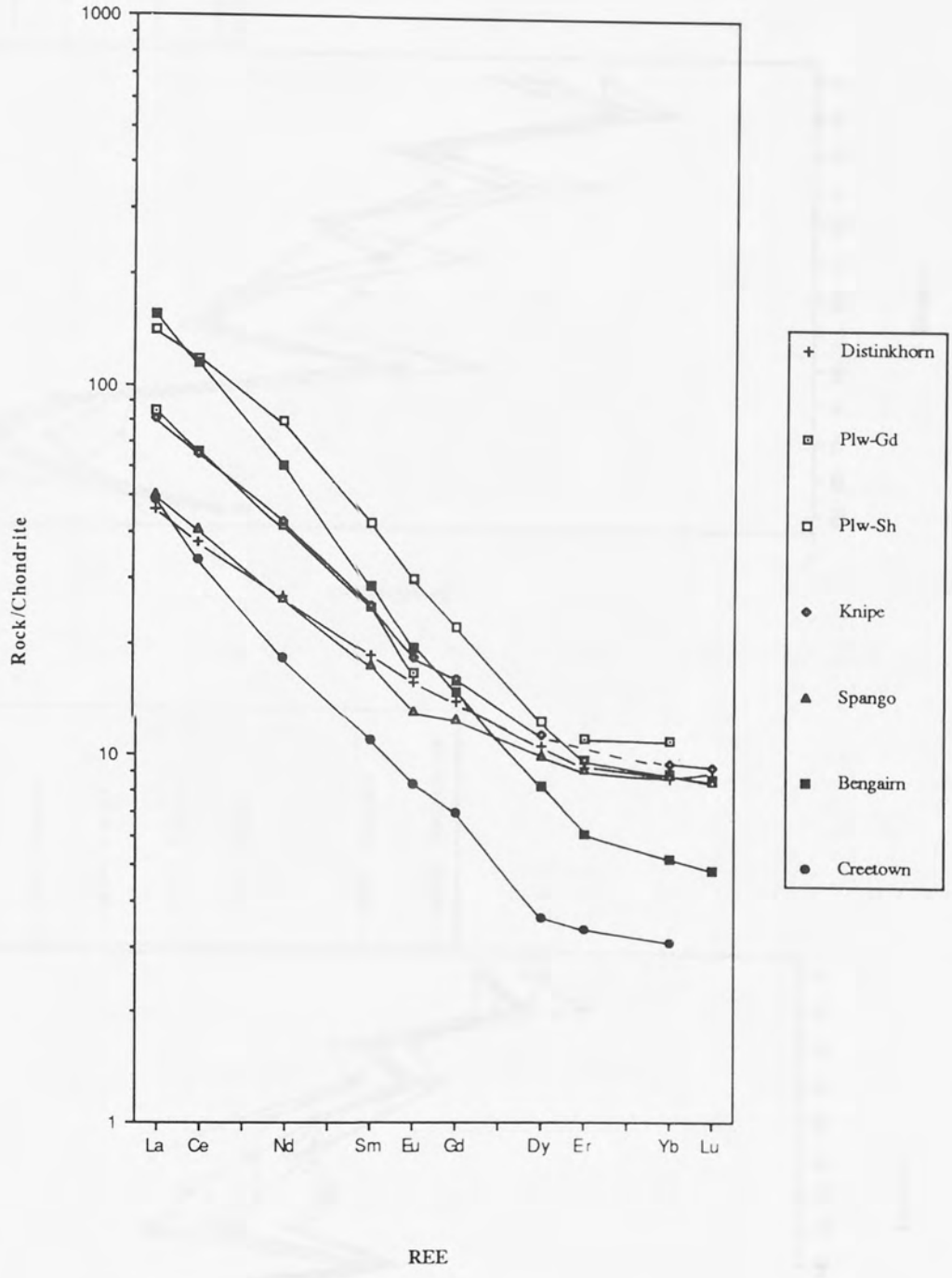

Figure 5.5 Chondrite normalised REE diagram showing selected samples of granitoid plutons from the Midland Valley to the southern Southern Uplands.

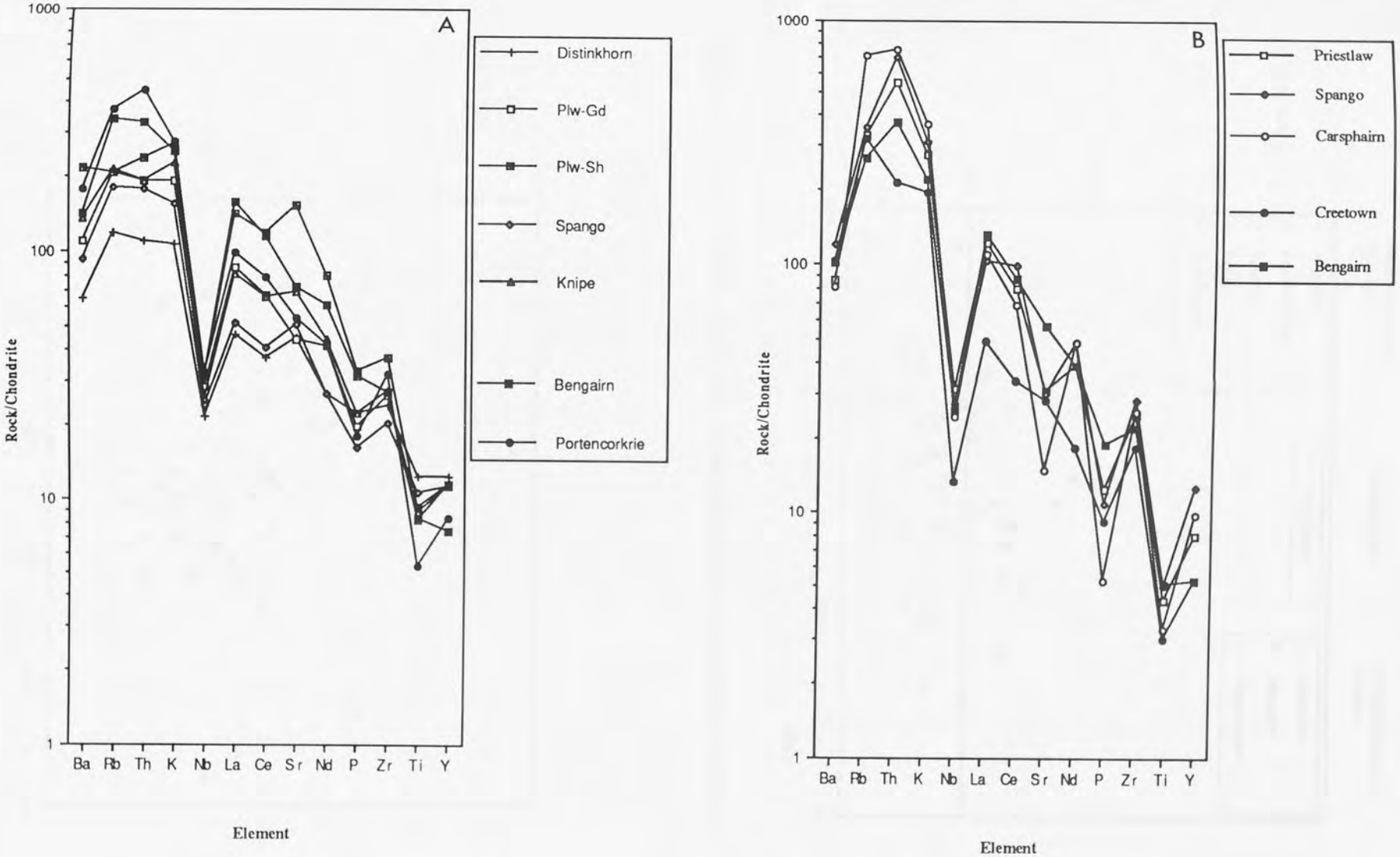

Figure 5.6 Spiderdiagrams for southern Scotland granitoid plutons for the least evolved (A) and more evolved (B) samples.

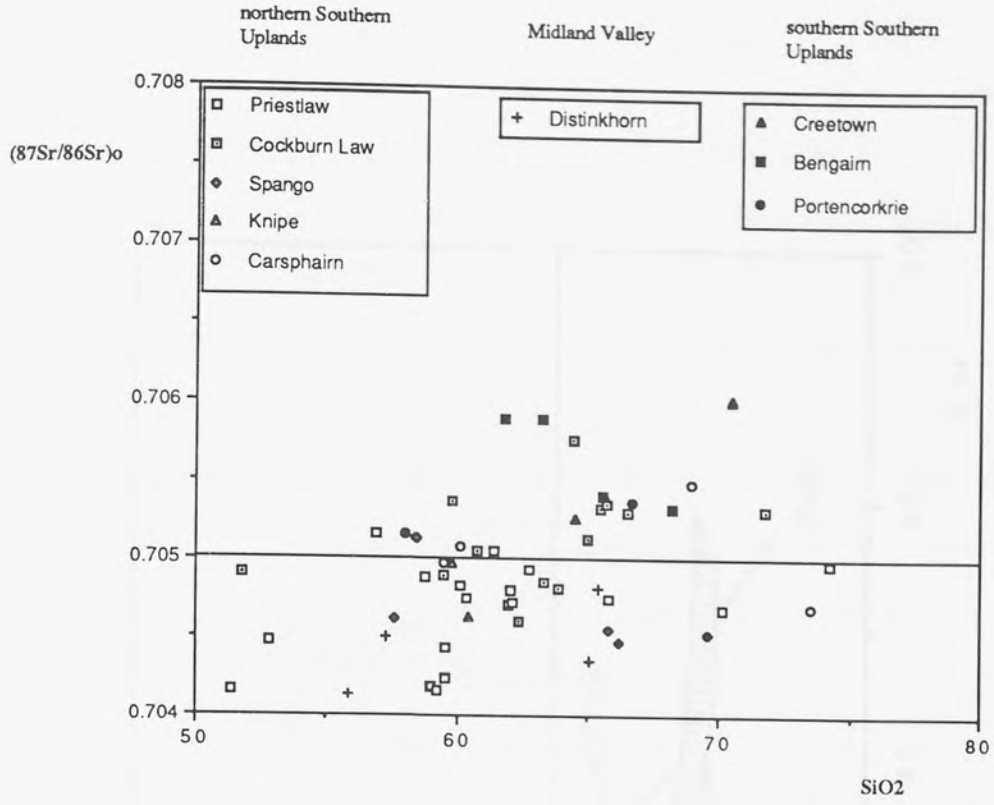

Figure 5.7 ($^{87}Sr/^{86}Sr$)o - SiO_2 plot of southern Scotland granitoid plutons.

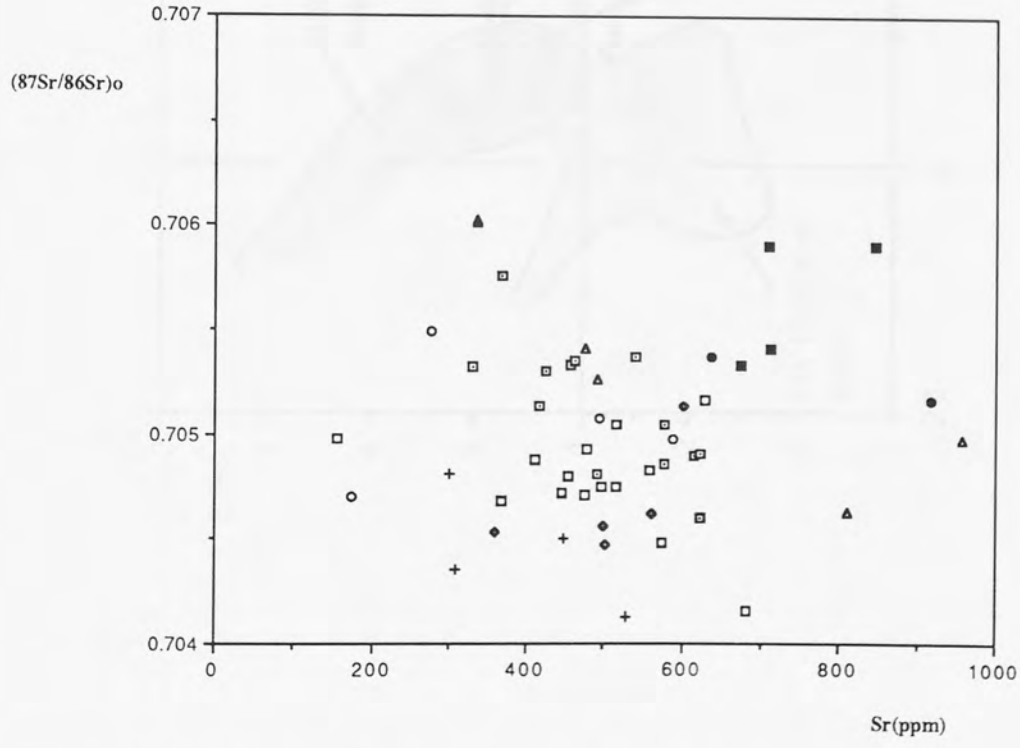

Figure 5.8 ($^{87}Sr/^{86}Sr$)o - Sr plot of southern Scotland granitoid plutons.

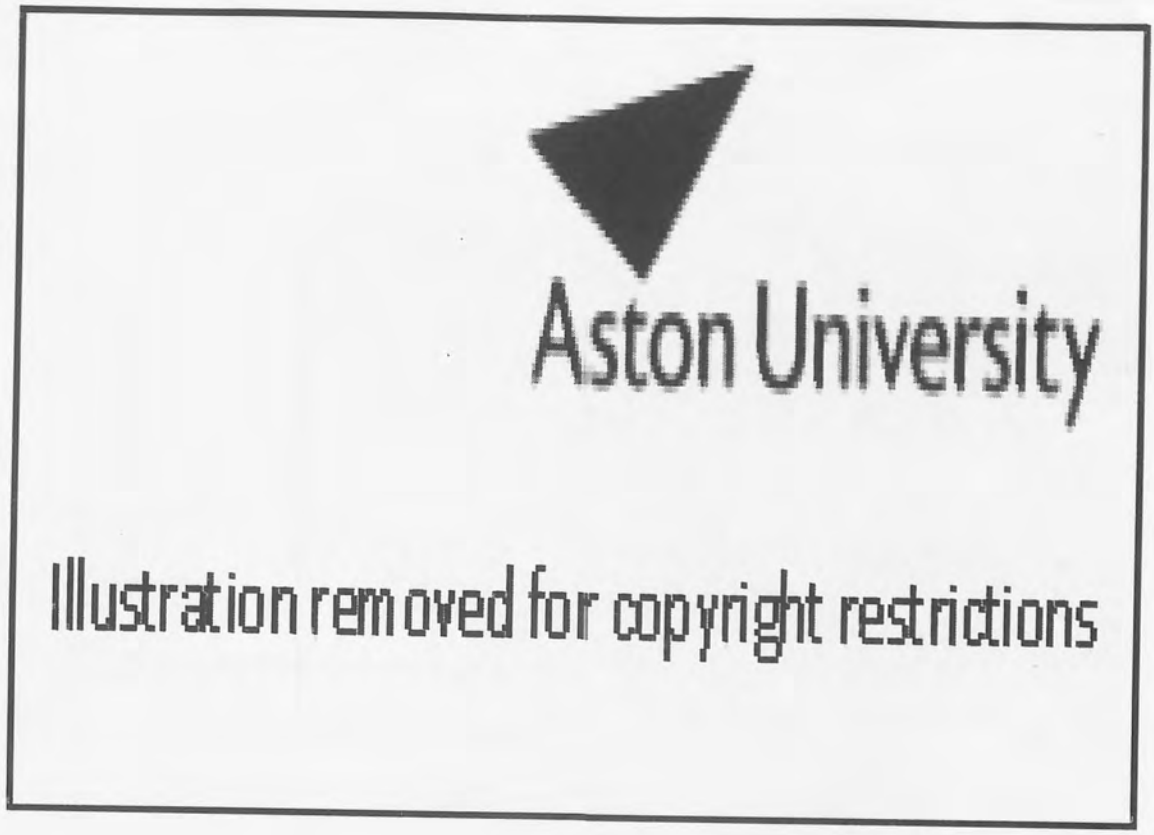

Figure 5.9 εNd - εSr diagram, showing new data southern Scotland granitoid plutons (line plots), and previously published data for Midland Valley and SW Highland lavas (Thirlwall, 1982a), and the Criffell, Fleet and Doon plutons (Halliday, 1984; Holden *et al* 1987).

right quadrant, in a similar position to the nearby Loch Doon intrusion (Halliday, 1984), and both these bodies have more enriched isotopic ratios than others elsewhere in the northern Southern Uplands. The reason for this probably is a function of analysing more evolved compositions: although there is a range in initial Sr ratios in Loch Doon from as low as 0.7041 (Halliday *et al.* 1980), the only two samples that were analysed for $^{143}Nd/^{144}Nd$ have initial Sr ratios $\geq$ 0.7050 (Halliday, 1984). The nearby Knipe intrusion has initial Sr isotopic ratios as low as 0.7046 with corresponding ε Nd= + 1.1. Initial ratios of 0.7050 have corresponding ε Nd = -1.2 which is comparable to the Sr and Nd values for Loch Doon. It is likely therefore that the more basic diorites of Loch Doon with low initial Sr isotopic ratios will also have comparably high initial Nd isotopic signatures.

Data for three samples from the St. Abbs lavas are also shown on Figure 5.9. Two samples from the 'flat trend' of Thirlwall (1979) lie near the less evolved granitoids and the third from the 'rapid enrichment' trend, lies in the lower right quadrant. These lavas and the smaller plutonic bodies have a rather restricted range and have similar overall geochemistry (chapter 2). The flat to concave downwards trends of Priestlaw and Cockburn Law are however not present in the other small plutons which display steeper concave upwards trends more typical of mixing/AFC (Figure 5.9).

Data from the southern Southern Uplands plutons are displaced to higher εSr and lower ε Nd relative to the northern ones. As shown previously all have initial Sr isotopic ratios >0.7050 and low ε Nd. Mafic inclusions in the Criffell pluton (Holden *et al.* 1987) and the one sample analysed from Creetown have ε Nd > 0 (Fig 5.9).

5.6 Discussion

(a) Crustal addition vs. crustal recycling

A knowledge of the source(s) of granitoids is necessary in order to place constraints on models for the evolution of the continental crust through geological time. Although it is generally accepted that much of the Earth's crust had formed during the Pre-Cambrian (Moorbath, 1975), there is debate as to whether the production of

Phanerozoic granitoids at destructive plate margins represent additions to the crust or are merely recycled crust (Allegre & Ben Othman, 1980, Samson *et al.* 1989). There is no general consensus concerning either the proportions or mechanisms of mixing of the various components of calc-alkaline granitoids. Much of the ambiguity arises from expecting too much identity of source, and from the extrapolation of the results from individual plutons to large areas.

Several authors have suggested that the late Caledonian granitoids of Scotland are mixtures of both mantle melts and crustal materials, whereas others have proposed that they are dominantly or totally crustal melts. Debate about the importance of crustal recycling during the later stages of the Caledonian orogeny has centred around plutons in the Highlands particularly in the area around the present exposure of the Lorne lavas (Hamilton *et al.* 1980; Frost *et al.* 1985; Thirlwall, 1986; Clayburn, 1988). Much of the evidence for crustal recycling comes from Pb isotope systematics (Clayburn, 1988), however mantle derived Pb may be swamped by Pb from assimilation of crustal melts/fluids which may contain ten to fifty times the concentration of that in a basalt from the mantle. Although there can be little doubt that a crustal component forms at least part of the S.W. Highlands granitoids the least evolved granitoid is isotopically and geochemically very similar to the primitive Lorne lavas (Thirlwall, 1986) . These lavas provide evidence for an enriched mantle beneath the south west part of the Highlands (Thirlwall, 1982a).

Primitive magmas are the best insights into the characteristics of the mantle, thus it is worthwhile to compare their isotope characteristics with those of the plutons. The extensive late Caledonian volcanics of the Midland Valley are probably derived from a long term, LREE depleted mantle modified by subducted lithosphere (Thirlwall, 1982a). The Distinkhorn in the Midland Valley likewise displays radiogenic Nd and unradiogenic Sr isotopic ratios similar to those of the lavas (Figure 5.9). The variation in isotopic ratios however, is an indication that the pluton did not evolve as a closed system and that AFC processes are likely to have occurred.

The only lavas, contemporaneous with plutons in the northern Southern

Uplands, are those of St. Abbs/Eyemouth. Although the least evolved of these are basic andesites (Thirlwall, 1979) they have high Ni and Cr values and thus it is unlikely that they have suffered extensive crustal contamination. All of the lavas in northern Southern Uplands, particularly the most basic ones, have low ε Sr and high ε Nd implying either a large mantle or recently derived mantle source. The data are strongly similar to the least evolved parts of the plutons of the northern Southern Uplands. This similarity is worth discussion in the light of a recent model of melting, assimilation, storage and homogenisation (MASH) (Hildreth & Moorbath, 1988). This model was based on a detailed study of arc magmas in central Chile, all of which lie at the same distance from the trench and above the subducting plate, which traversed crust of different ages. In the MASH model base-level characteristics for each volcano are established by "blending of sub-crustal and deep-crustal magmas in zones of melting, assimilation, storage and homogenization (MASH) at the mantle-crust transition". It is therefore possible that the similarities in the least evolved northern Southern Uplands intrusions and lavas is the base-level of a ponded, mantle-derived magma. Although it is extremely likely that crustal contamination occurs as magmas pass through the crust it can be argued that isotopic ratios in the more basic parts of the plutons remain relatively close to those of the underlying primary mantle and are not simply a product of MASH because:

(1) The similarity of trace and major elements of the most basic rocks of the plutons to high Ni and Cr magmas at St.Abbs Head and Eyemouth. Primitive lavas however are unknown along the arc in central Chile (Hildreth & Moorbath, 1988).

(2) For a more depleted source (e.g. highest εNd Midland Valley lavas Figure 5.9) to be parental to the plutons it would require two contaminants in order to produce the required S-shaped pattern of the eastern Southern Uplands on an ε Nd- ε Sr diagram. It would be very unlikely that two contaminants would produce similar characteristics in several plutons and primitive lavas separated by ca.100km.

(3) Hildreth & Moorbath (1988) stated that "...real constancy in base level values would require consistent homogenisation prior to resumed ascent and would suggest that

the mixing proportions of crustal and mantle melts, the mineral assemblages residual to crustal melting, and probably therefore the depth of the MASH zone all remain more or less fixed". This might be feasible in long lived or large magma chambers such as those which occur in Chile. The similarities of the plutons and lavas of the northern Southern Uplands would, in the MASH hypothesis, be coincidental. It is thought to be extremely unlikely that the Priestlaw shoshonitic diorites and the parent to the Main Series gabbro both of which have very different Sr and Nd abundances would end up with almost identical isotope ratios. This would require that the fine-grained diorites either have suffered much more contamination, which is unlikely (Chapter 2), or to have had a different contaminant, which is also extremely unlikely considering the similarity in Pb isotopes between the two (Thirlwall *et al.* 1989). The similarity in isotopic ratios of Spango, Knipe and the St. Abbs lavas across a strike area of ca.130 km. is further evidence against a dominant MASH control. The slightly lower ε Nd and higher ε Sr in Spango and Knipe are likely to have been produced by minor contamination consistent with their more evolved nature (57-60% SiO_2). The overall evidence therefore suggests that the mantle composition below the northern Southern Uplands is isotopically close to that of the Basic pyroxene-mica diorites and norite of Priestlaw i.e. εNd ca. +2.2, initial $^{87}Sr/^{86}Sr$ ca. 0.7041

It is evident from the variation in isotopic ratios (Figure 5.7-9) that the magmas for the plutonic rocks did not remain as closed systems. However the zonations in both the Loch Doon and Carsphairn intrusions have been modelled as closed system fractional crystallisation based on both least squares modelling and the good trends observed in selected trace elements (Tindle & Pearce, 1981; Tindle *et al.* 1988). Although fractional crystallisation is an important control in the evolution of zoned calc-alkaline plutons, the isotopic evidence clearly shows that at least two components, generally both a mantle and a crustal source, are necessary. This has been shown for the Priestlaw and Cockburn Law intrusions in which fractional crystallisation has been an important control (Chapter 2), and where the well-defined trends are consistent with a simple model of fractional crystallisation. Progressive contamination of a basic/intermediate magma by a

silica-rich (minimum melt) contaminant may thus simply appear to enhance the fractional crystallisation process which in itself is essentially progressively producing a minimum-melt composition.

Isotope ratios in the plutons generally correlate with fractionation thus a model akin to AFC is dominant in their evolution; however it is not unusual to find rocks with lower SiO_2 with higher ε Sr than that of more evolved ones. This implies, along with field evidence (Chapter 2; Tindle *et al.* 1988), that in most cases the units were emplaced as separate pulses from a single chamber and that they were very closely, but not necessarily directly, related. Without detailed isotopic data for the individual plutons it is difficult to model their evolution in any quantitative way. The similarities between the northern plutons are consistent with their having similar histories and it is evident that a crustal contribution is present in all plutons. AFC processes have probably operated in all northern Southern Upland plutons and, since all have a narrow range in isotope ratios, it is likely that fractional crystallisation is the more dominant control on zonation with Ma/Mc (r in AFC calculations) ratios being low. AFC processes generally require less contamination than simple mixing in order produce changes in isotopic ratios (see Figure 2.7) and may require reductions in modelling of as much as tenfold (Pankhurst *et al.* 1988). The crustal contributions thus are probably small in the Spango and Knipe intrusions like those of Priestlaw and Cockburn Law. The larger pluton of Loch Doon has a large range in initial $^{87}Sr/^{86}Sr$ ratios (0.7041-0.7059) and, along with Carsphairn, contains more evolved compositions (e.g aplites, cordierite microgranites). Many of these evolved rocks have similarities to the S-type Fleet intrusion, thus it is likely that their centres contain a significant crustal component. High-SiO_2 rocks are much less common in the smaller intrusions, but this is perhaps not surprising because their heat budget is unlikely to promote melting on a large scale.

Plutons in the southern Southern Uplands, nearer to the trace of the Iapetus Suture, are much younger (ca.397 Ma.) than those further north (Thirlwall, 1988). A similar age for the granite and lavas of the Cheviot, which lie across the presumed

Iapetus Suture, shows that this period of magmatism post-dates closure of the Iapetus Ocean. The larger plutons show correlated increases in SiO_2, initial $^{87}Sr/^{86}Sr$, $^{18}O/^{16}O$ (Stephens *et al.* 1985) and age corrected $^{206}Pb/^{204}Pb$, reflecting large components of crustal melt in their centres. The quartz diorites of Bengairn (adjacent to Criffell) have similar enriched isotopic characteristics (Figure 5.9) which may also imply crustal involvement. Lack of a Eu anomaly in the samples analysed from this pluton is not clear evidence against crustal contamination, because the production of an anomaly is dependent on fO_2, and a feldspar free contaminant could also produce smooth REE patterns. The presence of mafic syn-plutonic dykes in the Criffell pluton with higher initial $^{143}Nd/^{144}Nd$ than the pluton itself (Holden *et al.* 1987) implies a mantle component as opposed to an infracrustal I-type parent (Stephens *et al.* 1985). The presence of abundant, mantle-derived hornblende lamprophyres around Criffell, with variable $^{143}Nd/^{144}Nd$ and relatively high $^{87}Sr/^{86}Sr$, which may have played a parental role (Henney *et al.* 1989) also supports the concept of a mantle component. The data from the syn-plutonic dykes and lamprophyres indicate that, if these are parents to the plutons, the large plutons near to the Iapetus Suture are to some degree contaminated. This is consistent with the evidence for more enhanced crustal melting (e.g. Fleet, centre of Criffell) at this time. The more basic rocks do however have generally more radiogenic Sr and less radiogenic Nd than in the northern Southern Uplands granitoids and lavas. The least evolved plutonic rocks in the southern Southern Uplands are present in the marginal parts of the Portecorkrie pluton, and all have high initial $^{87}Sr/^{86}Sr$ >0.7050 (J.W. Gaskarth, in prep.). Andesites associated with the Cheviot pluton further east also have similarly elevated initial ratios (Thirlwall, 1988). Mafic lamprophyres spatially associated with the Criffell pluton are likely to represent melts little modified by crustal interaction (Henney *et al.* 1989). Their isotopic signatures (ε Nd= -2 to +2; ε Sr= +15 to +30) imply the presence of a heterogeneous mantle below the southern part of the Southern Uplands. A difference in the mantle composition between that beneath the southern Southern Uplands, and that under the northern part is probable, rather than having to postulate large amounts of contamination in southern diorites and

lamprophyres, the latter which have primary characteristics.

The proposal that lamprophyres are parental, by AFC and mixing processes, to the Criffell and other Late Caledonian granitoids (Henney *et al.* 1989, Rock & Hunter, 1987) is based on the spatial and temporal association of the two, and on isotopic evidence. It has been shown, on the basis of isotope and major and trace elements, that lamprophyres are not parental to the plutons of the northern Southern Uplands, which require a basaltic/basaltic andesite parent (Chapters 2 & 4). Basaltic rocks are also present in vents near the Criffell pluton (Rock *et al.* 1986a). Although the isotope characteristics are consistent with the lamprophyre parent hypothesis, the necessary contaminating siliceous melts would be unusual, being rich in Al_2O_3 and Na_2O and low in CaO, K_2O and most trace elements particularly Sr, Rb and the HFS elements. It is not clear what melting phases can give rise to such an unusual assemblage. The mechanisms of contamination however are likely to be complex in volatile-rich liquids, particularly when combined with crystallisation of the magma. It is thought more likely that the lamprophyres represent very small degree partial melts formed at the initiation of a melting event, consistent with their general early emplacement, and that later, larger degree partial melting (essentially the same source isotopically) has given rise to the parents of the granitoids. This would partly explain the relatively low Y and middle REE abundances in the southern plutons compared with their very high abundances in lamprophyres. A general model of lamprophyres being the parental source to granitoids is unlikely from the lack of evidence of similar lower crustal lithologies worldwide. The generally high Th, U and K contents of lamprophyres would also enhance heat flow if extensive underplating had occurred, and there is little evidence for this. Another difficulty is with the large volumes of small degree partial melts necessary for a lamprophyre parent. Increasing the degree of melting (in which case lamprophyres would not be produced), and ponding the magma would not produce a primary assemblage for minettes. The higher SiO_2 and generally lower incompatible element concentrations in the hornblende-lamprophyres and basalts compared to mica lamprophyres may be related to higher degrees of partial melting in the former and thus

explain their closer association with plutons in the southern part of the southern Uplands.

Based on the limited Nd data available it would appear that, as in the northern Southern Upland plutons, contamination is more important for the larger plutons. The likely presence of a variably enriched mantle below this area however makes quantitative estimates difficult.

(b) Granitoid suites

The granitoids of the Southern Uplands form part of a suite: the "S of Scotland Suite": comprising plutons from the southern Highlands, the Midland Valley and the Southern Uplands (Stephens & Halliday, 1984). The Criffell and Fleet plutons are excluded from this classification because they have some S-type characteristics. Stephens & Halliday (1984) defined a suite as being "of various petrographic types but related regionally by distinctive chemical characteristics". Plutons in the SW Grampian Highlands for example show large enrichments in Sr and Ba compared with the other suites. Such a classification however excludes suites based on age and source, which may have been important in defining the geochemical nature of the suites. In many classification schemes it is tempting to relate differences relative to some arbitrary reference e.g.SiO_2 =58%. The problem here however is that granitoids may represent the products of different degrees of melting, fractionation and contamination, all of which which may be a function of physical as opposed to chemical parameters. An example of this are the A-type granitoids of the Cairngorm suite that are associated with thickened crust to >60km, produced during the Grampian orogeny (Atherton & Plant, 1984), which may have allowed more extensive crystallisation and contamination to occur. Different degrees of partial melting of a similar source may also give rise to contrasting geochemical units in single plutons, as in the case of Priestlaw, where the shoshonitic pyroxene-mica diorites have very similar major and trace element contents to the SW Highland Suite, and yet were derived from a similar source to the Main Series of the pluton (Chapter 2). Because individual specimens or groups of specimens may have a separate history (e.g. AFC, fractional crystallisation,

simple mixing) it is probably better to view the data set as a whole. The pyroxene-mica diorites taken alone, for example, do not fit the suites of Stephens & Halliday (1984), but are unique to the S of Scotland Suite. Since Sr and Nd isotopes are not affected by fractional crystallisation or melting, they provide more constraints as to the components involved and help to highlight differences in primary sources and contaminants.

The new data presented both in this chapter and Chapter 2 allow a subdivision of the southern Scotland (Midland Valley and Southern Uplands) granitoids into three suites. The Nd and Sr isotopic data are interpreted to indicate three possible mantle sources in the south of Scotland: a) the Midland Valley, b) northern Southern Uplands and c) the southern Southern Uplands. Because there is a distinct age difference for magmatism between the northern (c.a.410ma) and southern (c.a. 394ma) Southern Uplands a clear separation into two suites is justified. The mantle below the northern Southern Uplands at 410Ma. was isotopically depleted, but more enriched than that below the Midland Valley, whereas that below the southern part is much more enriched and heterogeneous than that in the north (Figure 5.9). Differences in major and trace element contents also exist between the northern and southern areas (e.g. La/Yb). A chemical as well as a temporal difference therefore exists between the northern and southern Southern Uplands plutons.

Terrane boundaries, once proven, can also be used to define suites Differences in the composition of the crust, as well as the mantle, may occur between different terranes. In the south of Scotland the basement is covered by Lower Palaeozoic sediments and characterisation of the basement must be by indirect means. A clear indication of different basement terranes is produced from a study of Pb isotopes. Plutons in southern Scotland, all have relatively flat trends in $^{206}Pb/^{204}Pb$ - $^{207}Pb/^{204}Pb$ plots, and at constant $^{206}Pb/^{204}Pb$ there is an increase in $^{207}Pb/^{204}Pb$ from the Midland Valley through the northern Southern Uplands to the southern Southern Uplands (Thirlwall *et al.* 1989). The highest $^{207}Pb/^{204}Pb$ and $^{206}Pb/^{204}Pb$ values of the southern plutons (correlated with initial $^{87}Sr/^{86}Sr$ and $\delta\,^{18}O$) are similar to those of the English Lake District

magmas and do not match those of the Lower Paleozoic sediments. Because no Midland Valley magmas have such high $^{206}Pb/^{204}Pb$ and $^{207}Pb/^{204}Pb$, this implies a lack of any common crustal unit for the Midland Valley and the Southern Uplands. On the basis of this information the granitoids and lavas are considered to form three suites based on isotopic characteristics and the ages of emplacement. In the northern Southern Uplands there is however spatial overlapping of the 410ma plutons in the eastern Southern Uplands with the younger lamprophyres which are similar to magmas produced in the southern Southern Uplands. This will be discussed in the following section.

(c) Tectonic models

A direct relationship between late Caledonian magmatism and subduction relies on the precise dating of closure of the Iapetus Ocean. Ideas for this relationship have varied from a direct one (Thirlwall 1982a,1983,1988) to post closure with melting of mantle previously metasomatised by subduction being triggered from above by vertical and horizontal block movements (Watson, 1984). Evidence for the position of the suture of the closed Iapetus Ocean comes from the provincialism of lower Palaeozoic fauna (McKerrow & Cocks, 1976) and the presence of oceanic igneous and sedimentary rocks (Lambert *et al.* 1981). There is little evidence however to provide direct dating of the time of closure, however the Cheviot intrusion and associated lavas (396 Ma) are located above the postulated suture (Solway Line) thus closure was complete by that time (Thirlwall, 1988). On the basis of stratigraphic and structural evidence ocean closure is likely to have been either Ashgillian or post-early Gendinian (Thirlwall, 1988). Silurian pelagic sediments in the Southern Uplands are difficult to reconcile with early closure and therefore closure in the early Devonian is favoured (Thirlwall, 1988). This would imply a direct relationship of 410ma and older magmatism to subduction, with the probable onset of magmatism occurring when sediment ceased to be accreted in the Wenlock (Thirlwall, 1988).

In comparison with recent trench-arc gaps (~140km, Thorpe, 1982), magmatism in the northern part of the Southern Uplands is very close (~60km.) to the

Iapetus Suture. Late Caledonian movements between terranes may however be responsible for the juxtaposition of terranes that were originally separated by large distances. The Orlock Bridge Fault for example, separating the Northern and Central Belts, has been proposed to be a major strike slip fault separating two terranes, but several of the northern Southern Uplands plutons lie south of this fault (Carsphairn, Priestlaw, Cockburn Law). The geochemical data indicate that if this fault separates two terranes, then its position at depth must be different from that at the surface. Crystalline rocks occur at a shallow depth below parts of the north eastern Southern Uplands and the geophysical evidence indicates that this basement continues to the south of both Priestlaw and Cockburn Law (Hall *et al.* 1983). A crustal high velocity refractor crosses the Southern Uplands Fault (Hall *et al.* 1983), but its apparent continuity is not necessarily equivalent to the continuity of a structural marker (Freeman *et al.* 1988), and the same lower-middle crust is not necessarily common to both. A model of the Southern Uplands as a "pop-up" structure (Kneedham & Knipe, 1986), partly allochtonous onto Midland Valley-type basement, and partly underthrust by Lake District basement, can be fitted with the different basement blocks suggested for the Southern Uplands.

A similar, but more detailed study, using the results of the NEC deep crustal profile (Freeman *et al.* 1988) recognised four crustal / terrane types in southern Scotland/northern England : Midland Valley (zone A), a sub-continental subduction complex (zone B), Lake District (zone C) and Midland Platform (zone D). Zones A and B in the northern part are taken to have originated from the northern continent. They are separated from zones C and D further south by a strong northerly dipping reflector, which is taken to represent the Iapetus Suture, with the southern continent being partially subducted beneath the northern one. At the northerly junction of the suture two parallel reflectors transect beyond the Moho, to a depth of 6-7 km. It was suggested that the termination of these reflectors delimits the northerly extent of a decollement, or shear zone, active during the later stages of collision, when mantle originally beneath the southern continent, underthrust the crust of the collision zone.

The chemical similarity of southern Southern Uplands plutons to those further south in the Lake District provides further evidence for underthrusting of lithosphere below part of the Southern Uplands. It has been suggested elsewhere, on the basis of Pb isotopes, that magmatism around 394 Ma was initiated in response to underthrusting of ancient fertile English lithosphere (Thirlwall *et al.* 1989). The geochemical data presented, are therefore consistent with geophysical data in implying the presence of at least two different terranes below the Southern Uplands. The final configuration based on the geochemical data is shown in simplified form in Figure 5.10.

In the proposed model the southern part of the Southern Uplands, and the ocean trench, probably lay further south during the 410 Ma magmatism which occurred close to the Southern Uplands Fault, therefore negating the problem of these rocks being too close to the subduction zone. The differences in Pb and Nd isotope compositions across the Southern Uplands Fault however implies that the northern part and the Midland Valley do not share a common crustal source. Strike-slip faulting was important for the development of the Caledonides. The source of clasts in Wenlock conglomerates in the Midland Valley was from the south, which Bluck (1983) shows was not the present Southern Uplands, whereas the late Silurian conglomerates can be matched with Southern Upland lithologies. It is possible therefore that the northern Southern Upland basement was brought to its present position during the Late Silurian and this is dated by the change in lithology of conglomerate clasts present in the Midland Valley rocks (Bluck, 1983). The timing of these large scale movements is consistent with the period of sinistral strike-slip faulting observed elsewhere in the Caledonides (Watson, 1984). This model is not necessarily inconsistent with the idea that the northern belt is allochthonous as postulated by Hutton & Murphy (1987) and indicated by granitoid clasts in conglomerates which are similar to granitoids in Newfoundland (Elders, 1987), but it requires that the boundary between terranes be located further south and at depth.

The occurrence of the younger lamprophyres (similar to those further south) spatially associated with 410 Ma activity in the eastern Southern Uplands, can also

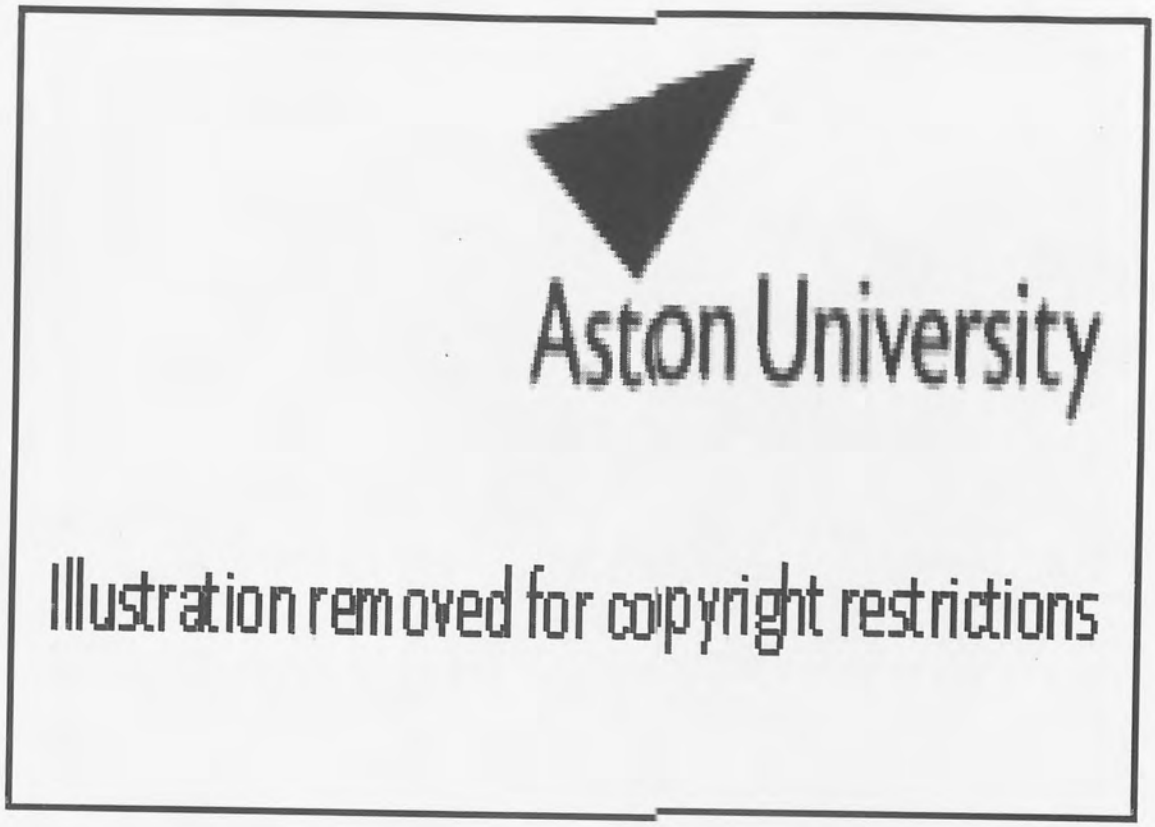

Figure 5.10 Configuration of basement terranes in southern Scotland based on geochemistry of Late Caledonian igneous rocks. Modified from Needham & Knipe (1986).

be explained by this model, and gives the clearest indication of the time of final closure of Iapetus. The isotopic data for the northern plutons suggests a depleted mantle source not too dissimilar from that below the Midland Valley. Although the source of the lamprophyres is from an isotopically time-integrated enriched mantle, it is extremely surprising that this mantle was not sampled by the earlier 410 Ma magmatism. This implies that the source of the lamprophyres was not in its present position at this time. The decoupling of mantle from crust of the southern continent, and the underthrusting of this mantle beneath crust from the northern continent, was implied from the NEC deep reflection studies (Freeman *et al.* 1988). This underthrusting of enriched mantle (representing the source of the lamprophyres) can explain the absence of lamprophyres during subduction (410Ma.), and their emplacement once subduction had ceased. It further suggests that underthrusting, and therefore final closure of the Iapetus Ocean occurred between 410 Ma (the age of the northern granitoids and lavas), and the emplacement of the lamprophyres at ca. 400 Ma. It substantiates therefore, a direct relationship between 410 Ma and earlier magmatism, and subduction.

The change in age of magmatism across Scotland, becoming younger towards the suture (Thirlwall, 1988), may be explained by this model as the trench is moved seaward partly due to the introduction of terranes, and partly due to steepening of the subducting plate during impingement of the English continent.

5.7 Summary

(1) The least evolved parts of plutons from the northern Southern Uplands have high ε Nd and low ε Sr. This is interpreted to indicate that they were derived from a long term depleted mantle modified by subducted lithosphere similar to Midland Valley lavas (Thirlwall, 1986).

(2) Plutons from the southern Southern Uplands have generally higher ε Sr, La/Yb and lower ε Nd and are derived from a more enriched mantle.

(3) None of the plutons studied appears to have remained as a closed system. General

correlations of Sr and Nd isotopes with SiO_2 imply that a process similar to AFC best explains the data. Because Pb isotope ratios do not match with presently exposed Lower Palaeozoic sediments, the contaminant is probably crust from below the accretionary prism.

(4) A combination of Sr and Nd from this study and published Pb isotopes (Thirlwall *et al.* 1989), combined with age dates and geochemistry shows three different magmatic suites to be present in southern Scotland: (a) Midland Valley (b) northern Southern Uplands and (c) southern Southern Uplands. These suites have distinctive mantle and crustal sources.

(5) The data are consistent with geophysical models in implying northward underthrusting of English lithosphere below the southern part of the Southern Uplands and of further underthrusting of decoupled mantle below northern Southern Uplands crust. Differences between isotopic characteristics of the Midland Valley magmas and the northern Southern Uplands magmas imply that they are derived from different terranes which may have been juxtaposed in the Silurian by strike-slip faulting prior to the onset of magmatism.

(6) Closure of the Iapetus Ocean by underthrusting of English mantle and crust occurred post 410 Ma and prior to ca 397 Ma. The 410 Ma magmatism occurred therefore whilst subduction was active hence the two must be directly linked.

(7) The change in age of magmatism across Scotland, becoming younger southward, may be the result of seaward migration of the trench as terranes are introduced in the fore-arc region and the steepening of the subducting plate resulting from impingement of the English plate during closure the of Iapetus Ocean.

REFERENCES

AGUE, J.J. & BRIMHALL, G.H. 1987. Granites of the batholiths of California: products of local assimilation and regional-scale crustal contamination. *Geology*, **15**, 63-66.

ALIBERT, C., MICHARD, A. & ALBAREDE, F. 1986. Isotope and trace element geochemistry of Colorado Plateau volcanics. *Geochimica et Cosmochimica Acta*, **50**, 2735-2750

ALLEGRE, C.J. & MINSTER, J.F. 1978. Quantitative models of trace element behaviour in magmatic processes. *Earth and Planetary Science Letters*, **38**, 1-25.

ALTHERR, A., HENJES, F., MATTHEWS, A., FRIEDRICHSEN, H. & TAUBER HANSEN, B. 1988. O-Sr isotopic variations in Miocene granitoids from the Aegean: evidence for an origin by combined assimilation and fractional crystallization. *Contributions to Mineralogy and Petrology*, **100**, 528-541.

ANDERSON, T.B. & OLIVER G.J.H. 1986. The Orlock Bridge fault: a major late-Caledonian sinistral fault in the Southern Uplands terrane, British Isles. *Transactions of the Royal Society of Edinburgh:: Earth Sciences*, 77, 203-222.

ARIMA, M. & EDGAR, A.D. 1983. A high pressure experimental study on a magnesian-rich leucite-lamproite from the West Kimberly area, Australia: petrogenetic implications. *Contributions to Mineralogy and Petrology*, **84**, 228-234.

BACHINSKI, S.W. & SCOTT, R.B. 1979. Rare-earth and other trace element contents and the origin of minettes (mica-lamprophyres). *Geochimica et Cosmochimica Acta*, **43**, 93-100.

BAILEY, E.B. & MAUFE, H.B. 1960. The geology of Ben Nevis and Glen Coe and the surrounding country. *Memoir of the Geological Survey of Great Britain* (Scotland).

BAKER, B.H. & McBIRNEY, A.R. 1985. Liquid fractionation. part III: Geochemistry of zoned magmas and the compositional effects of liquid fractionation. *Journal of Volcanology and Geothermal Research*, **24**, 55-81.

BAMFORD, D., NUNN, K., PRODEHL, C. & JACOB, B. 1977. LISPB-IV. Crustal structure of northern Britain. *Geophysical Journal of the Royal Astronomical Society*, **54**, 43-60.

BAMFORD, D., NUNN, K., PRODEHL, C. & JACOB, B. 1978. LISPB-IV. Crustal structure of northern Britain. *Geophysical Journal of the Royal Astronomical Society*, **54**, 43-60.

BARNES, R.P., ROCK, N.M.S. & GASKARTH, J.W.G. 1986. Late Caledonian dyke-swarms in southern Scotland: new field, petrological and geochemical data from the Wigtown Peninsula, Galloway. *Geological Journal*, **21**, 101-125.

BARTON, M. & HAMILTON, D.L. 1982. Water-undersaturated melting experiments bearing upon the origin of potassium-rich magmas. *Mineralogical Magazine*, **45**, 267-278.

BATEMAN, P.C. & CHAPPELL, B.W. 1979. Crystallization, fractionation and solidification of the Tuolumne Intrusive Series, Yosemite National Park, California. *Geological Society of America Bulletin* , **90**, 465-482.

BENNET, J.R.P. 1969. Institute of Geological Sciences Report, GP/AG/70/13.

BLUCK, B.J. 1983. Role of the Midland Valley of Scotland in the Caledonian orogeny. *Transactions of the Royal Society of Edinburgh:: Earth Sciences*, **74**, 119-136.

BOWEN, N.L. 1928. *The evolution of the igneous rocks*, Princeton University Press, Princeton, New Jersey, 332p.

BOWES & WRIGHT 1967. The explosion-breccia pipes near Kentallen, Scotland and their geological setting. *Transactions of the Royal Society of Edinburgh*, **67**, 109-143.

BOWES 1962. Kentallenite-lamprophyre-granite age relations at Kentallen, Argyll. *Geological Magazine*, **99**, 119-122.

BROWN, P.E., MILLER, J.A. & GRASTY, R.L. (1968). Isotopic ages of Late Caledonian granitic intrusions in the British Isles. *Proceedings of the Yorkshire Geological Society*, **36**, Part 2, Number 15, 251-276.

CANTAGREL, J.M., DIDIER, J. & GOURGAUD, A. 1984. Magma mixing: origin of intermediate rocks and "enclaves" from volcanism to plutonism. *Physics of the Earth and Planetary Interiors*, **35**, 63-76.

CHAPPELL, B.W. & STEPHENS, W.E. 1988. Origin of infracrustal (I-type) granite magmas. *Transactions of the Royal Society of Edinburgh:: Earth Sciences*, **79**, 71-86.

CHAPPELL, B.W. & WHITE, A.J.R. 1974. Two contrasting granite types. *Pacific Geology* , **8**, 173-174.

CHEN, C.H. & MOORE, J.G. 1979. Late Jurassic Independance dike swarm in eastern California. *Geology*, **7**, 129-133.

CLARKE, D.B. & MUECKE, G.K. 1985. Review of the petrochemistry and origin of the South Mountain Batholith and associated plutons, Nova Scotia, Canada. In: Hall, C. (ed.) *High Heat Production Granites, Hydrothermal Circulation, and Ore Genesis*, Institute of mining and metallurgy, London, 41-54.

CLAYBURN, J.A.P. 1988. The crustal evolution of central Scotland and the nature of the lower crust: Pb, Nd and Sr isotope evidence from Caledonian granites. *Earth and Planetary Science Letters*, **90**, 41-51.

DePAOLO, D.J. 1980. Sources of continental crust: Neodymium isotope evidence from the Sierra Nevada and Peninsular Ranges. *Science*, **209**, 684-687.

DePAOLO, D.J. 1981a. Trace element and isotopic effects of combined wallrock assimilation and fractional crystallisation. *Earth and Planetary Science Letters*, **53**, 189-202.

DePAOLO, D.J. 1981b. A Neodymium and Strontium isotopic study of the Mesozoic calc-alkaline granitic batholiths of the Sierra Nevada and Peninsular Ranges, California. *Journal of Geophysical Research*, **86**, 10470-10488.

DePAOLO, D.J. & WASSERBURG, G.J. 1976. Inferences about magma sources and mantle structure from variations of $^{143}Nd/^{144}Nd$. *Geophysical Research Letters*, **3**, 743-746.

DePAOLO, D.J. & WASSERBURG, G.J. 1977. The source of island arcs as indicated by Nd and Sr isotopic studies. *Geophysical Research Letters*, **4**, 465-468.

EGGLER, D.H. 1987. Solubility of major and trace elements in mantle metasomatic fluids: experimental constraints. In: *Mantle Metasomatism*, Menzies, M.A. & Hawkesworth, C.J. (eds.), Academic Press, London, 21-44.

EHRENBERG, S.N. 1982. Petrogenesis of garnet lherzolite and megacrystalline nodules from the Thumb, Navajo Volcanic Field. *Journal of Petrology*, **23**, 507-547

EHRENBERG, S.N. 1977. The Washington Pass volcanic center: evolution and eruption of minette magmas of the Navajo volcanic field. *Extended abstracts, Second International Kimberlite Conference*, Santa Fe, 1977 (unpaged).

EICHELBERGER, J.C. & GOOLEY, R. 1977. Evolution of silicic magma chambers and their relationship to basaltic volcanism. *American Geophysical Union Monogragh*, **20**, 57-77

ELDERS, C.F. 1987. The provenance of granite boulders in conglomerates of the Northern and Central Belts of the Southern Uplands of Scotland. *Journal of the Geological Society, London,* **144**, 853-863.

ESPERANCA, S. & HOLLOWAY, J.R. 1987. On the origin of some mica-lamprophyres: experimental evidence from a mafic minette. *Contributions to Mineralogy and Petrology*, **95**, 207-216.

FOLEY, S. 1988. The genesis of continental basic alkaline magmas: an interpretation in terms of redox melting. In: Menzies, M.A. & Cox, K.G. (eds.), *Oceanic and Continental Lithosphere: Similarities and Differences,* Special volume, journal of Petrology, Oxford University Press, 139-162.

FOURCADE, S. & ALLEGRE, C.J. 1980. Trace element behaviour in granite genesis: A case study. The calc-alkaline plutonic association from the Querigut Complex (Pyrenees, France). *Contributions to Mineralogy and Petrology*, **76**, 177-195.

FREEMAN, B., KLEMPERER, S.L. & HOBBS, R.W. 1988. The deep structure of northern England and the Iapetus suture zone from BIRPS deep seismic reflection profiles. *Journal of the Geological Society, London,* **145**, 727-740.

FREY, F.A., CHAPPELL, B.W. & ROY, S.D. 1978. Fractionation of rare-earth elements in the Tuolumne Intrusive Series, Sierra Nevada batholith, California. *Geology*, **6**, 239-242.

FROST, C.D. & O'NIONS, R.K. 1985. Caledonian magma genesis and crustal recycling. *Journal of Petrology*, **26**, 515-544.

GLADNEY, E.S. & ROELANDTS. 1988. 1987 compilation of elemental standards for USGS BHVO-1, MAG-1, QLO-1, RGM-1, SCo-1, SDC-1, SGR-1 and STM-1. *Geostandards Newsletter* , **12**, No.2, 253-362.

GOAD, B.E. & CERNY, P. 1981. Peraluminous pegmatitic granites and their pegmatitic aureoles in the Winnipeg River District, south-eastern Manitoba. *Canadian Mineralogist*, **19**, 177-194.

GREEN, D.H. & WALLACE, M.E. 1988. Mantle metasomatism by ephemeral carbonatite melts. *Nature*, **336**, 459-462.

GROMET, L.P. & SILVER, L.T. 1983. Rare earth element distributions among minerals in a granodiorite and their petrogenetic implications. *Geochimica et Cosmochimica Acta*, **47**, 925-939.

HALL, J., POWELL, D.W., WARNER, M.R., EL-ISA, Z.H.M., ADESANYA, O. & BLUCK, B.J. 1983. Seismological evidence for shallow crystalline basement in the Southern Uplands of Scotland. *Nature*, **305**, 418-420.

HALLIDAY, A.N., STEPHENS, W.E. & HARMON, R.S. 1980. Rb-Sr and O isotopic relationships in 3 zoned Caledonian granitic plutons, Southern Uplands, Scotland: evidence for varied sources and hybridization of magmas. *Journal of the Geological Society, London,* **137**, 329-348.

HALLIDAY, A.N. 1984. Coupled Sm-Nd and U-Pb systematics in late Caledonian granites and the basement under northern Britain. *Nature*, **307**, 229-233.

HALLIDAY,A.N., STEPHENS, W.E., HUNTER, R.H., MENZIES, M.A., DICKIN, A.P. & HAMILTON, P.J. 1985. Isotopic and chemical constraints on the building of the deep Scottish lithosphere. *Scottish Journal of Geology*, **21**, 465-491.

HAMILTON, P.J., O'NIONS, R.K. & PANKHURST, R.J. 1980. Isotopic evidence for the provenance of some Caledonian granites. *Nature*, **287**, 279-284.

HANSON, G.N. 1978. The application of trace elements to the petrogenesis of igneous rocks of granitic composition. *Earth and Planetary Science Letters*, **38**, 26-43.

HARMON, R.S., HALLIDAY, A.N., CLAYBURN, J.A.P. & STEPHENS, W.E. 1984. Chemical and isotopic systematics of the Caledonian intrusions of Scotland and northern England: a guide to magma source region and magma-crust interaction. *Philosophical Transactions of the Royal Society of London,* **A 310**, 709-742.

HARRIS, A.L. 1983. The growth and structure of Scotland. In: Craig, G.Y. (ed.), *Geology of Scotland*, 1-22. Scottish Academic Press, Edinburgh.

HAWKESWORTH, C.J., VAN CALSTREN, P. & MENZIES, M.A. 1984. Mantle enrichment processes. *Nature*, **311**, 773-776.

HENDERSON, P. *Inorganic Geochemistry*. Permagon Press, London.

HENNEY, P.J., EVANS, J.A., HOLDEN, P. & ROCK, N.M.S. 1989. Granite-lamprophyre associations in the Scottish Caledonides: trace element and isotopic evidence for mantle involvement in Caledonian granite genesis. *TERRA abstracts,* in press.

HICKEY, R.L. & FREY, F.A. 1982. Geochemical characteristics of boninite series volcanics: implications for their source. *Geochimica et Cosmochimica Acta,* **46**, 2099-2115.

HILDRETH. W. 1981. Gradients in silicic magma chambers: implications for lithosphere magmatism. *Journal of Geophysical Research*, **86**, No. B11, 10153-10192.

HILDRETH. W. & MOORBATH, S. 1988. Crustal contributions to arc magmatism in the Andes of Central Chile. *Contributions to Mineralogy and Petrology*, **98**, 455-489.

HOLDEN, P., HALLIDAY, A.N. & STEPHENS, W.E. 1987. Neodymium and strontium isotope content of microdiorite enclaves points to mantle input to granitoid production. *Nature*, **330**, 53-56.

HURLEY, P.M. & FAIRBAIRN, H.W. 1957. Abundance and distribution of uranium and thorium in zircon, sphene, apatite, epidote, and monazite in granitic rocks. *Transactions of the American Geophysical Union*, **38**, 939-944.

HUTTON, D.H.W. 1987. Strike-slip terranes and a model for the evolution of the British and Irish Caledonides. *Geological Magazine*, **124**, 405-425.

HUTTON, D.H.W. & MURPHY, F.C. 1987. The Silurian of the Southern Uplands and Ireland as a successor basin to the end-Ordovician closure of Iapetus. *Journal of the Geological Society, London,* **144**, 765-772.

JONES, A.P. & SMITH, J.V. 1983. Petrological significance of mineral chemistry in the Agaltha Peak and the Thumb minettes, Navajo volcanic field. *Journal of Geology*, **91**, 643-656.

JOPLIN, G.A. 1968. The shoshonite association: a review. *Journal of the Geological Society of Australia*, **15**, 275-294.

JORDAN, T.H. 1988. Structure and formation of the continental Tectosphere. *Journal of Petrology, Special Lithosphere Issue*, 11-37.

KAY, R.W. & KAY, S.M. 1983. Crustal recycling and the Aleutian arc. *Geochimica et Cosmochimica Acta*, **52**, 1351-1359.

KING, B.C. 1937. The minor intrusives of Kirkudbrightshire. *Proceedings of the Geologists Association*, **48**, 282-306.

KISTLER, R.W., CHAPPELL, B.W., PECK, D.L. & BATEMAN, P.C. 1986. Isotopic variation in the Tuolumne Intrusive Suite, central Sierra Nevada, California. *Contributions to Mineralogy and Petrology*, **94**, 205-220.

KISTLER, R.W. & PETERMAN, Z.E. 1978. Reconstruction of crustal blocks of California on the basis of initial strontium isotopic compositions of Mesozoic granitic rocks. *United States Geological Survey, Professional Paper*, **1071**.

LAGIOS, E. & HIPKIN, R.G. 1979. The Tweedale granite - a newly discovered batholith in the Southern Uplands. *Nature*, **280**, 672-675.

LAMBERT, R.ST.J., HOLLAND, J.G. & LEGGETT, J.K. 1981. Petrology and tectonic setting of some Ordovician volcanic rocks from the Southern Uplands of Scotland. *Journal of the Geological Society, London,* **138**, 421-436.

LEAKE & COOPER 1983. The Black Stockarton Moor sub-volcanic complex. *Journal of the Geological Society, London,* **140**, 665-676.

LEAT, P.T., THOMPSON, R.N., MORRISON, M.A., HENDRY, G.L. & TRAYHORN, S.C. 1986. Geodynamic significance of post-Variscan intrusive and extrusive potassic magmatism in SW England. *Transactions of the Royal Society of Edinburgh:: Earth Sciences*, **77**, 349-360.

LEGGETT, J.K. 1987. The Southern Uplands as an accretionary prism: the importance of analogues in reconstructing palaeogeography. *Journal of the Geological Society, London,* **144**, 737-752.

LEGGETT, J.K., McKERROW, W.S. & EALES, M.H. 1979a. The Southern Uplands of Scotland: a lower Palaeozoic accretionary prism.*Journal of the Geological Society, London,* **136**, 755-770.

LEGGETT, J.K., McKERROW, W.S., MORRIS, J.H., OLIVER, G.J.H. & PHILLIPS, W.E.A. 1979b. The north-western margin of the Iapetus Ocean. *In* : Harris, A.L., Holland, C.H. & Leake, B.E. (eds.) *The Caledonides of the British Isles -reviewed.* Geological Society, London, Special Publication, **8**, 683-698.

LONGMANN, C.D., BLUCK, B.J. & VAN BREEMAN, O. 1979. Ordovician conglomerates and the evolution of the Midland Valley. *Nature.* **280**, 578-581.

MACDONALD, R., THORPE, R.S., GASKARTH, J.W.G. & GRINROD, A.R. 1985. Multi-component origin of Caledonian lamprophyres of northern England. *Mineralogical Magazine*, **49**, 485-494.

MACDONALD, R., ROCK, N.M.S., RUNDLE, C.C. & RUSSEL, O.J. 1986. Relationships between Caledonian lamprophyric and acidic magmas in a differentiated dyke, SW Scotland. *Mineralogical Magazine*, **49**, 547-557.

MacKASKIE, D.R. 1984. Identification of petrogenetic processes using covariance plots of trace-element data. *Chemical Geology*, **47**, 11-30.

MAHOOD, G.A. & HILDRETH, W. 1983. Large partition coefficients for trace elements in high silica rhyolites. *Geochimica et Cosmochimica Acta*, **47**, 11-30.

MARSH, J.S. 1989. Geochemical constraints on coupled assimilation and fractional crystallisation involving upper crustal compositions and continental tholeiitic magma. *Earth and Planetary Science Letters*, **92**, 70-80.

McCARTHY, T.S. & HASTY, R.A. 1976. Trace element distribution patterns and their relationship to the crystallisation of granitic melts. *Geochimica et Cosmochimica Acta*, **40**, 1351-1358.

McADAM, A.D. & TULLOCH, W. 1985. Geology of the Haddington district. Memoir for 1:50 000 sheet 33W and part of sheet 41. *Memoir of the Geological Survey of Great Britain* (Scotland).

McCULLOCH, M. & CHAPPELL, B.W. 1982. Nd isotope characteristics of S- and I-type granites. *Earth and Planetary Science Letters*, **58**, 51-64.

McKENZIE, D. 1985. The extraction of magma from the crust and mantle. *Earth and Planetary Science Letters*, **74**, 81-91.

McKERROW, W.S. 1987. The Southern Uplands controversy. Report of a discussion. *Journal of the Geological Society of London*, **144**, 735-736.

McKERROW, W.S., LEGGETT, J.K. & EALES, M.H. 1977. Imbricate thrust model for the Southern Uplands of Scotland. *Nature*, **267**, 237-9.

McKERROW, W.S. & COCKS, L.R.M. 1976. Progressive faunal migration across the Iapetus Suture. *Nature*, **263**, 304-306.

MENZIES, M. A. & HALLIDAY, A.N. 1988. Lithospheric Mantle Domains beneath the Archean and Proterozoic crust of Scotland. *Journal of Petrology, Special Lithosphere Issue*, 275-302.

MENZIES, M.A. & HAWKESWORTH, C.J. 1987. Upper mantle processes and composition. In: Nixon, p. (ed.) *Mantle Xenoliths*. London: Wiley and Sons. 725-738.

MENZIES, M.A., KEMPTON, P. & DUNGAN, M. 1985. Interaction of continental lithosphere and asthenospheric melts below the Geronimo volcanic field Arizona, USA. *Journal of Petrology*, **26**, 663-693.

MENZIES, M.A. & MURTHY, V.R. 1980. Enriched mantle: Nd and Sr isotopes in diopsides from kimberlite nodules, *Nature*, **283**, 634-636.

MENZIES, M.A., ROGERS, N., TINDLE, A. & HAWKESWORTH, C.J. 1987. Metasomatic and enrichment processes in lithospheric peridotites, an effect of asthenosphere-lithosphere interaction. In: *Mantle Metasomatism*, Menzies, M.A. & Hawkesworth, C.J. (eds.), Academic Press, London, 21-44.

MIDGELY, H.G. 1946. The geology and petrology of the Cockburn Law intrusion, Berwickshire. *Geological Magazine*, **83**, 49-66.

MILLER, C.F. & MITTLEFEHLDT, D.W. 1982. Depletion of light rare-earth elements in felsic magmas. *Geology*, **10**, 129-133.

MOORBATH, S. 1975. The geological significance of early Precambrian rocks. *Proceedings of the Geologists Association*, **86**, Part 3, 259-279.

MORRIS, J.H. 1983. The stratigraphy of the Lower Palaeozoic rocks in the western end of the Longford-Down inlier, Ireland. *Journal of Earth Sciences of the Royal Dublin Society*, **5**, 201-218.

MORRIS, J.H. 1987. The Northern Belt of the Longford-Down Inlier, Ireland and Southern Uplands, Scotland: an Ordovician back-arc basin. *Journal of the Geological Society of London*, **144**, 773-786.

MORRISON, M.A., HENDRY, G.L. & LEAT, P.T. 1986. Regional and tectonic implications of parallel Caledonian and Permo-Carboniferous lamprophyre dyke swarms from Lismore, Ardgour. *Transactions of the Royal Society of Edinburgh:: Earth Sciences*, **77**, 279-288.

MORSE, S.A. 1980. *Basalts and Phase diagrams*. Springer-Verlag, Berlin.

MUECKE, G.K. & CLARKE, D.B. 1981. Geochemical evolution of the South Mountain batholith, Nova Scotia: rare-earth-element evidence. *Canadian Mineralogist*, **19**, 133-145.

NAKAMURA, N. 1974. Determination of REE, Ba, Fee, Mg, Na and K in carbonaceous and ordinary chondrites. *Geochimica et Cosmochimica Acta*, **38**, 757-775.

NEEDHAM, D.T. & KNIPE, R.J., 1986. Accretion- and collision-related deformation in the Southern Uplands accretionary wedge, southwestern Scotland. *Geology*, **14**, 303-306.

NOCKOLDS, S.R. 1941. The Garabal Hill-Glen Fyne igneous complex. *Quarterly Journal of the Geological Society of London*, **96**, 451-511.

O'HARA, M.J. 1977. Geochemical evolution during fractional crystallisation of a periodically refilled magma chamber. *Nature*, **266**, 503.

OLIVER, G.J. & LEGGETT, J.K. 1980. Metamorphism in an accretionary prism: prehnite-pumpellyite facies metamorphism of the Southern Uplands of Scotland. *Transactions of the Royal Society of Edinburgh*, **71**, 235-246.

O'NIONS, R.K., HAMILTON, P.J. & HOOKER, P.J. 1983. A Nd isotope investigation of sediments related to crustal development in the British Isles. *Earth and Planetary Science Letters*, **63**, 229-240.

PANKHURST, R.J. 1979. Isotope and trace element evidence for the origin and evolution of Caledonian granites in the Scottish Highlands. *In* : Atherton, M.P. & Tarney, J. (eds) *Origin of granite batholiths-geochemical evidence*, 18-33. Shiva Publications, Orpington, England.

PANKHURST, R.J. & SUTHERLAND, D.S. 1985. Caledonian granites and diorites of Scotland and Ireland. In: Sutherland, D.S. (ed.), *Igneous rocks of the British Isles*, 149-190. John Wiley & Sons, Chichester, England.

PANKHURST, R.J., HOLE, M.J. & BROOK, M. 1988. Isotope evidence for the origin of Andean granites. *Transactions of the Royal Society of Edinburgh:: Earth Sciences*, **79**, 123-133.

PEARCE, J.A. 1982. Trace element characteristics of lavas from destructive plate boundaries. In: *Andesites* (Ed. Thorpe, R.S.), 525-548. John Wiley & Sons, New York.

PEARCE, J.A. 1983. Role of the sub-continental lithosphere in magma genesis at active continental margins. In: Hawkesworth, C.J. & Norry, M.J. (eds.); *Continental basalts and mantle xenoliths*, 230-249. Shiva Publications.

PEARCE, J.A. & CANN, J.R. 1973. Tectonic setting of basic volcanic rocks determined using trace element analysis. *Earth and Planetary Science Letters*, **19**, 290-300.

PEARCE, J.A. & NORRY, M.J. 1979. Petrogenetic implications of Ti, Zr, Y and Nb variations in volcanic rocks. *Contributions to Mineralogy and Petrology*, **69**, 33-47.

PECCERILLO, A & TAYLOR, S.R. 1976. Geochemistry of Eocene calc-alkaline volcanic rocks from the Katsamonu area, northern Turkey. *Contributions to Mineralogy and Petrology*, **58**, 63-81.

PHILLIPS, W.E.A., STILLMAN, C.J. & MURPHY, T. 1976. A Caledonian plate tectonic model. *Journal of the Geological Society, London,* **132**, 579-609.

PHILLIPS, W.J. 1956. The minor intrusive suite associated with the Criffell-Dalbeattie granodiorite complex. *Proceedings of the Geologists Association*, **67**, 103-121.

PIDGEON, R.T. & AFTALION, M. 1978. Cogenetic and inherited zircon U-Pb systems in granites: Palaeozoic granites of Scotland and England. In: Bowes, B.E. & Leake, B.E. (eds.) *Crustal evolution in northwestern Britain and adjacent regions*, Geological Journal Special Issue No. 10, 183-220.

PLANT, J.A., BROWN, G.C., SIMPSON, P.R. & SMITH, R.T. 1980. Signatures of metalliferous granites in the Scottish Caledonides. *Transactions of the Institute of Mining and Meattalurgy*, **89**, B198-210.

REID, J.B., EVANS, O.C. & FATES, D.G. 1983. Magma mixing in granitic rock of the central Sierra Nevada. *Earth and Planetary Science Letters*, **66**, 243-261.

RICHARDSON, S.H., ERLANK, A.J. & HART, S.R. 1985. Kimberlite-borne garnet peridotite xenoliths from old enriched subcontinental lithosphere. *Earth and Planetary Science Letters*, 75, 116-128.

RICHEY, J.E. 1939. The dykes of Scotland. *Transactions of the Edinburgh Geological Society*, **13**, 393-435.

RINGWOOD, A.E. 1975. *Composition and Petrology of the Earths mantle.*: McGraw-Hill, United States.

ROCK, N.M.S. 1984. Nature and origin of Calc-alkaline lamprophyres: minettes, vogesites, kersantites and spessartites. *Transactions of the Royal Society of Edinburgh:: Earth Sciences*, **74**, 193-227.

ROCK, N.M.S., COOPER, C. & GASKARTH, J.W.G. 1986a. Late Caledonian subvolcanic vents and associated dykes in the Kirkudbright area, Galloway, SW Scotland. *Proceedings of the Yorkshire Geological Society*, **1**, 1-2.

ROCK, N.M.S., GASKARTH, J.W.G., HENNEY, P.J. & SHAND, P. 1988. Late Caledonian dyke-swarms of northern Britain: some preliminary petrogenetic and tectonic implications of their province-wide distribution and chemical variation. *Canadian Mineralogist*, **26**, 3-22.

ROCK, N.M.S., GASKARTH, J.W.G. & RUNDLE, C.C. 1986b. Late Caledonian dyke-swarms in southern Scotland: a regional zone of primitive K-rich lamprophyres and associated vents. *Journal of Geology*, **94**, 505-522.

ROCK, N.M.S. & HUNTER, R.H. 1987. Late Caledonian dyke-swarms of northern Britain: spatial and temporal intimacy between lamprophyric and granitic magmatism around the Ross of Mull pluton, Inner Hebrides. *Geologische Rundschau*, **76**, 805-826.

ROCK. N.M.S. & RUNDLE, C.C. 1986. Lower Devonian age for the 'Great (basal) Conglomerate' of the Scottish Borders. *Scottish Journal of Geology*, **22**, 285-288.

RODEN, M.F. 1981. Origin of coexisting minette and ultramafic breccia, Navajo Volcanic Field. *Contributions to Mineralogy and Petrology*, **77**, 195-206.

RODEN, M.F. & SMITH, D. 1979. Field geology, chemistry, and petrology of Buell Park minette diatreme, Apache County, Arizona. *In* Boyd, F.R. & MEYER, H.O.A. (eds.). *Kimberlites, Diatremes and Diamonds*. 364-381. Washington: American Geophysical Union.

RUDDOCK, D.I. & HAMILTON, D.L. 1978a. The system KAlSi2O6-CaMgSi2O6-SiO2 at 4Kb. *Progress in Experimental Petrology, NERC Publications Series D*, **11**, 25-27.

RUDDOCK, D.I. & HAMILTON, D.L. 1978b. Stability of carbonate in a simple potassium-rich model. *Progress in Experimental Petrology, NERC Publications Series D*, **11**, 28-31.

SAWKA, W.N., CHAPPELL, B.W. & NORRISH, K. 1984. Light-rare-earth-element zoning in sphene and allanite during granitoid fractionation. *Geology*, **12**, 131-134.

SCHOTT, J. 1983. Thermal diffusion and magmatic differentiation: a new look at an old problem. *Bulletin of Mineralogy*, **106**, 247-262.

SMEDLEY, P.L. 1986. The relationship between calc-alkaline volcanism and within-plate continental rift volcanism: evidence from Scottish Palaeozoic lavas. *Earth and Planetary Science Letters*, **77**, 113-128.

SMEDLEY, P.L. 1988. The geochemistry of Dinantian volcanism in south Kintyre and the evidence for provincialism in the southern Scottish mantle. *Contributions to Mineralogy and Petrology*, **99**, 374-384.

SMITH, D.I. 1979. Caledonian minor intrusions of the N Highlands of Scotland. *In* : Harris, A.L., HOLLAND, C.H. & LEAKE, B.E. (eds.) *The Caledonides of the British Isles-reviewed*. Geological Society, London, Special Publication, **8**, 683-698.

SOPER, N.J., WEBB, B.C. & WOODCOCK, N.H. 1987. Late Caledonian (Acadian) transpression in north-west England: timing, geometry and geotectonic significance. *Proceedings of the Yorkshire Geological Society*, **46**, 175-192.

STEPHENS, W.E. & HALLIDAY, A.N. 1984. Geochemical contrasts between late Caledonian granitoid plutons of northern, central and southern Scotland. *Transactions of the Royal Society of Edinburgh:: Earth Sciences*, **75**, 259-273.

STEPHENS, W.E., WHITLEY, J.E., THIRLWALL, M.F. & HALLIDAY, A.N. 1985. The Criffell zoned pluton: correlated behaviour of rare earth element abundances with isotopic systems. *Contributions to Mineralogy and Petrology*, **89**, 226-238.

STONE, P., FLOYD, J.D., BARNES, R.P. & LINTERN, B.C. 1987. A sequential back-arc and foreland basin thrust duplex model for the Southern Uplands of Scotland. *Journal of the Geological Society, London,* **144**, 753-764.

SUZUKI, K. & SHIRAKI, K. Chromite-bearing spessartites from Kasuga-mura, Japan and their bearing on possible mantle origin andesite. *Contributions to Mineralogy and Petrology*, **71**, 313-322.

TAYLOR, H.P. 1980. The effects of assimilation of country rocks by magmas on $^{18}O/^{16}O$ and $^{87}Sr/^{86}Sr$ systematics in igneous rocks. *Earth and Planetary Science Letters*, **47**, 243-254.

THIRLWALL, M.F. 1979. *The petrochemistry of the British Old Red Sandstone volcanic province*. PhD thesis, University of Edinburgh.

THIRLWALL, M.F. 1982a. Systematic variation in chemistry and Nd-Sr isotopes across a Caledonian calc-alkaline volcanic arc: implications for source materials. *Earth and Planetary Science Letters*, **58**, 27-50.

THIRLWALL, M.F. 1982b. A triple-filament method for rapid and precise analysis of rare-earth elements by isotope dilution. *Chemical Geology*, **35**, 155-166.

THIRLWALL, M.F. 1983. Isotope geochemistry and origin of calc-alkaline lavas from a Caledonian continental margin volcanic arc. *Journal of Volcanology and Geothermal Research*, **18**, 589-631.

THIRLWALL, M.F. 1988. Geochronology of Late Caledonian magmatism in northern Britain. *Journal of the Geological Society, London*, **145**, 951-967.

THIRLWALL, M.F. 1989. Short Paper. Movement on proposed terrane boundaries in northern Britain: constraints from Ordovician-Devonian igneous rocks. *Journal of the Geological Society, London*, **146**, 373-376.

THIRLWALL, M.F., MAYNARD, J., STEPHENS, W.E. & SHAND, P. 1989. Calc-alkaline magmagenesis in the Scottish Southern Uplands forearc: a Pb-Sr-Nd Isotope study. *TERRA abstracts*, **1**, 178.

THOMPSON, R.N. 1982. Magmatism of the British Tertiary Volcanic Province. *Scottish Journal of Geology*, **18**, 49-107.

THOMPSON, R.N. & FOWLER, M.B. 1987. Subduction-related shoshonitic and ultrapotassic magmatism: a study of Siluro-Ordovician syenites from the Scottish Caledonides. *Contributions to Mineralogy and Petrology*, **94**, 507-522.

THOMPSON, R.N., MORRISON, M.A., HENDRY, G.L. & PARRY, S.J. 1984. An assessment of the relative roles of crust and mantle in magma genesis: an elemental approach. *Philosophical Transactions of the Royal Society of London*, **A310**, 549-590.

THORPE, 1982. (ed.) *Andesites: orogenic andesites and related rocks*. John Wiley, London,

TINDLE, A.G., McGARVIE, D.W. & WEBB, P.C. 1988. The role of hybridization and crystal fractionation in the evolution of the Cairnsmore of Carsphairn intrusion, Southern Uplands of Scotland. *Journal of the Geological Society, London*, **145**, 11-21.

TINDLE, A.G. & PEARCE, J.A. 1981. Petrogenetic modelling of in situ fractional crystallisation in the zoned Loch Doon pluton, Scotland. *Contributions to Mineralogy and Petrology*, **78**, 196-207.

TINDLE, A.G. & PEARCE, J.A. 1983. Assimilation and partial melting of continental crust: evidence from the mineralogy and geochemistry of autoliths and xenoliths. *Lithos*, **16**, 185-202.

TURPIN, L., VELDE, D. & PINTE, G. 1988. Geochemical comparison between minettes and kersantites from the western European Hercynian orogen: trace element and Pb-Sr-Nd isotope constraints on their origin. *Earth and Planetary Science Letters*, **87**, 73-86.

UPTON, B.J.G., ASPEN, P. & CHAPMAN, N.A. 1983. The upper mantle and deep crust beneath the British Isles: evidence from inclusions in volcanic rocks. *Journal of the Geological Society, London,* **140**, 105-121.

VANCE, J.A. 1961. Zoned granitic intrusions-an alternative hypothesis of origin. *Geological Society of America Bulletin*, **72**, 1723-1728.

VARNE, R. 1985. Ancient subcontinental mantle: a source for K-rich orogenic volcanics. *Geology*, **13**, 405-408.

VELDE, D. 1968. Les transformations de l'olivine dans le lamprophyres et lamproites. *Bull. Soc. Geol. Fr.* **10**, 601-612.

VENTURELLI, G., THORPE, R.S., DAL PIAZ, G.V., DEL MORO, A. & POTTS, P.J. 1984. Petrogenesis of calc-alkaline, shoshonitic and associated ultrapotassic Oligocene volcanic rocks from the northwestern Alps, Italy. *Contributions to Mineralogy and Petrology*, **86**, 209-220.

VERNON, 1983. Restite, xenoliths and microgranitoid enclaves in granites. *Journal of the Proceedings of the Royal Society of New South Wales*, **116**, 77-103.

WALKER, D. & DeLONG, S.E. 1982 Soret separation of mid-ocean ridge basalt magma. *Contributions to Mineralogy and Petrology*, **79**, 231-240.

WALKER, D. & DeLONG, S.E. 1984. A small Soret effect in spreading center gabbros. *Contributions to Mineralogy and Petrology*, **85**, 203-208.

WALL, V.J., CLEMENS, J.D. & CLARKE, D.B. 1987. Models for granitoid evolution and source compositions. *Journal of Geology*, **95**, 731-749.

WATSON, E.B. 1979. Zircon saturation in felsic liquids: experimental results and applications to trace element geochemistry. *Contributions to Mineralogy and Petrology*, **70**, 407-419.

WATSON, E.B. & HARRISON, T.M. 1984. Accessory minerals and the geochemical evolution of crustal magmatic systems: a summary and prospectus of experimental approaches. *Physics of the Earth and Planetary Interiors*, **35**, 19-30.

WATSON, J. 1984. The ending of the Caledonian orogeny in Scotland. *Journal of the Geological Society, London,* **141**, 193-214.

WENDLANDT, R.F. & EGGLER, D.H. 1980a. The origins of potassic magmas. 1. Melting relations in the system $KAlSiO_4$-Mg_2SiO_4-SiO_2 and $KAlSiO_4$-MgO-SiO_2-CO_2 to 30 kilobars. *American Journal of Science*, **280**, 385-420.

WENDLANDT, R.F. & EGGLER, D.H. 1980b. The origins of potassic magmas. 2. Stability of phlogopite in natural spinel lherzolite and in the system $KAlSiO_4$-MgO-SiO_2-CO_2 at high pressures and temperatures. *American Journal of Science*, **280**, 421-458.

WHALEN, J.B. 1983. The Ackley City batholith, southeastern Newfoundland: evidence for crystal versus liquid-state fractionation. *Geochimica et Cosmochimica Acta*, **47**, 1443-1457.

WHITE, A.J.R. & CHAPPELL, B.W. 1977. Ultrametamorphism and granitoid genesis. *Tectonophysics*, **43**, 7-22.

WHITE, A.J.R., CLEMENS, J.D., HOLLOWAY, J.R., SILVER, L.T., CHAPPELL, B.W. & WALL, V.J. 1986. S-type granites and their probable absence in southwestern North America. *Geology*, **14**, 115-118.

WRIGHT, A.E. & BOWES, D.R. 1979. Geochemistry of the Appinite Suite. *In* : Harris, A.L., Holland, C.H. & Leake, B.E. (eds.) *The Caledonides of the British Isles-reviewed*. Geological Society, London, Special Publication, **8**, 699-704.

WYLLIE, P.J. 1978. Magmas and volatile components. *American Mineralogist*, **64**, 469-500.

WYLLIE, P.J. 1979. Mantle fluid compositions buffered in peridotite-CO_2-H_2O by carbonates, amphibole and phlogopite. *Journal of Geology*, **86**, 687-713.

Appendices

APPENDIX 1: XRF preparation

A1.1 Sample preparation

Samples of at least 2kg were collected in the field from the freshest part of surface outcrops. These were trimmed of weathered surfaces and split into fragments of < 6cm diameter. This was followed by crushing in a steel plated jaw crusher to ca. 5mm, and finally reduced to a fine powder (-200 mesh) in a Siebtechnic tema mill with tungsten carbide discs for 3-5 minutes.

A1.2 Preparation of fused discs and powder briquettes

Sample powders were initially dried in an oven at 110°C for three hours. Approximately 0.75gm. of this powder was weighed in a Pt/Au crucible and an amount of La oxide doped flux (Johnson Matthey Spectroflux 105) equivalent to 5.33333 times the sample weight was added. The mixture was then fused at 1100°C in a furnace for 20 minutes. After cooling the crucible was reweighed and more flux added up to the original weight above. The crucible was then reheated using a Meker burner and the contents poured into a graphite mould and pressed into a glass disc.

Sample powders were dried in an oven at 110°C for three hours. Approximately 8.5 gm. of powder was weighed onto paper, and binder (Bakelite resin RO214/1) equivalent to 0.17646 times the powder weight was added. The mixture was subsequently transferred to a mixing bottle containing 6 glass balls and shaken vigorously for ca. 15 minutes until homogenised. This was then made into powder briquettes in a Specac press at 20 tons pressure. The briquettes were finally cured in an oven at 120 110°C for 12 hours.

APPENDIX 2: Rare-earth element and isotope preparation

A2.1 Sr isotope preparation

The preparation of samples for Sr isotope analysis was as follows:

(a) Boil 30ml Teflon beakers in deionized water for 20 minutes, and then rinse with ultra high quality (UHQ) water. Add approximately 1ml of sample to the beakers and rinse from the sides using UHQ water.

(b) Transfer to a fume cupboard and add about 2ml conc. S.B. HNO_3 and 6-8ml 40% HF. Cover the beakers with parafilm, and leave to stand overnight.

(c) Evaporated to dryness before adding ca. 2ml of SB HNO_3, again evaporate to dryness.

(d) Add ca. 6ml S.B. 6M HCl and evaporate to dryness.

(e) Add approximatley 5ml of 2.5 M HCl .

(f) Transfer samples to centrifuge tubes and centrifuge for 5 minutes at 1000 rrp.

(g) Add 1ml of solution to ion exchange columns with pipette previously rinsed in 2.5 M HCl.

(h) Allow resin bed to dry and rinse in with 1ml 2.5 M HCl.

(i) Repeat with a second 1ml of 2.5 M HCl.

(j) Elute and collect samples with 2.5 M HCl.

(k) Evaporate collected solutions to dryness.

(l) Mount the samples onto single Tantalum filaments on single beads with phosphoric acid.

A2.2 Nd isotope and REE preparation

(a) Add equal quantities of HNO_3 and HF to Teflon beakers, and leave overnight. Clean with UHQ water and leave in vacuum oven overnight.

(b) Weigh out ca. 0.2 gm. into beakers and rinse in with conc. (sub-boiled) HNO_3. Add HF to slightly less than half full and leave on hot plate for half an hour before evaporating.

(c) Add fresh HF and HNO_3 and leave on hot plate for 2 days.

(d) Add ca. 2ml conc. HNO_3 and evaporate.

(e) Add 10% HNO_3 up to less than half full and leave on hot plate overnight.

(f) Pour solution into centrifuge tubes previously rinsed with 10% HNO_3, and centrifuge for 5-10 minutes.

(g) Split into two fractions, ca. nine tenths of solution for Nd isotope analysis and one tenth for REE analysis.

(h) Sample solutions for REE to be spiked, with REE spike chosen depending on approximate concentrations of REE (XRF) in sample. Half fill beakers with 10% HNO_3 and evaporate. Add 5 ml 75% HOAC/25% 5M HNO_3 and leave to equilibrate overnight.

(i) Evaporate samples for Nd, add 5 ml 75% HOAC/25% 5M HNO_3 and leave to equilibrate.

(j) Elute and collect samples using HOAC/HNO_3, orange and yellow cocktails in respective columns.

(k) Mount REE and Nd isotopic solutions on triple filament beads (centre Rhenium/side Tantalum).

Sr and Nd isotopes and REE were then analysed on the VG 354 mass spectrometer at Royal Holloway and Bedford New College.

Appendix 3a. Major and trace element data: granitoids

No.	1540	1542	1542d	PS13	PS15	PS16	PS17	PS18	PS25
Grid ref.	NT749 627	NT648 642	NT648 642	NT615 651	NT626 642	NT626 643	NT629 643	NT631 643	NT641 643
G [a]	Gd[b]	Plw/Gd	Plw/Po	Plw/N	Plw/N	Plw/Gd	Plw/Gd	Plw/Gd	Plw/Di
SiO_2	57.58	59.45	73.90	45.92	50.50	52.23	51.42	59.14	58.06
Al_2O_3	17.26	17.59	13.76	20.69	18.57	16.40	17.74	15.16	16.66
Fe_2O_3	5.73	5.99	1.69	9.22	7.28	7.23	8.16	7.41	6.66
MgO	3.70	3.05	0.78	4.14	8.89	7.63	6.62	3.49	4.73
CaO	5.04	4.60	1.21	9.64	9.53	8.28	7.40	3.16	6.18
K_2O	2.25	2.69	4.96	1.34	0.29	1.50	1.51	2.99	1.96
Na_2O	3.36	3.97	2.99	2.50	2.63	2.53	3.00	3.33	3.43
MnO	0.09	0.11	0.03	0.14	0.12	0.13	0.12	0.16	0.10
TiO_2	0.88	0.85	0.23	2.11	0.42	0.66	1.19	1.45	0.89
P_2O_5	0.25	0.25	0.06	0.27	0.03	0.18	0.18	0.30	0.17
LOI	3.35	1.11	0.76	3.16	1.35	2.06	2.21	2.21	1.01
Total	**99.49**	**99.65**	**100.37**	**99.13**	**99.60**	**98.82**	**99.55**	**98.80**	**99.84**
Zn	79	78	29	76	69	66	81	82	73
Cu	13	17	6	90	10	23	8	69	28
Ni	38	46	89	15	129	92	75	51	72
Rb	57	73	104	24	11	44	34	74	55
Sr	509	492	152	855	680	520	557	339	405
Y	24	30	14	20	8	23	29	37	25
Zr	148	196	106	128	17	126	108	228	153
Nb	10	11	12	18	2	7	6	10	7
Ba	597	750	280	477	214	499	443	830	470
U	2	2	8	0	0	3	2	5	3
Th	5	12	36	3	1	5	4	9	6
Pb	10	14	26	4	5	12	14	19	17
V	156	109	26	275	98	170	212	207	155
Cr	68	18	22	2	274	237	153	103	117

No.	PS26	PS27	PS28	PS29	PS30G	PS31	PS32	PS33	PS34
NGR	NT642 641	NT642 641	NT643 641	NT644 641	NT644 641	NT644 641	NT644 640	NT644 640	NT645 640
	Plw/Di	Plw/Di	Plw/Di	Plw/Di	Plw/Di	Plw/Di	Plw/Di	Plw/Gd	Plw/Gd
SiO_2	58.93	58.12	58.86	58.32	61.24	66.29	61.33	59.29	61.97
Al_2O_3	16.40	15.62	15.89	15.63	16.76	16.83	16.80	16.97	17.09
Fe_2O_3	6.25	6.25	5.86	6.26	5.72	4.36	5.49	6.48	5.30
MgO	4.26	4.95	4.61	4.67	2.95	2.10	3.04	3.29	2.79
CaO	4.97	5.23	5.18	5.40	4.29	3.35	4.64	4.71	3.93
K_2O	2.20	4.21	4.04	3.85	2.59	3.14	2.61	2.94	2.84
Na_2O	3.64	2.76	3.03	2.91	3.98	3.93	3.86	3.78	3.83
MnO	0.10	0.11	0.10	0.11	0.09	0.08	0.09	0.11	0.09
TiO_2	0.82	0.96	0.92	0.95	0.80	0.59	0.77	0.89	0.75
P_2O_5	0.17	0.32	0.35	0.32	0.19	0.17	0.19	0.21	0.22
LOI	0.96	1.18	1.13	0.81	0.98	1.13	0.85	1.09	1.18
Total	**98.69**	**99.70**	**99.96**	**99.22**	**99.58**	**101.95**	**99.66**	**99.78**	**99.98**
Zn	71	77	89	75	73	53	72	79	66
Cu	23	16	18	27	11	10	24	21	18
Ni	63	57	49	66	54	58	62	48	57
Rb	65	69	67	68	70	70	72	67	76
Sr	392	1713	1773	1707	436	428	450	545	470
Y	25	26	25	26	29	20	30	27	24
Zr	167	240	266	271	190	175	194	176	241
Nb	9	10	11	10	8	9	10	10	12
Ba	473	1596	1518	1484	682	783	639	812	749
U	5	1	3	3	4	4	5	3	3
Th	8	7	12	14	11	10	9	11	9
Pb	15	19	22	17	20	16	19	21	18
V	141	139	140	134	112	73	116	127	103
Cr	118	129	115	132	71	46	67	48	54

No.	PS36	PS38	PS39	PS41	PS42	PS43	PS44	PS45	PS60
NGR	NT644 642	NT648 642	NT648 642	NT657 636	NT657 636	NT656 639	NT644 642	NT642 647	NT645 634
	Plw/Gd	Plw/Gd	Plw/Gd	Plw/Gd	Plw/Gd	Plw/Gd	Plw/Gd	Plw/Di	Plw/Po
SiO_2	58.74	60.27	61.15	55.20	61.45	60.72	53.88	61.16	69.56
Al_2O_3	16.62	17.24	17.00	18.79	17.13	17.18	16.73	16.62	14.71
Fe_2O_3	6.56	5.85	5.63	7.70	5.47	5.19	7.65	4.40	2.99
MgO	4.21	2.92	2.81	4.91	3.02	3.14	6.48	4.21	1.74
CaO	4.73	4.46	4.14	0.23	4.20	3.83	7.12	4.64	2.03
K_2O	2.08	2.66	2.79	4.43	2.83	2.65	1.59	2.73	4.14
Na_2O	3.72	3.94	3.90	0.20	3.75	3.61	3.28	3.32	3.41
MnO	0.11	0.11	0.10	0.04	0.11	0.09	0.14	0.05	0.06
TiO_2	0.87	0.83	0.77	0.83	0.81	0.73	1.04	0.95	0.42
P_2O_5	0.18	0.24	0.22	0.14	0.21	0.18	0.19	0.24	0.13
LOI	1.53	0.79	0.95	4.06	1.00	1.78	1.51	1.46	0.98
Total	**99.33**	**99.30**	**99.63**	**96.52**	**99.97**	**99.09**	**99.59**	**99.77**	**100.15**
Zn	81	82	71	96	68	69	72	84	31
Cu	10	20	17	23	36	11	25	35	5
Ni	74	40	49	67	40	47	77	116	64
Rb	34	69	82	129	75	76	53	79	103
Sr	557	505	472	44	470	428	479	379	359
Y	29	29	31	37	27	27	28	27	21
Zr	110	176	197	146	175	155	136	230	168
Nb	6	11	12	14	10	10	6	13	12
Ba	425	692	646	580	649	636	438	645	600
U	2	1	4	0	3	2	1	4	4
Th	5	9	12	12	12	10	4	10	26
Pb	12	20	19	7	18	14	11	21	15
V	208	108	98	174	119	109	174	129	51
Cr	141	33	25	156	32	43	159	228	47

No.	PS61	PS62	PS63	PS65	PS79	PS81	PS198	PS199	PS202
NGR	NT646 633	NT646 631	NT644 628	NT645 626	NT643 627	NT645 634	NT642 647	NT645 635	NT626 642
	Plw/Gd	Plw/Gd	Plw/Di	Plw/Gd	Plw/Gd	Plw/Po	Plw/Di	Plw/Po	Plw/N
SiO_2	64.08	55.40	58.94	60.30	60.39	65.40	58.70	64.61	48.88
Al_2O_3	15.72	17.23	17.41	16.82	17.59	15.89	15.79	15.94	16.52
Fe_2O_3	3.81	7.16	6.23	6.06	5.21	3.85	6.34	3.94	10.26
MgO	2.54	4.72	3.18	3.17	2.37	2.45	6.05	2.37	11.27
CaO	3.26	5.69	5.20	4.12	4.13	2.88	5.57	3.25	9.40
K_2O	3.73	2.05	3.15	2.76	3.02	3.85	2.06	3.65	0.32
Na_2O	3.59	3.68	3.48	3.82	3.79	3.59	3.17	3.68	1.50
MnO	0.07	0.12	0.11	0.10	0.09	0.06	0.09	0.06	0.18
TiO_2	0.53	1.02	0.97	0.85	0.71	0.53	0.88	0.55	0.27
P_2O_5	0.16	0.28	0.26	0.21	0.20	0.16	0.17	0.16	0.03
LOI	2.48	2.32	0.81	1.80	1.93	1.23	0.32	1.16	1.08
Total	**99.95**	**99.66**	**99.73**	**100.00**	**99.43**	**99.86**	**99.14**	**99.37**	**99.71**
Zn	29	66	75	59	58	35	66	30	81
Cu	5	49	10	14	11	9	42	8	28
Ni	47	44	38	48	43	52	182	52	259
Rb	93	55	65	76	90	96	61	92	12
Sr	478	609	1044	503	510	464	391	503	560
Y	23	24	28	28	24	26	28	24	9
Zr	191	160	209	178	145	193	179	198	22
Nb	9	8	10	9	11	10	9	11	3
Ba	895	710	1120	725	975	893	610	855	181
U	4	3	4	2	2	4	3	5	0
Th	17	8	8	12	11	15	8	15	2
Pb	11	11	20	12	11	11	21	14	6
V	75	170	132	126	106	79	127	79	116
Cr	65	71	26	47	30	56	284	46	436

No.	PS234	PS235	PL1	PL2	PL3	PL4	PL5	PL6	PS82
NGR	NT639 632	NT642 647	NT646 632	NT646 632	NT646 632	NT646 633	NT646 633	NT646 633	NT771 587
	Plw/Di	Plw/Gd	Plw/Po	Plw/Po	Plw/Po	Plw/Po	Plw/Po	Plw/Po	Clw/Gd
SiO_2	57.10	47.65	63.20	63.19	64.48	64.16	64.78	64.89	48.48
Al_2O_3	17.93	21.49	15.54	15.76	15.70	15.52	15.47	15.45	18.91
Fe_2O_3	7.28	8.65	3.81	3.95	4.11	3.66	3.68	3.72	6.98
MgO	3.57	5.54	2.58	2.93	2.54	2.24	2.24	2.38	2.62
CaO	4.85	2.93	3.25	3.09	2.83	3.63	3.45	3.33	10.14
K_2O	2.69	1.16	3.90	3.85	3.73	3.62	3.74	3.73	1.10
Na_2O	3.32	2.06	3.54	3.54	3.49	3.47	3.61	3.61	3.52
MnO	0.13	0.13	0.05	0.06	0.05	0.06	0.06	0.06	0.09
TiO_2	1.03	1.47	0.55	0.57	0.54	0.52	0.52	0.52	1.42
P_2O_5	0.25	0.22	0.16	0.18	0.19	0.16	0.15	0.16	0.35
LOI	1.29	7.60	2.51	2.31	1.55	2.01	1.74	1.48	5.61
Total	**99.40**	**98.90**	**99.09**	**99.41**	**99.20**	**99.03**	**99.43**	**99.30**	**99.24**
Zn	79	80	34	38	37	32	31	28	61
Cu	12	22	8	8	11	6	7	13	25
Ni	19	37	47	50	49	47	57	53	41
Rb	65	44	90	90	93	88	89	92	29
Sr	698	176	498	522	470	478	466	480	588
Y	32	28	23	25	27	21	23	23	23
Zr	163	158	184	190	192	177	189	181	80
Nb	10	7	11	10	11	9	11	10	8
Ba	844	810	815	878	889	852	822	815	326
U	6	1	4	4	2	2	2	5	2
Th	13	6	16	14	17	16	15	17	3
Pb	16	11	12	11	15	10	10	10	14
V	181	177	79	86	75	75	73	80	174
Cr	44	138	60	60	54	54	48	58	30

No.	PS83	PS84	PS85	PS85b	PS85f	PS86	PS87a	PS87b	PS88
NGR	NT771 587	NT771 590	NT771 591	NT771 591	NT771 591	NT775 594	NT775 594	NT775 594	NT773 593
	Clw/Gd	Clw/Gd	Clw/Gd	Clw/Gd	Clw/G	Clw/Di	Clw/Di	Clw/Di	Clw/Gd
SiO_2	54.33	63.04	64.50	65.02	71.02	59.72	53.08	49.93	64.33
Al_2O_3	17.87	15.78	15.05	15.08	12.87	16.44	16.78	16.11	16.32
Fe_2O_3	7.16	4.90	4.55	4.49	3.53	5.66	3.66	2.49	4.50
MgO	4.45	3.28	3.15	3.04	2.41	3.83	2.23	1.63	2.89
CaO	4.25	4.07	3.56	3.47	1.87	5.32	9.98	12.25	2.96
K_2O	2.16	3.12	3.49	3.76	3.97	2.52	2.91	2.81	3.65
Na2O	3.70	3.59	3.27	3.13	2.55	3.70	3.04	0.00	3.61
MnO	0.10	0.07	0.06	0.08	0.05	0.08	0.09	0.10	0.08
TiO_2	1.16	0.69	0.70	0.70	0.57	0.76	0.83	0.81	0.63
P_2O_5	0.17	0.20	0.18	0.17	0.11	0.21	0.21	0.21	0.19
LOI	3.72	1.10	1.33	0.92	1.03	1.14	7.12	14.09	1.15
Total	**99.07**	**99.84**	**99.84**	**99.84**	**99.98**	**99.39**	**99.98**	**100.22**	**100.30**
Zn	67	66	63	61	49	72	46	34	57
Cu	40	40	18	20	14	42	33	9	8
Ni	47	59	68	71	90	69	84	55	67
Rb	51	88	88	93	92	64	74	63	96
Sr	475	484	450	459	322	574	532	102	503
Y	25	26	22	22	17	26	26	31	23
Zr	141	198	227	245	169	180	163	153	189
Nb	9	11	10	9	10	8	8	8	10
Ba	492	613	680	813	621	633	646	522	741
U	2	6	1	3	1	3	2	3	2
Th	5	15	9	10	16	7	8	6	14
Pb	11	20	23	22	22	23	19	11	21
V	167	94	98	92	76	126	152	133	90
Cr	34	88	80	70	94	87	180	154	68

No.	PS89	PS90	PS91	PS92	PS93	PS94	PS95	PS96	PS97
NGR	NT772 591	NT766 598	NT766 597	NT766 597	NT767 596	NT769 597	NT769 591	NT775 594	NT769 587
	Clw/Gd	Clw/Di	Clw/Di	Clw/Di	Clw/Di	Clw/Di	Clw/Gd	Clw/Gd	Clw/Di
SiO_2	62.56	59.45	58.78	64.16	59.18	62.93	61.66	60.60	61.28
Al_2O_3	16.00	17.13	17.50	16.27	15.74	16.15	16.23	16.47	16.70
Fe_2O_3	5.14	5.75	6.30	4.39	6.34	4.43	5.51	5.53	5.69
MgO	3.13	3.38	3.34	2.51	5.53	2.28	3.32	3.77	3.19
CaO	4.02	5.23	5.45	3.94	5.65	3.73	4.35	4.00	1.28
K_2O	3.42	2.46	2.45	2.62	2.42	3.16	3.08	2.90	4.42
Na_2O	3.56	3.76	3.69	4.03	3.18	3.57	3.74	3.40	2.66
MnO	0.09	0.10	0.10	0.08	0.10	0.07	0.10	0.09	0.06
TiO_2	0.71	0.83	0.93	0.61	0.67	0.68	0.74	0.77	0.83
P_2O_5	0.21	0.22	0.23	0.15	0.19	0.18	0.22	0.20	0.21
LOI	1.11	1.20	1.12	0.74	0.91	0.79	1.06	2.09	3.02
Total	**99.94**	**99.50**	**99.90**	**99.50**	**99.90**	**97.98**	**100.01**	**99.81**	**99.34**
Zn	62	64	80	66	70	76	64	71	54
Cu	22	15	23	61	28	11	28	21	31
Ni	65	45	50	56	112	34	59	53	64
Rb	86	69	68	74	65	70	77	73	92
Sr	561	363	602	411	529	503	604	472	344
Y	25	26	27	24	21	27	24	25	26
Zr	194	156	171	160	143	230	183	177	211
Nb	8	9	10	10	9	12	10	8	10
Ba	712	477	662	564	590	711	625	603	985
U	2	2	3	5	0	3	3	2	2
Th	13	10	8	12	11	9	11	10	12
Pb	18	19	24	23	21	21	20	16	14
V	96	116	144	95	143	85	102	132	138
Cr	83	49	52	60	253	23	83	93	126

No.	PS98	PS99	PS100	PS108	PS109	PS110	PS111	1474	1486
NGR	NT777 585	NT778 591	NT774 589	NT772 589	NT772 588	NT774 589	NT773 587	NT968 590	NT496 631
	Clw/Di	Clw/Di	Clw/Po	Clw/Po	Clw/Gd	Clw/Po	Clw/Gd	Lb/Gd	St/Gd
SiO_2	60.96	63.58	65.51	62.99	62.13	65.94	60.34	62.39	65.15
Al_2O_3	18.04	16.77	16.14	16.09	16.13	16.01	16.95	16.87	16.19
Fe_2O_3	4.96	4.35	3.89	4.61	4.82	3.84	5.48	3.55	3.96
MgO	1.85	2.37	2.30	3.05	3.18	2.31	3.66	3.14	1.05
CaO	4.70	4.59	2.74	3.97	3.60	2.09	4.31	2.14	2.50
K_2O	2.79	2.31	2.93	3.01	3.42	3.07	2.94	3.71	3.45
Na2O	3.81	3.80	4.26	3.57	3.70	4.06	3.94	3.28	3.38
MnO	0.08	0.06	0.07	0.07	0.08	0.08	0.08	0.04	0.05
TiO_2	0.81	0.66	0.53	0.64	0.71	0.54	0.81	0.92	0.52
P_2O_5	0.30	0.15	0.15	0.17	0.19	0.15	0.20	0.34	0.17
LOI	1.94	1.04	1.42	1.26	2.25	1.79	1.31	3.50	3.44
Total	**100.23**	**99.68**	**99.94**	**99.42**	**100.22**	**99.87**	**100.01**	**99.87**	**99.86**
Zn	62	62	46	63	59	51	75	73	42
Cu	11	15	16	18	19	13	52	7	3
Ni	55	42	61	52	54	52	53	35	9
Rb	87	70	81	78	82	77	74	86	114
Sr	392	363	414	536	504	385	552	369	238
Y	25	24	21	21	26	23	26	19	24
Zr	208	151	193	179	196	172	177	266	221
Nb	10	10	9	9	10	10	10	17	11
Ba	611	499	626	678	700	669	686	807	615
U	2	3	2	2	4	3	3	4	3
Th	13	11	11	12	9	10	7	17	12
Pb	20	18	19	19	16	20	19	21	15
V	89	124	78	99	101	74	111	142	55
Cr	36	69	42	46	64	39	55	75	18

No.	**1487**	**1488**	**1491**	**PS169**
NGR	NT495 640	NT495 640	NT511 643	NT 968 590
	St/Gd	St/Gd	Kd/Gd	Lb/Gd
SiO_2	63.41	53.14	63.55	60.08
Al_2O_3	16.82	17.28	16.70	17.17
Fe_2O_3	4.73	5.85	5.28	2.80
MgO	1.94	3.04	2.29	2.40
CaO	3.06	8.99	2.62	3.62
K_2O	3.37	1.88	2.89	3.53
Na_2O	3.45	2.88	3.66	3.77
MnO	0.08	0.07	0.10	0.07
TIO_2	0.66	1.20	0.80	0.97
P_2O_5	0.20	0.27	0.21	0.37
LOI	2.36	5.24	2.65	4.74
Total	**100.05**	**99.82**	**100.76**	**99.51**
Zn	57	58	69	49
Cu	4	11	7	16
Ni	13	54	18	45
Rb	99	49	80	84
Sr	378	475	376	534
Y	24	22	27	21
Zr	217	147	204	262
Nb	10	11	11	19
Ba	726	452	707	769
U	2	1	0	1
Th	10	4	11	16
Pb	15	10	16	16
V	66	146	101	155
Cr	34	200	42	90

a

Plw = Priestlaw
Clw = Cockburnlaw
St = Stobshiel
Kd = Kidlaw
Lb = Lamberton Beach

b

N = norite
Gd = hornblende diorite/granodiorite
Di = pyroxene-mica diorite
Po = porphyritic granodiorite/granite

Appendix 3b. Major and trace element data: minor intrusions and lavas

No.	1385	1386	1387	1389	1391	1392	1393	1394	1395
Grid Ref.	NT728 643	NT739 630	NT739 629	NT743 630	NT757 624	NT764 615	NT765 616	NT786 604	NT786 597
Type[a]	Fpt	Fmd	Fpt	Fpt	P	Fpt	Fpt	P	Fpt
SiO_2	62.59	56.07	61.20	63.54	58.36	64.51	64.46	50.70	70.37
Al_2O_3	15.47	17.14	15.09	15.60	16.61	15.91	16.10	15.22	15.79
Fe_2O_3	3.44	6.50	3.59	4.31	6.08	3.79	3.93	5.32	2.37
MgO	2.34	3.90	2.25	2.08	3.61	1.66	0.84	5.68	1.12
CaO	3.52	4.69	3.58	4.14	4.52	2.50	3.66	5.66	1.66
K_2O	2.90	2.70	2.88	2.11	2.54	2.60	2.80	2.87	2.92
Na_2O	3.29	3.44	3.54	3.23	3.46	3.48	3.32	2.44	3.32
MnO	0.09	0.09	0.08	0.09	0.11	0.07	0.10	0.11	0.06
TiO_2	0.58	1.09	0.55	0.61	0.88	0.54	0.57	0.83	0.36
P_2O_5	0.20	0.21	0.17	0.15	0.18	0.13	0.14	0.42	0.13
LOI	6.58	3.74	6.58	5.30	4.27	3.93	5.17	10.35	3.72
Total	**100.99**	**99.57**	**99.51**	**101.17**	**100.62**	**99.10**	**101.08**	**99.59**	**101.42**
Zn	36	81	50	91	55	70	48	56	39
Cu	7	9	18	31	3	13	8	3	6
Ni	67	22	56	32	24	38	21	125	31
Rb	73	75	74	75	73	69	79	91	75
Sr	293	409	272	387	231	422	273	182	98
Y	18	30	17	19	21	26	20	21	19
Zr	159	198	149	137	121	183	118	202	141
Nb	10	10	10	9	9	9	8	14	9
Ba	549	625	721	405	562	528	495	726	270
U	3	2	2	4	3	4	4	3	5
Th	7	9	9	9	5	7	7	12	7
Pb	13	19	10	39	7	13	11	8	11
V	82	134	77	84	87	128	83	153	38
Cr	71	53	72	53	38	66	27	172	11

No.	1396	1397	1398	1402	1405	1406	1407	1408a	1408b
Grid Ref.	NT786 597	NT785 600	NT787 603	NT544 519	NT471 591	NT470 592	NT470 592	NT470 592	NT470 592
	P	P	Fpt	Fpt	Fpt	Fpt	Fpt	Fpt	Fpt
SiO_2	56.01	61.05	64.47	70.90	63.05	65.07	63.85	63.70	63.70
Al_2O_3	14.98	14.72	15.69	15.20	16.49	16.28	15.92	16.36	16.40
Fe_2O_3	7.58	5.90	4.69	2.81	4.37	3.96	3.26	4.24	3.95
MgO	6.66	4.40	2.45	0.82	1.73	1.84	0.98	1.77	1.70
CaO	6.08	3.20	2.88	0.58	2.53	1.79	4.61	2.63	3.89
K_2O	2.75	3.41	3.25	3.24	2.94	3.28	2.64	2.63	2.42
Na2O	2.76	3.27	3.13	4.39	3.97	4.20	3.48	4.01	3.61
MnO	0.14	0.10	0.07	0.03	0.07	0.07	0.08	0.07	0.08
TiO_2	0.84	0.63	0.56	0.36	0.68	0.60	0.59	0.62	0.61
P_2O_5	0.26	0.22	0.14	0.10	0.17	0.15	0.16	0.15	0.17
LOI	2.68	3.11	2.41	1.51	3.47	3.00	5.68	3.88	4.91
Total	**100.74**	**100.01**	**99.73**	**99.94**	**99.47**	**100.24**	**101.24**	**100.07**	**100.95**
Zn	95	63	59	49	64	63	53	54	58
Cu	58	3	18	58	8	132	6	6	6
Ni	74	47	19	43	10	11	9	9	7
Rb	50	62	59	90	71	80	73	72	69
Sr	881	747	566	233	444	530	230	439	366
Y	24	21	19	17	23	17	20	21	19
Zr	169	167	146	144	142	140	135	137	136
Nb	8	9	9	10	9	11	10	9	9
Ba	1107	1376	927	616	594	616	405	603	333
U	3	3	6	3	3	3	3	2	4
Th	9	15	10	12	7	8	9	7	7
Pb	13	12	27	18	12	11	9	12	10
V	166	117	91	44	94	83	77	87	86
Cr	289	233	41	33	11	26	26	18	20

No.	1408c	1408d	1409	1410	1411	1412	1413	1416a	1416b
Grid Ref.	NT469 522	NT469 522	NT469 593	NT774 605	NT774 605	NT779 604	NT781 605	NT770 584	NT770 584
Type	Fpt	Fpt	Fpt	P	P	Fpt	Fpt	Fmd	Fmd
SiO_2	63.10	65.54	63.95	55.61	57.80	65.82	64.74	52.82	55.11
Al_2O_3	16.03	16.81	16.11	17.80	15.90	15.74	15.78	15.26	15.82
Fe_2O_3	4.10	3.98	2.25	7.09	6.96	4.24	4.75	7.69	7.05
MgO	1.76	1.64	0.61	4.19	4.73	2.15	2.47	5.75	4.98
CaO	4.13	1.49	5.46	5.88	6.05	3.06	2.65	3.73	3.81
K_2O	2.61	2.76	2.68	1.70	2.75	2.86	2.77	3.40	3.42
Na_2O	2.97	3.31	3.23	3.34	2.96	3.32	3.10	1.56	2.44
MnO	0.09	0.05	0.09	0.09	0.15	0.07	0.05	0.12	0.12
TiO_2	0.61	0.65	0.66	1.09	0.95	0.51	0.59	0.94	0.95
P_2O_5	0.17	0.18	0.18	0.19	0.32	0.12	0.15	0.30	0.32
LOI	3.56	3.57	6.33	3.20	2.09	1.99	2.43	7.59	6.75
Total	**99.12**	**99.97**	**101.55**	**100.18**	**100.66**	**99.88**	**99.47**	**99.17**	**100.76**
Zn	61	61	37	43	73	39	37	75	68
Cu	9	18	0	96	67	78	73	33	87
Ni	7	10	8	36	63	44	44	50	53
Rb	68	71	66	56	57	60	58	93	76
Sr	257	173	158	453	905	572	578	463	695
Y	20	20	22	27	27	17	22	22	23
Zr	133	137	148	164	214	137	144	191	185
Nb	9	10	9	8	10	8	9	10	9
Ba	337	295	325	461	1014	780	1016	779	1530
U	4	3	0	3	3	4	4	1	3
Th	8	8	6	6	10	9	8	11	14
Pb	10	15	6	10	8	12	8	10	13
V	81	91	72	180	145	88	93	173	183
Cr	20	19	25	42	135	57	61	146	123

No.	1416c	1416d	1416e	1416f	1417	1418	1425	1426	1427
Grid Ref.	NT770 584	NT770 584	NT770 584	NT770 584	NT730 601	NT752 640	NT899 661	NT947 647	NT958 602
Type	Fmd	Fmd	Fmd	Fmd	Fpt	P	AB	P	Fpt
SiO_2	54.14	53.87	55.77	56.27	67.20	59.79	60.42	60.87	63.67
Al_2O_3	15.06	14.55	15.10	15.52	16.09	16.37	15.11	14.45	15.80
Fe_2O_3	6.35	6.36	5.99	7.27	3.31	5.65	6.52	4.46	3.53
MgO	4.99	5.27	4.83	5.65	1.45	4.19	6.49	3.25	2.14
CaO	4.15	4.46	5.35	4.12	1.71	4.09	1.40	4.05	2.24
K_2O	3.44	3.02	3.20	2.71	3.15	2.27	0.67	0.96	3.52
Na2O	2.83	3.16	2.97	2.64	3.22	3.68	3.76	4.96	4.23
MnO	0.15	0.13	0.12	0.12	0.07	0.12	0.05	0.06	0.07
TiO_2	0.92	0.87	0.90	0.92	0.45	0.83	0.83	0.60	0.64
P_2O_5	0.28	0.27	0.27	0.29	0.15	0.24	0.19	0.18	0.24
LOI	6.78	6.91	4.82	5.49	4.26	4.58	5.91	5.72	3.20
Total	**99.09**	**98.87**	**99.33**	**101.00**	**101.05**	**101.81**	**101.36**	**99.55**	**99.26**
Zn	67	70	72	101	44	69	134	65	57
Cu	36	83	117	154	5	14	27	14	277
Ni	59	53	53	60	23	70	118	64	31
Rb	76	68	68	75	97	54	24	38	88
Sr	994	827	904	782	318	424	104	226	449
Y	23	23	25	26	21	20	24	21	19
Zr	183	171	180	171	133	165	149	188	249
Nb	9	9	9	9	10	11	9	11	15
Ba	1468	1026	1042	1236	773	667	182	216	783
U	3	5	4	2	3	1	2	4	3
Th	13	14	15	12	7	10	9	11	15
Pb	13	14	16	48	11	9	16	12	19
V	166	165	159	176	64	130	159	93	76
Cr	128	115	132	148	9	131	281	159	58

No.	1428	1429	1467	1468	1469	1470	1471	1472	1475
Grid Ref.	NT922	NT911	NT929	NT930	NT934	NT954	NT954	NT953	NT968
	603	637	627	627	626	627	626	627	590
Type	Fpt	Fpt	Fpt	Fpt	Fpt	Fpt	Fpt	P	P
SiO_2	71.19	70.46	64.22	60.78	70.17	64.79	68.31	51.66	62.98
Al_2O_3	15.70	15.59	16.65	14.86	14.99	14.70	15.17	15.86	16.21
Fe_2O_3	2.24	2.37	3.81	4.27	1.99	3.07	2.55	8.55	4.58
MgO	0.36	1.01	0.39	1.63	1.11	1.86	1.26	6.54	3.06
CaO	1.44	1.42	3.74	6.30	1.43	3.56	2.15	4.02	2.26
K_2O	2.62	2.50	1.53	2.39	2.19	1.94	2.77	1.75	4.13
Na_2O	4.66	3.98	5.79	3.49	5.88	4.66	3.05	4.08	3.75
MnO	0.02	0.04	0.06	0.07	0.01	0.07	0.04	0.11	0.05
TiO_2	0.32	0.32	0.74	0.65	0.30	0.45	0.45	0.96	0.79
P_2O_5	0.12	0.13	0.33	0.22	0.13	0.17	0.16	0.19	0.33
LOI	2.55	3.53	4.04	5.59	2.67	5.80	4.46	5.99	2.61
Total	**101.20**	**101.36**	**101.30**	**100.23**	**100.88**	**101.07**	**100.37**	**99.72**	**100.75**
Zn	43	47	30	49	31	38	33	106	71
Cu	14	4	6	13	4	21	69	35	17
Ni	3	7	60	89	3	15	11	95	35
Rb	72	78	42	65	49	59	71	39	108
Sr	254	82	173	467	159	275	237	472	412
Y	14	15	18	18	15	17	18	23	28
Zr	133	128	204	194	130	185	190	124	297
Nb	8	10	13	12	9	12	13	6	18
Ba	358	386	162	617	340	188	182	642	937
U	3	2	4	2	2	1	2	1	5
Th	10	9	11	12	10	15	16	6	19
Pb	11	13	19	19	8	17	12	24	11
V	38	35	78	77	33	44	46	236	92
Cr	20	14	176	153	13	35	31	260	61

No.	1476	1477	1478	1480	1481	1482	1483	1484	1485a
Grid Ref.	NT954	NT955	NT955	NT734	NT734	NT749	NT749	NT749	NT736
	584	578	578	607	608	627	628	629	668
Type	P	P	P	Fpt	Fpt	Fmd	P	P	Fpt
SiO_2	63.29	63.86	62.89	63.09	66.15	58.80	59.27	60.49	64.70
Al_2O_3	16.33	15.98	16.23	16.87	15.90	16.48	14.29	16.55	15.25
Fe_2O_3	3.92	4.54	5.25	4.46	3.01	5.58	4.06	5.14	3.18
MgO	2.44	3.62	3.95	1.47	1.64	3.30	3.19	2.16	1.50
CaO	3.14	1.09	1.00	2.69	2.33	4.94	4.19	3.63	2.62
K_2O	3.51	3.61	2.83	1.77	2.95	2.14	2.70	2.54	2.40
Na2O	4.21	3.90	4.73	4.22	3.93	3.55	3.07	3.80	3.94
MnO	0.07	0.05	0.05	0.08	0.07	0.10	0.08	0.08	0.11
TiO_2	0.75	0.76	0.88	0.67	0.47	0.83	0.52	0.75	0.51
P_2O_5	0.32	0.29	0.31	0.20	0.16	0.24	0.15	0.18	0.16
LOI	2.53	3.02	2.40	4.57	4.61	3.09	7.54	5.06	5.03
Total	**100.50**	**100.71**	**100.51**	**100.08**	**101.19**	**99.03**	**99.06**	**100.37**	**99.39**
Zn	64	71	98	57	32	64	43	68	49
Cu	76	6	22	7	3	18	6	3	6
Ni	32	51	62	13	15	41	57	12	31
Rb	78	95	66	51	74	59	76	63	67
Sr	528	411	331	294	218	453	459	264	191
Y	22	20	22	26	17	25	20	24	19
Zr	289	262	252	212	148	168	169	192	158
Nb	19	15	15	11	11	9	9	10	9
Ba	701	778	752	408	251	612	585	493	348
U	4	3	3	4	2	0	5	2	2
Th	21	17	15	10	10	9	14	10	9
Pb	17	15	17	42	11	11	8	12	10
V	85	99	99	91	62	131	97	102	66
Cr	73	97	128	30	22	66	102	27	55

No.	1485b	1493	1494	1495a	1495b	1496	1498	1509	1510
Grid Ref.	NT736 668	NT561 629	NT563 631	NT564 632	NT564 632	NT565 634	NT500 572	NT533 601	NT533 614
Type	Fpt	qFp	qFp	qFp	qFp	qFp	qFp	qFp	P
SiO_2	66.39	78.42	77.18	79.41	76.94	78.01	80.25	75.89	62.27
Al_2O_3	15.95	13.34	13.76	13.71	14.26	14.00	13.68	13.97	16.59
Fe_2O_3	4.04	1.51	1.21	1.03	1.42	0.93	0.84	1.43	4.83
MgO	1.44	0.32	0.17	0.18	0.28	0.17	0.22	0.24	3.10
CaO	1.67	0.41	0.34	0.03	0.30	0.03	0.06	0.18	3.04
K_2O	2.43	2.47	2.18	2.79	2.58	2.58	3.84	3.18	3.62
Na_2O	3.81	2.55	3.55	2.14	3.09	2.69	0.00	3.68	4.04
MnO	0.10	0.02	0.01	0.01	0.05	0.00	0.00	0.01	0.08
TiO_2	0.55	0.12	0.13	0.12	0.13	0.13	0.13	0.17	0.72
P_2O_5	0.18	0.14	0.06	0.06	0.05	0.05	0.03	0.05	0.31
LOI	4.12	1.81	1.49	1.57	1.71	1.52	2.05	1.15	2.29
Total	100.68	101.11	100.09	101.05	100.81	100.11	100.89	99.94	100.87
Zn	69	29	22	34	36	24	23	21	62
Cu	19	0	5	0	0	5	6	2	36
Ni	35	11	5	2	5	2	3	4	53
Rb	65	85	83	95	86	91	125	105	68
Sr	220	43	68	20	50	35	42	185	926
Y	19	18	18	19	18	19	17	17	21
Zr	163	80	86	84	86	87	83	104	214
Nb	9	12	14	12	13	12	12	13	13
Ba	329	394	352	338	349	284	296	606	2373
U	2	2	6	2	4	3	4	2	4
Th	10	14	14	17	14	15	15	17	11
Pb	9	11	16	11	18	12	10	34	18
V	73	6	11	10	10	10	11	13	90
Cr	37	10	7	8	5	10	7	7	69

No.	1512	1513	1514	1515	1516a	1517	1518	PS5	PS6
Grid Ref.	NT535 618	NT530 619	NT543 594	NT543 594	NT544 594	NT485 553	NT478 555	NT544 610	NT539 619
Type	qFp	qFp	Fpt	qFp	P	qFp	qFp	qFp	qFp
SiO_2	76.72	75.92	69.53	76.33	67.22	78.95	79.59	77.33	78.73
Al_2O_3	14.14	14.10	16.05	13.91	15.91	14.14	13.45	13.96	13.35
Fe_2O_3	0.86	0.99	3.62	1.04	4.05	1.19	1.88	0.95	1.04
MgO	0.12	0.17	0.91	0.16	1.64	0.21	0.13	0.15	0.12
CaO	0.36	1.05	0.34	0.16	1.77	0.12	0.08	0.16	0.10
K_2O	4.30	4.10	3.22	4.38	2.92	3.04	3.21	1.45	0.90
Na2O	3.49	3.55	3.77	3.31	4.05	1.48	0.00	4.94	4.60
MnO	0.04	0.03	0.07	0.02	0.07	0.01	0.00	0.00	0.00
TiO_2	0.13	0.13	0.57	0.12	0.65	0.12	0.13	0.06	0.05
P_2O_5	0.06	0.06	0.16	0.04	0.21	0.07	0.02	0.04	0.04
LOI	1.09	1.81	1.98	1.07	2.39	2.23	2.43	1.15	1.32
Total	101.31	101.90	100.22	100.54	100.88	101.57	100.81	100.18	100.24
Zn	21	47	38	24	68	25	19	15	17
Cu	4	0	19	5	10	6	5	42	13
Ni	6	2	17	7	20	5	6	32	38
Rb	120	122	90	138	71	102	104	53	44
Sr	119	126	265	111	343	33	14	80	56
Y	20	19	23	17	27	18	18	18	16
Zr	88	88	200	85	216	88	81	70	63
Nb	12	13	11	13	13	13	12	12	10
Ba	612	592	1172	591	1080	231	238	166	169
U	4	3	3	4	3	3	4	2	4
Th	18	15	15	16	14	16	13	15	13
Pb	8	32	10	19	26	4	6	7	9
V	8	10	70	9	76	10	12	4	5
Cr	11	11	46	7	40	9	6	10	17

No.	PS7	PS8a	PS8b	PS9a	PS9b	PS10	PS11	PS12	PS14a
Grid Ref.	NT675	NT682	NT682	NT683	NT683	NT651	NT652	NT615	NT619
	566	576	576	576	576	581	581	651	651
Type	qFp	qFp	qFp	qFp	qFp	Fpt	Fpt	P	P
SiO_2	75.52	75.80	75.53	75.59	75.48	66.59	66.32	53.33	56.09
Al_2O_3	14.39	13.09	14.07	14.19	14.01	15.56	15.72	16.92	17.61
Fe_2O_3	1.60	1.59	1.63	1.48	0.87	2.80	3.19	8.16	6.24
MgO	0.24	0.59	0.26	0.24	0.43	1.37	1.40	6.59	1.94
CaO	0.06	0.62	0.14	0.09	0.42	2.43	2.39	6.58	7.12
K_2O	4.52	4.45	4.93	4.68	4.20	2.44	2.31	1.28	2.36
Na_2O	1.30	1.26	1.48	2.31	2.42	3.66	3.87	3.24	3.79
MnO	0.03	0.05	0.02	0.01	0.02	0.09	0.05	0.12	0.09
TiO_2	0.08	0.08	0.08	0.11	0.12	0.49	0.50	1.20	1.03
P_2O_5	0.04	0.04	0.04	0.04	0.05	0.17	0.17	0.19	0.24
LOI	2.10	2.41	1.59	0.72	1.77	4.22	3.60	1.81	2.59
Total	99.87	99.98	99.77	99.46	99.78	99.82	99.53	99.43	99.09
Zn	30	32	33	31	27	47	58	80	53
Cu	0	24	19	12	2	18	9	31	14
Ni	25	33	36	29	32	21	25	40	35
Rb	133	128	153	127	109	73	60	42	65
Sr	92	98	96	45	59	219	314	243	385
Y	16	17	20	15	15	20	20	34	32
Zr	64	56	62	70	70	198	203	163	219
Nb	11	9	10	10	10	10	11	7	10
Ba	455	471	470	573	498	436	532	379	522
U	2	2	0	4	2	2	2	0	1
Th	8	11	9	8	9	14	13	2	9
Pb	7	8	8	7	5	12	17	10	18
V	11	6	10	11	13	54	54	203	125
Cr	12	39	31	23	33	40	54	183	52

No.	PS14b	PS19	PS20	PS22	PS24	PS54	PS55	PS56	PS57
Grid Ref.	NT619	NT633	NT636	NT638	NT640	NT625	NT399	NT393	NT394
	651	644	646	645	644	664	566	571	566
Type	P	Fpt	Fpt	Fpt	Fpt	Fpt	Fpt	Fpt	Fpt
SiO_2	59.33	72.69	70.39	70.94	65.43	69.55	67.67	64.32	65.74
Al_2O_3	17.11	15.77	16.11	16.57	16.68	15.36	16.20	15.18	15.29
Fe_2O_3	6.22	2.06	2.24	2.55	6.13	3.27	2.84	3.46	3.70
MgO	3.25	0.44	0.87	0.95	3.40	1.27	0.83	2.27	1.43
CaO	4.74	0.16	0.33	0.28	0.31	0.47	1.03	3.31	1.80
K_2O	2.41	3.35	3.12	2.56	0.75	3.19	2.51	1.62	2.78
Na2O	3.73	2.86	4.41	3.25	0.00	4.23	4.84	4.28	4.39
MnO	0.11	0.05	0.04	0.02	0.04	0.03	0.05	0.04	0.05
TiO_2	0.92	0.41	0.31	0.33	0.92	0.39	0.67	0.45	0.63
P_2O_5	0.22	0.11	0.11	0.11	0.20	0.12	0.22	0.12	0.21
LOI	1.34	1.81	1.68	2.18	6.16	1.54	2.17	4.44	2.90
Total	99.38	99.72	99.59	99.75	99.77	99.42	99.02	99.51	101.80
Zn	78	35	58	54	48	54	52	50	77
Cu	10	7	24	3	48	10	11	13	19
Ni	39	38	25	30	70	43	35	34	27
Rb	63	101	86	72	30	89	70	56	65
Sr	371	65	360	201	24	274	357	322	230
Y	28	23	14	14	21	18	25	19	23
Zr	202	169	130	131	187	161	245	147	233
Nb	10	10	8	7	9	11	15	8	23
Ba	520	398	540	234	140	927	716	836	14
U	2	5	3	1	0	3	2	4	450
Th	10	15	6	9	10	15	14	8	2
Pb	17	5	7	13	8	7	10	17	13
V	109	52	37	41	176	52	64	74	20
Cr	54	44	9	18	229	55	51	92	70

No.	PS77	PS105	PS106	PS114	PS115	PS117	PS121	PS123	PS131
Grid Ref.	NT644	NT634	NT635	NT658	NT660	NT648	NT664	NT596	NT622
	624	619	618	667	671	687	666	597	584
Type	Fpt	qFp	Fpt	P	P	P	P	qFp	Fpt
SiO_2	65.18	76.55	62.95	54.91	58.56	61.45	62.08	76.30	68.12
Al_2O_3	16.64	14.07	14.68	14.60	15.35	17.35	17.20	14.12	15.25
Fe_2O_3	4.54	1.34	3.59	6.16	5.49	5.16	5.34	0.80	3.00
MgO	1.41	0.38	2.36	4.51	3.69	2.30	2.74	0.14	1.38
CaO	1.76	0.35	3.29	6.15	3.81	1.99	1.29	0.10	1.36
K_2O	3.97	2.95	2.57	2.65	3.28	2.76	2.78	4.14	2.76
Na_2O	3.32	2.01	3.10	3.17	3.83	4.61	4.67	3.79	4.89
MnO	0.04	0.02	0.12	0.10	0.08	0.07	0.08	0.03	0.05
TiO_2	0.64	0.19	0.45	0.84	0.77	0.62	0.72	0.10	0.42
P_2O_5	0.19	0.06	0.13	0.35	0.28	0.14	0.19	0.03	0.13
LOI	1.70	2.13	5.92	5.35	3.50	2.30	2.32	0.77	2.03
Total	**99.09**	**100.04**	**99.14**	**98.77**	**98.64**	**98.74**	**99.41**	**100.29**	**99.39**
Zn	47	23	26	65	65	61	81	18	63
Cu	71	179	7	26	22	10	16	6	8
Ni	37	49	56	44	39	25	26	43	26
Rb	103	87	85	54	71	53	56	122	80
Sr	382	41	218	771	633	685	602	111	258
Y	20	31	18	27	26	23	24	23	23
Zr	195	94	155	206	207	121	183	72	213
Nb	10	12	10	9	10	6	10	15	9
Ba	887	298	613	1044	1725	893	794	365	608
U	2	5	5	3	5	3	1	2	3
Th	11	14	10	15	14	7	11	13	13
Pb	17	5	103	14	11	11	8	11	11
V	91	23	62	148	129	130	102	8	52
Cr	50	34	119	179	120	29	51	23	40

No.	PS132	PS140a	PS140b	PS150	PS154	PS156	PS157	PS163	PS166
Grid Ref.	NT623	NT618	NT618	NT607	NT603	NT602	NT601	NT958	NT960
	584	622	622	634	651	653	655	599	595
Type	P	qFp	qFp	P	P	P	qFp	P	P
SiO_2	58.19	76.35	76.69	61.59	60.04	63.72	77.18	60.33	61.77
Al_2O_3	15.18	14.02	14.26	15.39	15.43	14.74	13.73	15.93	16.64
Fe_2O_3	5.47	1.03	1.10	4.53	4.59	3.38	0.77	4.63	4.76
MgO	5.42	0.14	0.16	4.20	3.29	3.87	0.13	4.44	3.28
CaO	3.48	0.05	0.05	2.46	4.00	2.40	0.06	1.82	0.95
K_2O	2.20	3.68	3.37	2.21	2.16	1.62	4.07	3.56	3.30
Na2O	4.22	3.38	3.46	3.60	3.77	3.91	3.63	3.58	4.73
MnO	0.09	0.02	0.00	0.08	0.07	0.05	0.02	0.05	0.06
TiO_2	0.69	0.10	0.11	0.62	0.71	0.45	0.08	0.87	0.85
P_2O_5	0.26	0.03	0.03	0.16	0.20	0.13	0.03	0.28	0.34
LOI	4.12	1.02	1.09	4.56	5.49	5.57	n.d.	3.56	2.21
Total	**99.30**	**99.82**	**100.31**	**99.38**	**99.75**	**99.82**	**99.70**	**99.04**	**98.88**
Zn	81	24	21	65	60	53	19	74	84
Cu	31	1	2	32	17	10	0	36	49
Ni	52	39	49	85	65	128	45	103	32
Rb	41	104	104	49	54	55	121	73	100
Sr	754	133	142	310	441	326	78	574	357
Y	23	19	18	18	19	17	18	21	26
Zr	199	74	73	149	162	136	69	236	279
Nb	8	15	15	10	10	11	13	14	19
Ba	692	430	448	863	736	443	435	691	800
U	3	2	2	0	4	5	2	1	1
Th	12	16	13	9	10	7	16	11	18
Pb	14	11	12	15	12	11	7	19	13
V	143	9	9	99	115	67	7	112	103
Cr	225	37	26	180	126	236	34	194	53

No.	PS168	PS178	PS183	PS187	PS211
Grid Ref.	NT959	NT919	NT917	NT785	NT463
	595	664	688	600	540
Type	Fpt	qFp	AB	Fpt	qFp
SiO_2	65.74	77.08	53.33	63.55	76.99
Al_2O_3	16.36	13.89	15.39	15.38	14.06
Fe_2O_3	3.71	0.97	8.20	3.83	1.04
MgO	2.30	0.34	9.25	2.54	0.30
CaO	0.55	0.55	1.77	2.23	0.19
K_2O	3.91	2.37	1.91	3.22	4.17
Na_2O	3.96	2.46	2.87	3.36	1.84
MnO	0.04	0.02	0.05	0.08	0.01
TiO_2	0.65	0.04	1.26	0.55	0.12
P_2O_5	0.25	0.08	0.33	0.12	0.04
LOI	2.14	2.31	4.79	4.43	1.65
Total	99.61	100.10	99.16	99.29	100.41
Zn	118	60	119	45	21
Cu	104	4	149	5	4
Ni	54	43	186	32	30
Rb	89	70	46	102	113
Sr	468	40	214	255	22
Y	15	12	25	21	19
Zr	263	57	228	130	81
Nb	18	12	15	9	14
Ba	827	159	316	470	501
U	2	3	0	4	4
Th	20	6	10	7	15
Pb	72	7	21	8	10
V	75	1	137	95	8
Cr	73	16	412	75	22

a

P:	Porphyrite
Fpt:	Acid porphyrite
qFp:	Quartz porphyry
Fmd:	Microgranodiorite
AB:	St. Abbs Head andesite

Appendix 3c. Major and trace element data: lamprophyres

No.	1388	1399	1414	1415	1421	1422	1423	1424	1433
NGR	NT740 630	NT786 602	NT782 605	NT771 583	NT919 685	NT919 685	NT918 681	NT899 691	NT512 144
Type[a]	Lm	Lm	Lm	Lm	Lm	Lm	Lm	Lm	Lm
SiO_2	53.40	57.32	50.20	51.15	54.38	52.54	50.58	45.19	44.81
Al_2O_3	13.92	13.98	13.29	13.55	12.11	12.10	11.14	13.01	13.28
Fe_2O_3	6.37	6.56	8.88	5.50	5.79	6.62	5.88	7.27	9.79
MgO	7.08	5.50	11.70	5.58	5.88	5.62	5.27	7.73	9.03
CaO	5.88	5.19	6.05	5.63	5.13	5.33	8.57	9.12	6.93
K_2O	4.97	3.70	2.49	5.49	5.31	5.67	3.72	4.01	3.37
Na_2O	2.58	2.47	1.54	2.11	0.34	0.04	0.74	1.86	1.98
MnO	0.12	0.13	0.16	0.13	0.08	0.12	0.10	0.11	0.10
TiO_2	1.08	0.89	1.02	1.17	1.43	1.48	1.34	1.14	1.17
P_2O_5	0.83	0.54	0.36	0.95	0.65	0.67	0.62	1.06	1.68
LOI	4.23	2.93	2.98	7.78	8.45	9.66	11.46	8.90	6.74
Total	100.47	99.21	98.65	99.04	99.55	99.85	99.41	99.39	98.88
Zn	84	74	86	57	50	50	54	93	137
Cu	55	15	34	38	25	44	21	134	122
Ni	264	124	345	110	202	195	204	297	279
Rb	111	69	100	115	124	108	105	84	73
Sr	1248	775	544	731	235	261	483	1532	1079
Y	25	26	23	27	23	25	23	36	31
Zr	337	333	167	333	773	804	728	525	376
Nb	22	11	7	20	17	15	15	32	22
Ba	2048	1511	612	2058	1431	1451	1319	1878	4940
U	5	6	0	4	6	4	1	3	5
Th	24	20	10	22	17	16	11	20	34
Pb	26	12	8	19	10	11	14	21	26
V	125	127	183	146	143	145	128	150	252
Cr	301	220	860	280	462	470	420	335	459

No.	1443	1452	1473	1492	1497	1511	PS1	PS1c	PS1m
NGR	NT494 155	NT428 201	NT968 590	NT502 557	NT503 571	NT526 622	NT512 114	NT512 114	NT512 114
	Lm	Lm	Lm	Lm	Lm	Lm	Lm	Lm	Lm
SiO_2	41.25	52.22	52.10	47.03	49.15	50.67	47.76	48.89	26.67
Al_2O_3	14.30	14.66	12.79	13.04	12.87	13.90	13.77	13.98	7.46
Fe_2O_3	8.65	6.31	5.22	9.44	8.76	6.56	6.58	7.15	4.04
MgO	6.75	6.94	6.34	3.58	3.89	5.67	7.41	7.41	2.91
CaO	11.45	5.47	7.54	8.08	8.39	7.43	7.31	6.72	29.58
K_2O	2.70	3.68	3.34	4.11	3.47	4.24	5.47	5.51	3.02
Na2O	2.78	2.98	2.71	3.56	3.69	2.61	1.22	1.36	0.15
MnO	0.17	0.11	0.11	0.12	0.11	0.11	0.09	0.08	0.29
TiO_2	1.21	0.97	1.48	2.20	2.17	1.15	0.93	1.01	0.48
P_2O_5	1.48	0.53	1.12	0.99	0.93	0.89	0.68	0.69	0.39
LOI	9.61	4.76	7.72	7.88	7.09	7.47	7.72	7.30	25.46
Total	100.35	98.62	100.47	100.03	100.52	100.68	98.92	100.10	100.44
Zn	101	74	107	91	113	79	92	92	49
Cu	45	41	44	55	52	67	52	56	65
Ni	172	222	204	50	42	177	303	309	124
Rb	62	81	76	64	51	89	120	122	60
Sr	1794	1090	713	1181	908	1142	443	464	281
Y	32	20	40	17	18	23	25	24	19
Zr	384	355	422	243	254	310	341	341	169
Nb	29	15	25	23	24	18	18	19	9
Ba	8656	1774	1204	8057	1644	1666	1529	1480	632
U	4	3	4	2	4	2	6	6	2
Th	26	20	25	12	11	23	29	31	17
Pb	42	23	13	6	7	9	30	32	18
V	217	145	169	212	214	156	172	180	74
Cr	223	343	479	130	134	362	416	436	158

No.	PS173	PS174	PS181	PS182	PS184a	PS184b	PS184c	PS186	PS188
NGR	NT968 590	NT968 590	NT918 680	NT919 684	NT954 642	NT954 642	NT954 642	NT786 597	NT774 605
Type	Lm	Lm	Lm	Lm	Lm	Lm	Lm	Lm	Lm
SiO_2	46.46	52.16	51.24	59.28	47.94	48.96	54.91	55.34	52.85
Al_2O_3	13.04	7.63	11.74	12.23	12.94	13.69	9.60	14.90	14.39
Fe_2O_3	6.27	4.18	6.77	5.97	7.92	7.49	4.74	7.52	8.24
MgO	6.42	5.13	6.19	4.72	7.64	7.42	4.22	7.03	8.05
CaO	9.09	14.01	6.82	3.60	7.29	6.72	10.98	5.63	7.69
K_2O	4.36	1.28	2.20	3.82	2.95	1.46	0.97	3.02	1.65
Na_2O	2.21	1.29	0.17	0.13	1.50	3.29	1.94	2.49	2.36
MnO	0.12	0.18	0.12	0.06	0.11	0.09	0.09	0.13	0.15
TiO_2	1.41	0.81	1.46	1.46	0.82	0.89	0.62	0.82	1.03
P_2O_5	1.09	0.65	0.63	0.66	0.22	0.24	0.15	0.24	0.25
LOI	8.49	12.99	11.93	6.91	9.56	9.88	11.19	2.09	2.77
Total	**98.95**	**100.31**	**99.27**	**98.85**	**98.88**	**100.12**	**99.41**	**99.22**	**99.43**
Zn	100	71	74	51	83	82	58	101	67
Cu	44	27	26	33	25	16	26	30	62
Ni	197	112	243	191	232	196	65	81	108
Rb	101	32	70	89	74	42	37	56	47
Sr	705	403	257	217	173	178	187	852	1052
Y	44	29	24	24	23	25	25	25	28
Zr	414	237	740	794	126	134	168	168	193
Nb	26	16	17	18	7	8	10	9	10
Ba	1524	528	1085	1227	499	239	1069	1255	627
U	5	5	4	5	0	3	2	3	1
Th	27	14	15	16	7	9	7	11	9
Pb	19	19	12	12	28	25	13	10	6
V	170	110	148	159	203	231	89	176	188
Cr	458	286	447	483	651	613	148	305	356

No.	PS191	PS192	PS192m	PS192c	PS215	PS216	PS218	PS219	PS220m
NGR	NT740 630	NT771 583	NT771 583	NT771 583	NT501 302	NT502 302	NT451 233	NT452 228	NT449 189
Type	Lm	Lm	Lm	Lm	Lm	Lm	Lm	Lm	Lh
SiO_2	53.62	49.36	51.97	49.30	54.41	52.46	53.71	47.02	55.67
Al_2O_3	14.26	13.12	13.95	13.02	13.00	12.32	14.34	15.40	16.51
Fe_2O_3	5.82	6.40	6.41	6.62	5.57	5.63	6.20	8.20	6.57
MgO	6.74	7.26	4.27	7.21	4.39	5.10	7.24	6.89	4.04
CaO	4.22	5.44	4.96	5.47	6.73	7.98	3.67	7.39	2.92
K_2O	5.17	5.19	5.84	5.05	5.15	4.32	3.45	1.55	3.76
Na2O	2.78	2.08	2.33	2.02	2.16	2.59	3.08	3.52	4.98
MnO	0.11	0.13	0.09	0.13	0.07	0.08	0.07	0.12	0.07
TiO_2	1.08	1.18	1.15	1.13	0.93	0.95	0.93	1.31	1.54
P_2O_5	0.83	0.97	0.92	0.90	0.72	0.72	0.44	0.24	0.62
LOI	4.23	7.49	6.84	8.28	6.63	7.44	5.08	6.19	2.13
Total	**98.86**	**98.62**	**98.73**	**99.12**	**99.74**	**99.57**	**98.22**	**97.82**	**98.79**
Zn	76	67	38	68	125	129	82	70	73
Cu	61	44	18	25	100	97	78	48	21
Ni	211	160	72	163	231	292	206	115	29
Rb	112	109	116	104	88	77	42	47	96
Sr	1005	858	597	797	936	534	642	453	552
Y	25	25	46	26	26	26	25	28	25
Zr	343	327	344	325	342	325	216	162	211
Nb	24	21	23	21	15	14	7	8	14
Ba	1888	2000	1955	1893	1872	1373	2734	466	1812
U	4	4	5	2	11	9	1	2	4
Th	24	24	27	27	40	37	11	3	8
Pb	13	15	21	20	29	40	19	14	11
V	140	149	121	142	124	132	140	213	201
Cr	322	312	229	303	342	415	402	359	34

No.	PS220c	PS221	PS222	PS223	PS224	PS225	PS226	PS227m	PS227mc
NGR	NT449 189	NT508 114	NT483 118	NT457 101	NT458 101	NT498 168	NT489 157	NT494 152	NT494 152
Type	Lh	Lm	Lh	Lm	Lm	Lm	Lh	Lmh	Lmh
SiO_2	54.63	47.45	55.84	57.52	56.29	42.49	56.57	42.60	42.23
Al_2O_3	12.97	16.37	14.30	14.86	15.08	14.15	16.82	14.52	15.19
Fe_2O_3	7.41	8.09	5.83	6.37	6.39	8.11	6.37	9.33	8.50
MgO	8.20	8.01	6.33	7.19	5.77	11.62	5.80	8.77	6.02
CaO	7.86	3.79	4.17	1.14	3.55	5.13	0.89	7.77	9.08
K_2O	1.81	5.13	2.78	3.02	3.64	3.83	2.83	2.11	3.28
Na_2O	2.17	2.50	3.19	3.46	3.72	2.16	5.03	3.09	2.99
MnO	0.11	0.06	0.07	0.06	0.06	0.13	0.08	0.12	0.15
TiO_2	1.18	1.44	0.84	0.83	0.86	1.43	1.22	1.62	1.59
P_2O_5	0.40	0.76	0.26	0.26	0.35	1.03	0.44	1.37	1.19
LOI	2.93	5.31	5.85	3.78	5.01	6.39	3.24	7.68	6.21
Total	**99.67**	**98.90**	**99.44**	**98.50**	**100.72**	**96.48**	**99.28**	**98.99**	**96.40**
Zn	77	139	78	111	79	175	101	122	99
Cu	27	64	26	17	44	51	33	49	55
Ni	257	169	158	164	149	269	113	193	115
Rb	45	74	49	56	70	79	67	49	80
Sr	744	403	335	311	361	960	326	694	2810
Y	22	31	22	26	23	28	26	35	34
Zr	167	362	156	167	172	412	295	406	401
Nb	10	25	9	10	11	25	20	33	31
Ba	784	2633	682	614	963	1838	605	2316	11214
U	1	3	3	2	3	2	2	2	5
Th	2	23	8	9	8	21	15	22	22
Pb	13	20	15	9	12	53	21	35	108
V	162	231	151	165	155	254	198	251	221
Cr	535	346	347	378	310	528	213	249	173

No.	PS227c	PS229
NGR	NT494 152	NT
Type	Lmh	Lm
SiO_2	40.79	52.60
Al_2O_3	13.69	16.23
Fe_2O_3	9.08	6.74
MgO	8.46	6.86
CaO	9.45	4.11
K_2O	2.34	2.82
Na2O	2.62	3.79
MnO	0.13	0.07
TiO_2	1.50	1.07
P_2O_5	1.37	0.56
LOI	8.21	4.18
Total	**97.62**	**99.02**
Zn	105	103
Cu	46	44
Ni	215	240
Rb	57	53
Sr	1016	1133
Y	32	26
Zr	393	386
Nb	30	18
Ba	3688	1918
U	4	1
Th	25	19
Pb	28	51
V	227	159
Cr	241	424

a Lm: Mica lamprophyre
Lh: Hornblende lamprophyre
Lmh: Kersantitic spessartite

Appendix 3d. Major and trace element data: sediments

No.	PS2	PS3	PS4	PS3Os	PS35	PS45	PS75	PS130	PS164
Grid ref.	NT550 618	NT543 612	NT543 610	NT658 638	NT643 643	NT642 647	NT643 624	NT612 588	NT958 599
Type [a]	Gywk	Gywk	Gywk	Hfls	Hfls	Gywk	Gywk	Gywk	Gywk
SiO_2	60.50	73.86	63.86	73.36	59.87	61.16	73.64	71.47	56.83
Al_2O_3	17.57	11.15	10.10	11.06	17.83	16.62	10.70	8.86	11.08
Fe_2O_3	4.32	4.95	3.85	4.57	0.81	4.40	4.16	3.05	5.03
MgO	0.37	2.50	2.63	2.84	3.80	4.21	2.74	1.81	3.57
CaO	2.36	0.85	5.75	1.88	0.80	4.64	2.29	5.25	9.05
K_2O	0.88	1.86	2.42	1.83	4.10	2.73	0.99	1.40	1.59
Na_2O	8.64	1.22	0.93	1.36	1.43	3.32	2.31	1.62	1.76
MnO	0.11	0.06	0.08	0.04	0.04	0.05	0.06	0.06	0.08
TiO_2	0.96	0.75	0.75	0.63	0.81	0.95	0.70	0.49	0.66
P_2O_5	0.03	0.15	0.18	0.12	0.18	0.24	0.13	0.09	0.15
LOI	3.14	2.31	9.31	2.41	3.71	1.46	1.98	n.d.	9.46
Total	**98.88**	**99.65**	**99.86**	**100.10**	**99.54**	**99.77**	**99.67**	**94.10**	**99.25**
Zn	26	76	64	62	92	84	62	47	78
Cu	16	23	35	19	47	35	22	8	7
Ni	26	90	75	66	117	116	65	49	65
Rb	38	65	81	69	132	79	37	54	57
Sr	298	115	293	132	157	379	197	118	162
Y	30	29	25	31	30	27	21	25	29
Zr	364	282	272	227	219	230	293	223	181
Nb	14	12	10	11	15	13	12	8	12
Ba	328	680	415	327	858	645	366	212	195
U	2	2	2	1	4	4	3	1	4
Th	10	9	8	11	12	10	8	9	10
Pb	7	19	11	14	27	21	11	12	13
V	90	116	103	87	135	129	106	67	91
Cr	285	297	243	122	171	228	207	184	166

No.	PS164wr	PS167	PS185	PS200
Grid ref.	NT958 599	NT960 595	NT955 637	NT646 625
Type	Gywk	Shl	Gywk	Gywk
SiO_2	65.91	51.68	59.95	59.82
Al_2O_3	12.90	18.15	11.31	18.14
Fe_2O_3	5.82	8.98	5.19	6.52
MgO	3.78	8.09	3.47	2.87
CaO	1.99	1.64	6.92	1.49
K_2O	1.85	3.51	1.83	4.50
Na2O	2.00	1.54	1.83	1.69
MnO	0.10	0.07	0.06	0.03
TiO_2	0.91	0.95	0.75	0.77
P_2O_5	0.20	0.18	0.17	0.26
LOI	4.20	4.72	8.21	2.35
Total	**99.65**	**99.51**	**99.69**	**98.44**
Zn	86	112	70	103
Cu	11	24	18	23
Ni	85	111	73	78
Rb	67	119	64	116
Sr	74	141	129	303
Y	29	30	29	31
Zr	267	149	216	184
Nb	14	16	12	15
Ba	210	426	196	1189
U	4	3	0	1
Th	11	14	9	10
Pb	15	15	16	21
V	119	196	102	130
Cr	207	180	172	108

a Gywk: Graywacke
Hfls: Hornfelsed graywacke
Shl: Shale

Appendix 3e. Major and trace element data: Carboniferous intrusions

No.	1400a	1400b	1401a	1401b	1453	1466b	1466c	PS72	PS112
Grid ref.	NT568 390	NT568 390	NT569 397	NT569 397	NT443 259	NT928 626	NT928 626	NT645 625	NT665 658
Type	F	F	F	F	F	D	D	D	D
SiO_2	61.42	59.10	63.84	63.02	62.60	45.61	44.20	53.01	45.85
Al_2O_3	17.67	17.31	17.94	18.20	15.50	14.48	14.13	17.85	17.80
Fe_2O_3	5.47	7.13	4.41	5.22	7.47	6.97	10.21	12.40	12.74
MgO	0.26	0.80	0.57	0.19	1.49	2.37	1.41	0.28	4.46
CaO	0.69	1.16	0.52	0.50	1.83	16.38	16.69	0.45	0.84
K_2O	5.96	5.49	5.83	5.91	4.03	0.62	0.63	8.72	8.49
Na_2O	5.48	5.29	6.05	5.95	1.36	1.65	1.51	0.00	0.00
MnO	0.09	0.12	0.09	0.07	0.05	0.21	0.19	0.13	0.12
TiO_2	0.25	0.44	0.26	0.27	0.35	1.96	1.91	2.04	3.75
P_2O_5	0.09	0.15	0.07	0.08	0.09	0.21	0.21	0.36	0.54
LOI	1.13	1.55	0.60	0.67	5.05	10.48	9.78	n.d.	n.d.
Total	98.50	98.53	100.20	100.07	99.81	100.94	100.87	95.16	94.44
Zn	47	90	41	37	655	108	61	111	196
Cu	21	23	21	7	11	27	26	28	189
Ni	27	21	26	21	9	125	54	70	169
Rb	113	93	114	116	70	26	27	143	69
Sr	93	157	82	80	22	376	395	119	29
Y	68	56	55	52	71	23	24	58	39
Zr	982	970	997	1013	1334	124	121	623	212
Nb	108	96	115	115	88	11	13	64	24
Ba	544	1038	534	449	256	334	296	624	666
U	2	3	3	1	4	1	0	4	1
Th	14	12	14	15	12	1	4	9	2
Pb	34	40	35	42	9	42	58	47	17
V	0	1	3	5	0	224	271	113	309
Cr	12	11	3	7	18	248	264	54	231

No.	PS135	PS177	PS201	PS214	PS217
Grid ref.	NT637 581	NT928 627	NT645 625	NT545 517	NT443 259
Type	D	D	D	Cm	F
SiO_2	50.00	49.37	54.91	45.81	62.98
Al_2O_3	13.14	13.87	18.30	13.47	16.10
Fe_2O_3	14.87	11.32	11.42	12.85	6.93
MgO	4.87	6.62	0.43	6.26	1.03
CaO	5.75	11.35	0.47	5.53	1.14
K_2O	1.36	0.51	6.85	3.76	5.23
Na2O	2.14	1.61	0.00	2.65	0.96
MnO	0.13	0.17	0.13	0.15	0.06
TiO_2	3.00	1.89	2.07	2.64	0.37
P_2O_5	0.44	0.19	0.37	1.16	0.10
LOI	3.25	2.40	n.d.	4.66	4.35
Total	98.94	99.29	94.77	98.94	99.24
Zn	131	87	114	324	491
Cu	20	44	28	41	24
Ni	22	106	93	40	28
Rb	40	18	112	80	77
Sr	384	336	29	1247	23
Y	44	26	69	36	78
Zr	259	122	626	497	1378
Nb	19	13	67	115	95
Ba	549	389	513	1649	215
U	0	2	3	5	4
Th	3	4	12	16	13
Pb	29	11	44	59	13
V	419	304	109	149	0
Cr	17	244	70	31	12

a F: Felsite
D: Dolerite
Cm: Monchiquite

Appendix 4. Rare-earth element data

Sample no:	PS15	PS17	PS27	PS28	PS32	PS60	PS65
Pluton:	Plw	Plw	Plw	Plw	Plw	Plw	Plw
La	2.49	13.07	39.63	46.25	25.76	39.81	28.01
Ce	5.31	30.52	87.77	101.66	52.68	68.58	57.20
Nd	3.1738	18.337	43.761	50.279	24.14	24.450	26.278
Sm	0.8471	4.5091	7.4991	8.621	4.829	4.0094	5.0905
Eu	0.671	1.267	2.062	2.292	1.187	0.9007	1.293
Gd	n.d.	4.74	n.d.	6.20	4.400	3.25	4.45
Dy	1.038	4.961	3.973	4.307	4.445	2.657	4.32
Er	0.696	2.872	2.089	2.203	2.649	1.596	2.50
Yb	0.65	2.464	1.875	1.975	2.490	1.746	2.410
Lu	0.097	0.354	0.273	0.288	n.d.	n.d.	n.d.

Sample no:	PS82	PS92	PS95	PS99	80007	80009	80010
Pluton:	Plw	Plw	Plw	Plw	Sp	Sp	Sp
La	13.37	23.34	30.89	23.23	n.d.	32.86	16.793
Ce	29.22	46.09	65.54	47.53	n.d.	65.18	35.28
Nd	16.551	20.118	30.604	21.476	25.568	26.634	16.816
Sm	3.7691	4.0287	5.7088	4.4474	4.6287	4.8557	3.5526
Eu	1.444	1.0355	1.390	1.0778	0.942	1.1148	1.0145
Gd	3.850	3.67	n.d.	n.d.	n.d.	4.182	3.49
Dy	3.680	3.373	3.91	3.813	n.d.	3.850	3.448
Er	1.973	1.979	2.14	2.194	n.d.	2.291	2.079
Yb	1.703	1.906	2.07	2.068	2.449	2.248	1.966
Lu	0.27	0.310	n.d.	n.d.	n.d.	n.d.	0.2896

Sample no:	K57	K72	K73	TA6	TG13	AS40	AS48
Pluton/type:	Kn	Kn	Kn	Bn	Bn	Cp	Cp
La	29.62	26.58	28.62	51.38	36.72	24.40	47.30
Ce	57.39	56.90	58.16	99.38	69.12	51.56	86.5
Nd	25.249	27.052	25.484	38.249	25.369	24.1826	37.960
Sm	4.8615	5.1524	4.9988	5.8188	3.8461	5.0084	6.9518
Eu	1.429	1.432	1.1863	1.5216	1.006	1.3669	1.068
Gd	4.435	4.46	4.47	4.137	2.68	4.7	6.1
Dy	4.011	3.927	4.008	2.834	1.78	4.435	5.65
Er	2.309	2.21	2.282	1.379	0.88	2.546	3.28
Yb	2.189	2.102	2.144	1.148	0.76	2.3798	3.16
Lu	0.333	0.316	0.391	0.165	n.d.	n.d.	0.44

Sample no:	AS49	78/GDTE1	80012	SA1	SA5	SA13	1388
Pluton/type:	Cp	Cr	Dst	AB	AB	AB	L
La	28.38	16.07	15.25	36.22	21.31	21.89	123.9
Ce	44.72	29.36	32.49	74.87	42.75	67.36	246.98
Nd	25.496	11.5847	16.8598	34.149	20.936	19.2741	97.833
Sm	4.8116	2.2397	3.7750	6.4736	4.2356	3.6224	13.609
Eu	0.8021	0.6469	1.2149	1.7293	1.2480	0.7693	3.356
Gd	4.28	1.92	3.86	5.61	3.86	3.06	8.34
Dy	3.919	1.245	3.647	4.79	n.d.	n.d.	n.d.
Er	2.349	0.761	2.102	2.642	1.91	1.62	2.16
Yb	2.196	0.6803	1.905	2.37	1.79	1.56	1.702
Lu	0.325	n.d.	0.303	0.3444	0.2650	0.2277	n.d.

Sample no:	1424
Pluton/type:	L
La	169.8
Ce	342.7
Nd	145.876
Sm	22.021
Eu	5.043
Gd	14.01
Dy	7.36
Er	2.94
Yb	2.109
Lu	0.299

a

Plw: Priestlaw
Clw: Cockburn Law
Sp: Spango
Kn: Knipe
Bn: Bengairn
Cp: Carsphairn
Cr: Creetown
AB: St.Abbs/Eyemouth lavas
L: Lamprophyres

Appendix 5. Sr and Nd isotope data

A5.1 Sr isotopes:

Sample No.	Rb[a]	Sr[a]	$^{87}Rb/^{86}Sr$	$^{87}Sr/^{86}Sr$	$(^{87}Sr/^{86}Sr)_o$	ε Sr
Priestlaw:						
1542	77.30	495.0	0.451	0.707401 ±10	0.70477	+10.8
1542d	117.9	155.1	2.201	0.717825 ±9	0.70498	+13.8
PS15	4.601	681.0	0.0197	0.704271 ±9	0.70416	+2.1
PS17	33.08	572.5	0.168	0.705464 ±9	0.70448	+6.7
PS25	57.20	410.0	0.405	0.707243 ±10	0.70488	+12.4
PS27	71.55	1731.0	0.119	0.704900 ±8	0.70420	+2.7
PS28	69.53	1773.0	0.113	0.704890 ±9	0.70423	+3.1
PS29	70.96	1719.0	0.119	0.704869 ±8	0.70417	+2.3
PS30	74.73	445.7	0.486	0.707572 ±9	0.70473	+10.2
PS32	74.40	452.0	0.477	0.707608 ±9	0.70482	+11.5
PS33	71.86	557.1	0.373	0.707027 ±12	0.70485	+11.9
PS34	82.28	477.5	0.498	0.707848 ±8	0.70494	+13.2
PS39	84.68	475.6	0.515	0.707739 ±7	0.70473	+10.2
PS60	114.7	367.2	0.906	0.709981 ±10	0.70469	+9.7
PS62	58.59	626.5	0.272	0.706753 ±8	0.70516	+16.3
PS63	68.43	1064.0	0.186	0.705535 ±9	0.70445	+6.2
PS65	80.74	515.3	0.454	0.707707 ±10	0.70505	+14.8
PS199	103.0	514.0	0.579	0.708162 ±7	0.70478	+10.8
Cockburn Law						
PS82	26.36	621.1	0.122	0.705631 ±9	0.70492	+12.9
PS84	94.45	491.0	0.555	0.708077 ±10	0.70483	+11.6
PS85	96.06	455.4	0.610	0.708915 ±9	0.70535	+19.0
PS85b	98.99	462.0	0.619	0.708985 ±10	0.70537	+19.3
PS85f	102.1	330.0	0.894	0.710590 ±7	0.70537	+19.3
PS86	66.16	576.0	0.334	0.706995 ±8	0.70505	+14.8
PS89	93.32	577.0	0.469	0.707600 ±6	0.70486	+12.1
PS91	70.62	615.0	0.333	0.706852 ±10	0.70491	+12.8
PS92	78.81	416.0	0.547	0.708342 ±9	0.70515	+16.2
PS93	67.75	540.2	0.362	0.707504 ±11	0.70539	+19.6
PS95	82.16	623.0	0.382	0.706839 ±8	0.70461	+8.5
PS99	72.44	368.0	0.570	0.709108 ±9	0.70578	+25.1
PS100	87.70	423.0	0.599	0.708825 ±10	0.70533	+18.7

Sample No.	$^{87}Rb/^{86}Sr^{b}$	$^{87}Sr/^{86}Sr$	$(^{87}Sr/^{86}Sr)_{o}$	ε Sr
Spango				
K76	0.243	0.706041±10	0.70462	+8.7
80007	1.007	0.710410 ±8	0.70453	+7.4
80008	0.651	0.708360 ±8	0.70456	+7.8
80009	0.567	0.707788 ±9	0.70448	+6.7
80010	0.307	0.706925 ±7	0.70513	+15.9
Knipe				
K57	0.197	0.706124 ±9	0.70497	+13.6
K72	0.266	0.706187 ±9	0.70463	+8.8
K73	0.570	0.708737 ±10	0.70541	+19.9
K74	0.529	0.708356 ±8	0.70527	+17.9
Carsphairn				
AS30	0.356	0.707058 ±9	0.70498	+13.8
Bengairn				
B3	0.286	0.707029 ±8	0.70541	+19.7
B6	0.373	0.707259 ±8	0.70515	+16.0
TA6	0.405	0.708186 ±12	0.70590	+26.6
TG13	0.532	0.708541 ±11	0.70553	+21.4
Portencorkrie				
PHF7	0.185	0.706208 ±9	0.70516	+16.1
PHF125	0.599	0.708755 ±6	0.70537	+19.1
Creetown				
78/GDTE1	0.964	0.711459 ±8	0.70601	+28.2
St.Abbs Head/Eyemouth lavas				
SA1	0.292	0.70632 ±3	0.70462	+8.7
SA5	0.364	0.70676 ±2	0.70463	+8.8
SA13	0.304	0.70688 ±3	0.70510	+15.5

Sample No.	Rb[a]	Sr[a]	$^{87}Rb/^{86}Sr$	$^{87}Sr/^{86}Sr$	$(^{87}Sr/^{86}Sr)_o$	ε Sr
Sediments						
PS30s	72.23	137.5	1.521	0.72180 ±2	0.71292	+126.6
PS35	147.2	162.1	2.632	0.727885 ±7	0.71252	+120.9
Lamprophyres						
1388	127.2	1320.0	0.275	0.707131 ±9	0.70556	+21.8
1424	97.68	1691.0	0.168	0.706807 ±10	0.70585	+26.0

A5.2 Nd isotopes:

Sample No.	Sm	Nd	$^{147}Sm/^{144}Nd$	$^{143}Nd/^{144}Nd$	$(^{143}Nd^{144}Nd)_o$	ε Nd
Priestlaw:						
PS15	0.8587	3.217	0.1614	0.512637 ±7	0.512209	+1.9
PS17	4.611	18.75	0.1487	0.512600±5	0.512201	+1.8
PS27	7.589	44.28	0.1036	0.512489 ±4	0.512211	+2.0
PS28	8.720	50.85	0.1037	0.512503 ±4	0.512225	+2.2
PS32	4.870	24.35	0.1209	0.512515 ±4	0.512190	+1.6
PS60	4.049	24.69	0.0992	0.512469 ±4	0.512203	+1.8
PS65	5.184	26.76	0.1171	0.512475 ±4	0.512161	+1.0
Cockburn Law						
PS82	3.993	17.53	0.1378	0.512572 ±4	0.512202	+1.8
PS92	4.059	20.27	0.1211	0.512472 ±5	0.512147	+0.7
PS95	5.770	30.93	0.1128	0.512494 ±6	0.512191	+1.6
PS99	4.494	21.71	0.1252	0.512359 ±10	0.512023	-1.7
Spango						
80007	4.629	25.59	0.109	0.512430±4	0.512137	+0.53
80009	4.856	26.63	0.110	0.512452 ±5	0.512157	+0.92
80010	3.553	16.82	0.128	0.512449 ±4	0.512106	-0.08
Knipe						
K57	4.862	25.25	0.117	0.512361 ±3	0.512047	-1.23
K72	5.152	27.05	0.115	0.512480 ±4	0.512171	+1.19
K73	4.999	25.48	0.119	0.512310 ±4	0.511990	-2.34

Sample No.	Sm	Nd	$^{147}Sm/^{144}Nd$	$^{143}Nd/^{144}Nd$	$(^{143}Nd^{144}Nd)_o$	ε Nd
Carsphairn						
AS40	5.008	24.18	0.125	0.512406±5	0.512070	-0.8
AS48	6.952	37.96	0.111	0.512377±5	0.512079	-0.6
AS49	4.817	25.50	0.114	0.512383±4	0.512077	-0.6
Bengairn						
TA6	5.819	38.25	0.092	0.512329±3	0.512090	-0.7
TG13	3.846	25.37	0.092	0.512340±4	0.512101	-0.5
Creetown						
78/GDTE1	2.240	11.58	0.117	0.512453±5	0.512149	+0.4
Distinkhorn						
80012	3.775	16.86	0.135	0.512631±6	0.512269	+3.1
St.Abbs Head/Eyemouth lavas						
SA1	6.474	34.15	0.115	0.512396±4	0.512087	-0.45
SA5	4.236	20.94	0.122	0.512521±4	0.512193	+1.6
SA13	3.622	19.27	0.114	0.512461±4	0.512155	+0.9
Lamprophyres						
1388	14.21	102.2	0.084	0.512320±4	0.512100	-0.4
1424	24.17	160.2	0.091	0.512205±4	0.511967	-3.0

a Rb and Sr determined by XRF at Royal Holloway and Bedford New College.

b Rb and Sr data from M.F. Thirlwall (unpublished data).